Universiteit
Leiden
The Netherlands

Pathogenesis and treatment of skeletal metastasis : studies in animal models

Buijs, J.T.

Citation
Buijs, J. T. (2009, January 21). *Pathogenesis and treatment of skeletal metastasis : studies in animal models*. Retrieved from https://hdl.handle.net/1887/13413

Version:	Corrected Publisher's Version
License:	Licence agreement concerning inclusion of doctoral thesis in the Institutional Repository of the University of Leiden
Downloaded from:	https://hdl.handle.net/1887/13413

Note: To cite this publication please use the final published version (if applicable).

Pathogenesis and Treatment of Skeletal Metastasis

Studies in animal models

Jeroen T. Buijs

Jeroen_Buijs_18.indd 1 26-11-2008 10:18:07

Pathogenesis and Treatment of Skeletal Metastasis – Studies in Animal Models
J.T. Buijs
Thesis, University of Leiden, 2009 – with references – with a summary in dutch

Lay-out and cover design: www.textcetera.nl

Cover: photo of the "Tree of Ténéré" (Niger), once considered the most isolated tree on earth. In the early 1970s photo taken by dr. Peter Krohn ©, www.krohn-photos.com.

ISBN 978-90-9023684-1
Printed by: Gildeprint

© 2009, J.T.Buijs, The Netherlands. All right reserved. No part of this thesis may be reproduced or transmitted in any form, by any means, electronic or mechanical, without prior written permission of the author

Jeroen_Buijs_18.indd 2 26-11-2008 10:18:07

Pathogenesis and Treatment of Skeletal Metastasis

Studies in animal models

Proefschrift

ter verkrijging van

de graad van Doctor aan de Universiteit Leiden,

op gezag van Rector Magnificus prof.mr. P.F. van der Heijden,

volgens besluit van het College voor Promoties

te verdedigen op woensdag 21 januari 2009

klokke 15:00 uur

door

Jeroen Theodorus Buijs

geboren te Amsterdam

in 1979

Jeroen_Buijs_18.indd 3 26-11-2008 10:18:07

Promotiecommissie

Promotor	prof.dr. S.E. Papapoulos
Co-promotor	dr. G. van der Pluijm
Referent	prof.dr. T.A. Guise (Univ. of Virginia, Charlottesville, VA, USA)
Overige leden	prof.dr. C.W.G.M. Löwik
	prof.dr. P. ten Dijke

The studies presented in this thesis were performed at the departments of Endocrinology and Metabolic Diseases, Pathology, and Urology at the Leiden University Medical Center, Leiden, The Netherlands and at the department of Urology, University of Bern, Inselspital, Switzerland.

The research described in this thesis was financially supported by grants from the Dutch Cancer Society (RUL2001-2485) and the European Sixth Framework programme PRIMA (FP504-587).

The printing of this thesis was financially supported by:
Jurriaanse Stichting
Procter & Gamble Pharmaceuticals Nederland B.V.
Astellas Pharma B.V.
Merck Sharp and Dohme B.V.
Eli Lilly Nederland B.V.
AstraZeneca B.V.
Amgen B.V.
Servier Nederland Farma B.V.
Merck Serono B.V.
Medtronic Spine
Novartis Oncology

Jeroen_Buijs_18.indd 4 26-11-2008 10:18:07

Aan mijn ouders,
voor Nurka,

Jeroen_Buijs_18.indd 5 26-11-2008 10:18:07

Contents

Chapter 1.	General introduction partly published in *Cancer Letters, in press.*	9
Chapter 2.	Prognostic significance of periodic acid-Schiff-positive patterns in primary breast cancer and its lymph node metastases *Breast Cancer Res Treat* 2004; 84:117-30.	71
Chapter 3.	Optical imaging of cancer metastasis to bone marrow: a mouse model of minimal residual disease *Am J Pathol* 2002; 160:1143-53.	91
Chapter 4.	Interference with the microenvironment supports impairs the de novo formation of bone metastasis in vivo *Cancer Res* 2005; 65:7682-90.	109
Chapter 5.	Inhibition of bone resorption and growth of breast cancer in the bone microenvironment *Bone, in press*.	133
Chapter 6.	Bone morphogenetic protein 7 in the development and treatment of bone metastases from breast cancer. *Cancer Res* 2007; 215:8742-51	147
Chapter 7.	BMP7, a putative regulator of epithelial homeostasis in the human prostate, is a potent inhibitor of prostate cancer bone metastasis in vivo. *Am J Pathol* 2007; 171:1047-57.	171
Chapter 8.	General discussion	195
Chapter 9.	Summary – Samenvatting	225
List of abbreviations		235
List of publications		237
Curriculum vitae		239

Jeroen_Buijs_18.indd 7 26-11-2008 10:18:07

Jeroen_Buijs_18.indd 8 26-11-2008 10:18:07

Chapter 1

General Introduction

Partly published in
Cancer Letters 2008, *in press*

Jeroen T Buijs[1]
Gabri van der Pluijm[1,2]

Departments of Urology[1] and Endocrinology[2],
Leiden University Medical Center,
Leiden, The Netherlands

Jeroen_Buijs_18.indd 9 26-11-2008 10:18:07

Jeroen_Buijs_18.indd 10 26-11-2008 10:18:07

General introduction

Table of Contents		**11**
1	**Clinical Problem of Skeletal Metastasis**	**13**
2	**Paget's 'Seed and Soil' Hypothesis**	**15**
3	**'The Seed': Tumor Progression and Metastasis**	**15**
3.1	Carcinogenesis	15
3.2	Angiogenesis	17
3.3	Acquisition of an Invasive Phenotype: Epithelial-to-Mesenchymal Transition	19
3.4	Intravasation, Circulation and Extravasation	22
3.4.1	Vertebral Venous System	23
4	**'The Soil': Bone/Bone Marrow Microenvironment**	**23**
4.1	Bone	24
4.1.1	Bone Cells	24
4.1.2	Bone Matrix	26
4.1.3	Bone Turnover	26
4.2	Bone Marrow	26
4.3	TGF-**ß** Superfamily	29
4.4.1	Signaling Pathways	29
4.4.2	Regulation of Activity	33
4.4.3	Physiologic and Pathophysiologic Functions	36
5	**'Seed–Soil' Interactions**	**37**
5.1	Bone Turnover and Skeletal Metastasis	39
5.2	Bone Metastatic Phenotype	40
5.2.1	Osteolytic Bone Metastasis	40
5.2.2	Osteosclerotic Bone Metastasis	42
6	**Animal Models of Bone Metastasis**	**44**
6.1	Spontaneous Mammary and Prostate Cancer in Animals	44
6.2	Transgenic Induction of Mammary and Prostate Cancer in Mice	45
6.3	Syngeneic and Xenograft Models of Bone Metastasis	45
6.3.1	Routes of Cancer Cell Inoculation	45

Jeroen_Buijs_18.indd 11 26-11-2008 10:18:07

6.4	Subcutaneous Transplantation of Human Bone	47
6.5	*In Vivo* Imaging	47
7	**Treatment of Bone Metastases**	**47**
7.1	Treatment Strategies	48
7.1.1	Bone Resorption Inhibitors	48
7.2	Future Perspectives	50
8	**Aim and Outline of Thesis**	**50**
9	**References**	**51**

Jeroen_Buijs_18.indd 12 26-11-2008 10:18:07

1 Clinical Problem of Skeletal Metastasis

Cancers account for over 20% of deaths in Western countries and these are primarily due to the spread of cancer to distant organs [1]. It has long been recognized that primary cancers spread to distant organs with characteristic preference [2], and the skeleton is one of the most common organs to be affected by metastatic cancer [3-6]. Breast and prostate cancer are osteotropic tumors, i.e., carcinomas that have a special predilection to form bone metastases. At postmortem examination ~70% of patients dying of these cancers have evidence of metastatic bone disease (Table 1) [5,7]. Carcinomas of thyroid, kidney and bronchus also commonly give rise to bone metastases, with an incidence of 30% to 40%, but tumors of the gastrointestinal tract rarely (<10%) produce bone metastases. In these routine autopsies, the true incidence of metastases in the skeleton is most likely underestimated, and more accurate assessments may be determined by scintigrams. Together, breast and prostate cancer probably account for more than 80% of cases of metastatic bone disease [6].

Table 1 **Incidence of skeletal metastases at autopsy**
Based on all autopsy studies listed by Galasko [5] + study from Walther [7]

		Incidence (%) of bone metastases	
Primary tumor site	**Number of studies**	**Median**	**Range**
Breast	13	67	47– 85
Prostate	8	66	33 – 85
Thyroid	5	38	28 – 60
Lung	6	36	30 – 55
Kidney	4	34	33 – 40
Esophagus	3	6	5 – 7
Gastro-intestinal tract	5	7	3 – 11
Rectum	3	11	8 – 13
Uterine/ cervix	1	50	x
Ovaries	1	9	x
Liver	1	16	x

Breast and prostate cancer are the most commonly diagnosed malignancies [1] and the second leading cause of cancer death in the western world in women and men, respectively [1]. At time of diagnosis, most patients with breast [3] and prostate [8] cancer do not have clinicopathologic signs of overt distant metastases. Thus, after resection of the primary tumor and all positive lymph nodes, these patients are in complete clinical remission. However, disseminated tumor cells (DTCs) can already be present in bone marrow (BM) [9-13], a clinical situation called *minimal residual disease (MRD)*. The DTCs that are still present in BM are frequently resistant to current treatment (chemo-/hormone therapy), and can stay

dormant for many years [10,14,15]. So, only the very small subfraction of the DTCs that have acquired the abilities of metastasizing to, surviving in, and colonizing the bone/BM microenvironment, can eventually result in the development of an overt bone metastasis. Only this subpopulation of DTCs can, therefore, be regarded as true *metastasis-initiating cells* (MICs). Even though, the general presence of DTCs in BM at time of diagnosis is significantly associated with the formation of distant metastases, particularly to bone [9,10].

The clinical courses of patients with breast and prostate cancer with a first recurrence in bone are relatively long, with a median survival of 24 and 40 months [4]. This is in marked contrast to those with first recurrence of breast cancer in the liver (3 months)[3]. Moreover, patients with disease that remains confined to the skeleton have a better prognosis than those with subsequent visceral involvement [16]. In these patients, the decline in quality of life and eventual death is due almost entirely to skeletal complications and their subsequent treatment [17,18]. The prognostic indicators that metastatic breast cancer remains confined to skeleton are low histological grade (well-differentiated), lobular subtype (vs. ductal), postmenopausal state and a low number of positive lymph nodes at time of surgery. For patients with breast cancer, good prognostic factors for survival after the development of bone metastases are low histological grade (well-differentiated), positive estrogen receptor status, a long disease free interval, and increasing age [16].

Bone pain is the most common complication of metastatic bone disease, resulting from structural damage, periosteal irritation, and nerve entrapment [19]. In addition, hypercalcemia occurs in 5–10% of all patients with advanced cancer but is most common in patients with breast cancer, multiple myeloma, and squamous carcinomas of the lung [20,21]. Pathologic fractures are a relatively late complication of bone involvement.

Bone metastases in prostate cancer patients are predominantly osteoblastic (osteosclerotic), characterized by increased bone formation due to exaggerated osteoblastic activity. In contrast, patients with breast, lung, and kidney cancers have predominantly osteolytic bone metastases, characterized by increased bone degradation resulting from enhanced osteoclastic activity [18,21,22]. However, patients can have both osteolytic and osteoblastic bone metastases, or mixed lesions containing both elements (see paragraph 5.2, 'Bone Metastatic Phenotype').

In this chapter, a brief introduction into the multistep process of metastasis will be given. Subsequently, this chapter will give an overview of our current understanding of the molecular and biological mechanisms involved in the process of bone metastasis formation, including a summary of normal bone physiology and therapeutic opportunities. Finally, the outline of this thesis will be presented. But first, to set the scene, the next paragraph will describe the well-established 'seed and soil' hypothesis as postulated by Stephen Paget in 1889.

Jeroen_Buijs_18.indd 14 26-11-2008 10:18:07

2 Paget's 'Seed and Soil' Hypothesis

Over a century ago Stephen Paget was the one of the first who observed a non-random pattern of metastasis to certain organs by analyzing autopsy records of 735 women who had died of breast cancer [2]. He proposed the 'seed and soil' hypothesis in which he compared the seeding of cancer cells to the dispersal of the seeds of plants. Accordingly, circulating cancer cells ('seeds') disperse in all directions, but can accomplish metastases only in the organs where the microenvironment ('soil') is permissive for their growth, i.e., osteotropic cancer cells posses certain properties that enable them to grow in bone, and the bone/bone marrow microenvironment provides a fertile soil on which to grow. Ever since, the hypothesis holds forth. Based on this hypothesis, the 'seed' (see paragraph 'The Seed: Tumor Progression and Metastasis'), the 'soil ('The Soil: Bone/Bone Marrow') and their interactions ('Seed–Soil Interactions') will be specifically addressed in this chapter.

3 'The Seed': Tumor Progression and Metastasis

Since Paget postulated the 'seed and soil' hypothesis, our understanding of the metastatic process has increased tremendously. It has now been well-established that tumor progression and metastasis is a multistep process characterized sequentially by carcinogenesis and growth of the primary tumor, angiogenesis, cell invasion, access to the systemic blood circulation (intravasation), survival in circulation, arrest in microvasculature and subsequent extravasation, and growth at distant organs, (reviewed in [23]) (Fig. 1). These processes will be discussed in more detail in the next paragraphs.

3.1 Carcinogenesis

The great majority of cancers (>80%) occur in epithelial tissues, yielding carcinomas [1,24]. Epithelial tissues are generally built according to a common set of architectural principles; relatively thin sheets of epithelial cells are separated from complex layers of stroma by a basement membrane. By definition, carcinomas begin on the epithelial side of the basement membrane as hyperplastic and dysplastic growth progressing to a carcinoma *in situ,* and are considered to be *benign*. Nevertheless, carcinoma *in situ* may develop into an invasive malignancy as it breaks through the basement membrane and, by then, is classified as *malignant*, and commonly called a cancer [24].

In the normal, healthy situation tissue fibroblasts regulate the proliferation and differentiation of epithelial tissues [25]. Likewise, tumor–stroma interactions also play a critical role in development and progression of carcinomas [26,27]. For example, transformed stroma can induce malignancy in lung [28] and mammary epithelia [29], and conversely, normal fibroblasts have been reported to convert malignant epithelia to morphologically benign lesions

[30]. Cancer-associated fibroblasts (CAFs) could also induce tumorigenesis in non-malignant prostatic epithelial cells, mediated via CAF-secreted stromal-derived factor (SDF-1) and transforming growth factor-ß (TGF-ß) [31]. This is in line with the dual role that is implicated for TGF-ß in carcinogenesis. In normal and non-malignant epithelial cells TGF-ß actc as a potent growth inhibitor [32,33]. However, different types of carcinomas (e.g., Ras-transformed cells) can become refractory to growth inhibition. In fact, TGF-ß can potentiate tumorigenesis and contribute to invasiveness by stimulating an epithelial-to-mesenchymal transition (EMT) [34-38] (see paragraph 3.3 'Acquisition of an Invasive Phenotype: Epithelial-to-Mesenchymal Transition')

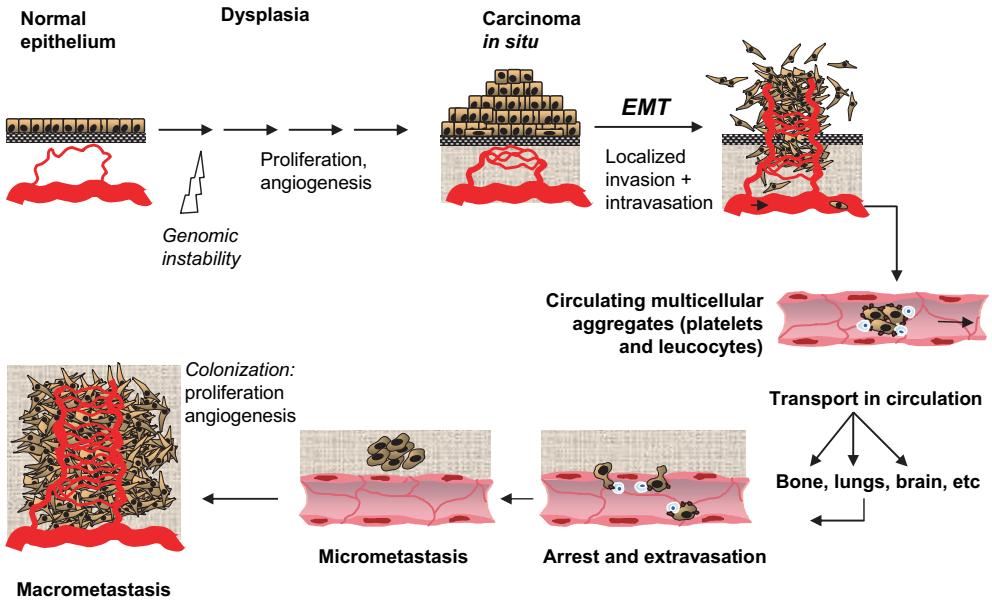

Figure 1 **Main steps in tumor progression and metastasis**. Cellular transformation due to genomic instability and changes can result in dysplasia, which may eventually result in a carcinoma *in situ*. At the same time, new blood vessel are formed (angiogenesis). This will facilitate cancer cells to enter into the systemic circulation (intravasation), after they have undergone an epithelial-to-mesenchymal transition (EMT). The EMT confers an invasive phenotype to the cancer cells, including loss of cell-cell adhesion, increased motility and matrix degradation. Aggregates of cancer cells with platelets and leukocytes may form cell embolis that may consequently be protected from the immune reaction. Arrest in the capillaries may be facilitated by mechanical mechanism and by adhesion to endothelium-specific cell adhesion molecules. Eventually some of the micrometastases may acquire the ability to colonize the tissue in which they have landed, enabling them to form a macrometastasis. The small probability of successfully completing all steps of this cascade explains the low likelihood that any single cancer cell leaving a primary tumor will succeed in becoming the founder of a distant, macroscopic metastasis.

Jeroen_Buijs_18.indd 16 26-11-2008 10:18:09

Many other tumor–stroma interactions are also mediated by members of the TGF-ß superfamily [39], e.g., the involvement of TGF-ß signaling in fibroblasts was determined by conditional inactivation of the TGF-ß type II receptor (TßRII) gene in mouse fibroblasts ($TßRII^{fspKO}$) [40]. The loss of TGF-ß responsiveness in fibroblasts resulted in intra-epithelial neoplasia in prostate and invasive squamous cell carcinoma of the forestomach, both associated with an increased abundance of stromal cells. TGF-ß and other members of the TGF-ß superfamily will be discussed in greater detail in the section 'TGF-ß superfamily members'.

For over 150 years, it has been anticipated that only a minority of cells within a tumor are responsible for tumor growth and development (reviewed in [41]). Over the past few years it has become possible to isolate and characterize these tumor-initiating cells, first from hematological malignancies [42,43] and recently also from many solid tumors, including breast [44] and prostate cancer [45,46]. Cell fractions of as few as 100 to 200 sorted cells with a particular phenotype from human primary breast [44] and prostate cancer [46] could successfully be orthotopically transplanted in immune-deficient mice, whereas much larger numbers (10^4–10^5) of the rest of the cells depleted of that particular phenotype could not. Many of these isolated tumor-initiating cells share (surface) markers with somatic stem cells and both share the characteristics of 1) self-renewal, 2) an indefinite proliferative potential, 3) differentiation along one or several diverse lineages, and 4) homing to allow cells to migrate and seek their niche. For these reasons, tumor-initiating cells have been given the popular name 'cancer stem cells (CSCs)' [47,48]. The concept of CSCs underscores the importance of targeting the correct cells for cancer therapy. Eliminating only the more differentiated, rapidly dividing cells by chemo- or radiotherapy is not likely to result in successful long term remission if the less differentiated and slower proliferating CSCs remain to repopulate the tumor. At present, much remains to be learned about the identification, molecular signature and functional plasticity of the CSCs [49].

3.2 Angiogenesis

Angiogenesis, also referred to as neovascularization, is the process of new capillary formation from pre-existing vessels [50,51]. Angiogenesis is a complex multistep process that involves dissolution of the basement membrane of the vessel, extracellular matrix degradation, migration and proliferation of endothelial cells, capillary differentiation, stabilization and anastomosis. These processes are tightly regulated by inducers and inhibitors of endothelial proliferation, migration and differentiation [52].

In malignancy, tumor cells can switch from an angiogenesis-inhibiting phenotype to an angiogenesis-stimulating phenotype, the so-called *'angiogenic switch'* [53]. This angiogenic switch is essential for tumor growth beyond 1–2 mm^3 without neovascularization [54]. In breast cancer, tumor-induced angiogenesis is already evident at the pre-invasive stage of ductal carcinoma *in situ*, characterized by a rim of microvessels formed around the ducts that are filled with proliferative epithelial cells. So before carcinoma cells breach the base-

ment membrane, they often succeed in stimulating angiogenesis on the stromal side of the membrane, by dispatching angiogenic factors through this porous barrier to endothelial cells within the stroma [55]. Angiogenesis is not only required to meet the growing metabolic demands of the tumor by supplying nutrients and oxygen, but also provides routes for tumor dissemination and metastasis [54,56]. Not surprisingly, high blood vessel counts or production of factors that stimulate angiogenesis are independent predictors of poor prognosis in many primary solid cancers [57-61]. A variety of factors, including hypoxia and genetic changes in the tumor cells, contribute to the increase in production of angiogenic factors. Furthermore, cells within the activated tumor stroma also play an important role in increasing the production of vascular endothelial growth factors (VEGFs) and other angiogenic factors, including basic fibroblast growth factor (bFGF) and platelet-derived growth factor (PDGF) [26,62].

VEGF-A is a specific endothelial cell mitogen and regarded as the most important inducer of angiogenesis. It is constitutively expressed in many cancers [62,63]. Its importance was underlined when it was demonstrated that monoclonal antibodies against VEGF-A inhibited the growth of various tumors in animal models [64]. Angiogenesis is not only essential for the primary tumor to grow and metastasize, but is required for the outgrowth of a micrometastasis into an overt (bone) metastasis as well [65,66].

Besides weakly stimulating angiogenesis, VEGF-C and VEGF-D are the main inducers of tumor lymphangiogenesis, and are overexpressed in breast and prostate cancers as well [67]. Accordingly, VEGF-C and VEGF-D expression levels have been correlated with increased number of lymph vessels in cancer patients, and have been shown to promote metastatic spread via the lymphatics [68,69].

In addition to (lymph)angiogenesis, evidence is accumulating that malignant tumors are often capable of inducing other structures that may contribute to (invasive) growth and dissemination (reviewed in [70]). Networks that stain positive with periodic acid-Schiff (PAS) have been observed in different types of cancers [62,71-73]. In both uveal and cutaneous melanoma, these structures have been shown to be of prognostic significance [73-75].

The PAS reaction is a non-specific indicator for polysaccharides, which are present in basement membranes, including those of blood vessels. The PAS-positive patterns may represent (a mixture of): blood vessels/vascular network [72,74], fibrovascular tissue [76,77], tumor cells [78], or a fluid conducting meshwork [71]. Maniotis and co-workers have shown that highly aggressive, but not non-aggressive, melanoma cells are capable of forming highly patterned vascular channels *in vitro* that are composed of a PAS-positive basement membrane in the absence of endothelial cells and fibroblasts [78]. These channels formed *in vitro* are morphologically identical to PAS-positive channels in histological preparations of highly aggressive primary and metastatic uveal and cutaneous melanomas. The generation of microvascular channels by aggressive tumor cells was termed "vasculogenic mimicry" (VM) to emphasize their *de novo* generation without participation by endothelial cells [78-80]. Since then, VM has

Jeroen_Buijs_18.indd 18 26-11-2008 10:18:09

been identified in several cancers, including prostate [81] and inflammatory breast cancer [82]. However, the and co-workers remains a debatable subject, and
Although some investigators state that the original findings of VM by Maniotis are not convincing [83,84], or lack novelty [85], VM is becoming increasingly accepted as a concept for tumor cell plasticity

3.3 Acquisition of an Invasive Phenotype: Epithelial-to-Mesenchymal Transition

In the pre-invasive stage of carcinoma *in situ*, with or without increased neovascularization in the underlying stroma, the first step leading to dissemination is the acquisition of local invasiveness [23]. The organization of the epithelial cell layers in normal tissue is incompatible with the motility and invasiveness displayed by malignant cancer cells. Therefore, in order to acquire motility and invasiveness, cancer cells must shed many of their epithelial characteristics, detach from epithelial sheets, and undergo a drastic alteration, which is referred to as the epithelial-to-mesenchymal transition (EMT) [37,86].
In order to invade adjacent cell layers carcinoma cells are required to remodel the nearby tissue environment by excavating passageways through the extracellular matrix (ECM) and pushing aside any cells that stand in their path [87]. The most important effectors to create space in the ECM are matrix metalloproteinases (MMPs)(reviewed in [88]). In carcinomas, the great bulk of these proteases are secreted by recruited stromal cells, notably macrophages, mast cells and fibroblasts, rather than neoplastic cells [26,89]. During the course of degrading ECM components (e.g., fibronectin, tenascin, laminin, collagens, and proteoglycans), MMPs can also activate certain growth factors that have been tethered in inactive form to the ECM or to cell-surfaces [88].

The EMT displayed by cancer cells is reminiscent of the highly conserved and fundamental process of EMT that occurs during early embryonic development [90-93]. During gastrulation, embryonic epithelial cells need to undergo an EMT in order to migrate to a new environment. Eventually these embryonic cells may regain a fully differentiated epithelial phenotype via a mesenchymal-to-epithelial transition (MET) (Fig. 2) [94-98]. The transition to a more mesenchymal, motile cellular phenotype is the result of a complex physiological process that includes dissolution of adherens junctions, loss of cell polarity, a change to spindle-like cell morphology, cytoskeletal reorganization, increased cell motility, loss of epithelial markers and induction of mesenchymal markers [90-93,99]. Increased vimentin expression and perturbation of E-cadherin-mediated cell adhesion appear as hallmarks of this process [37,100-102]. Accordingly, it has been shown that once E-cadherin expression is suppressed, other cell-physiologic changes associated with the EMT seem to follow suit. Additionally, re-expression of E-cadherin in different types of cancer strongly suppressed the invasiveness and metastatic dissemination [103,104].

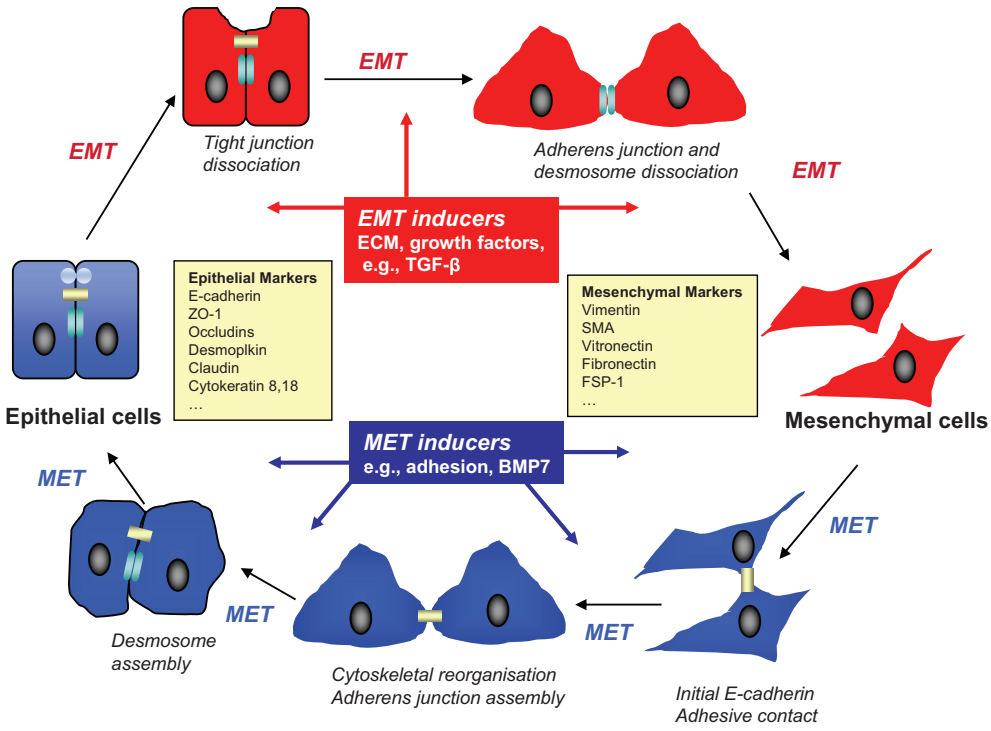

Figure 2 **The cycle of epithelial-cell plasticity as observed in embryonic development during gastrulation.** The diagram shows the cycle of events during which epithelial cells are transformed into mesenchymal cells and vice versa. The different stages during EMT (epithelial–to-mesenchymal transition) and the reverse process MET (mesenchymal–to-epithelial transition) are regulated by effectors of EMT and MET, which influence each other. Important events during the progression of EMT and MET, including the regulation of the tight junctions and the adherens junctions, are indicated. ECM, extracellular matrix; ZO-1, zona occludens 1; SMA, smooth muscle actin; FSP-1, fibroblast-specific protein-1; adapted from [97].

Under non-pathological conditions, EMT and MET are both non cell-autonomous processes, and thus require an external stimulus to be initiated [92,93,105]. In malignancy, both genetic alterations and tumor environment may be able to induce EMT in tumor cells. Transformed mammary epithelial cells that are in direct contact with the surrounding stromal cells can undergo an EMT, indicated by expression of vimentin and an elongated, fibroblastic shape [105]. However, established metastases of most cancers recapitulate the differentiated phenotype of their primary tumors including re-expression of E-cadherin [106,107]. Therefore, the important steps that enable metastasis can be reversible, and are not explained solely by irreversible genetic alterations, indicating the existence of a dynamic component to human tumor progression [108,109].

TGF-ß is one of the main inducers of EMT as was demonstrated in Ras-transformed mammary and other epithelial cells [110-112] (Fig. 3). These mammary epithelial cells were even able to maintain the mesenchymal, fibroblast-like state through autocrine TGF-ß signaling [110,111]. However, when TGF-ß was removed (by adding fresh medium or neutralizing antibodies) they reverted back to their epithelial appearance [110], indicating that they had undergone an MET. Another example of a self-sustaining positive feedback loop for EMT is the expression of αvß6 integrin by tumor cells, which can activate the latent form of TGF-ß produced by the stroma cells [113].

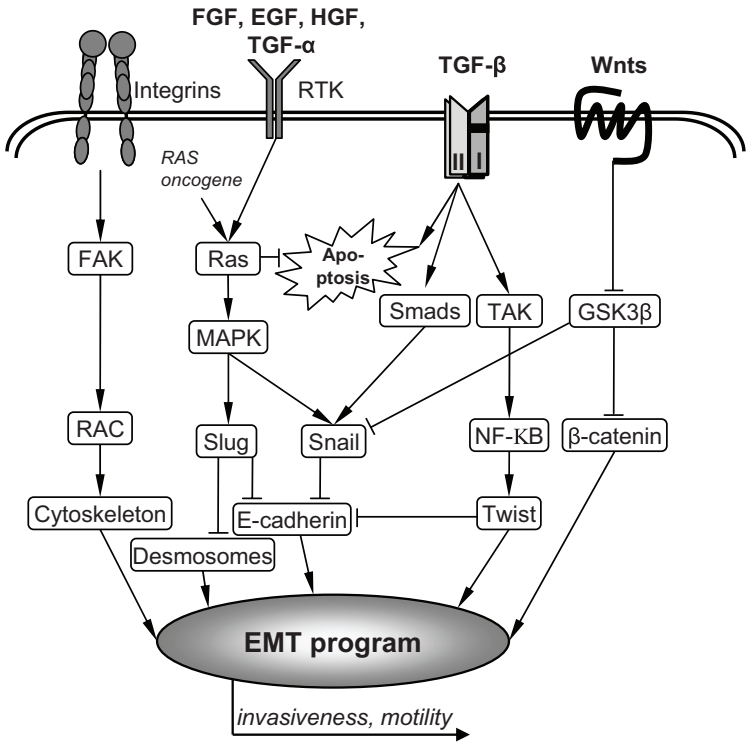

Figure 3 **Overview of the molecular networks that regulate EMT.** A small selection of EMT regulators, and a limited representation of their crosstalks are illustrated. TGF-ß is one of the main inducers of EMT. However, several normal and transformed epithelial cell lines need co-activation of Ras-signaling, to overcome transforming growth factor-ß (TGF-ß)-induced apoptosis. It is likely that the EMT is normally triggered in response to a mixture of signals that carcinoma cells receive from the stroma together with intracellular signals, e.g. the signal released by the Ras oncogene. FGF, fibroblast growth factor; HGF, hepatocyte growth factor; EGF, epidermal growth factor; RTK, receptor tyrosine kinase; FAK, focal adhesion kinase; GSK3ß, glycogen-synthase kinase-3ß; MAPK, mitogen-activated protein kinase; NF-κB, nuclear factor-κB; TAK1, TGF-ß-activated kinase-1.

Additional microenvironmental signals that can induce EMT are ECM components and soluble factors, including other members of the TGF-ß superfamily, fibroblast growth factor (FGF) family, epidermal growth factor (EGF), hepatocyte growth factor (HGF, alias scatter factor) [114], insulin-like growth factor (IGF)-II [115] and proteins of the wingless (Wnt) and Hedgehog (Hh) families (Fig. 3) (reviewed in [86,97]). It is important to take into account that besides the tumor–stroma interactions at the edge of tumor, infiltrating cells (e.g., lymphocytes, macrophages) might also be able to induce EMT in tumor cells. Moreover, accumulation of irreversible mutations could also trigger invasive behavior, particularly resulting in poorly differentiated anaplastic cancers, in which no re-differentiation is detectable in primary cancers and metastases [116,117].

Both the EMT concept and the CSC concept cover distinct aspects of tumor progression and metastasis, but can be converged into a single concept, which subdivides CSCs in the *stationary cancer stem cell* (SCS cell) and the *migrating cancer stem cell* (MCS cell) [109]. SCS cells, which are still embedded in the epithelial tissue, are already active in benign precursor lesions, such as carcinoma *in situ*, and persist in differentiated areas throughout all steps of tumor progression; however SCS cells cannot disseminate. MCS cells, which are located predominantly at the tumor–stroma interface, are derived from SCS cells through the acquisition of a (transient) EMT in addition to stemness. This concept takes into account two important requirements — CSCs that have undergone EMT can disseminate, and DTCs that retain stem-cell functionality can form metastatic colonies. So, the MCS cell concept combines the important current tumor initiation and progression concepts — the cancer stem cell and EMT concept — and it integrates both genetic alterations and the tumor environment as combined driving forces of malignant progression. However, the concept still awaits verification in different models of tumor progression for various types of cancer.

3.4 Intravasation, Circulation and Extravasation

Once tumor cells detach from the primary tumor via EMT, they can intravasate into the blood or lymphatic system. Via the lymphatic system, tumor cells can form lymph node metastases in close proximity of the primary tumor, or eventually enter the blood circulation in the left and right subclavian veins. Tumor cells that directly, or indirectly, enter the blood vessels can spread via the pulmonary circulation throughout the whole body, where they may found new colonies. However, the event of a successful development of a distant metastasis is very rare, and most cancer cells are not able to by-pass the capillary bed of the lungs. This is substantiated by the fact that in animal models, it has been estimated that 3–4 10^6 cancer cells/g of tumor can reach the bloodstream per day [118], but that only a very small minority of cancer cells reaching the blood will survive and grow at the distant sites.

In the blood circulation, cancer cells may interact with platelets [119,120] and leucocytes, to create aggregates or emboli. These may increase resistance to shear stress and protect from immune-cell–mediated tumor cell clearance [23,121]. These aggregates may also

facilitate mechanical trapping in the capillaries of different organs, and promote extravasation [122]. Once the tumor cells have exited the circulation, the activated platelets are a source of factors that are able to induce angiogenesis [123], stimulate tumor cell proliferation, and indirectly enhance osteoclastic activity in the bone environment [119,120].

3.4.1 Vertebral Venous System

As first demonstrated by Batson, there exists a *vertebral venous system*, which is composed of three freely communicating thin-walled valveless networks: intraosseous vertebral veins, epidural and paravertebral venous complexus [124,125]. The pressure in the intraosseous veins is always 35–50% higher than on the caval side of the venous circulatory system, enabling blood to flow along this pressure gradient from the vertebrae to the inferior vena cava. However, the absence of valves makes it possible that an increase of abdominal pressure, such as caused by coughing, lifting or palpation, could cause retrograde flow. Moreover, Batson showed in human cadaver and animal experiments that venous blood from both the pelvis and the breast flowed not only into the vena cava, but also directly into the vertebral venous system [124,125]. This system, in which blood is thus continuously subjected to arrest and reversal of the direction of the flow, could enable cancer cells from the pelvic region and breast to by-pass the pulmonary circulation, providing an explanation for the predilection of breast and prostate cancer to produce metastases in the axial skeleton. This hypothesis was tested by Coman and De Long, who performed an inoculation with cancer cells in the femoral veins during a moderate temporarily increase in intra-abdominal pressure in experimental animals. Indeed, an increased abdominal pressure enabled cancer cells to directly enter, and form metastases within the vertebral venous system [124,126].

Although the system of blood flow in the *vertebral venous system* can, at least in part, explain the high incidence of bone metastases in the vertebrae, it cannot explain that human cancers, particularly breast and prostate cancer, metastasize with high frequency to other bones [5]. For this explanation, we may need to have a closer look at the interactions between the 'seed' and the 'soil'. But before these interactions will be discussed, the next paragraph will first comprehensively describe the properties of the soil.

4 ' The Soil': Bone/Bone Marrow Microenvironment

In addition to anatomy, the pathophysiology of bone metastasis is determined by multiple direct and indirect interactions between metastatic cancer cells and the bone/BM microenvironment (including BM cells, bone cells, and bone matrix). First, the normal physiology of the bone/BM microenvironment will first be dilineated below.

4.1 Bone

Bone is a highly mineralized tissue that provides mechanical support and metabolic functions to the skeleton. It can be formed by either intramembraneous ossification or endochondral ossification. Intramembranous ossification occurs when mesenchymal precursor cells differentiate directly into bone-forming osteoblasts, a process employed in generating the flat bones of the skull as well as in adding new bone to the outer surfaces of long bones. In contrast, endochondral bone formation entails the conversion ofan initialcartilage template into bone and is responsible for generating most bones of the skeleton (reviewed in [127]).

4.1.1 Bone Cells

The formation and degradationof bone matrix is regulated by normal bone cells, namely the osteoblast and osteoclast, respectively. In normal bone, there is a balanced remodeling sequence: first, osteoclasts resorb bone matrix, and then osteoblasts form bone matrix at the same site (reviewed in [127]).

4.1.1.1 Osteoclasts

Osteoclasts are specialized cells derived from the monocyte–macrophage hematopoietic lineage that adhere to and, once activated, degrade bone matrix (reviewed in [128,129]). Activated osteoclasts resorb bone by secreting the protease cathepsin K that dissolves the matrix, and produce acid that releases bone mineral into the extracellular space under the ruffled border of the plasma membrane of osteoclasts, which faces bone (reviewed in [129]). The adherence of osteoclasts to the bone surface is critical for the bone resorptive process, since agents that interfere with osteoclast attachment block bone resorption [130]. Although osteoclasts can be influenced by various locally produced cytokines as well as systemic hormones, two specific hematopoietic factors — macrophage colony stimulating factor (M-CSF, alias CSF1) and receptor activator of nuclear factor κB ligand (RANKL) — are both necessary and sufficient for the formation and activation of osteoclasts. M-CSF is produced by stromal cells and osteoblasts and interacts with its receptor c-fms expressed on macrophage precursors to stimulate proliferation. Accordingly, op/op mice that lack expression of M-CSF due to a gene mutation are deficient in osteoclasts (and macrophages), resulting in enhanced bone formation [131-133]. Substitution of M-CSF reversed the osteopetrotic phenotype in op/op mice [134]. While M-CSF is crucially important in the early steps of osteoclastogenesis, RANKL — expressed on osteoblasts and stromal cells — is critically involved in maturation and activation of the osteoclasts. Interaction of RANKL with the membrane receptor RANK on osteoclast precursors induce — by signaling through the nuclear factor-κB (NF-κB) and Jun N-terminal kinase (JNK) pathways — commitment of the monocyte–macrophage precursor to the osteoclast lineage [135-139]. The importance of RANK–RANKL binding in the formation of osteoclasts has been demonstrated clearly by *RANKL* [140,141] and *RANK* [142] knock-out mice. Both knock-out mice lack osteoclasts, and

Jeroen_Buijs_18.indd 24 26-11-2008 10:18:10

as a result, severe osteopetrosis develops. In addition, the development of B cells and T cells is defective in these animals. Likewise, mice bearing mutations or deletions in intracellular signal molecules critically involved in RANK signaling, such as c-Fos [143], c-Jun [144] and NFATc [145], also develop osteopetrosis. Various locally produced cytokines as well as systemic calcitropic hormones — including parathyroid hormone (PTH), 1,25-dihydroxyvitamin D3, and prostaglandins — indirectly stimulate osteoclastogenesis by upregulation of RANKL expression on marrow stromal cells and osteoblasts [139,146,147]. In addition, many cytokines, such as interleukin (IL)-1 and tumor necrosis factor-α, are also able to directly affect osteoclasts [128].

Osteoprotegerin (OPG) was identified as the decoy receptor for RANKL, and is normally present in the BM [139,148]. OPG is a member of the superfamily of tumor necrosis factor receptors and inhibits the differentiation and resorption of osteoclasts *in vitro* and *in vivo* [136,148,149]. The ratio of RANKL to OPG regulates the formation and activity of osteoclasts [150]. Accordingly, OPG-deficient mice display marked osteoporosis [151,152], whereas overproduction of OPG in these mice causes severe osteopetrosis [153].

4.1.1.2 Osteoblasts and Osteocytes

Osteoblasts are the bone-forming cells, responsible for the production of the matrix constituents. They are always found lining the layer of bone matrix that they are producing before it is calcified, referred to as osteoid tissue. Osteoid tissue exists because of a time lag between matrix formation and its subsequent calcification (the osteoid maturation period), which is approximately 10 days [127,154]. Osteoblasts never appear to function individually, and are always found in clusters of cuboidal cells along the bone surface (~100 to 400 cells per bone-forming site). Osteoblasts arise from local mesenchymal stem cells (MSCs), which are precursor cells for many cell types involved in bone formation, such as osteoblasts, osteocytes and chondrocytes, and for other mesenchymal cell lineages, such as fibroblasts, myoblasts, adipocytes, and neuronal cells [155]. For differentiation towards an osteoblast, MSCs first undergo proliferation, become committed and then differentiate into a pre-osteoblast — producing alkaline phosphatase — and subsequently into a mature osteoblast, producing increasing amounts of osteocalcin and calcified matrix [156]. Runt-related transcription factor 2 (Runx2; alias core-binding factor α1) and Osterix are crucial transcription factors that drive the expression of most genes associated with osteoblast differentiation [157,158]. Accordingly, bone does not develop in mice that lack the *Runx2* gene [159,160]. The commitment of MSCs to the osteoblast lineage is regulated by at least three major morphogenetic pathways, the BMP [161,162], the Hh [163], and the Wnt [164] signaling pathway. These pathways can still be influenced and fine-tuned by factors, such as PTH, PTH-related protein (PTHrP), platelet-derived growth factor (PDGF), fibroblast growth factors (FGFs), TGF-β, sex steroids and other hormones (reviewed in [154]). When osteoblasts become embedded in the bone matrix, they differentiate into *osteocytes*, the most abundant cells in

mature bone. Because they can function as mechanosensors, osteocytes are considered to modulate bone remodeling in response to bone loading (reviewed in [127,165]).

4.1.2 Bone Matrix

Bone is composed of an organic matrix that is strengthened by deposits of calcium salts. Type I collagen constitutes approximately 90-95% of the organic bone matrix, whereas noncollagenous proteins comprise the remaining 5-10%. Crystalline salts deposited in the matrix are primarily calcium and phosphate in the form of hydroxyapatite [127]. Noncollagenous proteins can be subdiveded in 1) cell attachment proteins, 2) proteoglycans, 3) γ-carboxylated (gla) proteins, and 4) growth factors (e.g., IGFs, TGF-ßs, FGFs, PDGFs, and BMPs) (reviewed in [166]). Any of the attachment proteins, e.g., osteopontin (OPN), bone sialoprotein (BSP), and vitronectin and collagen type I facilitate interactions with integrins that are expressed by specialized bone and HSC cells as well as osteotropic cancer cells [167,168]. The mineralized bone also stores a variety growth factors, including IGFs, TGF-ßs, FGFs, PDGFs, and BMPs. Since bone continuously remodels, bone-stored growth factors, such as IGFs, TGF-ßs, FGFs, PDGFs, and BMPs [169,170], are constantly released in the BM cavity by osteoclastic bone resorption, affecting growth of bone metastatic cells as will be discussed in detail in paragraph 5: 'Seed-Soil Interactions'. IGF-I is the growth factor that is stored most abundantly in the bone matrix, and upon release, it can play an important role in stimulation of (cancer) cell proliferation and chemotaxis, and inhibition of apoptosis [171]. TGF-ßs and BMPs will be discussed in detail in paragraph 4.4.

4.1.3 Bone Turnover

Adult bone is continuously remodeled by bone resorption and subsequent bone formation in temporary anatomic structures, called the basic multicellular units (BMUs), described by Frost more than forty–years ago [172] (Fig. 4). These two phases are in a balanced sequence and the net result is replacement of old bone with new bone, thus maintaining structural integrity of the skeleton throughout adult life [172-174]. The actual number and activity of these BMUs determine the bone turnover rate (or status) and they are under the control of mechanical stress, cytokines and hormones. Upon resorption, local mitogenic factors, such as TGF-ß, that are embedded within the calcified matrix are released and activated [175]. These local factors, along with the systemic factors PTH, estrogen, and prostaglandin, recruit new osteoblasts at the BMU to fill the gap created by osteoclasts.

4.2 Bone Marrow

Bones are not entirely compact, and the center of the bone generally consists of spongy bone or a bone cavity, which are lined by endosteal cells. These spaces are occupied by red or yellow bone marrow (BM). Red BM facilitates active hematopoiesis, but with increasing age, the rate of hematopoiesis diminishes and more and more of it is converted to yellow BM —

consisting almost entirely of fat cells. However, under appropriate stimuli, such as extreme blood loss, yellow BM can convert to red BM again. In adults, red marrow is found mainly in the spongy bone of flat bones, such as iliac creast and sternum, and in the proximal ends of the long bones femur and humerus. Interestingly, these bones are relatively often affected by cancer metastasis, suggesting that red BM might be somehow involved [2,5].

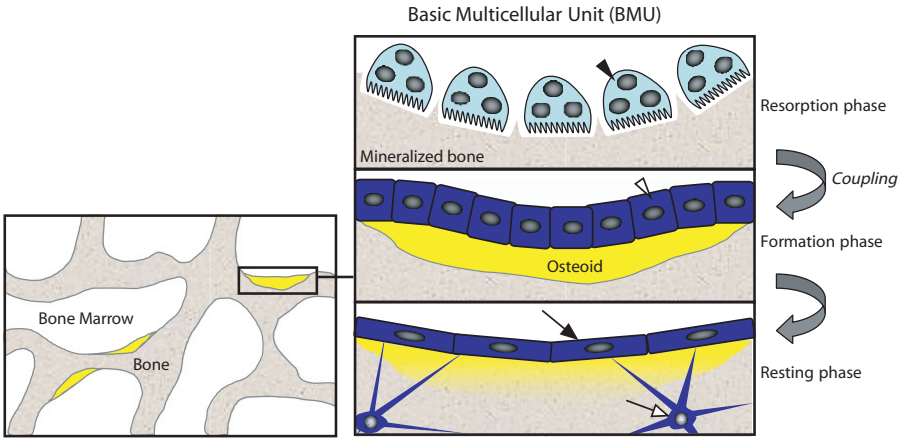

Figure 4 **The basic multicellular unit.** Bone is continuously remodeled by basic multicellular units (BMUs), the temporary anatomic structures that resorb bone and subsequently induce bone formation. Multinucleated osteoclasts (arrowhead) resorb the calcified matrix of a bone trabecula, the *'resorption phase'*. In a tight coupling, pre-osteoblasts migrate and differentiaite into osteoblasts (empty arrowheads). These lay down new bone matrix, which is not yet calcified and is reffered to as osteoid, the *'formation phase'*. Subsequently, the osteoid becomes mineralized. At the end phase of this remodeling, the surface of new bone is covered by flattened osteoblasts or 'lining cells' characterized by low/absent bone forming activity, the *'resting phase'*. Osteoblasts that are trapped in the matrix become osteocytes (arrow with empty arrowhead); others die or form new, flattened osteoblast or 'lining cells' (arrow). The number of BMUs can be modulated by mechanical loading, hormones and cytokines, marrow hematopoiesis and drugs (bone resorption inhibitors); adapted from [344].

Hematopoietic stem cells (HSCs) can reside in BM in two niches, the osteoblastic niche and the vascular niche (reviewed in [176-178]). The osteoblastic niche is formed by endosteal osteoblasts that provide a quiescent environment for HSCs maintenance, support expansion of HSCs into the different hematopoietic lineages, and control HSC numbers [179,180]. In contrast, the vascular niche has been identified in association with fenestrated endothelium of sinusoids, and facilitates HSC transendothelial migration during mobilization or homing, dependent on endothelium-derived factors (Fig. 5) [177,178,181].

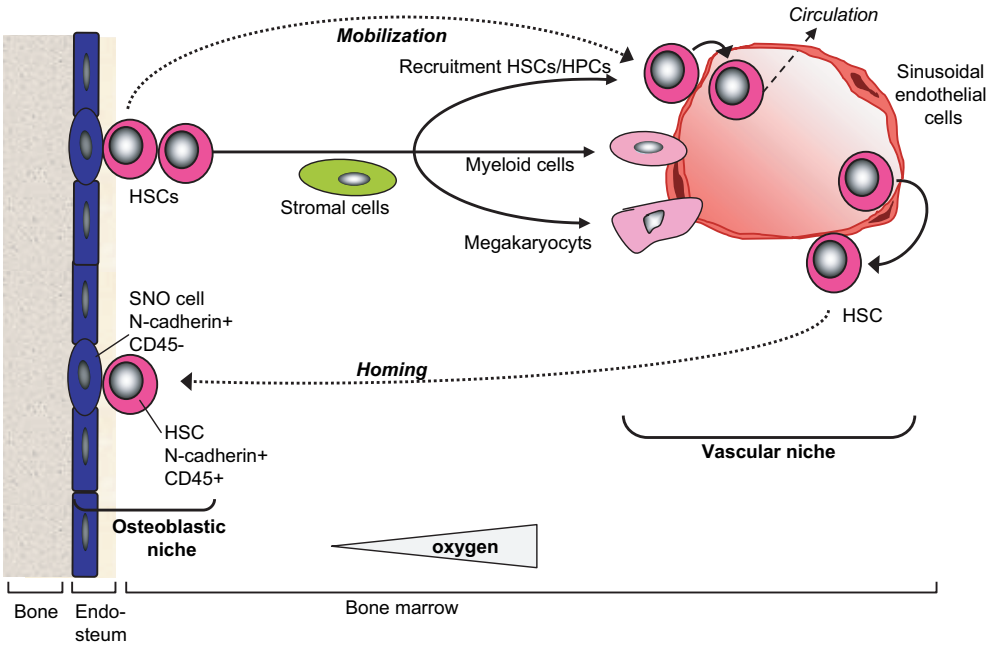

Figure 5 **Osteoblastic and vascular niche in bone.** Under normal physiological conditions, HSCs reside in either the osteoblastic or vascular niche. In response to low levels of SDF-1 in the bone marrow, a portion of HSC daughter cells will leave the bone marrow and begin to mobilize and circulate. HSC homing is the reverse of mobilization, occurring in response to higher levels of SDF-1 in the bone marrow, particularly produced by the immature osteoblasts that align the periosteum. The osteoblastic niche may provide a quiescent microenvironment for HSC maintenance. In contrast, the vascular niche facilitates HSC transendothelial migration during mobilization or homing and may favor HSC proliferation and further differentiation. Higher oxygen concentration gradients as the cells progress from the osteoblastic niche to the vascular niche might play a role in recruitment, proliferation, and differentiation of HSCs/HPCs. Stress such as thrombocytopenia can induce HSCs to enter into the cell cycle, mobilize to the vascular niche, and differentiate. SNO, spindle shaped N-cadherin+ osteoblast; adapted from [178].

Endothelial cells, osteoblasts, and other stromal cells constitutively express the chemoattractive cytokine, or chemokine, SDF-1 (alias CXCL12), while HSCs express its receptor CXCR4 [182]. SDF-1 generated by endothelial cells induces HSCs from the circulation to undergo transendothelial migration mediated by E- and P-selectins [183,184]. Subsequently, HSCs could migrate toward the osteoblastic niche, where HSCs have been shown to adhere only to a subset of immature osteoblasts, the spindle-shaped N-cadherin^{+}CD45^{-} osteoblastic (SNO) cells [180]. Accordingly, an increase of these SNO cells correlated with an increase in HSCs, suggesting that SNO cells function as key components of the osteoblastic niche [180]. Little is presently known about the molecules that define the vascular niche, and its relationship with the osteoblastic niche.

Granulocyte-macrophage colony stimulating factor (GM-CSF, alias CSF2) induces HSC and progenitor cell mobilization and is widely used clinically during stem cell-based transplantation procedures. The mechanism involved is a reduced concentration of SDF-1 in BM, whereas SDF-1 in the peripheral circulation is less affected after GM-CSF treatment [185]. In bone marrow, GM-CSF induces proteolytic enzymes such as elastase, cathepsin G, MMP-2, and MMP-9, which inactivate SDF-1 and are required for cells to penetrate the endothelium [186]. In addition, GM-CSF could regulate SDF-1 expression in osteoblasts at the transcriptional level [187,188].

4.3 TGF-ß Superfamily

The TGF-ß superfamily consists of more than 30 proteins in mammals, including TGF-ßs, activins, BMPs, growth/differentiation factors and anti-Müllerian hormone (Fig. 6). These growth factors, and their antagonists, control many different biological processes such as proliferation, differentiation, apoptosis, and invasiveness in many different epithelial as well as non-epithelial cells [189-192]. In mammals, three isoforms of TGF-ß, i.e., TGF-ß1, TGF-ß2 and TGF-ß3, and more than 20 BMP–related proteins have been identified [193]. In general, TGF-ß isoforms have highly comparable structures and *in vitro* biological activities [194]. In contrast, different BMPs often exert different, and even opposing, effects [161]. Therefore, they should be regarded as individual proteins rather than be classified as a group in respect to cell function.

TGF-ß1 is the most abundant isoform with the largest sources in platelets (20 mg/kg) [195] and bone (200 mg/kg) [196,197]. In comparison, the sources of BMP2, BMP4, and BMP7 in bone are 21 mg/kg, 6 mg/kg, and 84 mg/kg, respectively [170].

The source of TGF-ß/BMPs in the bone/BM microenvironment may be acellular, released by osteoclastic resorption of the extracellular bone matrix, or cellular, derived from cells that reside in bone (e.g., osteoclasts, osteoblasts, and osteocytes) or in bone marrow (e.g., megakaryocytes) (reviewed in [198]).

4.4.1 Signaling Pathways

Members of the TGF-ß superfamily mediate their pleiotropic effects by signaling through transmembrane serine/threonine kinase type I and type II receptors (Fig. 7) [39,193,199]. The type II receptor kinases are constitutively active without ligand stimulation. Upon ligand–induced heteromeric complex formation between type II receptors and type I receptors, type I receptors become phosphorylated by the type II receptors and activate downstream signaling components among which Smad (Sma-Mad related protein) molecules proteins play a pivotal role [193,200]. Unlike other members of the TGF-ß superfamily, BMPs have a higher affinity for the type I receptor, rather than for the type II receptors [201,202]. In mammals, five type II receptors and seven type I receptors have been identified [39,161,203] (Table 2). The type II receptors include activin type II and type IIB receptors (ActRII and ActRIIB), TGF-ß type II receptor (TßRII), BMP type II receptor (BMPRII) and anti-mullerian hormone type II recep-

tor (AMHRII). Type I receptors are termed activin receptor-like kinases (ALKs) 1 through 7. It is theoretically possible to form more than 30 different combinations of type II and type I receptors. However, under physiological conditions the combinations of type II and type I receptors appear to be limited by the variety of ligands that converge at the receptor level.

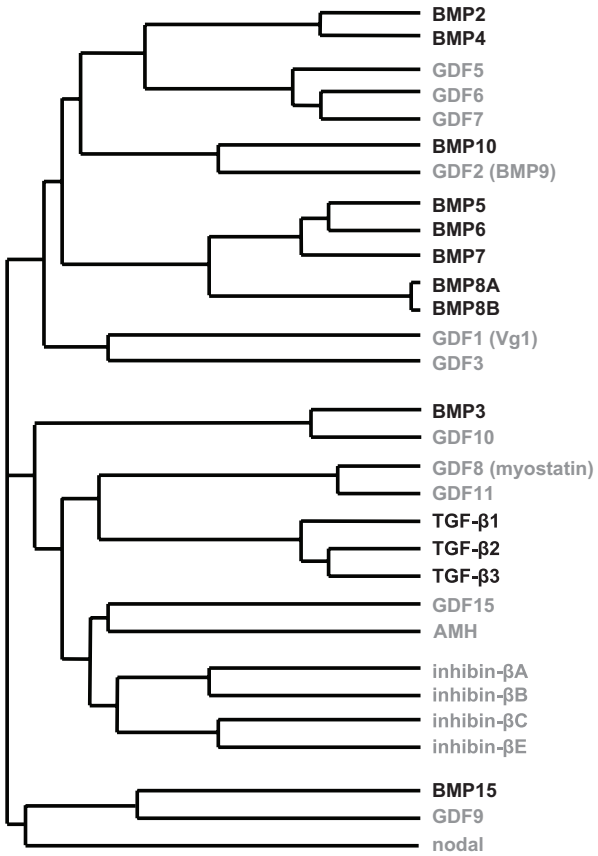

Figure 6 **Phylogenetic tree of TGF-ß superfamily**. The phylogenetic tree is derived from protein alignment of the human, putative mature and fully processed forms. The length of the horizontal lines connecting one sequence to another is proportional to the estimated difference between the proteins. BMPs and TGF-ßs are shown in black, other members of TGF-ß superfamly in grey. AMH, anti-Müllerian hormone; BMP, bone morphogenetic protein; GDF, growth and differentiation factor; TGF-ß, transforming growth factor-ß; based on [415].

In most cell types, ALK5 (TGF-ß type I receptor) is the predominant type I receptor that is activated by TGF-ß through TßRII (Fig. 8) [204]. ALK3 and ALK6 (BMP type IA and IB, respectively) are structurally highly comparable to each other and function as BMP type

Jeroen_Buijs_18.indd 30 26-11-2008 10:18:10

I receptors for BMPs. In addition, BMP6 and BMP7 have also been shown to bind ALK2 [201,205]. Different BMPs bind with different affinity to the type I receptors, e.g., BMP6 and BMP7 binds with higher affinity to ALK2 and ALK6 than to ALK3 [201,206] (Fig. 8). The expression of ALK3, ALK6 and BMPRII was observed in normal and benign prostate tissue, and was found to correlate with low tumor grade (well-differentiated) in prostate cancer. In addition, loss of BMPRII expression correlated with poor prognosis in prostate cancer patients [207,208].

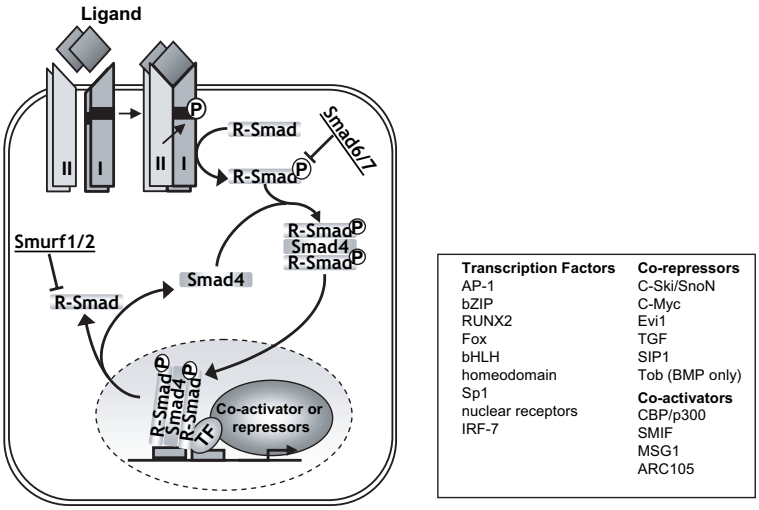

Figure 7 **General Mechanisms of TGF-ß/BMP-induced Smad activation.** At the cell surface, a ligand (homo- or heterodimer) binds a complex of transmembrane receptor serine/threonine kinases (types I and II) and induces transphosphorylation of the GS segments (black) in the type I receptor by the type II receptor kinases. The consequently activated type I receptors phosphorylate selected Smads at C-terminal serines, and these receptor-activated Smads (R-Smads) then form a complex with the common Smad, Smad4. Activated Smad complexes translocate into the nucleus, where they regulate transcription of target genes, through physical interaction and functional cooperation with DNA-binding transcription factors (TF) and coactivators or repressors. Activation of R-Smads by type I receptor kinases is inhibited by Smad6 or Smad7. The E3 ubiquitin ligases Smurf1 and Smurf2 mediate ubiquitination and consequent degradation of R-Smads; based on [199].

Table 2 **Type I and II receptors for TGF-ß superfamily members in mammals.** Alk, activin receptor-like kinase; ActRII and ActRIIB, activin type II and IIB receptors; TßRII, TGF-ß type II receptor; BMPRII, BMP type II receptor.

Type I receptor	*alias*	Type II receptor
Alk1		BMPRII
Alk2	ActR1A	ActRII
Alk3	BMPR1A	ActRIIB
Alk4	ActR1B	TßRII
Alk5	TßR1	AMHRII
Alk6	BMPR1B	
Alk7		

Besides the signaling type I and type II receptor, several accessory type III receptors, are known, e.g., betaglycan (TβRIII) [209] and endoglin (CD105) [210]. While endoglin inhibits TGF-ß1-induced ALK5–Smad3 signaling, it promotes BMP7–Smad1/Smad5 signaling [211,212]. On the other hand, betaglycan acts as a co-receptor for TGF-ß that modulates the binding of TGF-ß to its receptors, thus enhancing signaling via ALK5 [213]. Moreover, it can also function as a co-receptor for inhibin, disrupting activin and BMP signaling [214].

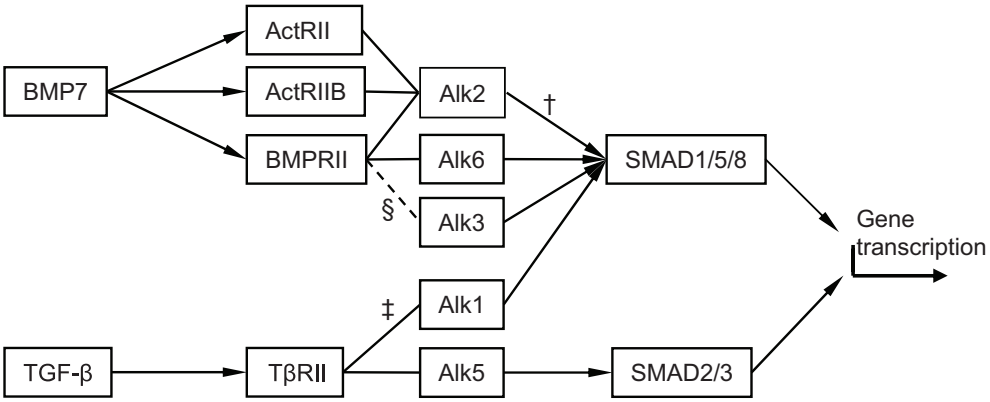

Figure 8 **Type I and II receptors, and R-Smads involved in BMP7 and TGF-ß signaling.** It is important to note that the presence of particular type I and II receptors, and R-Smads greatly differs in various cell types. † = activates only SMAD1 and -5, but not -8; § = BMP7 binds with low affinity to BMPRII/Alk3 complex; ‡ = pathway known in endothelial, but not epithelial, cells. Alk, activin receptor-like kinase; ActRII and ActRIIB, activin type II and IIB receptors; TßRII, TGF-ß type II receptor; BMPRII, BMP type II receptor; based on data from [201,205,416-419].

Smads, which are intra-cellular substrates for the TGF-ß superfamily receptors can be subdivided into: 1) receptor-activated Smads (R-Smads) which include Smad2 and Smad3 for TGF-ß and activin signaling, and Smad1, Smad5, and Smad8 for BMP signaling, 2) the common mediator Smad (Co-Smad), commonly refeered to as Smad4, and 3) inhibitory Smads (I-Smads), which include Smad6 and Smad7 [39,193]. R-Smads contain a conserved SSXS phosphorylation motif in their very C-termini, of which the last two serine residues become phosphorylated following interaction with activated type I receptors [39]. Phosphorylation of R-Smads results in their heteromerization with Smad4 followed by nuclear translocation and regulation of gene transcription in association with other transcription factors [161,200].

Smads are not equally activated by their cognate receptors. For example, ALK3 and ALK6 activate all three BMP R-Smads, whereas ALK2 can activate only Smad1 and Smad5, but not Smad8 [205,206]. Although Smad2 and Smad3 are structurally very similar to each other, Smad3 can directly bind DNA, whereas Smad2 signaling requires a specific combination of other transcription factors [215]. In fibroblasts, TGF-ß-mediated induction of matrix metalloproteinase-2 (MMP-2) was selectively dependent on Smad2, whereas induction of c-fos,

Jeroen_Buijs_18.indd 32 26-11-2008 10:18:10

Smad7, and TGF-ß1 autoinduction relied on expression of Smad3 [216]. Moreover, in tubular epithelial cells it was found that TGF-ß-induced increases in CTGF and decreases in E-cadherin expression were Smad3-dependent, whereas an increase in MMP-2 expression was Smad2–dependent [217]. In NMuMG mammary epithelial cells it was reported that complexes of Smad4 with both Smad2 or Smad3 can induce full EMT, however, the Smad3–Smad4 complex was most efficient [36]

Non-Smad pathways may also play an important role in understanding the diversity of signals generated by the TGF-ß superfamily proteins. MAP (mitogen-activated protein) kinases, including ERK (extracellular-signal-related kinase), JNK (JunN-terminal kinase), and p38MAPK, can, among many other growth factors, also be activated by BMPs and TGF-ßs in certain cell types. Moreover, signaling by Smads is modulated by various other signaling pathways allowing TGF-ß superfamily ligands to elicit different biological responses in target cells (reviewed in [193,199,200]).

4.4.2 Regulation of Activity

The level of activity of the TGF-ß superfamily members is determined by the regulation of 1) bioavailability and 2) cellular signaling.

The bioavailability of TGF-ß superfamily members is regulated by several types of mechanism, including proteolytic processing, secretion, interaction with ECM components, and extracellular binding proteins, and each step in the activation pathway is tightly controlled. For TGF-ß and BMP7 post-translational processing is shown in figure 9 [198,218-222]. During transit through the rough endoplasmic reticulum, the signal peptide is removed from the pre-pro-protein and, following dimerization, another cleavage occurs by the convertase family of endoproteases [219]. Within the secretory vesicles or in the extracellular space, these proteases cleave the precursor into a C-terminal mature peptide and an N-terminal precursor remnant, referred to as latency associated peptide (LAP) for TGF-ß, and prodomain for BMP7. Thus control and/or localization of convertase activity may represent an important level of regulation. After cleavage, mature TGF-ß and LAP remain attached via non-covalent bonds to form the small latent complex (SLC). LAP shields the receptor interacting epitopes in the mature protein and this keeps TGF-ß in its latent form [223]. The SLC can covalently attach to the large latent TGF-ß-binding protein (LTBP) to form the large latent complex (LLC) [224,225]. Most cell types secrete TGF-ß as part of LLC, although some cells (such as the bone cell line UMR-106) secrete SLC [226]. Four different LTPBs have been identified, of which LTBP1, LTBP3 and, to a lesser degree, LTBP4 covalently bind to LAPs of all three TGF-ß isoforms [227]. After secretion, LLC is targeted to ECM molecules, e.g., in the bone matrix. LTBP show remarkable homology with fibrillins, which are extracellular glycoproteins that are required for elastic fiber formation. Besides binding to ECM molecules, the C-terminal region of LTBP1 can also bind to the N-terminal region of fibrillin-1, linking LLC also to elastic microfibrils [228].

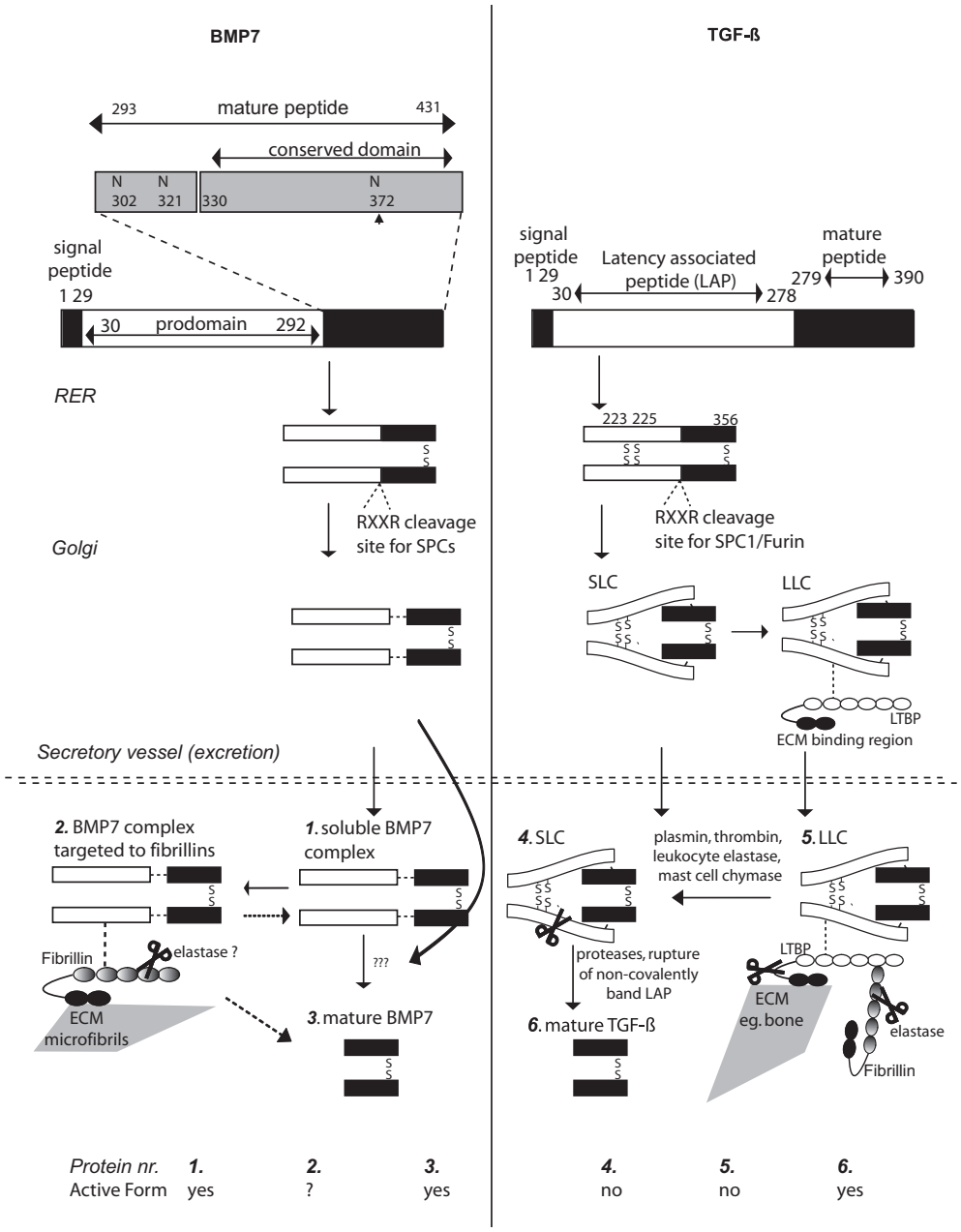

Figure 9 **TGF-ß and BMP7 posttranslational processing.** The mature BMP7 has three potential N-linked glycosylation sites, from which only the glycosylation sites at residue 372 in the TGF-ß conserved domain region is heavily or completely glycosylated (*top of figure:* arrowhead). The signal peptide, which targets the proteins to the secretory pathway, is cleaved off during transit through the *rough endoplasmatic*

Jeroen_Buijs_18.indd 34 26-11-2008 10:18:11

reticulum (RER). Subsequently, two monomers dimerize by way of disulfide bridges between cysteine residues. The protein is cleaved by subtilisin-like proprotein convertases (SPCs) at the RXXR motif. This yields the prodomain, or latency associated protein for TGF-ß, and the mature peptide. This mature petide stays noncovalently associated with its prodomain, forming the soluble BMP7 complex for BMP7 or the small latent complex (SLC) for TGF-ß. The noncovalent association prevents the premature activation of mature TGF-ß. The SLC can become covalently attached to a Large Latent Binding Protein (LTBP) to form the Large Latent Complex (LLC), and the SLC to LLC ratio depends on the cell type. After its secretion, the LLC is directed to fibrillin-1 and/or the ECM and stored through binding of the LTBP with these components. Inflammatory proteolytic enzymes, including elastase, release LLC from fibrillin-1, and Several proteases, such as plasmin, mast-cell chymase and thrombin, release LLC from the ECM. The SLC is more readily available for activation, and can be activated by proteases or conformational change in the LAP induced by interaction with, e.g., thrombospondin or integrins. The pro-domain of BMP7 targets the soluble BMP7 complex to the fibrilin-1 and -2 in the extracellular matrix. The precise mechanisms of posttranslational processing are less well understood for BMP7 and remains to be elucidated. Based on data from [219-221] (BMP7) and [198,222] (TGF-ß).

In order to exhibit their biological activity, the latent TGF-ß complexes need to be released from microfibrils and ECM. A recent study revealed that LLC release can be initiated by the displacement of LTBP bound to fibrillin-1 [218]. Degradation of microfibrils by inflammatory proteolytic enzymes (such as elastase) releases fragments of fibrillin-1, including an internal fibrillin fragment that efficiently binds to the N-terminal region of fibrillin-1 and displaces LTBP, releasing LLC from microfibrils [218]. The release of LLC from the ECM in bone and other tissue is mediated by several proteases, including plasmin, mast-cell chymase and thrombin (reviewed in [198,222]).

Subsequently, the truncated LLC and SLC can be subjected to three different mechanisms of *in vivo* activation: 1) degradation of the latency-associated peptide (LAP) by proteases, 2) induction of a conformational change in the LAP, e.g., by interaction with integrins and thrombospondin, and 3) rupture of the noncovalent bonds between LAP and mature TGF-ß [223]. In contrast, the soluble BMP7 complex — consisting of the mature peptide and its noncovalently associated prodomain — is already active, and is targeted to fibrillin-1 and -2 [220]. Therefore, it may be that proteases, such as elastases, are critically involved in the release of the soluble BMP7 complex from the elastic microfibers. However, the precise mechanisms of post-translational processing, secretion and interaction with ECM components are less well understood for BMP7 and remain to be elucidated.

In contrast, extracellular BMP antagonists are relatively well-studied secreted peptides that bind BMPs with high affinity and prevent their interaction with their cognate receptors. These antagonists can be categorized into subgroups, i.e., noggin [229], twisted gastrulation protein [230], the chordin family [231], and the DAN family [232].

TGF-ß/BMP signaling is limited by 1) dominant negative non-signaling membrane pseudoreceptors, 2) I-Smads, 3) ubiquitination and proteasomal degradation of signaling effec-

tors, 4) corepressors, and 5) phoshorylation of the linker region of R-Smads (reviewed in [233,234]). Many of the negative regulators involved are potently induced by BMP/TGF-ß signaling, and may thus participate in a negative feedback loop to control the intensity and duration of TGF-ß signaling [235-239]. The pseudoreceptor BAMBI (BMP and activin membrane-bound inhibitor) is a truncated, kinase-deficient, type I receptor that binds to ligand competitively and thereby inhibits BMP and TGF-ß signaling [240].

The I-Smads, Smad6 [237,241] and Smad7 [242], inhibit signal transduction by interference with the activation of R-Smads and prevention of heterodimerization between R-Smads and Smad4. In addition, I-Smads can also interact with type I receptors through Smurfs (Smad ubiquitin regulatory factors), inducing ubiquitination and degradation of the activated receptor complexes [244-247]. The Smurf1/2–Smad7 complexes play an important role in regulating ubiquitination of TGF-ß receptor complexes [248-250], Smurf1–Smad6/7 complexes appear to target BMP receptor complexes for degradation [247]. So, whereas Smad7 acts as a general inhibitor of TGF-ß superfamily member signaling pathway (BMP and TGF-ß), Smad6 preferentially blocks BMP signaling [236,237,241-243].

TGIF (TGF-ß-induced factor) is a transcriptional corepressor, i.e., a Smad binding protein that interferes with the ability of Smads to bind coactivators. It binds Smad2 and -3, thereby preventing the interaction of Smads with coactivators, resulting in reduced target gene expression. The competition for Smad binding between coactivators and corepressors determines the magnitude of the transcriptional output from a given level of signaling. Sloan-Kettering retrovirus (Ski) and and its relative Ski-related novel gene N (SnoN) [251,252] are also corepressors, which suppress Smad signaling by associating with the MH2 binding domain of Smads. Both Ski and SnoN bind Smad2 and -3, thereby inhibiting TGF-ß signaling [238,251-254]. In addition, Ski, but not SnoN, can also interact with Smad1 and -5 and antagonize BMP signaling [251,255-257]. By interacting with Smad1, -5, -6, -7, and -8, the transducer of ErbB-2 (Tob) also represses BMP signaling [258,259].

Inhibition of the Smad pathway can also occur via growth factor induced phosphorylation of the linker region of R-Smads, reducing ligand-induced nuclear accumulation of R-Smads. Acivation of Erk by EGF and HGF, or activated Ras can induce this phosphorylation [260-262].

4.4.3 Physiologic and Pathophysiologic Functions

BMPs are paradigmatic molecules directly regulating osteoblast generation and were first identified by their ability to form new bone *in vivo* (reviewed in [161,263]). They play a crucial role in skeletal and joint morphogenesis, bone remodeling, and fracture repair by inducing proliferation, lineage determination, differentiation, and apoptosis in chondrocyte and osteoblast precursors [203,264]. Subsequently, they were shown to act as multifunctional regulators of embryonic patterning and organogenesis, tissue remodeling, and repair [265].

BMPs have also been implicated in cancer development. Elevated levels of BMP6 are associated with higher grade primary tumors and advanced prostate cancer with metasta-

Jeroen_Buijs_18.indd 36 26-11-2008 10:18:11

sis [266,267], and BMP2 induces migration and invasion in breast [268] and prostate [269-271] cancer cells. BMP7 regulates multiple cellular processes including cell proliferation, migration, and apoptosis. In cells from the osteoblast lineage, exogenous addition of BMP7 can result in inhibition or stimulation of cell proliferation, totally dependent on the cell line type [272,273]. In PC-3 and DU 145 prostate cancer cells, BMP7 inhibited cell proliferation by arresting cells in G1 phase via up-regulation of the cyclin-dependent kinase (Cdk)-inhibitors. However, in C4-2B prostate cancer cells, BMP7 promotes cell survival by inhibiting stress-induced apoptosis via both the Smad/survivin and c-jun NH2-terminal kinase pathways [274].

Yet a different function for BMP signaling was demonstrated when Zhang and co-workers demonstrated that conditional deletion of ALK3 (BMPRIA) lead to increased numbers of SNO cells and subsequently to higher HSC numbers. Thus BMP signaling via ALK3 complex controls the number of HSCs by regulating the niche size [180].

TGF-ß is a potent growth inhibitor in normal and non-malignant epithelial cells [32,33]. However, different types of carcinomas often escape this tumor-suppressing activity and become refractile to growth inhibition [33,111,275]. In fact, TGF-ß can potentiate tumorigenesis and contribute to the progression and invasiveness of various carcinomas by inducing EMT [34-38]. Accordingly, it has been shown that a blockade of TGF-ß (signaling) inhibits tumor cell viability, migration, and metastasis [276-279]. Moreover, TGF-ß stimulates the PTHrP production in metastatic cancer cells, thereby being an important mediator in lytic bone destruction (as discussed in more detail in the paragraph 5.2.1, 'Osteolytic Bone Metastasis').

Although some BMPs, such as BMP2 [280] and BMP4 [281], have also been shown to induce an EMT in certain cell types under specific conditions, the homodimeric protein BMP7 can induce the opposite, a mesenchymal-to-epithelial transition (MET) in normal and non-transformed cells [192,282]. For instance, during kidney development, BMP7 is essential for the condensation and epithelialization of the metanephric mesenchyme in the kidney, resulting in the formation of the tubular epithelium [95,96,98]. In the adult kidney, BMP7 appears to be involved in the preservation of the epithelial phenotype of renal tubular cells [283], and inhibition of fibrosis [284,285] and inflammation [286,287]. Moreover, BMP7 treatment partly inhibited the pathologic effects in experimentally induced acute [287] and chronic [284,288,289] kidney disease, including its complications renal osteodystrophy [290,291] and vascular calcification [292]. In clinical practice, BMP7 is used as an osteoinductive agent in treatment of non-union fractures [293].

5 'Seed–Soil' Interactions

The establishment of a metastasis is dependent on the reciprocal interactions between cancer cells and the microenvironment. In order to form an overt bone metastasis, cancer cells first have to extravasate into, colonize and then grow in, the BM. Thus, the first interaction between the 'seed' and the 'soil', is when circulating cancer cell in blood interact with the endothelium of a specific tissue [294]. In most tissues, the endothelium differs in surface

markers, morphological phenotype and specialized functions [295], and is still susceptible to further modification by specific stimuli, such as inflammation. The specific combination of chemoattractive and adhesion molecules on the endothelium in the BM has been demonstrated to be particularly favorable for the retention and extravasation of circulating cancer cells [294].

As discussed in paragrapgh 4.2, BM endothelium-derived SDF-1 induces CXCR-4 expressing HSCs to undergo transendothelial migration mediated by E- and P-selectins [183,184]. Similarly, metastatic prostate cancer cells that adhere specifically to BM endothelial cells have also been reported to make use of E-selectin ligands for entry into BM [296-298]. Moreovcer, the chemokine receptors CXCR4 and CCR7 are also expressed by a variety of osteotropic epithelial cancer cell types [298-301], also mediating their adhesion to BM endothelium.

OPN, BSP, and type I collagen are major components of mineralized bone. These proteins mediate local adhesion, motility, survival and growth by interactions with matrix adhesion molecules, namely integrins, and are expressed by several types of cells, including HSCs. Similarly, cancer cell adhesion to OPN, BSP and type I collagen is also integrin-dependent [167,168]. So, integrin expression may not only be critical for guiding HSC to hematopoietic sites, but also for BM colonization by cancer cells [302]. Mainly the αvß3 (alias vitronectin receptor) and αIIbß3 integrins seem to participate in determining the osteotropism of cancer cells [303-306]. Accordingly, the MDA-MB-231-BO2 breast cancer cell line, which is a subclone of MDA-MB-231 (MDA-231), constitutively overexpresses αvß3 integrin and only metastasizes to bone [307]. Similarly, *de novo* expression of αvß3 integrin in 66cl4 breast cancer and CHO ovarian cancer cells that metastasize to lungs, but not to bone, is sufficient to promote their dissemination to bone [307,308]. Moreover, αvß3 integrin was shown to cooperate with BSP, MMP-2 and -9 in promoting osteotropic cancer cell invasion [309,310]. CD44 is a non-integrin, ubiquitous and multifunctional surface adhesion molecule, which has been identified as a receptor for both the glycosaminoglycan hyaluronan and OPN. It is expressed by various cancer cell types and has a well-established role in skeletal metastasis [311]. Taken together, the bone/BM microenvironment is able to actively allow circulating cancer cells to preferentially arrest in, extravasate into, and colonize BM, adopting similar pathways that are used by the homing of normal HSC to the bone/BM microenvironment [312].

Besides high affinity for bone matrix, breast and prostate cancer cells can also produce bone matrix proteins such as OPN, osteonectin [313], and BSP [314]. This acquisition of bone cell-like properties by tumor cells, is called *osteomimicry* [313,315,316], and improves homing, adhesion, proliferation, and survival in the bone/BM microenvironment.

According to the 'Seed and Soil' hypothesis, interaction between tumor cells and the microenvironment is supposed to occur only after tumor cells reach the microenvironment. However, this classical 'Seed and Soil' hypothesis appears to be too simplistic, since the recent discovery of the so-called *pre-metastatic niche* (PMN) [317]. Kaplan and co-workers showed that VEGFR1$^+$ BM-derived hematopoietic progenitor cells (HPCs) were mobilized by

Jeroen_Buijs_18.indd 38 26-11-2008 10:18:11

factors secreted from primary tumors (melanoma and lung carcinoma) to form fibronectin-rich patches in (non-bone) target organs. Remarkably, these niches are formed prior to the arrival of metastatic tumor cells. Blocking the PMN formation by VEGFR1 antibodies significantly inhibited metastasis. Strikingly, the PMN was shown to dictate the metastatic pattern, since conditioned media from a melanoma cell line could redirect lung carcinoma cells to metastatic sites that are favored by melanoma, but not lung cancer. Two cytokines produced by primary tumors, VEGF and placental growth factor (PlGF), were suggested to mediate the formation of the PMN, although additional chemokines or growth factors are certainly necessary to facilitate different organ-specific metastasis [317,318]. In summary, the PMN-model indicates that long range communication between tumor cells and target organs can occur before the arrival of tumor cells at distant sites. Understanding the molecular mechanisms involved in the formation and maintenance of PMNs and normal HSC niches (osteoblastic and vascular) and their role in supporting organ-specific metastasis may provide new approaches for developing novel treatment strategies. However, it remains to be investigated whether the PMN-model is also applicable to other types of cancer, including breast and prostate cancer.

5.1 Bone Turnover and Skeletal Metastasis

The rate of bone turnover is closely associated with the number of sites with increased paracrine availability of growth factors due to osteoclastic bone resorption, and, accordingly, the probability that the cancer cell (the 'seed') will find a favorable 'soil' in the bone/BM environment. The latter part of this hypothesis is based on experimental studies, which have shown that the rate of bone turnover is associated to the occurrence and progression of bone metastases indicating that the growth support provided by the bone microenvironment is active during bone resorption [319-321] (see 'Osteolytic Bone Metastasis'). Recently, this view was further substantiated by clinical studies, showing a strong and highly significant association between the rate of bone resorption and incidence of subsequent skeletal complications in breast and prostate cancer patients [322-325].

Serum alkaline phosphatase (sALP) and urinary hydroxyproline are common and non-expensive markers of bone formation and bone resorption, respectively. They are useful tools for assessing the overall bone turnover rate in cancer patients at risk to develop bone metastasis. Recently, more sensitive and specific biochemical markers have become available. Immunoassays for bone-specific alkaline phosphatase and type I collagen propeptides are currently the most sensitive markers for assessing bone formation. Best indices of bone resorption are the immunoassay for the pyridinoline cross-links and the related peptides that can be measured in urine and serum [326]. These markers for bone turnover may be useful in planning the rational use of preventive treatment with bone resorption inhibitors as will be discussed in more detail in paragraph 7, 'Treatment of Bone Metastasis'.

5.2 Bone Metastatic Phenotype

Whereas prostate cancer predominantly elicits an osteoblastic response resulting in osteosclerotic lesions, breast, lung and kidney cancer preferentially trigger an osteoclastic reaction mainly resulting in osteolytic lesions (reviewed in [18,22]). Although an osteolytic lesion is dominantly destructive, there is usually also a local bone formation response, which presumably represents an attempt at bone repair. Moreover, up to 25% of patients with bone metastases from breast cancer also have blastic lesions that are similar in appearance to those from patients with metastatic prostate cancer, and vice versa, some prostate cancer patients have osteolytic lesions that are similar in nature to those seen in patients with metastatic breast cancer. In other words, the common concept that there are basically two types of bone metastases, should rather be replaced by a view that the type of lesion is the result from a (dis)balance between anabolic and catabolic factors.

With regard to bone integrity, bone regions affected by either osteolytic or osteosclerotic lesions are both more prone to pathological fractures due to architectural distortion and deposition of bone of the woven (immature or embryonic) type, which is much less mechanically competent than the lamellar (mature) type.

An increase in the RANKL to OPG ratio is one of the major determinants of an osteolytic phenotype, and vice versa, a decrease in the ratio is a major determinant of an osteoblastic phenotype (reviewed in [146,327]).

5.2.1 Osteolytic Bone Metastasis

In osteolytic bone metastases, the destruction of bone is mediated by osteoclasts, as could histologically be observed by the numerous osteoclasts eroding the relatively scarce bone matrix [328,329].

PTHrP is regarded as the main mediator of osteoclast activation in bone metastatic breast cancer [18,20]. PTHrP induces RANKL and downregulates OPG in cells of the osteoblast lineage [330]. It is produced by most solid osteotropic cancers [331,332], and plays a major role in the development of the osteolytic features of their bone metastatic lesions [333]. Furthermore, PTHrP is considered to be responsible for the humoral hypercalcemia of malignancy (reviewed in [20]). In breast cancer 90% of metastases in bone were found to express PTHrP, compared to only 17% at non-bone sites and 60% of the primary tumors [331,334]. Initially, expression of PTHrP in the primary tumor appeared to be associated with formation of bone metastases [335,336]. However, a large prospective study of 526 consecutive patients with operable breast cancer demonstrated the opposite, PTHrP expression in primary breast cancer was significantly associated with fewer (bone) metastases [337,338]. Therefore, the most likely explanation for the observed increased PTHrP expression in bone metastases [334,339], is that the bone microenvironment induces cancer cells to express PTHrP rather than cancer cells that metastasize to the bone have an intrinsically higher PTHrP expression.

The hypothesis that PTHrP is induced by the bone microenvironment is also substantiated

Jeroen_Buijs_18.indd 40 26-11-2008 10:18:11

by experimental evidence from Yin and co-workers demonstrating that PTHrP production in MDA-231 breast cancer cells was stimulated by TGF-ß [340]. Accordingly, introduction of a TßRII lacking a cytoplasmic domain (TßRIIDcyt) that exhibited dominant-negative effects into these cells prevented an increase in PTHrP production in response to TGF-ß. Moreover, in an experimental model of bone metastasis (see paragraph 6, 'Animal Models of Bone Metastasis'), mice receiving MDA-231 cells lacking TGF-ß signaling had fewer and smaller osteolytic lesions than mice inoculated with parental or empty vector-transfected cells. Taken together, PTHrP increases osteoclastic bone resorption with consequent release and activation of matrix-integrated growth factors, especially TGF-ß and IGFs, stimulating both tumor growth and further secretion of PTHrP, thus establishing a 'vicious cycle' (Fig. 10).

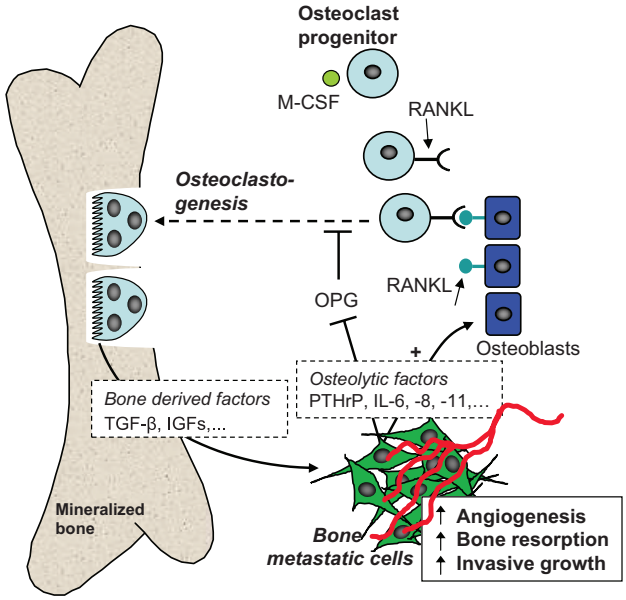

Figure 10 **The vicious cycle of the osteolytic bone metastasis.** Release of osteolytic factors, such as parathyroid hormone-related protein (PTHrP), by bone metastatic breast cancer cells causes nearby osteoblasts to change the mix of signals that they release: they increase RANKL synthesis. RANKL induces osteoclast precursors to mature into functional osteoclasts. The latter undertakes osteolysis, which causes bone demineralization, exposes the extracellular matrix within the bone, and results in liberation of various growth factors, including TGF-ß, IGFs, BMPs, PDGF. These growth factors cause cancer cell proliferation and survival, and the additional presence of TGF-ß stimulates production of PTHrP by the cancer cell, resulting in a self-sustaining positive-feedback loop that has been termed the 'vicious cycle' of osteolytic metastasis.

In addition to PTHrP, RANKL expression on osteoblasts/stromal cells can be upregulated by many other tumor secreted factors such as IL-1, IL-6, IL-8, IL-11, and tumor necrosis factor (TNF)-α. In addition, these osteolytic factors are also capable of modulating osteoclas-

togenesis independent of RANKL (reviewed in [341]). For example, IL-8 was shown to directly bind to CXCR1 present on osteoclast precursors [342]. More recently, the intra-cellular component NF-κB was demonstrated to play a crucial role in osteolytic bone metastases from breast cancer [343]. GM-CSF (alias CSF-2) was identified as the key target of NF-κB that mediates osteolytic bone metastasis of breast cancer by stimulating osteoclast development, thereby identifying new potential targets for prevention and treatment of skeletal metastasis from breast cancer.

The concept of the 'vicious cycle', in which cancer cells express osteolytic factors under influence of growth factors that are released from the bone matrix, has important therapeutic consequences: inhibition of bone resorption may interrupt this vicious cycle and thus may preserve bone mass, prevent pathological bone fractures, and even arrest tumor progression in the bone metastasis.

5.2.2 Osteosclerotic Bone Metastasis

Compared to osteolytic bone metastasis, mechanisms determining the exaggerated response in osteosclerotic bone metastasis are still poorly understood. It is believed that the excess production of mineralized bone matrix adjacent to the metastatic tumor cell deposit is due to an increased secretion of factors inducing proliferation, differentiation, and recruitment of osteoblast progenitors by the metastatic cancer cells (Fig. 11) (reviewed in [18,21,22,344]). Nonetheless, markers of bone resorption are also increased in metastatic prostate cancer, accurately reflecting the extent of disease progession [322-325,345]. In fact, bone resorption markers are even more elevated than in patients suffering from lesions from breast cancer [325], providing the rationale for treatment with bone resorption inhibitors, such as bisphosphonates, in prostate cancer patients (see paragrapgh 7.1.1, 'Bone Resorption Inhibitors').

BMPs are paradigmatic molecules that directly regulate osteoblast proliferation and differentiation (reviewed in [263]). Both normal and neoplastic human prostate tissue have been shown to express a variety of BMPs, namely BMP2, BMP3, BMP4, BMP6, and BMP7 [346]. Therefore, BMPs have been postulated to play an important role in the etiology of the osteoblastic phenotype of bone metastasis. Indeed, prostate cancer secreted BMPs in culture media were shown to promote mineralization *in vitro* (potency from high to low: BMP6 > BMP7 > BMP4) [347]. Moreover, forced overexpression of noggin — a BMP2, -4, -6, and -7 antagonist — in osteoinductive cell lines abrogated the osteoblastic response *in vivo* [270,348], however, tumor progression was not significantly affected [270,348]. Direct experimental evidence that a specific BMP could affect the osteoblastic response was provided by using neutralizing BMP6 antibodies, which inhibited the blastic response [269].

Prostate and breast cancer cells express a variety of Wnt proteins, which can enhance bone mass [349]. Interestingly, in breast cancer and myeloma — characterized by osteolytic lesions with suppression of osteoblastic activity — Wnt signaling is inhibited by the extra-

Jeroen_Buijs_18.indd 42 26-11-2008 10:18:11

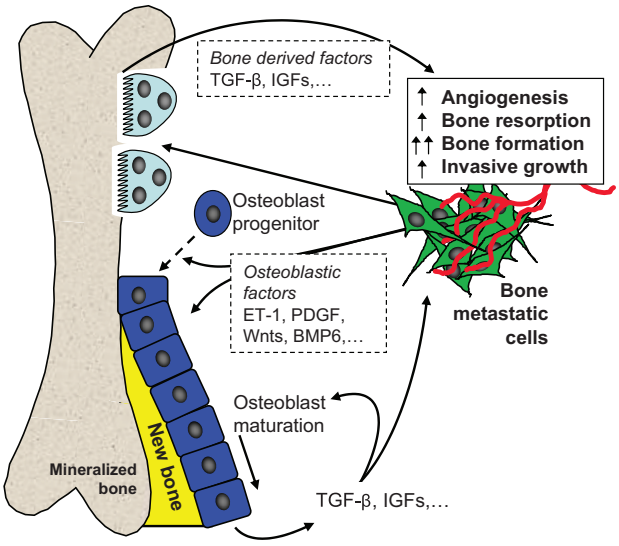

Figure 11 Pathophysiology of osteosclerotic bone metastasis. Release of endothelin (ET-1) and different Wnts by bone metastatic prostate cancer cells causes nearby osteoblasts progenitors to differentiate into osteoblasts. Mature osteoblasts also secrete growth factors such as TGF-ß that may stimulate bone metastatic growth. Therefore, a 'vicious cycle' is also considered to occur in osteoblastic metastasis.

cellular Wnt-antagonist dickkopf (DKK-1) expressed by the tumor cells [348,350,351]. Moreover, *in vitro* differential expression analysis in breast and prostate cancer cell lines showed that the expression of the Wnt and BMP antagonists, DKK-1 and noggin, respectively, rather than expression of Wnts and BMPs determines the manifestation (blastic/lytic) of the bone metastasis [348].

Other factors that have also been implicated as direct stimulators of osteoblast recruitment, proliferation, and differentiation in osteosclerotic bone metastases are IGF-I and -II, FGF-1 and -2, VEGF, platelet derived growth factor (PDGF-BB), and TGF-ß [346,349,352].

Prostate cancer patients with osteoblastic metastases have high serum levels of endothelin-1 (ET-1) [353]. Besides being a potent vasoconstrictor, ET-1 is also a direct mitogen for osteoblast progenitors [354]. A causative role for ET-1 in the pathophysiology of osteosclerotic bone metastasis has been demonstrated in pre-clinical models from prostate [354,355] and breast cancer [356]. The inhibition of bone metastatic but not primary tumor growth by treatment with ET-1-selective receptor antagonists in pre-clinical models suggests that a vicious cycle may also occur in osteoblastic metastasis [356].

In addition to factors that directly affect osteoblasts, prostate cancer cells also produce factors that indirectly affect osteoblast function by modifying the bone microenvironment, such as VEGF, and the proteases urokinase-type plasminogen activator (uPA) and prostate-specific antigen (PSA) [352]. uPA stimulates osteoblast proliferation, probably by hydrolyzing IGF-binding proteins and thereby increasing free IGF levels [357]. PSA is a serine protease of

the kallikrein family and a well-known marker of prostate cancer progression. It can cleave IGF-binding protein (IGFBP)-3, thereby reducing the ability of IGFBP-3 to antagonize the effects of IGF-I [358]. In addition, PSA can cleave PTHrP, thus allowing the osteoblastic reaction to predominate by decreasing bone resorption [359].

In conclusion, tumor cells (the 'seeds') can accomplish metastases only in the organs where the microenvironment (the 'soil') is permissive for their growth, i.e., reciprocal interaction between the bone/BM microenvironment and cancer cells is fundamental for establishing bone metastatic growth. Subsequently, the reciprocal interaction can result in exaggarated stimulation of bone degradation and/or formation, ultimately determining the bone metastatic phenotype.

6 Animal Models of Bone Metastasis

In clinical studies, the possibility to manipulate different variables is, obviously, very limited. Therefore, animal models have become important tools to investigate the pathogenesis of bone metastasis as well as to develop novel therapeutic strategies. In general, the incidence of bone metastases from spontaneous breast and prostate cancer in rodents and non-human primates is extremely rare. So, bone metastases in animal models need to be induced experimentally. These include syngeneic transplantation of spontaneously occurring rodent cancers and xenograft models with tumors or cell lines derived from human cancers into immunodeficient rodents (e.g., nude mice and rats, and severely compromised immunodeficient (SCID) mice). Furthermore, newly developed transgenic mice and immunodeficient mice transplanted with human bone fragments have been actively pursued as alternative models (reviewed in [360,361]).

6.1 Spontaneous Mammary and Prostate Cancer in Animals

Benign and malignant mammary neoplasms frequently develop in rats and mice, and the incidence is dependent on the strain. Unfortunately, these may not be good models for human disease. Most spontaneous mammary carcinomas in mice and rats have mild local tissue invasion, with low incidence of spontaneous metastasis to regional lymph nodes or lungs, and bone metastases are very rare. Moreover, spontaneous tumors can have long latency-periods. Compared to breast cancer, the incidence of prostate cancer in rodents and non-human primates is very rare [362]. However, specific strains of rats exist that have increased incidence of prostate neoplasia, but again, the incidence of bone metastasis formation is very rare [363,364]. Spontaneous prostate cancer occurs most commonly in dogs, including the formation of osteoblastic bone metastases [362].

6.2 Transgenic Induction of Mammary and Prostate Cancer in Mice

Mutations introduced in the genome — e.g., in the tumor suppressor p53 — by genetic engi-

neering have yielded transgenic mice that are prone to spontaneous development of a variety of neoplasms [365]. Tumors arising specifically in the mammary or prostate gland can be accomplished using oncogene expression — such as SV40 large T antigen — driven by tissue selective promoters. The whey acidic protein, C(3)1, and MMTV promoters are often used for the mammary gland [366], whereas the probasin, C(3)1, PSP94 and PSA promoters are used for the prostate gland [367]. Similarly, tissue-specific inactivation of (tumor suppressor) genes using the Cre/loxP site-specific recombination system could also result in tissue-specific carcinogenesis, as was shown by inactivation of p53 and E-cadherin genes [368]. The advantages of transgenic models of cancer include their predictability and the autochtonous development of cancer, i.e., originating where normally found. The disadvantage of the transgenic models is the low incidence of metastasis often due to rapid progression of the primary neoplasm. Moreover, in the transgenic models that do metastasize, metastases are usually found in lungs, but not in other organs such as bone [277].

6.3 Syngeneic and Xenograft Models of Bone Metastasis

Compared to transgenic mice, one of the major advantages of both syngeneic and xenograft models — using cancer cells and mice with an identical or different genetic background, respectively — is that cancer cells can be relatively easily subjected to genetic engineering *ex vivo*. In addition, these models also facilitate selection of cancer cell lines that have specific properties, such as a high propensity to spread to bone. These cell lines can be grown *in vitro* and, subsequently, re-injected intravenously, intracardially, orthotopically, or directly into the BM cavity. It is important to keep in mind that with respect to immunology, the use of immunocompetent mice in the 4T1 and other syngeneic models is preferred over xenograft models, which uses immunodeficient mice. On the other hand, cancer cells in the syngeneic model are not of human origin which may also lead to pitfalls when translating to the human situation.

6.3.1 Routes of Cancer Cell Inoculation

In syngeneic and xenograft experimental bone metastasis models, three major routes of cancer cell inoculation are commonly used, including 1) direct injection into bone microenvironment, 2) systemic injection, particularly intracardially, and 3) injection at orthotopic sites.

Cancer cells can be injected locally adjacent to a bone surface [369] or into a marrow cavity [370,371] (this thesis, chapter 2–6) to create an animal model for tumor growth in the bone microenvironment. However, local injection of tumor cells does not represent the entire process of bone metastasis and there can be distortions from injection caused by the injury to the bone (environment). Therefore, orthotopic or systemic injection is preferred.

Arguello and co-workers were the first who systemically injected cancer cells directly into the left ventricle of the heart [372]. Subsequently, cancer cells are dispersed throughout

the whole body, and metastases only develop in particular organs, i.e., reciprocal interaction between the cancer cell (the 'seed') and the microenvironment (the 'soil') is fundamental for establishing metastatic growth. The original model used immunocompetent mice, but later models used immunocompromised mice. At present, this technique has been adopted by many research groups using different types of cell lines, including the PC-3M-Pro4 prostate cancer cell line [373] (this thesis, chapter 7) and the broadly used MDA-231 breast cancer cell line [66,333,374,375] (this thesis, chapter 4,6). When MDA-231 wild type cells are intracardiacally injected into young (4–6 weeks old) female nude (or SCID) mice, metastases develop in specific organs, including bone. In this model, bone metastases can be clearly monitored by radiography after 3–4 weeks. Histologically, numerous osteoclasts and aggressive tumor colonization can be detected [66,333,374,375]. Bone metastases occur particularly in the metaphyses of the long bones, which are sites of active bone modeling and remodeling in young mice. Active bone turnover, high blood flow, and fenestrated sinusoids at these sites may predispose the metaphyses to the development of tumor growth. Blood vessels at the metaphyses have 180° turns and are common sites for embolization in young animals. Therefore, the anatomic arrangement of blood vessels in metaphyses may predispose to tumor cell embolization and development of bone metastases in growing rodents [376]. One of the disadvantages of the intracardiac injection model is that it lacks the critical early steps occurring between early growth at the primary site and entry into the circulation.

Kuperwasser and co-workers have developed an orthotopic xenograft model in which both the stromal and epithelial component of the reconstructed mammary gland are of human origin, enabling to genetically modify both epithelial and stromal cells *ex vivo*. They demonstrated that an altered stromal environment — stromal cells overexpressing TGF-ß or HGF — promoted breast cancer progression [377]. However, this model as well as other orthotopic models — including syngeneic and xenograft models — rarely show involvement of bone metastases. An exception is the 4T1 syngeneic model, in which orthotopic injection of 4T1 murine breast cancer cells results in formation of a primary tumor that disseminates to lung, adrenal glands, and bone [378,379]. Even more, syngeneic as well as xenograft models facilitate selection of sublines of cancers *in vivo* that have an increased incidence of bone metastasis after injection *in vivo*. For example, the 4T1.2 subclone of the 4T1 subline has an increased incidence of metastasis to bone after re-injection into the mammary fat pad [378].

Alternatively, experimental models can also use tumor tissue instead of tumor cells. Tumor tissue can be generated by implanting human cancer cell lines subcutaneously in nude mice, resulting in hybrid tumors containing a mixture of human cancer cells and murine stroma and blood vessels. Implantation of such a hybrid tumor, containing human MDA-MB-435 breast cancer cells, into the mammary glands of nude mice resulted in formation of bone metastases [380].

Human prostate cancer cell lines have also been transplanted orthotopically in mice, successfully representing different stages of cancer progression *in vivo* ranging from

Jeroen_Buijs_18.indd 46 26-11-2008 10:18:11

androgen-dependent growth, androgen-independent growth to metastatic growth, including formation of osteoblastic bone metastases [381-383].

6.4 Subcutaneous Transplantation of Human Bone

Human fetal bone has been transplanted successfully to the subcutis of immunodeficient SCID mice to serve as a preferential site of metastasis of human prostate cancer cells injected into the left ventricle of the heart or as a site of tumor growth after local injection of cancer cells near the viable bone substrate [384]. Similar results were also reported with the use of adult human bone in SCID mice [385]. Similarly, orthotopic injection of a specific human breast cancer cell line, SUM1315, into SCID mice resulted in metastasis to the engrafted human bone, and not to mouse skeleton [386]. Hence, these models demonstrated a preferential selection of human cancer cells to localize and proliferate in human bones compared with mouse bones. Furthermore, it was very recently demonstrated that SUM1315 cells were also able to metastasize to tissue-engineered bone, manufactured by BMP2-stimulated human BM stromal cells on a silk scaffold *in vitro* [387].

6.5 *In Vivo* Imaging

Studying bone metastasis in small animal models has often relied on histological analyses, PCR amplification, and radiography. However, assays that utilize excised tissues are subject to sampling limitations and cannot assess the overall extent of disease in a given animal. To overcome this limitation, *in vivo* detection of bone metastases using high-resolution Faxitron radiography has been used in an attempt to provide temporal information. However, it does not detect micrometastatic lesions, the desired targets for therapeutic intervention, or the actual tumor burden. Therefore, newer imaging modalities — e.g., based on the optical imaging — need to be developed and utilized to improve detection and quantification bone metastases in animal models [388,389] (this thesis, chapter 3).

7 Treatment of Bone Metastases

Once patients show evidence of bone metastasis, the disease is incurable with currently available therapies. At present, therapies focus on symptomatic management and limiting the progression of established disease (reviewed in [17,18]). Therefore, the ultimate goal is to develop new and better treatment strategies that can either prevent or treat bone metastases. For this we need a better understanding of which processes are crucially important in the formation and development of bone metastases.

7.1 Treatment Strategies

The selection of the appropriate systemic anti-tumor treatments, hormone and cytotoxic treatments, that are presently given are very much dependent on the type of cancer. In addition,

external beam radiotherapy can provide excellent palliation for localized metastatic bone pain, which can be achieved with a short treatment schedule of one to five fractions in most clinical situations [390]. Radiopharmaceuticals are now also available for the palliation of metastatic bone pain, with Strontium-89 as an effective wide-field radiotherapeutic in prostate cancer [391].

7.1.1 Bone Resorption Inhibitors

Other treatment strategies for bone metastatic disease are based on the interference with the bone microenvironment and the concomitant release of growth factors from mineralized bone during bone resorption that may support bone metastatic growth. Differently from most other tissues, drugs that can limit local turnover are available for bone. Suppression of bone turnover should interfere with the growth support for the tumor. Consequently, bone resorption inhibitors are becoming an attractive strategy for preventive and adjuvant therapies in patients with bone lesions.

7.1.1.1 Bisphosphonates

Bisphosphonates (BPs) are non-hydrolysable pyrophosphate analogues, and effective pharmacological bone resorption inhibitors that bind preferentially to bone at sites of active bone metabolism. They are released from the bone matrix during bone resorption and taken up by osteoclasts. BPs potently inhibit osteoclast activity and survival, thereby reducing osteoclast-mediated bone resorption [392-394]. In clinical practice, BPs have been widely used to control skeletal complications in various neoplastic diseases. The bisphosphonates zoledronic acid, ibandronate, clodronate and pamidronate are currently given to breast and prostate cancer patients with already established bone metastases to efficiently reduce the number of skeletal-related events (SREs) [392,395-398]. In addition, BPs may delay the progression and prevent the development of new bone metastatic foci in patients either established or without bone metastasis at the beginning of the treatment [399,400]. However, a similar study failed to demonstrate a reduction in the number of metastases [401]. Subsequently, three clinical trials primarily focused their investigation on the possibility that BP may prevent the development of metastases in women affected by primary breast cancer, but free of bone metastases at the moment of diagnosis. In two of these studies the preventive administration of BP significantly reduced the number of patients developing bone metastases and the number of bone metastases per patient [397,402]. In one study there was also a significant reduction of the number of visceral metastases [402]. However, in the third study BP treatment did not prevent the development of bone metastases and even seemed to increase the development of non-skeletal metastases [403]. To resolve the apparent contradiction, two large phase III trials using BPs as adjuvant therapy for primary breast cancer, each enrolling more than 3000 patients with early-stage breast cancer, are underway. The National Surgical Adjuvant Breast Project B-34 trial will determine whether orally administered clodronate (1600 mg daily for 3 years) alone or in combination with chemotherapy

Jeroen_Buijs_18.indd 48 26-11-2008 10:18:11

and/or hormonal therapy reduces the incidence of skeletal and non-skeletal metastases or improves overall or relapse-free survival. The Southwest Oncology Group 0307 trial will compare zoledronic acid (4 mg administered intravenously every 4 weeks for 6 months, then every 3 months for 2.5 years), clodronate (1600 mg taken orally daily for 3 years), and the BP ibandronate (50 mg taken orally daily for 3 years) as adjuvant therapy for primary breast cancer. The first results from these clinical trials are expected to be available in 2008. For prostate cancer similar prevention trials are ongoing.

7.1.1.2 Osteoprotegerin

Although the current therapy with BP results in a significant reduction in morbidity, an unmet medical need remains for a more convenient, effective, and safe therapy. Parental BPs must be administered by i.v. infusion. They are not effective in all patients, and renal toxicity and osteonecrosis may limit the dose and use of these agents in certain patients.

OPG is a potent natural bone resorption inhibitor that antagonizes the ability of RANKL to bind its receptor RANK [139,147,148]. Using the model of intracardiac injection with MDA-231 cells, treatment with Fc-OPG inhibited bone metastases formation from breast cancer [374]. In addition, in murine models of hypercalcemia, the Fc-OPG was shown to have a greater effect on reduction of bone turnover and osteoclast numbers than BP (pamidronate or zoledronic acid) treatment [404]. Moreover, in a phase I trial a single s.c. dose of OPG (AMGN-0007) suppressed bone resorption in patients with multiple myeloma and bone metastases from breast cancer at least as potently as with i.v. infusion with pamidronate [405]. Furthermore, Denosumab — a fully humanized, neutralizing monoclonal antibody to RANKL — decreased bone turnover markers in patients with multiple myeloma and bone metastases from breast cancer by a similar magnitude but more sustained than with pamidronate (i.v.) [406]. Phase III clinical trials are now focusing their investigation on whether or not denosumab is able to prevent formation of bone metastases from breast cancer and inhibit bone loss induced by hormone ablation therapy in prostate and breast cancer.

7.1.1.3 Cathepsin K Inhibitors

Another class of bone resorption inhibitors that also target osteoclastic bone resorption are cathepsin K inhibitors. In a recent preclinical study, it was shown that a cathepsin K inhibitor reduced breast cancer-induced osteolysis and skeletal tumor burden [407].

7.1.1.4 Other Treatments

Atrasentan is a small molecule that blocks the functional binding of ET-1 to ETA receptor [408]. ET-1 is a potent mitogen for both prostate cancer cells and osteoblasts, and it is considered to be involved in the generation of pain [409]. Prospective randomized placebo-controlled Phase II and III trials showed that atrasentan (10 mg/day, orally) provided adequate analgesia and a consistent trend demonstrating a delay in disease progression in patients with

metastatic hormone-refractory prostate cancer [408,410,411]. In theory, ET receptor antagonists seem better suited to act in the early phases of the cancer cell-bone interaction. Therefore, atrasentan is under investigation in a maturing phase 3 study in >900 men with non-metastatic hormone refractory prostate cancer to test the hypothesis that it delays the onset of metastatic disease.

7.2 Future Perspectives

Advances in structural deciphering of biomolecules that are involved in the pathogenesis of bone metastasis — such as OPG, integrins and MMPs — have allowed scientists to design molecules that mimic these critical targets. These artificially designed molecules can be used to block or increase the activity of a particular therapeutic target, and have significant potential in the treatment of bone metastasis. Measurements of bone turnover markers may be beneficial for the planning of a preventive treatment with bone resorption inhibitors, either newly designed molecules or more conventional ones. In the near future, gene signatures from primary cancers that predict bone metastatic potential are also very promising tools to plan adequate treatment [412-414].

8 Aim and Outline of Thesis

Once a bone metastasis has developed, patients cannot be cured. From then on, their quality of life is often adversely affected by the frequency and morbidity of skeletal-related events (SRE). Therefore, new and better treatments need to be developed, both to inhibit SRE as well as to inhibit the initial formation of bone metastases. To determine the efficacy of such treatments, more sensitive and less invasive methods to directly detect and monitor *in vivo* minimal residual disease (MRD) in preclinical cancer models are required.

In **chapter 2** of this thesis, the possible contribution to metastasis in breast cancer of periodic-acid Schiff (PAS)-positive structures in the primary tumor and its lymph node metastases is studied. In **chapter 3**, whole-body bioluminescent reporter imaging (BLI) is described as a new and better method to detect, monitor and quantify microscopic bone metastases in experimental models. Therefore, optical imaging is used in the following chapters to detect and quantify the effects of different kinds of treatments. In **chapter 4**, clinically relevant doses of bisphosphonate, given in a preventive or treatment protocol, are used to investigate the effects on progression of bone metastases. Subsequently, in **chapter 5**, high-dose bisphosphonate (BP) and osteoprotegerin (OPG) are given to maximally inhibit bone resorption using two different mechanisms of action to study the effects on established bone metastases. In **chapters 6** and **7**, bone morphogenetic protein (BMP7) is tested as a novel therapeutic molecule for repression of local and bone metastatic growth of breast and prostate cancer. Finally, general conclusions and discussions are described in **chapter 8**.

Jeroen_Buijs_18.indd 50 26-11-2008 10:18:12

9 References

1. Jemal A, Siegel R, Ward E, Murray T, Xu J, Thun MJ. Cancer statistics, 2007. *CA Cancer J Clin* 2007; 57:43-66.
2. Paget S. The distribution of secondary growths in cancer of the breast. *Lancet* 1889; 1:571-3.
3. Coleman RE, Rubens RD. The clinical course of bone metastases from breast cancer. *Br J Cancer* 1987; 55:61-6.
4. Coleman RE. Skeletal complications of malignancy. *Cancer* 1997; 80:1588-94.
5. Galasko C Incidence and distribution of skeletal metastases. In: *Skeletal Metastasis*, pp. 14-21. London, Butterworths, 1986.
6. Rubens RD The nature of metastatic bone disease. In: RD Rubens and Fogelman I. (eds.), *Bone metastases – diagnosis and treatment*, pp. 1-10. London, Springer-Verlag, 1991.
7. Walther HE. *Krebsmetastase*. Basel, Beno Schwabe & Co, 1948.
8. Chisholm GD, Rana A, Howard GC. Management options for painful carcinoma of the prostate. *Semin Oncol* 1993; 20:34-7.
9. Berg A, Berner A, Lilleby W, Bruland OS, Fossa SD, Nesland JM *et al*. Impact of disseminated tumor cells in bone marrow at diagnosis in patients with nonmetastatic prostate cancer treated by definitive radiotherapy. *Int J Cancer* 2007; 120:1603-9.
10. Braun S, Kentenich C, Janni W, Hepp F, de Waal J, Willgeroth F *et al*. Lack of effect of adjuvant chemotherapy on the elimination of single dormant tumor cells in bone marrow of high-risk breast cancer patients. *J Clin Oncol* 2000; 18:80-6.
11. Braun S, Vogl FD, Naume B, Janni W, Osborne MP, Coombes RC *et al*. A pooled analysis of bone marrow micrometastasis in breast cancer. *N Engl J Med* 2005; 353:793-802.
12. Diel IJ, Kaufmann M, Costa SD, Holle R, von Minckwitz G, Solomayer EF *et al*. Micrometastatic breast cancer cells in bone marrow at primary surgery: prognostic value in comparison with nodal status. *J Natl Cancer Inst* 1996; 88:1652-8.
13. Balic M, Lin H, Young L, Hawes D, Giuliano A, McNamara G *et al*. Most early disseminated cancer cells detected in bone marrow of breast cancer patients have a putative breast cancer stem cell phenotype. *Clin Cancer Res* 2006; 12:5615-21.
14. Janni W, Rack B, Schindlbeck C, Strobl B, Rjosk D, Braun S *et al*. The persistence of isolated tumor cells in bone marrow from patients with breast carcinoma predicts an increased risk for recurrence. *Cancer* 2005; 103:884-91.
15. Thurm H, Ebel S, Kentenich C, Hemsen A, Riethdorf S, Coith C *et al*. Rare expression of epithelial cell adhesion molecule on residual micrometastatic breast cancer cells after adjuvant chemotherapy. *Clin Cancer Res* 2003; 9:2598-604.
16. Coleman RE, Smith P, Rubens RD. Clinical course and prognostic factors following bone recurrence from breast cancer. *Br J Cancer* 1998; 77:336-40.
17. Coleman RE. Metastatic bone disease: clinical features, pathophysiology and treatment strategies. *Cancer Treat Rev* 2001; 27:165-76.
18. Mundy GR. Metastasis to bone: causes, consequences and therapeutic opportunities. *Nat Rev Cancer* 2002; 2:584-93.
19. Mercadante S. Malignant bone pain: pathophysiology and treatment. *Pain* 1997; 69:1-18.
20. Clines GA, Guise TA. Hypercalcaemia of malignancy and basic research on mechanisms responsible for osteolytic and osteoblastic metastasis to bone. *Endocr Relat Cancer* 2005; 12:549-83.
21. Guise TA, Mundy GR. Cancer and bone. *Endocr Rev* 1998; 19:18-54.
22. Roodman GD. Mechanisms of bone metastasis. *N Engl J Med* 2004; 350:1655-64.
23. Langley RR, Fidler IJ. Tumor cell-organ microenvironment interactions in the pathogenesis of cancer metastasis. *Endocr Rev* 2007; 28:297-321.
24. Alberts B, Bray D, Lewis J, Raff M, Roberts K, and Watson JD Cancer. In: *Molecular Biology of the Cell*, 3rd ed, pp. 1255-1291. New York & London, Garland Publishing, Inc., 1994.
25. Ronnov-Jessen L, Petersen OW, Bissell MJ. Cellular changes involved in conversion of normal to malignant breast: importance of the stromal reaction. *Physiol Rev* 1996; 76:69-125.
26. Chung LW, Baseman A, Assikis V, Zhau HE. Molecular insights into prostate cancer progression: the missing link of tumor microenvironment. *J Urol* 2005; 173:10-20.

27. Liotta LA, Kohn EC. The microenvironment of the tumour-host interface. *Nature* 2001; 411:375-9.
28. Nakamura T, Matsumoto K, Kiritoshi A, Tano Y, Nakamura T. Induction of hepatocyte growth factor in fibroblasts by tumor-derived factors affects invasive growth of tumor cells: in vitro analysis of tumor-stromal interactions. *Cancer Res* 1997; 57:3305-13.
29. Barcellos-Hoff MH, Ravani SA. Irradiated mammary gland stroma promotes the expression of tumorigenic potential by unirradiated epithelial cells. *Cancer Res* 2000; 60:1254-60.
30. Hayashi N, Sugimura Y, Kawamura J, Donjacour AA, Cunha GR. Morphological and functional heterogeneity in the rat prostatic gland. *Biol Reprod* 1991; 45:308-21.
31. Ao M, Franco OE, Park D, Raman D, Williams K, Hayward SW. Cross-talk between paracrine-acting cytokine and chemokine pathways promotes malignancy in benign human prostatic epithelium. *Cancer Res* 2007; 67:4244-53.
32. Oft M, Peli J, Rudaz C, Schwarz H, Beug H, Reichmann E. TGF-beta1 and Ha-Ras collaborate in modulating the phenotypic plasticity and invasiveness of epithelial tumor cells. *Genes Dev* 1996; 10:2462-77.
33. Roberts AB, Wakefield LM. The two faces of transforming growth factor beta in carcinogenesis. *Proc Natl Acad Sci U S A* 2003; 100:8621-3.
34. Ellenrieder V, Hendler SF, Boeck W, Seufferlein T, Menke A, Ruhland C *et al*. Transforming growth factor beta1 treatment leads to an epithelial-mesenchymal transdifferentiation of pancreatic cancer cells requiring extracellular signal-regulated kinase 2 activation. *Cancer Res* 2001; 61:4222-8.
35. Peinado H, Quintanilla M, Cano A. Transforming growth factor beta-1 induces snail transcription factor in epithelial cell lines: mechanisms for epithelial mesenchymal transitions. *J Biol Chem* 2003; 278:21113-23.
36. Piek E, Moustakas A, Kurisaki A, Heldin CH, Ten Dijke P. TGF-(beta) type I receptor/ALK-5 and Smad proteins mediate epithelial to mesenchymal transdifferentiation in NMuMG breast epithelial cells. *J Cell Sci* 1999; 112:4557-68.
37. Thiery JP. Epithelial-mesenchymal transitions in tumour progression. *Nat Rev Cancer* 2002; 2:442-54.
38. Valcourt U, Kowanetz M, Niimi H, Heldin CH, Moustakas A. TGF-{beta} and the Smad Signaling Pathway Support Transcriptomic Reprogramming during Epithelial-Mesenchymal Cell Transition. *Mol Biol Cell* 2005; 16:1987-2002.
39. Massague J. TGF-beta signal transduction. *Annu Rev Biochem* 1998; 67:753-91.:753-91.
40. Bhowmick NA, Chytil A, Plieth D, Gorska AE, Dumont N, Shappell S *et al*. TGF-beta signaling in fibroblasts modulates the oncogenic potential of adjacent epithelia. *Science* 2004; 303:848-51.
41. Wicha MS, Liu S, Dontu G. Cancer stem cells: an old idea--a paradigm shift. *Cancer Res* 2006; 66:1883-90.
42. Bonnet D, Dick JE. Human acute myeloid leukemia is organized as a hierarchy that originates from a primitive hematopoietic cell. *Nat Med* 1997; 3:730-7.
43. Dick JE. Acute myeloid leukemia stem cells. *Ann N Y Acad Sci* 2005; 1044:1-5.:1-5.
44. Al Hajj M, Wicha MS, Benito-Hernandez A, Morrison SJ, Clarke MF. Prospective identification of tumorigenic breast cancer cells. *Proc Natl Acad Sci U S A* 2003; 100:3983-8.
45. Miki J, Furusato B, Li H, Gu Y, Takahashi H, Egawa S *et al*. Identification of putative stem cell markers, CD133 and CXCR4, in hTERT-immortalized primary nonmalignant and malignant tumor-derived human prostate epithelial cell lines and in prostate cancer specimens. *Cancer Res* 2007; 67:3153-61.
46. Collins AT, Berry PA, Hyde C, Stower MJ, Maitland NJ. Prospective identification of tumorigenic prostate cancer stem cells. *Cancer Res* 2005; 65:10946-51.
47. Reya T, Morrison SJ, Clarke MF, Weissman IL. Stem cells, cancer, and cancer stem cells. *Nature* 2001; 414:105-11.
48. Tang DG, Patrawala L, Calhoun T, Bhatia B, Choy G, Schneider-Broussard R *et al*. Prostate cancer stem/progenitor cells: identification, characterization, and implications. *Mol Carcinog* 2007; 46:1-14.
49. Hill RP. Identifying cancer stem cells in solid tumors: case not proven. *Cancer Res* 2006; 66:1891-5.
50. D'Amore PA, Shan Y.Ng., Darland D.C. Angiogenesis. *science and medicine* 1999; 44-53.

Jeroen_Buijs_18.indd 52 26-11-2008 10:18:12

51. Risau W. Mechanisms of angiogenesis. *Nature* 1997; 386:671-4.
52. Kumar R, Fidler IJ. Angiogenic molecules and cancer metastasis. *In Vivo* 1998; 12:27-34.
53. Hanahan D, Folkman J. Patterns and emerging mechanisms of the angiogenic switch during tumorigenesis. *Cell* 1996; 86:353-64.
54. Folkman J. Angiogenesis in cancer, vascular, rheumatoid and other disease. *Nat Med* 1995; 1:27-31.
55. Engels K, Fox SB, Whitehouse RM, Gatter KC, Harris AL. Distinct angiogenic patterns are associated with high-grade in situ ductal carcinomas of the breast. *J Pathol* 1997; 181:207-12.
56. Boudreau N, Myers C. Breast cancer-induced angiogenesis: multiple mechanisms and the role of the microenvironment. *Breast Cancer Res* 2003; 5:140-6.
57. de Jong JS, van Diest PJ, Baak JP. Hot spot microvessel density and the mitotic activity index are strong additional prognostic indicators in invasive breast cancer. *Histopathology* 2000; 36:306-12.
58. Gasparini G, Harris AL. Clinical importance of the determination of tumor angiogenesis in breast carcinoma: much more than a new prognostic tool. *J Clin Oncol* 1995; 13:765-82.
59. Heimann R, Ferguson D, Powers C, Recant WM, Weichselbaum RR, Hellman S. Angiogenesis as a predictor of long-term survival for patients with node-negative breast cancer. *J Natl Cancer Inst* 1996; 88:1764-9.
60. Weidner N, Carroll PR, Flax J, Blumenfeld W, Folkman J. Tumor angiogenesis correlates with metastasis in invasive prostate carcinoma. *Am J Pathol* 1993; 143:401-9.
61. Weidner N. Intratumor microvessel density as a prognostic factor in cancer. *Am J Pathol* 1995; 147:9-19.
62. Engels K, Fox SB, Harris AL. Angiogenesis as a biologic and prognostic indicator in human breast carcinoma. *EXS* 1997; 79:113-56.:113-56.
63. Neufeld G, Cohen T, Gengrinovitch S, Poltorak Z. Vascular endothelial growth factor (VEGF) and its receptors. *FASEB J* 1999; 13:9-22.
64. Shih T, Lindley C. Bevacizumab: an angiogenesis inhibitor for the treatment of solid malignancies. *Clin Ther* 2006; 28:1779-802.
65. van der Pluijm G, Lowik C, Papapoulos S. Tumour progression and angiogenesis in bone metastasis from breast cancer: new approaches to an old problem. *Cancer Treat Rev* 2000; 26:11-27.
66. van der Pluijm G, Sijmons B, Vloedgraven H, Deckers M, Papapoulos S, Lowik C. Monitoring metastatic behavior of human tumor cells in mice with species-specific polymerase chain reaction: elevated expression of angiogenesis and bone resorption stimulators by breast cancer in bone metastases. *J Bone Miner Res* 2001; 16:1077-91.
67. Mohammed RA, Green A, El Shikh S, Paish EC, Ellis IO, Martin SG. Prognostic significance of vascular endothelial cell growth factors -A, -C and -D in breast cancer and their relationship with angio- and lymphangiogenesis. *Br J Cancer* 2007; 96:1092-100.
68. Stacker SA, Caesar C, Baldwin ME, Thornton GE, Williams RA, Prevo R *et al*. VEGF-D promotes the metastatic spread of tumor cells via the lymphatics. *Nat Med* 2001; 7:186-91.
69. Skobe M, Hawighorst T, Jackson DG, Prevo R, Janes L, Velasco P *et al*. Induction of tumor lymphangiogenesis by VEGF-C promotes breast cancer metastasis. *Nat Med* 2001; 7:192-8.
70. Auguste P, Lemiere S, Larrieu-Lahargue F, Bikfalvi A. Molecular mechanisms of tumor vascularization. *Crit Rev Oncol Hematol* 2005; 54:53-61.
71. Clarijs R, Otte-Holler I, Ruiter DJ, de Waal RM. Presence of a fluid-conducting meshwork in xenografted cutaneous and primary human uveal melanoma. *Invest Ophthalmol Vis Sci* 2002; 43:912-8.
72. Folberg R, Pe'er J, Gruman LM, Woolson RF, Jeng G, Montague PR *et al*. The morphologic characteristics of tumor blood vessels as a marker of tumor progression in primary human uveal melanoma: a matched case-control study. *Hum Pathol* 1992; 23:1298-305.
73. Thies A, Mangold U, Moll I, Schumacher U. PAS-positive loops and networks as a prognostic indicator in cutaneous malignant melanoma. *J Pathol* 2001; 195:537-42.
74. Folberg R, Rummelt V, Parys-Van Ginderdeuren R, Hwang T, Woolson RF, Pe'er J *et al*. The prognostic value of tumor blood vessel morphology in primary uveal melanoma. *Ophthalmology* 1993; 100:1389-98.

75. Warso MA, Maniotis AJ, Chen X, Majumdar D, Patel MK, Shilkaitis A *et al*. Prognostic significance of periodic acid-Schiff-positive patterns in primary cutaneous melanoma. *Clin Cancer Res* 2001; 7:473-7.
76. Foss AJ, Alexander RA, Hungerford JL, Harris AL, Cree IA, Lightman S. Reassessment of the PAS patterns in uveal melanoma. *Br J Ophthalmol* 1997; 81:240-6.
77. McLean IW, Keefe KS, Burnier MN. Uveal melanoma. Comparison of the prognostic value of fibrovascular loops, mean of the ten largest nucleoli, cell type, and tumor size. *Ophthalmology* 1997; 104:777-80.
78. Maniotis AJ, Folberg R, Hess A, Seftor EA, Gardner LM, Pe'er J *et al*. Vascular channel formation by human melanoma cells in vivo and in vitro: vasculogenic mimicry. *Am J Pathol* 1999; 155:739-52.
79. Folberg R, Hendrix MJ, Maniotis AJ. Vasculogenic mimicry and tumor angiogenesis. *Am J Pathol* 2000; 156:361-81.
80. Zhang S, Zhang D, Sun B. Vasculogenic mimicry: Current status and future prospects. *Cancer Lett* 2007; 254:157-64.
81. Sharma N, Seftor RE, Seftor EA, Gruman LM, Heidger PM, Jr., Cohen MB *et al*. Prostatic tumor cell plasticity involves cooperative interactions of distinct phenotypic subpopulations: Role in vasculogenic mimicry. *Prostate* 2002; 50:189-201.
82. Shirakawa K, Kobayashi H, Heike Y, Kawamoto S, Brechbiel MW, Kasumi F *et al*. Hemodynamics in vasculogenic mimicry and angiogenesis of inflammatory breast cancer xenograft. *Cancer Res* 2002; 62:560-6.
83. McDonald DM, Munn L, Jain RK. Vasculogenic mimicry: how convincing, how novel, and how significant? *Am J Pathol* 2000; 156:383-8.
84. McDonald DM, Foss AJ. Endothelial cells of tumor vessels: abnormal but not absent. *Cancer Metastasis Rev* 2000; 19:109-20.
85. Bissell MJ. Tumor plasticity allows vasculogenic mimicry, a novel form of angiogenic switch. A rose by any other name? *Am J Pathol* 1999; 155:675-9.
86. Huber MA, Kraut N, Beug H. Molecular requirements for epithelial-mesenchymal transition during tumor progression. *Curr Opin Cell Biol* 2005; 17:548-58.
87. Friedl P. Prespecification and plasticity: shifting mechanisms of cell migration. *Curr Opin Cell Biol* 2004; 16:14-23.
88. Egeblad M, Werb Z. new functions for the matrix metalloproteinases in cancer progression. *nature reviews* 2002; 2:161-74.
89. Nielsen BS, Rank F, Lopez JM, Balbin M, Vizoso F, Lund LR *et al*. Collagenase-3 expression in breast myofibroblasts as a molecular marker of transition of ductal carcinoma in situ lesions to invasive ductal carcinomas. *Cancer Res* 2001; 61:7091-100.
90. Hay ED. An overview of epithelio-mesenchymal transformation. *Acta Anat (Basel)* 1995; 154:8-20.
91. Stoker M, Perryman M. An epithelial scatter factor released by embryo fibroblasts. *J Cell Sci* 1985; 77:209-23.
92. Thiery JP. Epithelial-mesenchymal transitions in development and pathologies. *Curr Opin Cell Biol* 2003; 15:740-6.
93. Vincent-Salomon A, Thiery JP. Host microenvironment in breast cancer development: epithelial-mesenchymal transition in breast cancer development. *Breast Cancer Res* 2003; 5:101-6.
94. Barasch J, Yang J, Ware CB, Taga T, Yoshida K, Erdjument-Bromage H *et al*. Mesenchymal to epithelial conversion in rat metanephros is induced by LIF. *Cell* 1999; 99:377-86.
95. Dudley AT, Lyons KM, Robertson EJ. A requirement for bone morphogenetic protein-7 during development of the mammalian kidney and eye. *Genes Dev* 1995; 9:2795-807.
96. Luo G, Hofmann C, Bronckers AL, Sohocki M, Bradley A, Karsenty G. BMP-7 is an inducer of nephrogenesis, and is also required for eye development and skeletal patterning. *Genes Dev* 1995; 9:2808-20.
97. Thiery JP, Sleeman JP. Complex networks orchestrate epithelial-mesenchymal transitions. *Nat Rev Mol Cell Biol* 2006; 7:131-42.
98. Vukicevic S, Kopp JB, Luyten FP, Sampath TK. Induction of nephrogenic mesenchyme by osteogenic protein 1 (bone morphogenetic protein 7). *Proc Natl Acad Sci U S A* 1996; 93:9021-6.

Jeroen_Buijs_18.indd 54 26-11-2008 10:18:12

99. Grunert S, Jechlinger M, Beug H. Diverse cellular and molecular mechanisms contribute to epithelial plasticity and metastasis. *Nat Rev Mol Cell Biol* 2003; 4:657-65.
100. Dandachi N, Hauser-Kronberger C, More E, Wiesener B, Hacker GW, Dietze O *et al*. Co-expression of tenascin-C and vimentin in human breast cancer cells indicates phenotypic transdifferentiation during tumour progression: correlation with histopathological parameters, hormone receptors, and oncoproteins. *J Pathol* 2001; 193:181-9.
101. Siitonen SM, Kononen JT, Helin HJ, Rantala IS, Holli KA, Isola JJ. Reduced E-cadherin expression is associated with invasiveness and unfavorable prognosis in breast cancer. *Am J Clin Pathol* 1996; 105:394-402.
102. Lombaerts M, van Wezel T, Philippo K, Dierssen JW, Zimmerman RM, Oosting J *et al*. E-cadherin transcriptional downregulation by promoter methylation but not mutation is related to epithelial-to-mesenchymal transition in breast cancer cell lines. *Br J Cancer* 2006; 94:661-71.
103. Frixen UH, Behrens J, Sachs M, Eberle G, Voss B, Warda A *et al*. E-cadherin-mediated cell-cell adhesion prevents invasiveness of human carcinoma cells. *J Cell Biol* 1991; 113:173-85.
104. Vleminckx K, Vakaet L, Jr., Mareel M, Fiers W, van Roy F. Genetic manipulation of E-cadherin expression by epithelial tumor cells reveals an invasion suppressor role. *Cell* 1991; 66:107-19.
105. Weinberg RA. *The Biology of Cancer*. New York, Garland Science, Taylor&Francis Group, 2004.
106. Bukholm IK, Nesland JM, Borresen-Dale AL. Re-expression of E-cadherin, alpha-catenin and beta-catenin, but not of gamma-catenin, in metastatic tissue from breast cancer patients [seecomments]. *J Pathol* 2000; 190:15-9.
107. Bryden AA, Freemont AJ, Clarke NW, George NJ. Paradoxical expression of E-cadherin in prostatic bone metastases. *BJU Int* 1999; 84:1032-4.
108. Barker N, Clevers H. Tumor environment: a potent driving force in colorectal cancer? *Trends Mol Med* 2001; 7:535-7.
109. Brabletz T, Jung A, Spaderna S, Hlubek F, Kirchner T. Opinion: migrating cancer stem cells – an integrated concept of malignant tumour progression. *Nat Rev Cancer* 2005; 5:744-9.
110. Janda E, Lehmann K, Killisch I, Jechlinger M, Herzig M, Downward J *et al*. Ras and TGF[beta] cooperatively regulate epithelial cell plasticity and metastasis: dissection of Ras signaling pathways. *J Cell Biol* 2002; 156:299-313.
111. Oft M, Heider KH, Beug H. TGFbeta signaling is necessary for carcinoma cell invasiveness and metastasis. *Curr Biol* 1998; 19;8:1243-52.
112. Deckers M, van Dinther M, Buijs J, Que I, Lowik C, van der Pluijm G *et al*. The tumor suppressor Smad4 is required for transforming growth factor beta-induced epithelial to mesenchymal transition and bone metastasis of breast cancer cells. *Cancer Res* 2006; 66:2202-9.
113. Bates RC, Bellovin DI, Brown C, Maynard E, Wu B, Kawakatsu H *et al*. Transcriptional activation of integrin beta6 during the epithelial-mesenchymal transition defines a novel prognostic indicator of aggressive colon carcinoma. *J Clin Invest* 2005; 115:339-47.
114. Muller T, Bain G, Wang X, Papkoff J. Regulation of epithelial cell migration and tumor formation by beta-catenin signaling. *Exp Cell Res* 2002; 280:119-33.
115. Morali OG, Delmas V, Moore R, Jeanney C, Thiery JP, Larue L. IGF-II induces rapid beta-catenin relocation to the nucleus during epithelium to mesenchyme transition. *Oncogene* 2001; 20:4942-50.
116. Brabletz T, Jung A, Reu S, Porzner M, Hlubek F, Kunz-Schughart LA *et al*. Variable beta-catenin expression in colorectal cancers indicates tumor progression driven by the tumor environment. *Proc Natl Acad Sci U S A* 2001; 98:10356-61.
117. Rocha AS, Soares P, Fonseca E, Cameselle-Teijeiro J, Oliveira MC, Sobrinho-Simoes M. E-cadherin loss rather than beta-catenin alterations is a common feature of poorly differentiated thyroid carcinomas. *Histopathology* 2003; 42:580-7.
118. Butler TP, Gullino PM. Quantitation of cell shedding into efferent blood of mammary adenocarcinoma. *Cancer Res* 1975; 35:512-6.
119. Boucharaba A, Serre CM, Gres S, Saulnier-Blache JS, Bordet JC, Guglielmi J *et al*. Platelet-derived lysophosphatidic acid supports the progression of osteolytic bone metastases in breast cancer. *J Clin Invest* 2004; 114:1714-25.
120. Boucharaba A, Serre CM, Guglielmi J, Bordet JC, Clezardin P, Peyruchaud O. The type 1 lysophosphatidic acid receptor is a target for therapy in bone metastases. *Proc Natl Acad Sci U S A* 2006; %20;103:9643-8.

121. Nieswandt B, Hafner M, Echtenacher B, Mannel DN. Lysis of tumor cells by natural killer cells in mice is impeded by platelets. *Cancer Res* 1999; 59:1295-300.
122. Karpatkin S, Pearlstein E, Salk PL, Yogeeswaran G. Role of platelets in tumor cell metastases. *Ann N Y Acad Sci* 1981; 370:101-18.:101-18.
123. Trikha M, Zhou Z, Timar J, Raso E, Kennel M, Emmell E *et al*. Multiple roles for platelet GPIIb/IIIa and alphavbeta3 integrins in tumor growth, angiogenesis, and metastasis. *Cancer Res* 2002; 62:2824-33.
124. Batson OV. The function of the vertebral veins and their role in the spread of metastasis. *Ann Surg* 1940; 112:138-49.
125. Ibukuro K, Fukuda H, Mori K, Inoue Y. Topographic anatomy of the vertebral venous system in the thoracic inlet. *AJR Am J Roentgenol* 2001; 176:1059-65.
126. Coman DR, deLong RP. The role of the vertebral venous system in the metastasis of cancer to the spinal column; experiments with tumor-cell suspensions in rats and rabbits. *Cancer* 1951; 4:610-8.
127. Baron R Anatomy and Ultrastructure of Bone. In: MJ Favus (ed.), *Primer on the Metabolic Bone Diseases an Disorders of Mineral Metabolism*, 4 ed, pp. 3-10. Philadelpia, Lippincott Williams&Wilkins, 1999.
128. Boyle WJ, Simonet WS, Lacey DL. Osteoclast differentiation and activation. *Nature* 2003; 423:337-42.
129. Teitelbaum SL. Osteoclasts: what do they do and how do they do it? *Am J Pathol* 2007; 170:427-35.
130. Engleman VW, Nickols GA, Ross FP, Horton MA, Griggs DW, Settle SL *et al*. A peptidomimetic antagonist of the alpha(v)beta3 integrin inhibits bone resorption in vitro and prevents osteoporosis in vivo. *J Clin Invest* 1997; 99:2284-92.
131. Marks SCJr, Lane PW. Osteopetrosis, a new recessive skeletal mutation on chromosome 12 of the mouse. *J Hered* 1976; 67:11-8.
132. Yoshida H, Hayashi S, Kunisada T, Ogawa M, Nishikawa S, Okamura H *et al*. The murine mutation osteopetrosis is in the coding region of the macrophage colony stimulating factor gene. *Nature* 1990; 345:442-4.
133. Felix R, Cecchini MG, Hofstetter W, Elford PR, Stutzer A, Fleisch H. Impairment of macrophage colony-stimulating factor production and lack of resident bone marrow macrophages in the osteopetrotic op/op mouse. *J Bone Miner Res* 1990; 5:781-9.
134. Felix R, Cecchini MG, Fleisch H. Macrophage colony stimulating factor restores in vivo bone resorption in the op/op osteopetrotic mouse. *Endocrinology* 1990; 127:2592-4.
135. Hsu H, Lacey DL, Dunstan CR, Solovyev I, Colombero A, Timms E *et al*. Tumor necrosis factor receptor family member RANK mediates osteoclast differentiation and activation induced by osteoprotegerin ligand. *Proc Natl Acad Sci U S A* 1999; 96:3540-5.
136. Lacey DL, Timms E, Tan HL, Kelley MJ, Dunstan CR, Burgess T *et al*. Osteoprotegerin ligand is a cytokine that regulates osteoclast differentiation and activation. *Cell* 1998; 93:165-76.
137. Nakagawa N, Kinosaki M, Yamaguchi K, Shima N, Yasuda H, Yano K *et al*. RANK is the essential signaling receptor for osteoclast differentiation factor in osteoclastogenesis. *Biochem Biophys Res Commun* 1998; 253:395-400.
138. Tsukii K, Shima N, Mochizuki S, Yamaguchi K, Kinosaki M, Yano K *et al*. Osteoclast differentiation factor mediates an essential signal for bone resorption induced by 1 alpha,25-dihydroxyvitamin D3, prostaglandin E2, or parathyroid hormone in the microenvironment of bone. *Biochem Biophys Res Commun* 1998; 19;246:337-41.
139. Yasuda H, Shima N, Nakagawa N, Yamaguchi K, Kinosaki M, Mochizuki S *et al*. Osteoclast differentiation factor is a ligand for osteoprotegerin/osteoclastogenesis-inhibitory factor and is identical to TRANCE/RANKL. *Proc Natl Acad Sci U S A* 1998; 95:3597-602.
140. Dougall WC, Glaccum M, Charrier K, Rohrbach K, Brasel K, De Smedt T *et al*. RANK is essential for osteoclast and lymph node development. *Genes Dev* 1999; 13:2412-24.
141. Kong YY, Yoshida H, Sarosi I, Tan HL, Timms E, Capparelli C *et al*. OPGL is a key regulator of osteoclastogenesis, lymphocyte development and lymph-node organogenesis. *Nature* 1999; 397:315-23.
142. Li J, Sarosi I, Yan XQ, Morony S, Capparelli C, Tan HL *et al*. RANK is the intrinsic hematopoietic cell surface receptor that controls osteoclastogenesis and regulation of bone mass and calcium metabolism. *Proc Natl Acad Sci U S A* 2000; 97:1566-71.

Jeroen_Buijs_18.indd 56 26-11-2008 10:18:12

143. Grigoriadis AE, Wang ZQ, Cecchini MG, Hofstetter W, Felix R, Fleisch HA *et al*. c-Fos: a key regulator of osteoclast-macrophage lineage determination and bone remodeling. *Science* 1994; 266:443-8.
144. Ikeda F, Nishimura R, Matsubara T, Tanaka S, Inoue J, Reddy SV *et al*. Critical roles of c-Jun signaling in regulation of NFAT family and RANKL-regulated osteoclast differentiation. *J Clin Invest* 2004; 114:475-84.
145. Asagiri M, Sato K, Usami T, Ochi S, Nishina H, Yoshida H *et al*. Autoamplification of NFATc1 expression determines its essential role in bone homeostasis. *J Exp Med* 2005; 202:1261-9.
146. Theoleyre S, Wittrant Y, Tat SK, Fortun Y, Redini F, Heymann D. The molecular triad OPG/RANK/RANKL: involvement in the orchestration of pathophysiological bone remodeling. *Cytokine Growth Factor Rev* 2004; 15:457-75.
147. Khosla S. Minireview: the OPG/RANKL/RANK system. *Endocrinology* 2001; 142:5050-5.
148. Simonet WS, Lacey DL, Dunstan CR, Kelley M, Chang MS, Luthy R *et al*. Osteoprotegerin: a novel secreted protein involved in the regulation of bone density. *Cell* 1997; 89:309-19.
149. Yasuda H, Shima N, Nakagawa N, Mochizuki SI, Yano K, Fujise N *et al*. Identity of osteoclastogenesis inhibitory factor (OCIF) and osteoprotegerin (OPG): a mechanism by which OPG/OCIF inhibits osteoclastogenesis in vitro. *Endocrinology* 1998; 139:1329-37.
150. Suda T, Takahashi N, Udagawa N, Jimi E, Gillespie MT, Martin TJ. Modulation of osteoclast differentiation and function by the new members of the tumor necrosis factor receptor and ligand families. *Endocr Rev* 1999; 20:345-57.
151. Bucay N, Sarosi I, Dunstan CR, Morony S, Tarpley J, Capparelli C *et al*. osteoprotegerin-deficient mice develop early onset osteoporosis and arterial calcification. *Genes Dev* 1998; 12:1260-8.
152. Mizuno A, Amizuka N, Irie K, Murakami A, Fujise N, Kanno T *et al*. Severe osteoporosis in mice lacking osteoclastogenesis inhibitory factor/osteoprotegerin. *Biochem Biophys Res Commun* 1998; 247:610-5.
153. Min H, Morony S, Sarosi I, Dunstan CR, Capparelli C, Scully S *et al*. Osteoprotegerin reverses osteoporosis by inhibiting endosteal osteoclasts and prevents vascular calcification by blocking a process resembling osteoclastogenesis. *J Exp Med* 2000; 192:463-74.
154. Lian JB, Gary S, Stein GS, Cancelas JA, Robey PG, and Boskey AL Bone Formation: Osteoblasts Lineage Cells, Growth Factors, Matrix Proteins, and the Mineralization Process. In: MJ Favus (ed.), *Primer on the Metabolic Bone Diseases an Disorders of Mineral Metabolism*, 4 ed, pp. 14-29. Philadelpia, Lippincott Williams&Wilkins, 1999.
155. Aubin JE. Bone stem cells. *J Cell Biochem Suppl* 1998; 30-31:73-82.:73-82.
156. Lian JB, Stein GS. Runx2/Cbfa1: a multifunctional regulator of bone formation. *Curr Pharm Des* 2003; 9:2677-85.
157. Ducy P, Zhang R, Geoffroy V, Ridall AL, Karsenty G. Osf2/Cbfa1: a transcriptional activator of osteoblast differentiation. *Cell* 1997; 89:747-54.
158. Ducy P. Cbfa1: a molecular switch in osteoblast biology. *Dev Dyn* 2000; 219:461-71.
159. Otto F, Thornell AP, Crompton T, Denzel A, Gilmour KC, Rosewell IR *et al*. Cbfa1, a candidate gene for cleidocranial dysplasia syndrome, is essential for osteoblast differentiation and bone development. *Cell* 1997; 89:765-71.
160. Komori T, Yagi H, Nomura S, Yamaguchi A, Sasaki K, Deguchi K *et al*. Targeted disruption of Cbfa1 results in a complete lack of bone formation owing to maturational arrest of osteoblasts. *Cell* 1997; 89:755-64.
161. Korchynskyi O, van Bezooijen RL, Löwik CWGM, and Ten Dijke P Bone morphogenetic protein receptors and nuclear effectors in bone formation. In: S Vukicevic and KT Sampath (eds.), *Bone Morphogenetic Proteins: Regeneration of Bone and Beyond*, pp. 9-44. Basel, Birkhäuser, 2004.
162. van der Horst G, van Bezooijen RL, Deckers MM, Hoogendam J, Visser A, Lowik CW *et al*. Differentiation of murine preosteoblastic KS483 cells depends on autocrine bone morphogenetic protein signaling during all phases of osteoblast formation. *Bone* 2002; 31:661-9.
163. van der Horst G., Farih-Sips H, Lowik CW, Karperien M. Hedgehog stimulates only osteoblastic differentiation of undifferentiated KS483 cells. *Bone* 2003; 33:899-910.

164. Kato M, Patel MS, Levasseur R, Lobov I, Chang BH, Glass DA *et al*. Cbfa1-independent decrease in osteoblast proliferation, osteopenia, and persistent embryonic eye vascularization in mice deficient in Lrp5, a Wnt coreceptor. *J Cell Biol* 2002; 157:303-14.
165. Knothe Tate ML, Adamson JR, Tami AE, Bauer TW. The osteocyte. *Int J Biochem Cell Biol* 2004; 36:1-8.
166. Robey PG, Fedarko NS, Hefferan TE, Bianco P, Vetter UK, Grzesik W *et al*. Structure and molecular regulation of bone matrix proteins. *J Bone Miner Res* 1993; 8 Suppl 2:S483-7.:S483-S487.
167. van der Pluijm G, Vloedgraven HJ, Ivanov B, Robey FA, Grzesik WJ, Robey PG *et al*. Bone sialoprotein peptides are potent inhibitors of breast cancer cell adhesion to bone. *Cancer Res* 1996; 56:1948-55.
168. van der Pluijm G, Vloedgraven H, Papapoulos S, Lowik C, Grzesik W, Kerr J *et al*. Attachment characteristics and involvement of integrins in adhesion of breast cancer cell lines to extracellular bone matrix components. *Lab Invest* 1997; 77:665-75.
169. Hauschka PV, Mavrakos AE, Iafrati MD, Doleman SE, Klagsbrun M. Growth factors in bone matrix. Isolation of multiple types by affinity chromatography on heparin-Sepharose. *J Biol Chem* 1986; 261:12665-74.
170. Pietrzak WS, Woodell-May J, McDonald N. Assay of bone morphogenetic protein-2, -4, and -7 in human demineralized bone matrix. *J Craniofac Surg* 2006; 17:84-90.
171. Yoneda T, Hiraga T. Crosstalk between cancer cells and bone microenvironment in bone metastasis. *Biochem Biophys Res Commun* 2005; 328:679-87.
172. Frost HM. *Bone biodynamics*. Boston, Little Brown, 1964.
173. Mundy GR Bone remodeling. In: MJ Favus (ed.), *Primer on the Metabolic Bone Diseases and Disorders of Mineral Metabolism*, 4 ed, pp. 30-38. Philadelphia, Lippincott Williams&Wilkins, 1999.
174. Seeman E, Delmas PD. Bone quality--the material and structural basis of bone strength and fragility. *N Engl J Med* 2006; 354:2250-61.
175. Dallas SL, Rosser JL, Mundy GR, Bonewald LF. Proteolysis of latent transforming growth factor-beta (TGF-beta)-binding protein-1 by osteoclasts. A cellular mechanism for release of TGF-beta from bone matrix. *J Biol Chem* 2002; 277:21352-60.
176. Rizo A, Vellenga E, de Haan G, Schuringa JJ. Signaling pathways in self-renewing hematopoietic and leukemic stem cells: do all stem cells need a niche? *Hum Mol Genet* 2006; 15 Spec No 2:R210-9.:R210-R219.
177. Taichman RS. Blood and bone: two tissues whose fates are intertwined to create the hematopoietic stem-cell niche. *Blood* 2005; 105:2631-9.
178. Yin T, Li L. The stem cell niches in bone. *J Clin Invest* 2006; 116:1195-201.
179. Calvi LM, Adams GB, Weibrecht KW, Weber JM, Olson DP, Knight MC *et al*. Osteoblastic cells regulate the hematopoietic stem cell niche. *Nature* 2003; 425:841-6.
180. Zhang J, Niu C, Ye L, Huang H, He X, Tong WG *et al*. Identification of the hematopoietic stem cell niche and control of the niche size. *Nature* 2003; 425:836-41.
181. Peled A, Petit I, Kollet O, Magid M, Ponomaryov T, Byk T *et al*. Dependence of human stem cell engraftment and repopulation of NOD/SCID mice on CXCR4. *Science* 1999; 283:845-8.
182. Cancelas JA, Lee AW, Prabhakar R, Stringer KF, Zheng Y, Williams DA. Rac GTPases differentially integrate signals regulating hematopoietic stem cell localization. *Nat Med* 2005; 11:886-91.
183. Mohle R, Bautz F, Denzlinger C, Kanz L. Transendothelial migration of hematopoietic progenitor cells. Role of chemotactic factors. *Ann N Y Acad Sci* 2001; 938:26-34; discussion 34-5.:26-34.
184. Katayama Y, Hidalgo A, Furie BC, Vestweber D, Furie B, Frenette PS. PSGL-1 participates in E-selectin-mediated progenitor homing to bone marrow: evidence for cooperation between E-selectin ligands and alpha4 integrin. *Blood* 2003; 102:2060-7.
185. Petit I, Szyper-Kravitz M, Nagler A, Lahav M, Peled A, Habler L *et al*. G-CSF induces stem cell mobilization by decreasing bone marrow SDF-1 and up-regulating CXCR4. *Nat Immunol* 2002; 3:687-94.

Jeroen_Buijs_18.indd 58 26-11-2008 10:18:12

186. McQuibban GA, Butler GS, Gong JH, Bendall L, Power C, Clark-Lewis I *et al*. Matrix metalloproteinase activity inactivates the CXC chemokine stromal cell-derived factor-1. *J Biol Chem* 2001; 276:43503-8.
187. Katayama Y, Battista M, Kao WM, Hidalgo A, Peired AJ, Thomas SA *et al*. Signals from the sympathetic nervous system regulate hematopoietic stem cell egress from bone marrow. *Cell* 2006; 124:407-21.
188. Semerad CL, Christopher MJ, Liu F, Short B, Simmons PJ, Winkler I *et al*. G-CSF potently inhibits osteoblast activity and CXCL12 mRNA expression in the bone marrow. *Blood* 2005; 106:3020-7.
189. Blobe GC, Schiemann WP, Lodish HF. Role of transforming growth factor beta in human disease. *N Engl J Med* 2000; 342:1350-8.
190. Ducy P, Karsenty G. The family of bone morphogenetic proteins. *Kidney Int* 2000; 57:2207-14.
191. Itoh S, Itoh F, Goumans MJ, Ten Dijke P. Signaling of transforming growth factor-beta family members through Smad proteins. *Eur J Biochem* 2000; 267:6954-67.
192. Simic P, Vukicevic S. Bone morphogenetic proteins in development and homeostasis of kidney. *Cytokine Growth Factor Rev* 2005; 16:299-308.
193. Miyazono K, Maeda S, Imamura T. BMP receptor signaling: transcriptional targets, regulation of signals, and signaling cross-talk. *Cytokine Growth Factor Rev* 2005; 16:251-63.
194. Massague J. The transforming growth factor-beta family. *Annu Rev Cell Biol* 1990; 6:597-641.:597-641.
195. Assoian RK, Komoriya A, Meyers CA, Miller DM, Sporn MB. Transforming growth factor-beta in human platelets. Identification of a major storage site, purification, and characterization. *J Biol Chem* 1983; 258:7155-60.
196. Seyedin SM, Thompson AY, Bentz H, Rosen DM, McPherson JM, Conti A *et al*. Cartilage-inducing factor-A. Apparent identity to transforming growth factor-beta. *J Biol Chem* 1986; 261:5693-5.
197. Seyedin SM, Thomas TC, Thompson AY, Rosen DM, Piez KA. Purification and characterization of two cartilage-inducing factors from bovine demineralized bone. *Proc Natl Acad Sci U S A* 1985; 82:2267-71.
198. Janssens K, Ten Dijke P, Janssens S, Van Hul W. Transforming growth factor-beta1 to the bone. *Endocr Rev* 2005; 26:743-74.
199. Derynck R, Zhang YE. Smad-dependent and Smad-independent pathways in TGF-beta family signalling. *Nature* 2003; 425:577-84.
200. Massague J. How cells read TGF-beta signals. *Nat Rev Mol Cell Biol* 2000; 1:169-78.
201. Ten Dijke P, Yamashita H, Sampath TK, Reddi AH, Estevez M, Riddle DL *et al*. Identification of type I receptors for osteogenic protein-1 and bone morphogenetic protein-4. *J Biol Chem* 1994; 269:16985-8.
202. Liu F, Ventura F, Doody J, Massague J. Human type II receptor for bone morphogenic proteins (BMPs): extension of the two-kinase receptor model to the BMPs. *Mol Cell Biol* 1995; 15:3479-86.
203. Chen D, Zhao M, Mundy GR. Bone morphogenetic proteins. *Growth Factors* 2004; 22:233-41.
204. Miyazono K, Kusanagi K, Inoue H. Divergence and convergence of TGF-beta/BMP signaling. *J Cell Physiol* 2001; 187:265-76.
205. Ebisawa T, Tada K, Kitajima I, Tojo K, Sampath TK, Kawabata M *et al*. Characterization of bone morphogenetic protein-6 signaling pathways in osteoblast differentiation. *J Cell Sci* 1999; 112:3519-27.
206. Aoki H, Fujii M, Imamura T, Yagi K, Takehara K, Kato M *et al*. Synergistic effects of different bone morphogenetic protein type I receptors on alkaline phosphatase induction. *J Cell Sci* 2001; 114:1483-9.
207. Kim IY, Lee DH, Ahn HJ, Tokunaga H, Song W, Devereaux LM *et al*. Expression of bone morphogenetic protein receptors type-IA, -IB and -II correlates with tumor grade in human prostate cancer tissues. *Cancer Res* 2000; 60:2840-4.
208. Kim IY, Lee DH, Lee DK, Ahn HJ, Kim MM, Kim SJ *et al*. Loss of expression of bone morphogenetic protein receptor type II in human prostate cancer cells. *Oncogene* 2004; 23:7651-9.

209. Lopez-Casillas F, Cheifetz S, Doody J, Andres JL, Lane WS, Massague J. Structure and expression of the membrane proteoglycan betaglycan, a component of the TGF-beta receptor system. *Cell* 1991; 67:785-95.
210. Gougos A, Letarte M. Primary structure of endoglin, an RGD-containing glycoprotein of human endothelial cells. *J Biol Chem* 1990; 265:8361-4.
211. Letamendia A, Lastres P, Botella LM, Raab U, Langa C, Velasco B *et al*. Role of endoglin in cellular responses to transforming growth factor-beta. A comparative study with betaglycan. *J Biol Chem* 1998; 273:33011-9.
212. Scherner O, Meurer SK, Tihaa L, Gressner AM, Weiskirchen R. Endoglin differentially modulates antagonistic transforming growth factor-beta1 and BMP-7 signaling. *J Biol Chem* 2007; 282:13934-43.
213. Lopez-Casillas F, Wrana JL, Massague J. Betaglycan presents ligand to the TGF beta signaling receptor. *Cell* 1993; 73:1435-44.
214. Lewis KA, Gray PC, Blount AL, MacConell LA, Wiater E, Bilezikjian LM *et al*. Betaglycan binds inhibin and can mediate functional antagonism of activin signalling. *Nature* 2000; 404:411-4.
215. Yagi K, Goto D, Hamamoto T, Takenoshita S, Kato M, Miyazono K. Alternatively spliced variant of Smad2 lacking exon 3. Comparison with wild-type Smad2 and Smad3. *J Biol Chem* 1999; 274:703-9.
216. Piek E, Ju WJ, Heyer J, Escalante-Alcalde D, Stewart CL, Weinstein M *et al*. Functional characterization of transforming growth factor beta signaling in Smad2- and Smad3-deficient fibroblasts. *J Biol Chem* 2001; 276:19945-53.
217. Phanish MK, Wahab NA, Colville-Nash P, Hendry BM, Dockrell ME. The differential role of Smad2 and Smad3 in the regulation of pro-fibrotic TGFbeta1 responses in human proximal-tubule epithelial cells. *Biochem J* 2006; 393:601-7.
218. Chaudhry SS, Cain SA, Morgan A, Dallas SL, Shuttleworth CA, Kielty CM. Fibrillin-1 regulates the bioavailability of TGFbeta1. *J Cell Biol* 2007; 176:355-67.
219. Constam DB, Robertson EJ. Regulation of bone morphogenetic protein activity by pro domains and proprotein convertases. *J Cell Biol* 1999; 144:139-49.
220. Gregory KE, Ono RN, Charbonneau NL, Kuo CL, Keene DR, Bachinger HP *et al*. The prodomain of BMP-7 targets the BMP-7 complex to the extracellular matrix. *J Biol Chem* 2005;..
221. Sampath TK, Maliakal JC, Hauschka PV, Jones WK, Sasak H, Tucker RF *et al*. Recombinant human osteogenic protein-1 (hOP-1) induces new bone formation in vivo with a specific activity comparable with natural bovine osteogenic protein and stimulates osteoblast proliferation and differentiation in vitro. *J Biol Chem* 1992; 267:20352-62.
222. Ten Dijke P, Arthur HM. Extracellular control of TGFbeta signalling in vascular development and disease. *Nat Rev Mol Cell Biol* 2007; 8:857-69.
223. Annes JP, Munger JS, Rifkin DB. Making sense of latent TGFbeta activation. *J Cell Sci* 2003; 116:217-24.
224. Kanzaki T, Olofsson A, Moren A, Wernstedt C, Hellman U, Miyazono K *et al*. TGF-beta 1 binding protein: a component of the large latent complex of TGF-beta 1 with multiple repeat sequences. *Cell* 1990; 61:1051-61.
225. Saharinen J, Taipale J, Keski-Oja J. Association of the small latent transforming growth factor-beta with an eight cysteine repeat of its binding protein LTBP-1. *EMBO J* 1996; 15:245-53.
226. Dallas SL, Park-Snyder S, Miyazono K, Twardzik D, Mundy GR, Bonewald LF. Characterization and autoregulation of latent transforming growth factor beta (TGF beta) complexes in osteoblast-like cell lines. Production of a latent complex lacking the latent TGF beta-binding protein. *J Biol Chem* 1994; 269:6815-21.
227. Saharinen J, Keski-Oja J. Specific sequence motif of 8-Cys repeats of TGF-beta binding proteins, LTBPs, creates a hydrophobic interaction surface for binding of small latent TGF-beta. *Mol Biol Cell* 2000; 11:2691-704.
228. Isogai Z, Ono RN, Ushiro S, Keene DR, Chen Y, Mazzieri R *et al*. Latent transforming growth factor beta-binding protein 1 interacts with fibrillin and is a microfibril-associated protein. *J Biol Chem* 2003; 278:2750-7.

Jeroen_Buijs_18.indd 60 26-11-2008 10:18:12

229. Groppe J, Greenwald J, Wiater E, Rodriguez-Leon J, Economides AN, Kwiatkowski W *et al*. Structural basis of BMP signalling inhibition by the cystine knot protein Noggin. *Nature* 2002; 420:636-42.
230. Ross JJ, Shimmi O, Vilmos P, Petryk A, Kim H, Gaudenz K *et al*. Twisted gastrulation is a conserved extracellular BMP antagonist. *Nature* 2001; 410:479-83.
231. Bachiller D, Klingensmith J, Kemp C, Belo JA, Anderson RM, May SR *et al*. The organizer factors Chordin and Noggin are required for mouse forebrain development. *Nature* 2000; 403:658-61.
232. Pearce JJ, Penny G, Rossant J. A mouse cerberus/Dan-related gene family. *Dev Biol* 1999; 209:98-110.
233. Gazzerro E, Canalis E. Bone morphogenetic proteins and their antagonists. *Rev Endocr Metab Disord* 2006; 7:51-65.
234. Massague J, Seoane J, Wotton D. Smad transcription factors. *Genes Dev* 2005; 19:2783-810.
235. Afrakhte M, Moren A, Jossan S, Itoh S, Sampath K, Westermark B *et al*. Induction of inhibitory Smad6 and Smad7 mRNA by TGF-beta family members. *Biochem Biophys Res Commun* 1998; %19;249:505-11.
236. Ishisaki A, Yamato K, Hashimoto S, Nakao A, Tamaki K, Nonaka K *et al*. Differential inhibition of Smad6 and Smad7 on bone morphogenetic protein- and activin-mediated growth arrest and apoptosis in B cells. *J Biol Chem* 1999; 274:13637-42.
237. Nakao A, Afrakhte M, Moren A, Nakayama T, Christian JL, Heuchel R *et al*. Identification of Smad7, a TGFbeta-inducible antagonist of TGF-beta signalling. *Nature* 1997; 389:631-5.
238. Stroschein SL, Wang W, Zhou S, Zhou Q, Luo K. Negative feedback regulation of TGF-beta signaling by the SnoN oncoprotein. *Science* 1999; 286:771-4.
239. Takase M, Imamura T, Sampath TK, Takeda K, Ichijo H, Miyazono K *et al*. Induction of Smad6 mRNA by bone morphogenetic proteins. *Biochem Biophys Res Commun* 1998; 244:26-9.
240. Onichtchouk D, Chen YG, Dosch R, Gawantka V, Delius H, Massague J *et al*. Silencing of TGF-beta signalling by the pseudoreceptor BAMBI. *Nature* 1999; 401:480-5.
241. Imamura T, Takase M, Nishihara A, Oeda E, Hanai J, Kawabata M *et al*. Smad6 inhibits signalling by the TGF-beta superfamily. *Nature* 1997; 389:622-6.
242. Hayashi H, Abdollah S, Qiu Y, Cai J, Xu YY, Grinnell BW *et al*. The MAD-related protein Smad7 associates with the TGFbeta receptor and functions as an antagonist of TGFbeta signaling. *Cell* 1997; 89:1165-73.
243. Hata A, Lagna G, Massague J, Hemmati-Brivanlou A. Smad6 inhibits BMP/Smad1 signaling by specifically competing with the Smad4 tumor suppressor. *Genes Dev* 1998; 12:186-97.
244. Lin X, Liang M, Feng XH. Smurf2 is a ubiquitin E3 ligase mediating proteasome-dependent degradation of Smad2 in transforming growth factor-beta signaling. *J Biol Chem* 2000; 275:36818-22.
245. Zhang Y, Chang C, Gehling DJ, Hemmati-Brivanlou A, Derynck R. Regulation of Smad degradation and activity by Smurf2, an E3 ubiquitin ligase. *Proc Natl Acad Sci U S A* 2001; 98:974-9.
246. Zhu H, Kavsak P, Abdollah S, Wrana JL, Thomsen GH. A SMAD ubiquitin ligase targets the BMP pathway and affects embryonic pattern formation. *Nature* 1999; 400:687-93.
247. Murakami G, Watabe T, Takaoka K, Miyazono K, Imamura T. Cooperative inhibition of bone morphogenetic protein signaling by Smurf1 and inhibitory Smads. *Mol Biol Cell* 2003; 14:2809-17.
248. Kavsak P, Rasmussen RK, Causing CG, Bonni S, Zhu H, Thomsen GH *et al*. Smad7 binds to Smurf2 to form an E3 ubiquitin ligase that targets the TGF beta receptor for degradation. *Mol Cell* 2000; 6:1365-75.
249. Suzuki C, Murakami G, Fukuchi M, Shimanuki T, Shikauchi Y, Imamura T *et al*. Smurf1 regulates the inhibitory activity of Smad7 by targeting Smad7 to the plasma membrane. *J Biol Chem* 2002; 277:39919-25.
250. Tajima Y, Goto K, Yoshida M, Shinomiya K, Sekimoto T, Yoneda Y *et al*. Chromosomal region maintenance 1 (CRM1)-dependent nuclear export of Smad ubiquitin regulatory factor 1 (Smurf1) is essential for negative regulation of transforming growth factor-beta signaling by Smad7. *J Biol Chem* 2003; 278:10716-21.

251. Luo K, Stroschein SL, Wang W, Chen D, Martens E, Zhou S *et al*. The Ski oncoprotein interacts with the Smad proteins to repress TGFbeta signaling. *Genes Dev* 1999; 13:2196-206.
252. Sun Y, Liu X, Ng-Eaton E, Lodish HF, Weinberg RA. SnoN and Ski protooncoproteins are rapidly degraded in response to transforming growth factor beta signaling. *Proc Natl Acad Sci U S A* 1999; 96:12442-7.
253. Akiyoshi S, Inoue H, Hanai J, Kusanagi K, Nemoto N, Miyazono K *et al*. c-Ski acts as a transcriptional co-repressor in transforming growth factor-beta signaling through interaction with smads. *J Biol Chem* 1999; 274:35269-77.
254. Sun Y, Liu X, Eaton EN, Lane WS, Lodish HF, Weinberg RA. Interaction of the Ski oncoprotein with Smad3 regulates TGF-beta signaling. *Mol Cell* 1999; 4:499-509.
255. Takeda M, Mizuide M, Oka M, Watabe T, Inoue H, Suzuki H *et al*. Interaction with Smad4 is indispensable for suppression of BMP signaling by c-Ski. *Mol Biol Cell* 2004; 15:963-72.
256. Wang W, Mariani FV, Harland RM, Luo K. Ski represses bone morphogenic protein signaling in Xenopus and mammalian cells. *Proc Natl Acad Sci U S A* 2000; %19;97:14394-9.
257. Xu W, Angelis K, Danielpour D, Haddad MM, Bischof O, Campisi J *et al*. Ski acts as a co-repressor with Smad2 and Smad3 to regulate the response to type beta transforming growth factor. *Proc Natl Acad Sci U S A* 2000; 97:5924-9.
258. Yoshida Y, von Bubnoff A, Ikematsu N, Blitz IL, Tsuzuku JK, Yoshida EH *et al*. Tob proteins enhance inhibitory Smad-receptor interactions to repress BMP signaling. *Mech Dev* 2003; 120:629-37.
259. Yoshida Y, Tanaka S, Umemori H, Minowa O, Usui M, Ikematsu N *et al*. Negative regulation of BMP/Smad signaling by Tob in osteoblasts. *Cell* 2000; 103:1085-97.
260. Calonge MJ, Massague J. Smad4/DPC4 silencing and hyperactive Ras jointly disrupt transforming growth factor-beta antiproliferative responses in colon cancer cells. *J Biol Chem* 1999; %19;274:33637-43.
261. Kretzschmar M, Doody J, Massague J. Opposing BMP and EGF signalling pathways converge on the TGF-beta family mediator Smad1. *Nature* 1997; 389:618-22.
262. Kretzschmar M, Doody J, Timokhina I, Massague J. A mechanism of repression of TGFbeta/Smad signaling by oncogenic Ras. *Genes Dev* 1999; 13:804-16.
263. Ten Dijke P, Korchynskyi O, Valdimarsdottir G, Goumans MJ. Controlling cell fate by bone morphogenetic protein receptors. *Mol Cell Endocrinol* 2003; 211:105-13.
264. Reddi AH. Role of morphogenetic proteins in skeletal tissue engineering and regeneration. *Nat Biotechnol* 1998; 16:247-52.
265. Graff JM. Embryonic patterning: to BMP or not to BMP, that is the question. *Cell* 1997; 89:171-4.
266. Barnes J, Anthony CT, Wall N, Steiner MS. Bone morphogenetic protein-6 expression in normal and malignant prostate. *World J Urol* 1995; 13:337-43.
267. Hamdy FC, Autzen P, Robinson MC, Horne CH, Neal DE, Robson CN. Immunolocalization and messenger RNA expression of bone morphogenetic protein-6 in human benign and malignant prostatic tissue. *Cancer Res* 1997; 57:4427-31.
268. Clement JH, Raida M, Sanger J, Bicknell R, Liu J, Naumann A *et al*. Bone morphogenetic protein 2 (BMP-2) induces in vitro invasion and in vivo hormone independent growth of breast carcinoma cells. *Int J Oncol* 2005; 27:401-7.
269. Dai J, Keller J, Zhang J, Lu Y, Yao Z, Keller ET. Bone morphogenetic protein-6 promotes osteoblastic prostate cancer bone metastases through a dual mechanism. *Cancer Res* 2005; 65:8274-85.
270. Feeley BT, Gamradt SC, Hsu WK, Liu N, Krenek L, Robbins P *et al*. Influence of BMPs on the formation of osteoblastic lesions in metastatic prostate cancer. *J Bone Miner Res* 2005; 20:2189-99.
271. Feeley BT, Krenek L, Liu N, Hsu WK, Gamradt SC, Schwarz EM *et al*. Overexpression of noggin inhibits BMP-mediated growth of osteolytic prostate cancer lesions. *Bone* 2006; 38:154-66.
272. Maliakal JC, Asahina I, Hauschka PV, Sampath TK. Osteogenic protein-1 (BMP-7) inhibits cell proliferation and stimulates the expression of markers characteristic of osteoblast phenotype in rat osteosarcoma (17/2.8) cells. *Growth Factors* 1994; 11:227-34.
273. Yeh LC, Adamo ML, Olson MS, Lee JC. Osteogenic protein-1 and insulin-like growth factor I synergistically stimulate rat osteoblastic cell differentiation and proliferation. *Endocrinology* 1997; 138:4181-90.

Jeroen_Buijs_18.indd 62 26-11-2008 10:18:12

274. Yang S, Lim M, Pham LK, Kendall SE, Reddi AH, Altieri DC *et al*. Bone morphogenetic protein 7 protects prostate cancer cells from stress-induced apoptosis via both Smad and c-Jun NH2-terminal kinase pathways. *Cancer Res* 2006; 66:4285-90.
275. Seoane J. Escaping from the TGFbeta anti-proliferative control. *Carcinogenesis* 2006; 27:2148-56.
276. Gorska AE, Jensen RA, Shyr Y, Aakre ME, Bhowmick NA, Moses HL. Transgenic Mice Expressing a Dominant-Negative Mutant Type II Transforming Growth Factor-beta Receptor Exhibit Impaired Mammary Development and Enhanced Mammary Tumor Formation. *Am J Pathol* 2003; 163:1539-49.
277. Muraoka RS, Dumont N, Ritter CA, Dugger TC, Brantley DM, Chen J *et al*. Blockade of TGF-beta inhibits mammary tumor cell viability, migration, and metastases. *J Clin Invest* 2002; 109:1551-9.
278. Yang YA, Dukhanina O, Tang B, Mamura M, Letterio JJ, MacGregor J *et al*. Lifetime exposure to a soluble TGF-beta antagonist protects mice against metastasis without adverse side effects. *J Clin Invest* 2002; 109:1607-15.
279. Yingling JM, Blanchard KL, Sawyer JS. Development of TGF-beta signalling inhibitors for cancer therapy. *Nat Rev Drug Discov* 2004; 3:1011-22.
280. Ma L, Lu MF, Schwartz RJ, Martin JF. Bmp2 is essential for cardiac cushion epithelial-mesenchymal transition and myocardial patterning. *Development* 2005; 132:5601-11.
281. Theriault BL, Shepherd TG, Mujoomdar ML, Nachtigal MW. BMP4 induces EMT and Rho GTPase activation in human ovarian cancer cells. *Carcinogenesis* 2007; 28:1153-62.
282. Zeisberg M, Shah AA, Kalluri R. Bone morphogenic protein-7 induces mesenchymal to epithelial transition in adult renal fibroblasts and facilitates regeneration of injured kidney. *J Biol Chem* 2005; 280:8094-100.
283. Kalluri R, Neilson EG. Epithelial-mesenchymal transition and its implications for fibrosis. *J Clin Invest* 2003; 112:1776-84.
284. Hruska KA, Guo G, Wozniak M, Martin D, Miller S, Liapis H *et al*. Osteogenic protein-1 prevents renal fibrogenesis associated with ureteral obstruction. *Am J Physiol Renal Physiol* 2000; 279:F130-F143.
285. Wang S, Hirschberg R. BMP7 antagonizes TGF-beta -dependent fibrogenesis in mesangial cells. *Am J Physiol Renal Physiol* 2003; 284:F1006-F1013.
286. Gould SE, Day M, Jones SS, Dorai H. BMP-7 regulates chemokine, cytokine, and hemodynamic gene expression in proximal tubule cells. *Kidney Int* 2002; 61:51-60.
287. Vukicevic S, Basic V, Rogic D, Basic N, Shih MS, Shepard A *et al*. Osteogenic protein-1 (bone morphogenetic protein-7) reduces severity of injury after ischemic acute renal failure in rat. *J Clin Invest* 1998; 102:202-14.
288. Wang S, Chen Q, Simon TC, Strebeck F, Chaudhary L, Morrissey J *et al*. Bone morphogenic protein-7 (BMP-7), a novel therapy for diabetic nephropathy. *Kidney Int* 2003; 63:2037-49.
289. Zeisberg M, Hanai J, Sugimoto H, Mammoto T, Charytan D, Strutz F *et al*. BMP-7 counteracts TGF-beta1-induced epithelial-to-mesenchymal transition and reverses chronic renal injury. *Nat Med* 2003; 9:964-8.
290. Gonzalez EA, Lund RJ, Martin KJ, McCartney JE, Tondravi MM, Sampath TK *et al*. Treatment of a murine model of high-turnover renal osteodystrophy by exogenous BMP-7. *Kidney Int* 2002; 61:1322-31.
291. Lund RJ, Davies MR, Brown AJ, Hruska KA. Successful treatment of an adynamic bone disorder with bone morphogenetic protein-7 in a renal ablation model. *J Am Soc Nephrol* 2004; 15:359-69.
292. Davies MR, Lund RJ, Hruska KA. BMP-7 is an efficacious treatment of vascular calcification in a murine model of atherosclerosis and chronic renal failure. *J Am Soc Nephrol* 2003; 14:1559-67.
293. Giannoudis PV, Tzioupis C. Clinical applications of BMP-7: the UK perspective. *Injury* 2005; 36 Suppl 3:S47-S50.
294. Springer TA. Traffic signals for lymphocyte recirculation and leukocyte emigration: the multistep paradigm. *Cell* 1994; 76:301-14.
295. Garlanda C, Dejana E. Heterogeneity of endothelial cells. Specific markers. *Arterioscler Thromb Vasc Biol* 1997; 17:1193-202.

296. Dimitroff CJ, Descheny L, Trujillo N, Kim R, Nguyen V, Huang W *et al*. Identification of leukocyte E-selectin ligands, P-selectin glycoprotein ligand-1 and E-selectin ligand-1, on human metastatic prostate tumor cells. *Cancer Res* 2005; 65:5750-60.
297. Dimitroff CJ, Lechpammer M, Long-Woodward D, Kutok JL. Rolling of human bone-metastatic prostate tumor cells on human bone marrow endothelium under shear flow is mediated by E-selectin. *Cancer Res* 2004; 64:5261-9.
298. Sipkins DA, Wei X, Wu JW, Runnels JM, Cote D, Means TK *et al*. In vivo imaging of specialized bone marrow endothelial microdomains for tumour engraftment. *Nature* 2005; 435:969-73.
299. Muller A, Homey B, Soto H, Ge N, Catron D, Buchanan ME *et al*. Involvement of chemokine receptors in breast cancer metastasis. *Nature* 2001; 410:50-6.
300. Sun YX, Schneider A, Jung Y, Wang J, Dai J, Wang J *et al*. Skeletal localization and neutralization of the SDF-1(CXCL12)/CXCR4 axis blocks prostate cancer metastasis and growth in osseous sites in vivo. *J Bone Miner Res* 2005; 20:318-29.
301. Taichman RS, Cooper C, Keller ET, Pienta KJ, Taichman NS, McCauley LK. Use of the stromal cell-derived factor-1/CXCR4 pathway in prostate cancer metastasis to bone. *Cancer Res* 2002; 62:1832-7.
302. Guo W, Giancotti FG. Integrin signalling during tumour progression. *Nat Rev Mol Cell Biol* 2004; 5:816-26.
303. Sun YX, Fang M, Wang J, Cooper CR, Pienta KJ, Taichman RS. Expression and activation of alpha(v)beta(3) integrins by SDF-1/CXC12 increases the aggressiveness of prostate cancer cells. *Prostate* 2007; 67:61-73.
304. Harms JF, Welch DR, Samant RS, Shevde LA, Miele ME, Babu GR *et al*. A small molecule antagonist of the alpha(v)beta3 integrin suppresses MDA-MB-435 skeletal metastasis. *Clin Exp Metastasis* 2004; 21:119-28.
305. Zhao Y, Bachelier R, Treilleux I, Pujuguet P, Peyruchaud O, Baron R *et al*. Tumor alphavbeta3 integrin is a therapeutic target for breast cancer bone metastases. *Cancer Res* 2007; 67:5821-30.
306. McCabe NP, De S, Vasanji A, Brainard J, Byzova TV. Prostate cancer specific integrin alphavbeta3 modulates bone metastatic growth and tissue remodeling. *Oncogene* 2007; 26:6238-43.
307. Pecheur I, Peyruchaud O, Serre CM, Guglielmi J, Voland C, Bourre F *et al*. Integrin alpha(v) beta3 expression confers on tumor cells a greater propensity to metastasize to bone. *FASEB J* 2002; 16:1266-8.
308. Sloan EK, Pouliot N, Stanley KL, Chia J, Moseley JM, Hards DK *et al*. Tumor-specific expression of alphavbeta3 integrin promotes spontaneous metastasis of breast cancer to bone. *Breast Cancer Res* 2006; 8:R20.
309. Karadag A, Ogbureke KU, Fedarko NS, Fisher LW. Bone sialoprotein, matrix metalloproteinase 2, and alpha(v)beta3 integrin in osteotropic cancer cell invasion. *J Natl Cancer Inst* 2004; 96:956-65.
310. Rolli M, Fransvea E, Pilch J, Saven A, Felding-Habermann B. Activated integrin alphavbeta3 cooperates with metalloproteinase MMP-9 in regulating migration of metastatic breast cancer cells. *Proc Natl Acad Sci U S A* 2003; 100:9482-7.
311. Hill A, McFarlane S, Johnston PG, Waugh DJ. The emerging role of CD44 in regulating skeletal micrometastasis. *Cancer Lett* 2006; 237:1-9.
312. Kucia M, Reca R, Miekus K, Wanzeck J, Wojakowski W, Janowska-Wieczorek A *et al*. Trafficking of normal stem cells and metastasis of cancer stem cells involve similar mechanisms: pivotal role of the SDF-1-CXCR4 axis. *Stem Cells* 2005; 23:879-94.
313. Bellahcene A, Castronovo V. Increased expression of osteonectin and osteopontin, two bone matrix proteins, in human breast cancer. *Am J Pathol* 1995; 146:95-100.
314. Bellahcene A, Kroll M, Liebens F, Castronovo V. Bone sialoprotein expression in primary human breast cancer is associated with bone metastases development. *J Bone Miner Res* 1996; 11:665-70.
315. Knerr K, Ackermann K, Neidhart T, Pyerin W. Bone metastasis: Osteoblasts affect growth and adhesion regulons in prostate tumor cells and provoke osteomimicry. *Int J Cancer* 2004; 111:152-9.

Jeroen_Buijs_18.indd 64 26-11-2008 10:18:13

316. Koeneman KS, Yeung F, Chung LW. Osteomimetic properties of prostate cancer cells: a hypothesis supporting the predilection of prostate cancer metastasis and growth in the bone environment. *Prostate* 1999; 39:246-61.
317. Kaplan RN, Riba RD, Zacharoulis S, Bramley AH, Vincent L, Costa C *et al*. VEGFR1-positive hematopoietic bone marrow progenitors initiate the pre-metastatic niche. *Nature* 2005; 438:820-7.
318. Kaplan RN, Rafii S, Lyden D. Preparing the "soil": the premetastatic niche. *Cancer Res* 2006; 66:11089-93.
319. Arguello F, Baggs RB, Graves BT, Harwell SE, Cohen HJ, Frantz CN. Effect of IL-1 on experimental bone/bone-marrow metastases. *Int J Cancer* 1992; 52:802-7.
320. Kostenuik PJ, Singh G, Suyama KL, Orr FW. Stimulation of bone resorption results in a selective increase in the growth rate of spontaneously metastatic Walker 256 cancer cells in bone. *Clin Exp Metastasis* 1992; 10:411-8.
321. Schneider A, Kalikin LM, Mattos AC, Keller ET, Allen MJ, Pienta KJ *et al*. Bone turnover mediates preferential localization of prostate cancer in the skeleton. *Endocrinology* 2005; 146:1727-36.
322. Brown JE, Thomson CS, Ellis SP, Gutcher SA, Purohit OP, Coleman RE. Bone resorption predicts for skeletal complications in metastatic bone disease. *Br J Cancer* 2003; 89:2031-7.
323. Brown JE, Cook RJ, Major P, Lipton A, Saad F, Smith M *et al*. Bone turnover markers as predictors of skeletal complications in prostate cancer, lung cancer, and other solid tumors. *J Natl Cancer Inst* 2005; 97:59-69.
324. Coleman RE, Major P, Lipton A, Brown JE, Lee KA, Smith M *et al*. Predictive value of bone resorption and formation markers in cancer patients with bone metastases receiving the bisphosphonate zoledronic acid. *J Clin Oncol* 2005; 23:4925-35.
325. Costa L, Demers LM, Gouveia-Oliveira A, Schaller J, Costa EB, de Moura MC *et al*. Prospective evaluation of the peptide-bound collagen type I cross-links N-telopeptide and C-telopeptide in predicting bone metastases status. *J Clin Oncol* 2002; 20:850-6.
326. Garnero P. Markers of bone turnover in prostate cancer. *Cancer Treat Rev* 2001; 27:187-92.
327. Blair JM, Zhou H, Seibel MJ, Dunstan CR. Mechanisms of disease: roles of OPG, RANKL and RANK in the pathophysiology of skeletal metastasis. *Nat Clin Pract Oncol* 2006; 3:41-9.
328. Clohisy DR, Ramnaraine ML. Osteoclasts are required for bone tumors to grow and destroy bone. *J Orthop Res* 1998; 16:660-6.
329. Kakonen SM, Mundy GR. Mechanisms of osteolytic bone metastases in breast carcinoma. *Cancer* 2003; 97:834-9.
330. Thomas RJ, Guise TA, Yin JJ, Elliott J, Horwood NJ, Martin TJ *et al*. Breast cancer cells interact with osteoblasts to support osteoclast formation. *Endocrinology* 1999; 140:4451-8.
331. Southby J, Kissin MW, Danks JA, Hayman JA, Moseley JM, Henderson MA *et al*. Immunohistochemical localization of parathyroid hormone-related protein in human breast cancer. *Cancer Res* 1990; 50:7710-6.
332. Iddon J, Bundred NJ, Hoyland J, Downey SE, Baird P, Salter D *et al*. Expression of parathyroid hormone-related protein and its receptor in bone metastases from prostate cancer. *J Pathol* 2000; 191:170-4.
333. Guise TA, Yin JJ, Taylor SD, Kumagai Y, Dallas M, Boyce BF *et al*. Evidence for a causal role of parathyroid hormone-related protein in the pathogenesis of human breast cancer-mediated osteolysis. *J Clin Invest* 1996; 98:1544-9.
334. Powell GJ, Southby J, Danks JA, Stillwell RG, Hayman JA, Henderson MA *et al*. Localization of parathyroid hormone-related protein in breast cancer metastases: increased incidence in bone compared with other sites. *Cancer Res* 1991; 51:3059-61.
335. Kissin MW, Henderson MA, Danks JA, Hayman JA, Bennett RC, Martin TJ. Parathyroid hormone related protein in breast cancers of widely varying prognosis. *Eur J Surg Oncol* 1993; 19:134-42.
336. Bundred NJ, Walker RA, Ratcliffe WA, Warwick J, Morrison JM, Ratcliffe JG. Parathyroid hormone related protein and skeletal morbidity in breast cancer. *Eur J Cancer* 1992; 28:690-2.
337. Henderson M, Danks J, Moseley J, Slavin J, Harris T, McKinlay M *et al*. Parathyroid hormone-related protein production by breast cancers, improved survival, and reduced bone metastases. *J Natl Cancer Inst* 2001; 93:234-7.

338. Henderson MA, Danks JA, Slavin JL, Byrnes GB, Choong PF, Spillane JB *et al*. Parathyroid hormone-related protein localization in breast cancers predict improved prognosis. *Cancer Res* 2006; 66:2250-6.
339. Kohno N, Kitazawa S, Sakoda Y, Kanbara Y, Furuya Y, Ohashi O *et al*. Parathyroid Hormone-related Protein in Breast Cancer Tissues: Relationship between Primary and Metastatic Sites. *Breast Cancer* 1994; 1:43-9.
340. Yin JJ, Selander K, Chirgwin JM, Dallas M, Grubbs BG, Wieser R *et al*. TGF-beta signaling blockade inhibits PTHrP secretion by breast cancer cells and bone metastases development. *J Clin Invest* 1999; 103:197-206.
341. Virk MS, Lieberman JR. Tumor metastasis to bone. *Arthritis Res Ther* 2007; 9 Suppl 1:S5.:S5.
342. Bendre MS, Montague DC, Peery T, Akel NS, Gaddy D, Suva LJ. Interleukin-8 stimulation of osteoclastogenesis and bone resorption is a mechanism for the increased osteolysis of metastatic bone disease. *Bone* 2003; 33:28-37.
343. Park BK, Zhang H, Zeng Q, Dai J, Keller ET, Giordano T *et al*. NF-kappaB in breast cancer cells promotes osteolytic bone metastasis by inducing osteoclastogenesis via GM-CSF. *Nat Med* 2007; 13:62-9.
344. Cecchini MG, Wetterwald A, van der Pluijm G, Thalmann GN. Molecular and Biological Mechanisms of Bone Metastasis. *EAU Update Series* 2005; 3:214-26.
345. Maeda H, Koizumi M, Yoshimura K, Yamauchi T, Kawai T, Ogata E. Correlation between bone metabolic markers and bone scan in prostatic cancer. *J Urol* 1997; 157:539-43.
346. Ye L, Lewis-Russell JM, Kyanaston HG, Jiang WG. Bone morphogenetic proteins and their receptor signaling in prostate cancer. *Histol Histopathol* 2007; 22:1129-47.
347. Dai J, Kitagawa Y, Zhang J, Yao Z, Mizokami A, Cheng S *et al*. Vascular endothelial growth factor contributes to the prostate cancer-induced osteoblast differentiation mediated by bone morphogenetic protein. *Cancer Res* 2004; 64:994-9.
348. Schwaninger R, Rentsch CA, Wetterwald A, van der Horst G, van Bezooijen RL, van der Pluijm G *et al*. Lack of noggin expression by cancer cells is a determinant of the osteoblast response in bone metastases. *Am J Pathol* 2007; 170:160-75.
349. Hall CL, Kang S, MacDougald OA, Keller ET. Role of Wnts in prostate cancer bone metastases. *J Cell Biochem* 2006; 97:661-72.
350. Tian E, Zhan F, Walker R, Rasmussen E, Ma Y, Barlogie B *et al*. The role of the Wnt-signaling antagonist DKK1 in the development of osteolytic lesions in multiple myeloma. *N Engl J Med* 2003; 349:2483-94.
351. Voorzanger-Rousselot N, Goehrig D, Journe F, Doriath V, Body JJ, Clezardin P *et al*. Increased Dickkopf-1 expression in breast cancer bone metastases. *Br J Cancer* 2007; 97:964-70.
352. Logothetis CJ, Lin SH. Osteoblasts in prostate cancer metastasis to bone. *Nat Rev Cancer* 2005; 5:21-8.
353. Nelson JB, Hedican SP, George DJ, Reddi AH, Piantadosi S, Eisenberger MA *et al*. Identification of endothelin-1 in the pathophysiology of metastatic adenocarcinoma of the prostate. *Nat Med* 1995; 1:944-9.
354. Nelson JB, Nguyen SH, Wu-Wong JR, Opgenorth TJ, Dixon DB, Chung LW *et al*. New bone formation in an osteoblastic tumor model is increased by endothelin-1 overexpression and decreased by endothelin A receptor blockade. *Urology* 1999; 53:1063-9.
355. Banerjee S, Hussain M, Wang Z, Saliganan A, Che M, Bonfil D *et al*. In vitro and in vivo molecular evidence for better therapeutic efficacy of ABT-627 and taxotere combination in prostate cancer. *Cancer Res* 2007; 67:3818-26.
356. Yin JJ, Mohammad KS, Kakonen SM, Harris S, Wu-Wong JR, Wessale JL *et al*. A causal role for endothelin-1 in the pathogenesis of osteoblastic bone metastases. *Proc Natl Acad Sci U S A* 2003; 100:10954-9.
357. Rabbani SA, Desjardins J, Bell AW, Banville D, Mazar A, Henkin J *et al*. An amino-terminal fragment of urokinase isolated from a prostate cancer cell line (PC-3) is mitogenic for osteoblast-like cells. *Biochem Biophys Res Commun* 1990; 173:1058-64.
358. Cohen P, Peehl DM, Graves HC, Rosenfeld RG. Biological effects of prostate specific antigen as an insulin-like growth factor binding protein-3 protease. *J Endocrinol* 1994; 142:407-15.
359. Cramer SD, Chen Z, Peehl DM. Prostate specific antigen cleaves parathyroid hormone-related protein in the PTH-like domain: inactivation of PTHrP-stimulated cAMP accumulation in mouse osteoblasts. *J Urol* 1996; 156:526-31.

Jeroen_Buijs_18.indd 66 26-11-2008 10:18:13

360. Singh AS, Figg WD. In vivo models of prostate cancer metastasis to bone. *J Urol* 2005; 174:820-6.
361. Rosol TJ, Tannehill-Gregg SH, LeRoy BE, Mandl S, Contag CH. Animal models of bone metastasis. *Cancer* 2003; 97:748-57.
362. Waters DJ, Sakr WA, Hayden DW, Lang CM, McKinney L, Murphy GP *et al*. Workgroup 4: spontaneous prostate carcinoma in dogs and nonhuman primates. *Prostate* 1998; 36:64-7.
363. Pollard M. Lobund-Wistar rat model of prostate cancer in man. *Prostate* 1998; 37:1-4.
364. Varma VA, Austin GE. Morphologic characterization of early prostatic carcinomas in the ACI rat: a light and electron microscopic study. *Exp Mol Pathol* 1990; 52:202-11.
365. Donehower LA, Harvey M, Slagle BL, McArthur MJ, Montgomery CA, Jr., Butel JS *et al*. Mice deficient for p53 are developmentally normal but susceptible to spontaneous tumours. *Nature* 1992; %19;356:215-21.
366. Muraoka RS, Koh Y, Roebuck LR, Sanders ME, Brantley-Sieders D, Gorska AE *et al*. Increased malignancy of Neu-induced mammary tumors overexpressing active transforming growth factor beta1. *Mol Cell Biol* 2003; 23:8691-703.
367. Duan W, Gabril MY, Moussa M, Chan FL, Sakai H, Fong G *et al*. Knockin of SV40 Tag oncogene in a mouse adenocarcinoma of the prostate model demonstrates advantageous features over the transgenic model. *Oncogene* 2005; 24:1510-24.
368. Derksen PW, Liu X, Saridin F, van der GH, Zevenhoven J, Evers B *et al*. Somatic inactivation of E-cadherin and p53 in mice leads to metastatic lobular mammary carcinoma through induction of anoikis resistance and angiogenesis. *Cancer Cell* 2006; 10:437-49.
369. Kostenuik PJ, Singh G, Suyama KL, Orr FW. A quantitative model for spontaneous bone metastasis: evidence for a mitogenic effect of bone on Walker 256 cancer cells. *Clin Exp Metastasis* 1992; 10:403-10.
370. Berlin O, Samid D, Donthineni-Rao R, Akeson W, Amiel D, Woods VL, Jr. Development of a novel spontaneous metastasis model of human osteosarcoma transplanted orthotopically into bone of athymic mice. *Cancer Res* 1993; 53:4890-5.
371. Corey E, Quinn JE, Bladou F, Brown LG, Roudier MP, Brown JM *et al*. Establishment and characterization of osseous prostate cancer models: intra-tibial injection of human prostate cancer cells. *Prostate* 2002; 52:20-33.
372. Arguello F, Baggs RB, Frantz CN. A murine model of experimental metastasis to bone and bone marrow. *Cancer Res* 1988; 48:6876-81.
373. Pettaway CA, Pathak S, Greene G, Ramirez E, Wilson MR, Killion JJ *et al*. Selection of highly metastatic variants of different human prostatic carcinomas using orthotopic implantation in nude mice. *Clin Cancer Res* 1996; 2:1627-36.
374. Morony S, Capparelli C, Sarosi I, Lacey DL, Dunstan CR, Kostenuik PJ. Osteoprotegerin inhibits osteolysis and decreases skeletal tumor burden in syngeneic and nude mouse models of experimental bone metastasis. *Cancer Res* 2001; 61:4432-6.
375. Sasaki A, Boyce BF, Story B, Wright KR, Chapman M, Boyce R *et al*. Bisphosphonate risedronate reduces metastatic human breast cancer burden in bone in nude mice. *Cancer Res* 1995; 55:3551-7.
376. Yoneda T. Arterial microvascularization and breast cancer colonization in bone. *Histol Histopathol* 1997; 12:1145-9.
377. Kuperwasser C, Chavarria T, Wu M, Magrane G, Gray JW, Carey L *et al*. Reconstruction of functionally normal and malignant human breast tissues in mice. *Proc Natl Acad Sci U S A* 2004; 101:4966-71.
378. Lelekakis M, Moseley JM, Martin TJ, Hards D, Williams E, Ho P *et al*. A novel orthotopic model of breast cancer metastasis to bone. *Clin Exp Metastasis* 1999; 17:163-70.
379. Aslakson CJ, Miller FR. Selective events in the metastatic process defined by analysis of the sequential dissemination of subpopulations of a mouse mammary tumor. *Cancer Res* 1992; 52:1399-405.
380. Hoffman RM. Orthotopic metastatic mouse models for anticancer drug discovery and evaluation: a bridge to the clinic. *Invest New Drugs* 1999; 17:343-59.
381. Thalmann GN, Anezinis PE, Chang SM, Zhau HE, Kim EE, Hopwood VL *et al*. Androgen-independent cancer progression and bone metastasis in the LNCaP model of human prostate cancer. *Cancer Res* 1994; 54:2577-81.
382. Thalmann GN, Sikes RA, Wu TT, Degeorges A, Chang SM, Ozen M *et al*. LNCaP progression model of human prostate cancer: androgen-independence and osseous metastasis. *Prostate* 2000; 44:91-103.

383. Wu TT, Sikes RA, Cui Q, Thalmann GN, Kao C, Murphy CF *et al*. Establishing human prostate cancer cell xenografts in bone: induction of osteoblastic reaction by prostate-specific antigen-producing tumors in athymic and SCID/bg mice using LNCaP and lineage-derived metastatic sublines. *Int J Cancer* 1998; 77:887-94.
384. Nemeth JA, Harb JF, Barroso U, Jr., He Z, Grignon DJ, Cher ML. Severe combined immunodeficient-hu model of human prostate cancer metastasis to human bone. *Cancer Res* 1999; 59:1987-93.
385. Yonou H, Yokose T, Kamijo T, Kanomata N, Hasebe T, Nagai K *et al*. Establishment of a novel species- and tissue-specific metastasis model of human prostate cancer in humanized non-obese diabetic/severe combined immunodeficient mice engrafted with human adult lung and bone. *Cancer Res* 2001; 61:2177-82.
386. Kuperwasser C, Dessain S, Bierbaum BE, Garnet D, Sperandio K, Gauvin GP *et al*. A mouse model of human breast cancer metastasis to human bone. *Cancer Res* 2005; 65:6130-8.
387. Moreau JE, Anderson K, Mauney JR, Nguyen T, Kaplan DL, Rosenblatt M. Tissue-engineered bone serves as a target for metastasis of human breast cancer in a mouse model. *Cancer Res* 2007; 67:10304-8.
388. Henriquez NV, van Overveld PG, Que I, Buijs JT, Bachelier R, Kaijzel EL *et al*. Advances in optical imaging and novel model systems for cancer metastasis research. *Clin Exp Metastasis* 2007; 24:699-705.
389. Kaijzel EL, van der Pluijm G, Lowik CWGM. Whole-body optical imaging in animal models to assess cancer development and progression. *Clin Cancer Res* 2007; 13:3490-7.
390. Janjan NA. Radiation for bone metastases: conventional techniques and the role of systemic radiopharmaceuticals. *Cancer* 1997; 80:1628-45.
391. Lewington VJ, McEwan AJ, Ackery DM, Bayly RJ, Keeling DH, Macleod PM *et al*. A prospective, randomised double-blind crossover study to examine the efficacy of strontium-89 in pain palliation in patients with advanced prostate cancer metastatic to bone. *Eur J Cancer* 1991; 27:954-8.
392. Coleman RE. Bisphosphonates in breast cancer. *Ann Oncol* 2005; 16:687-95.
393. Fleisch H. Development of bisphosphonates. *Breast Cancer Res* 2002; 4:30-4.
394. Michaelson MD, Smith MR. Bisphosphonates for treatment and prevention of bone metastases. *J Clin Oncol* 2005; 23:8219-24.
395. Body JJ, Diel IJ, Lichinitser MR, Kreuser ED, Dornoff W, Gorbunova VA *et al*. Intravenous ibandronate reduces the incidence of skeletal complications in patients with breast cancer and bone metastases. *Ann Oncol* 2003; 14:1399-405.
396. Lipton A, Theriault RL, Hortobagyi GN, Simeone J, Knight RD, Mellars K *et al*. Pamidronate prevents skeletal complications and is effective palliative treatment in women with breast carcinoma and osteolytic bone metastases: long term follow-up of two randomized, placebo-controlled trials. *Cancer* 2000; 88:1082-90.
397. Powles T, Paterson A, McCloskey E, Schein P, Scheffler B, Tidy A *et al*. Reduction in bone relapse and improved survival with oral clodronate for adjuvant treatment of operable breast cancer [ISRCTN83688026]. *Breast Cancer Res* 2006; 8:R13.
398. Rosen LS, Gordon DH, Dugan W, Jr., Major P, Eisenberg PD, Provencher L *et al*. Zoledronic acid is superior to pamidronate for the treatment of bone metastases in breast carcinoma patients with at least one osteolytic lesion. *Cancer* 2004; 100:36-43.
399. Kanis JA, Powles T, Paterson AH, McCloskey EV, Ashley S. Clodronate decreases the frequency of skeletal metastases in women with breast cancer. *Bone* 1996; 19:663-7.
400. Conte PF, Latreille J, Mauriac L, Calabresi F, Santos R, Campos D *et al*. Delay in progression of bone metastases in breast cancer patients treated with intravenous pamidronate: results from a multinational randomized controlled trial. The Aredia Multinational Cooperative Group. *J Clin Oncol* 1996; 14:2552-9.
401. van Holten-Verzantvoort AT, Hermans J, Beex LV, Blijham G, Cleton FJ, Eck-Smit BC *et al*. Does supportive pamidronate treatment prevent or delay the first manifestation of bone metastases in breast cancer patients? *Eur J Cancer* 1996; 32A:450-4.
402. Diel IJ, Solomayer EF, Costa SD, Gollan C, Goerner R, Wallwiener D *et al*. Reduction in new metastases in breast cancer with adjuvant clodronate treatment. *N Engl J Med* 1998; 339:357-63.

Jeroen_Buijs_18.indd 68 26-11-2008 10:18:13

403. Saarto T, Vehmanen L, Virkkunen P, Blomqvist C. Ten-year follow-up of a randomized controlled trial of adjuvant clodronate treatment in node-positive breast cancer patients. *Acta Oncol* 2004; 43:650-6.
404. Morony S, Warmington K, Adamu S, Asuncion F, Geng Z, Grisanti M *et al*. The inhibition of RANKL causes greater suppression of bone resorption and hypercalcemia compared with bisphosphonates in two models of humoral hypercalcemia of malignancy. *Endocrinology* 2005; 146:3235-43.
405. Body JJ, Greipp P, Coleman RE, Facon T, Geurs F, Fermand JP *et al*. A phase I study of AMGN-0007, a recombinant osteoprotegerin construct, in patients with multiple myeloma or breast carcinoma related bone metastases. *Cancer* 2003; 97:887-92.
406. Body JJ, Facon T, Coleman RE, Lipton A, Geurs F, Fan M *et al*. A study of the biological receptor activator of nuclear factor-kappaB ligand inhibitor, denosumab, in patients with multiple myeloma or bone metastases from breast cancer. *Clin Cancer Res* 2006; 12:1221-8.
407. Le Gall C, Bellahcene A, Bonnelye E, Gasser JA, Castronovo V, Green J *et al*. A cathepsin K inhibitor reduces breast cancer induced osteolysis and skeletal tumor burden. *Cancer Res* 2007; 67:9894-902.
408. Carducci MA, Jimeno A. Targeting bone metastasis in prostate cancer with endothelin receptor antagonists. *Clin Cancer Res* 2006; 12:6296s-300s.
409. Yuyama H, Koakutsu A, Fujiyasu N, Tanahashi M, Fujimori A, Sato S *et al*. Effects of selective endothelin ET(A) receptor antagonists on endothelin-1-induced potentiation of cancer pain. *Eur J Pharmacol* 2004; 492:177-82.
410. Carducci MA, Padley RJ, Breul J, Vogelzang NJ, Zonnenberg BA, Daliani DD *et al*. Effect of endothelin-A receptor blockade with atrasentan on tumor progression in men with hormone-refractory prostate cancer: a randomized, phase II, placebo-controlled trial. *J Clin Oncol* 2003; 21:679-89.
411. Cella D, Petrylak DP, Fishman M, Teigland C, Young J, Mulani P. Role of quality of life in men with metastatic hormone-refractory prostate cancer: how does atrasentan influence quality of life? *Eur Urol* 2006; 49:781-9.
412. Kang Y, Siegel PM, Shu W, Drobnjak M, Kakonen SM, Cordon-Cardo C *et al*. A multigenic program mediating breast cancer metastasis to bone. *Cancer Cell* 2003; 3:537-49.
413. Minn AJ, Kang Y, Serganova I, Gupta GP, Giri DD, Doubrovin M *et al*. Distinct organ-specific metastatic potential of individual breast cancer cells and primary tumors. *J Clin Invest* 2005; 115:44-55.
414. Smid M, Wang Y, Klijn JG, Sieuwerts AM, Zhang Y, Atkins D *et al*. Genes associated with breast cancer metastatic to bone. *J Clin Oncol* 2006; 24:2261-7.
415. Schmiere B, Hill CS. TGF-beta-SMAD signal transduction: molecular specificity and functional flexibility. *Nat Rev Mol Cell Biol* 2007; 8:970-82.
416. Goumans MJ, Valdimarsdottir G, Itoh S, Rosendahl A, Sideras P, ten Dijke P. Balancing the activation state of the endothelium via two distinct TGF-beta type I. *EMBO J* 2002; 21:1743-53.
417. Macias-Silva M, Hoodless PA, Tang SJ, Buchwald M, Wrana JL. Specific activation of Smad1 signaling pathways by the BMP7 type I receptor, ALK2. *J Biol Chem* 1998; 273:25628-36.
418 Tamaki K, Souchelnytskyi S, Itoh S, Nakao A, Sampath K, Heldin CH *et al.* Intracellular signaling of osteogenic protein-1 through Smad5 activation. *J Cell Physiol* 1998; 177:355-63.
419. Yamashita H, ten Dijke P, Huylebroeck D, Sampath TK, Andries M, Smith JC *et al.* Osteogenic protein-1 binds to activin type II receptors and induces certain activin-like effects. *J Cell Biol* 1995; 130:217-26.

Jeroen_Buijs_18.indd 70 26-11-2008 10:18:13

Chapter 2

Prognostic Significance of Periodic Acid-Schiff-positive Patterns in Primary Breast Cancer and its Lymph Node Metastases

Breast Cancer Res Treat 2004; 84:117-30.

Jeroen T Buijs[1]
Anne-Marie Cleton[2]
Vincent THBM Smit[2]
Clemens WGM Löwik[1]
Socrates E Papapoulos[1]
Gabri van der Pluijm

Departments of Endocrinology[1] and Pathology[2],
Leiden University Medical Center,
Leiden, The Netherlands

Jeroen_Buijs_18.indd 71 26-11-2008 10:18:13

Abstract

Invasive ductal carcinoma is by far the largest histological subtype of breast cancer, but clinical behavior can differ greatly. Reliable morphological markers are, therefore, of invaluable help to distinguish between patients with good and poor prognosis. Histological patterns stained with periodic acid-Schiff (PAS) were previously shown to be of prognostic significance in cutaneous and uveal melanoma. In this study, we examined the presence of different PAS-positive (PAS+) structures in 54 women with infiltrating ductal adenocarcinoma of the breast and at least one axillary lymph node metastasis but no distant metastases who were followed for at least 11 years.

We found that the complexity of the thin PAS+ patterns in lymph node metastases is associated with a shorter period of disease-free survival (DFS) as well as of total survival (Kaplan Meier curves). Furthermore, the presence of PAS+ networks – the most complex thin PAS+ pattern – in lymph node metastases is one of the two independent factors associated with the occurrence of a distant metastasis (multivariate Cox model). Moreover, the presence of PAS+ networks in positive lymph nodes is the feature most strongly associated with DFS.

In conclusion, the presence of PAS+ networks in lymph node metastases is a new, reliable and convenient indicator for prognosis of breast cancer patients.

Jeroen_Buijs_18.indd 72 26-11-2008 10:18:13

Introduction

Breast cancer is the most frequent type of cancer among women in industrialized countries. Approximately one in twelve women will develop breast cancer during their lifetime, and the incidence is increasing in many countries. Locoregional metastasis to adjacent lymph nodes is a crucial event of breast cancer progression and, consequently, axillary nodal status is the best predictor of survival [1].

During cancer progression blood supply is required for tumors to survive, grow, and metastasize [2,3]. Tumor angiogenesis, the process of blood vessel formation into a growing tumor, is necessary, as a tumor can not grow beyond 3 mm^3 in the absence of angiogenesis due to the concomitant lack of oxygen and nutrients [4-6]. Several groups have shown that high blood vessel counts in primary breast, and other, cancers provide an independent predictor of poor prognosis [7-10].

In addition to angiogenesis, evidence is accumulating that malignant tumors are often capable of inducing other structures that may contribute to (invasive) growth and dissemination. In both uveal and cutaneous melanoma the presence of networks that stain positive with periodic acid-Schiff (PAS) has been described [8,11-13] and these have been shown to be of prognostic significance [13-15]. The PAS reaction is a non-specific indicator for polysaccharides, which are present in the basement membranes, including those of blood vessels. The PAS+ patterns may represent (a mixture of): blood vessels/ vascular network [12,14], fibrovascular tissue [16,17], tumor cells [18] or a fluid conducting meshwork [11]. Hence, at present, no consensus exists about the exact nature and origin of the PAS+ pattern. In melanoma PAS+ meshworks that were most interconnected correlated with the poorest prognosis, suggesting that these structures may facilitate tumor growth and/or dissemination [13-15].

Invasive ductal carcinoma is by far the largest histological subtype of breast cancer (at least 80%), but clinical behavior can be quite different. Reliable morphological markers are, therefore, needed for distinguishing patients with good and poor prognosis. In the present study, we investigated the presence of different PAS+ patterns in the primary tumor and its lymph node metastases of women with infiltrating ductal adenocarcinoma of the breast. Our results show that the presence of these patterns has significant prognostic value for both disease-free survival and total survival.

Patients & Methods

Patients

Out of 251 women with breast cancer operated between April 1984 and November 1989 in the Leiden University Medical Center, 170 had infiltrating ductal adenocarcinomas, no distant metastases at the time of surgery, no other malignant tumors and at least one paraffin embedded tissue was available for examination. Of these, 79 had at least one positive lymph

node and were included in the study. Twenty-three patients were excluded for the following reasons: no follow-up (4), paraffin blocks of either the primary tumor or its lymph node metastases were not available (20), or paraffin blocks of the primary tumor or its lymph node metastases had such quality that tumor histology and staining could not be examined properly (1). This analysis, therefore, includes 54 patients with infiltrating ductal adenocarcinomas with at least one lymph node metastasis, but no distant metastases, in whom material from both the primary tumor and the lymph nodes was available. The excised breast carcinomas and lymph nodes were fixed with formalin and embedded in paraffin for routine histopathological examinations. All primary breast tumors were revised and graded according to Bloom and Richardson (BAR) by a pathologist (V.T.H.B.M.S.). Patients were followed periodically according to existing protocols.

Periodic Acid-Schiff (PAS)

Periodic acid-Schiff (PAS)-staining was performed on 5 μm paraffin embedded sections. Sections were deparaffinized and rehydrated in the following immersion steps: 5' Paraclear (2x)(Klinipath, Duiven, The Netherlands), 2' 100% ethanol (2x), 2' 96%, 2' 80%, 2' 70%, 2' 50% and 2' distilled water. The sections were incubated for 30 minutes in a 56 °C pre-warmed 0.6% periodic acid solution. The sections were rinsed with distilled water, and Schiff's reagent (Feulgen stain, Klinipath, Duiven, The Netherlands) was added. After 30 minutes, the sections were washed for 15 minutes with tap water. Samples were counterstained with Mayer's Hematoxylin (Merck, Amsterdam, The Netherlands) for 1 minute and washed with tap water for 10 minutes before being dehydrated and mounted in xylol under glass coverslips with Aquamount.

Immunohistochemistry

All 5 μm paraffin embedded sections were mounted on slides coated with aminopropylethoxysilane (APES) followed by glutaraldehyde. After overnight drying in an oven at 37 °C, slides were stored in slide boxes at a temperature of 4 °C, to avoid loss of antigen epitopes [19]. The sections were deparaffinized and rehydrated in the following steps: 5' Paraclear (2x) (Klinipath, Duiven, The Netherlands) and 2' 100% ethanol (2x). To block endogenous peroxide activity of the tissue, 20 minutes incubation at room temperature with 1% hydrogen peroxide in methanol was done. Microwave antigen retrieval (AR) was done for vimentin [20], in brief: sections were boiled for 10 minutes in a solution of 10 mmol/L citrate buffer pH 6 in a domestic microwave oven at full power (Electrolux 700W). Enzymatic digestion was performed with trypsin (CD31), treatment at 37 °C for 20 minutes, using 0.1% trypsin (Sigma T-8128) in 0.1% calcium chloride pH 7.4. All incubations and washing with phosphate-buffered saline were performed at room temperature. Sections were incubated with the primary antibodies overnight, followed by 30 minute incubations with biotin-labeled rabbit-anti-mouse Ig or biotin-labeled goat-anti-rabbit Ig and a preformed complex of biotin-labeled horserad-

Jeroen_Buijs_18.indd 74 26-11-2008 10:18:13

ish peroxidase and streptavidin (DAKO). CD31 (clone JC/70A, dilution 1:200) and von Willebrand Factor (vWF)(polyclonal, dilution 1:400) were supplied by DAKO (Glostrup, Denmark), vimentin (clone V9, dilution 1:300) by Monosan (Uden, The Netherlands) and Smooth Muscle Actin (clone ASM-1, dilution 1:1000) by Progen (Heidelberg, Germany). Immune complexes were visualized with 0.05% diaminobenzidine and 0.0015% hydrogen peroxide. Slides were counterstained in Mayer's hematoxylin (Merck, Amsterdam, The Netherlands) for 30 seconds and washed with tap water for 10 minutes before being dehydrated and mounted in xylol under glass coverslips with aquamount.

Statistical Analyses

Patients were divided into two groups, according to the presence or absence of a particular PAS+ pattern. Subsequently, Kaplan-Meier curves were calculated and compared with a log-rank test for survival and disease free survival. The level of significance was set at P = 0.05. Afterward, the relative importance of all PAS+ patterns and the major clinical and prognostic characteristics (histological grade, stage, age, the number of positive lymph nodes at time of surgery and treatment of primary tumor) were determined by multivariate analysis using the Cox proportional hazards model. The Cox model was constructed using a forward stepwise selection procedure on the basis of the likelihood ratio statistic with chi-square scores with significance levels of 0.05 or less for entry, and chi-square scores with significance levels of 0.10 or greater for removal.
SPSS-10 was used for all calculations.

Results

Patients

Stage, histological grade, treatment of primary tumor, kind of adjuvant treatment, age at time of surgery, disease free survival (DFS; end-point is the occurrence of a distant metastasis) and total survival (end-point is the occurrence of cancer-related death) are summarized in table 1.

Morphological PAS-positive Patterns

Sections stained with PAS were interpreted by two investigators (J.T.B. and G.v.d.P.) and a pathologist (V.T.H.B.M.S.). Different morphological patterns were identified within the tumor (Fig. 1). A subset of the patterns in this study, the 'thin PAS-positive (PAS+) patterns' or the 'thin PAS+ meshwork' (E-J), as described by Foldberg and co-workers [12], existed within a compact tumor mass. We discerned 10 distinct PAS+ patterns in primary breast cancer and their lymph node metastases:

A. *Small curves of extra cellular matrix*: curves of PAS+ connective tissue (CT) around small groups of tumor cells (3-10 cells)(Fig. 1*A*).

Table 1 **Classification of all patients included in the study.** Stage, Histological Grade (both a.), treatment of primary tumor, adjuvant therapy (b.), age, disease freesurvival (DFS) and survival (all c.) are summarized. MRM = modified radical mastectomy, BCT = breast conserving treatment, RT = radio therapy, Horm = hormone therapy and Chem = chemotherapy , Age = age at time of surgery, St.dev = standard deviation, SEM = standard error of the mean.

(a)

	Stage				Histological Grade		
All patients	**II A**	**II B**	**III A**	**III B**	**1**	**2**	**3**
54 (100%)	7 (13.0%)	19 (35.2%)	7 (13.0%)	21 (35.5%)	4 (7.4%)	17 (27.8%)	33 (61.1%)

(b)

		Adjuvant therapy						
		None	**Chem**	**Horm**	**RT**	**RT +**	**RT +**	**Total**
Treatment of primary tumor	**MRM**	11	3	1	21	9	4	49 (90.7%)
	BCT + RT	2	2	1	x	x	x	5 (9.3%)

(c)

	Age (in years)	**DFS (in years)**	**Survival (in years)**
Average	57.83	4.63	6.58
Median	57.29	3.74	5.72
St.dev	12.09	4.19	4.13
SEM	1.54	0.53	0.52
Range	27.77 - 84.20	0.20 - 16.15	0.20 - 16.15

B. *Small cellclusters surrounded by CT*: dominant PAS+ CT network with small cluster, <10 cells, of breast cancer cells (Fig. 1*B*).

C. *Large cellclusters surrounded by CT*: dominant PAS+ CT network with clusters, ≥ 10 cells, of breast cancer cells (Fig. 1*C*).

D. *Thick circular loops of CT*: composed of thick, circular PAS+ CT layers around clusters of breast cancer cells (>20 cells)(Figure 1.d). Because of their circular shape, these thick circular loops of CT may be confused with looping patterns that form networks. However, 'thick circular loops of CT' are presented as thick, dominant layers, obviously consisting of CT. (Fig. 1*D*)

E. The *parallel* pattern: straight thin PAS+ patterns are arranged parallel to one another without dichotomous branching or cross-linking (Fig. 1*E*).

F. The *parallel with cross-link* pattern: parallel straight thin PAS+ patterns are linked to each other in a fashion reminiscent of switching tracks in a rail yard (Fig. 1*F*).

G. *Arcs*: thin PAS+ arcs are incomplete loops (i.e. loops that are not closed). We made no attempt to obtain serial sections through tumors to determine whether these arcs become complete loops in deeper section planes (Fig. 1*G*).

H. *Arcs with branching*: PAS+ arcs demonstrate dichotomous branching (Fig. 1*H*).

I. *Loops*: completely closed thin PAS+ circles. The presence of one closed loop is sufficient evidence to record this pattern as present (Fig. 1*I*).
J. *Interconnected Loops*: back-to-back closed PAS+ loops. By definition, if interconnected loops are present, loops must be present (Fig. 1*J*).

Immunohistochemical Characterization of the Thin PAS+ Patterns

Antibodies to vWF or CD31 (PECAM-1) have been frequently used to visualize the blood vessels, and antibodies to Flt-4 (VEGFR-3) have been used to visualize lymph vessels, although blood vessels in a tumor might be stained as well [21].

In this study, the expression of vWF and Flt-4 (Fig. 2) was indeed mainly restricted to (blood) vessels (overview in Table 2). CD31 was also found to be expressed on blood vessels. In addition, the different thin PAS+ patterns depicted in figure 1 stained positive for smooth muscle actin (SMA)(Fig. 3). Occasionally, lumina were found in the PAS+ patterns. Lumina stained both unilaterally and bilaterally for SMA (Fig. 3*E,F*), but were negative vWF and Flt-4. Tumor cells and, sporadically, erythrocytes were found in these lumina. The vWF+/CD31+ tumor blood vessels (Fig. 2*A,B* and 4*A*), which contained numerous erythrocytes, were located in bifurcations of this SMA+/PAS+ meshwork and might be interconnected to these lumina, suggesting an additional form of perfusion/dissemination for the tumor in the PAS+ meshwork. In summary, two different types of structures were observed in the thin PAS+ meshwork:

1. Tumor blood vessels, vWF+/CD31+.
2. "Additional meshwork", PAS+/SMA+ (vWF-negative).

Table 2 **Summary of staining of specific tissues as seen in the study.** Vessels with erythrocytes were considered as blood vessels. Specific staining for lymph vessels was not scored, since lymph vessels and blood vessels without erythrocytes can not be distinguished. VWF = von Willebrand Factor, SMA = smooth muscle actin.

Antibody	Blood Vessels	Stroma	Arcs (G+H)	Loops (I)	Networks (J)
CD 31/PECAM-1	+	-	Patchy	Patchy	Patchy
VEGFR-3 (Flt-4)	+	-	-	-	-
VWF	+	-	-	-	-
SMA	+	+	+	+	+
Vimentin	+	+	Patchy	Patchy	Patchy
Other					
PAS-staining	+	+	+	+	+

The expression of CD31 in some primary breast carcinomas and concomitant lymph node metastases appeared not exclusive for blood vessels containing a lumen ((Fig. 4*C,D*). In addition, expression of CD31 was repeatedly found as a patchy, discontinuous staining alongside parts of the PAS+/SMA+ meshwork. Patchy staining alongside the entire meshwork was found for vimentin expression as well (data not shown).

Occasionally, it was found that breast cancer cells were polarized to the meshwork, resembling the organization of normal breast ductal epithelial cells that are polarized to myoepithelial cells (Fig. 4*D*).

PAS-positive Patterns and Prognosis

The presence or absence of each morphological pattern in both primary tumor and positive lymph node was recorded for each patient with no knowledge of the clinical outcome (Table 3). The identification of thin PAS+ patterns was highly reproducible (Table 4). Various types of thin PAS+ patterns were frequently observed within the same tumor. In primary breast cancer as well as in its lymph node metastasis the incidence of thin PAS+ patterns that were most interconnected, the PAS+ networks (14.8% and 13.0%, respectively) and loops (20.4% and 18.5%, respectively), was lower than the incidence of thin PAS+ patterns that were less interconnected. In the primary tumor and its positive lymph node the presence of any thin PAS+ pattern was 29.6% and 35.2%, respectively. The presence of any thin PAS+ pattern was for 63% concordant between the primary tumor and its positive lymph node (data not shown). Apart from 'thick circular loops of CT', other PAS+ structures, which were thick and associated with CT, were scored more frequently.

Table 3 **Distribution of Morphological PAS-positive (PAS-+) Patterns in Primary Breast Carcinomas and their lymph node metastases.** In brackets is the percentage of the patients having a particular PAS+ pattern.
ECM = extracellular matrix, CT = connective tissue.

	PAS+ patterns	Primary breast carcinoma	Lymph node metastasis
ECM-rich patterns	Small curves of ECM (A)	18 (33.3%)	32 (59,3%)
	Small cellclusters surrounded by CT (B)	33 (61.1%)	17 (27.8%)
	Large cellclusters surrounded by CT (C)	34 (63.0%)	15 (27.8%)
	Thick circular loops of CT (D)	12 (22.2%)	7 (13.0%)
	Parallel (E)	10 (18.5%)	14 (25.9%)
	Parallel with Cross-Links (F)	10 (18.5%)	13 (24.1%)
Thin PAS+ patterns	Arcs (G)	12 (22.2%)	14 (25.9%)
	Arcs with Branching (H)	12 (22.2%)	13 (24.1%)
	Loops (I)	11 (20.4%)	10 (18.5%)
	Networks (J)	8 (14.8%)	7 (13.0%)
	Any thin PAS+-pattern	16 (29.6%)	19 (35.2%)
	Total number of patients	54 (100%)	

To determine which of the ten PAS+ patterns might be associated with clinical outcome, Kaplan-Meier (KM) survival curves (Fig. 5 and 6) were estimated from the data (Table 5). None of the (thin) PAS+ patterns in the primary mammary carcinoma was significantly associated with poor prognosis.

Jeroen_Buijs_18.indd 78 26-11-2008 10:18:13

Table 4 Agreement between two independent observers for each thin PAS+ pattern.

Thin PAS+ patterns	% Agreement	Chance corrected measure of agreement (kappa statistics)
Parallel (E)	88	0.639
Parallel with Cross-Links (F)	88	0.639
Arcs (G)	85	0.677
Arcs with Branching (H)	85	0.677
Loops (I)	85	0.641
Networks (J)	88	0.693
any thin PAS+ pattern	85	0.687

Note: P ⩽ 0.001 for all observations

Table 5 Kaplan-Meier Analysis for Disease Free Survival (DFS) and Total Survival for the Presence of Morphological PAS-positive (PAS+) Patterns in Primary Breast Carcinomas and their Lymph Node Metastases. ECM =extra cellular matrix, CT = connective tissue.

		Primary breast carcinoma				Lymph node metastasis			
		Disease free survival		Total survival		Disease free survival		Total survival	
	PAS+ patterns	Log-rank X2	P	Log-rank X2	P	Log-rank X2	P	Log-rank 2	P
ECM rich patterns	Small curves of ECM (A)	0.54	0.4604	0.01	0.9302	1.18	0.2771	1.09	0.2975
	Small cellclusters surrounded by CT (B)	0.07	0.7929	< 0.01	0,9894	3.11	0,0779	5.16	0,0231
	Large cellclusters surrounded by CT (C)	0.02	0.8950	0.02	0.8950	1.10	0.2935	0.24	0,6221
	Thick circular loops of CT (D)	< 0.01	0.9791	0.01	0,9214	2.56	0,1094	11.88	0,0006
Thin PAS+ patterns	Parallel (E)	0.08	0.7808	0.05	0.8170	3.13	0.0770	0.18	0,6689
	Parallel with Cross-Links (F)	0.08	0.7808	0.05	0.8170	3.26	0,0711	0.16	0,6918
	Arcs (G)	0.02	0.8930	0.57	0.4485	8.48	0,0036	11.09	0.0009
	Arcs with Branching (H)	0.02	0.8930	0.57	0.4485	7.62	0,0058	8.92	0,0028
	Loops (I)	0.10	0.7503	0.80	0.3700	13.89	0,0002	17.49	< 0,0001
	Networks (J)	1.26	0.2620	1.06	0.3023	18.86	< 0,0001	17.02	< 0,0001
	Any thin PAS+-patterns	0.63	0.4275	0.67	0.4131	9.73	0,0018	3.00	0,083

Table 6 Cox Proportional Hazards Model Using Forward Stepwise Selection of Prognostic Factors in Breast Cancer for DFS. DF = degrees of freedom, SE = standard error.

Variable	DF	Paramater estimate	SE	Wald chi-square	P	Hazard ratio	95 % Confidence interval
PAS+ network	1	2.463	0.524	22.077	< 0.0001	8.78	3.27 - 23.60
Stage-classification	1	0.413	0.151	7.481	0.005	1.50	1.13 - 1.98

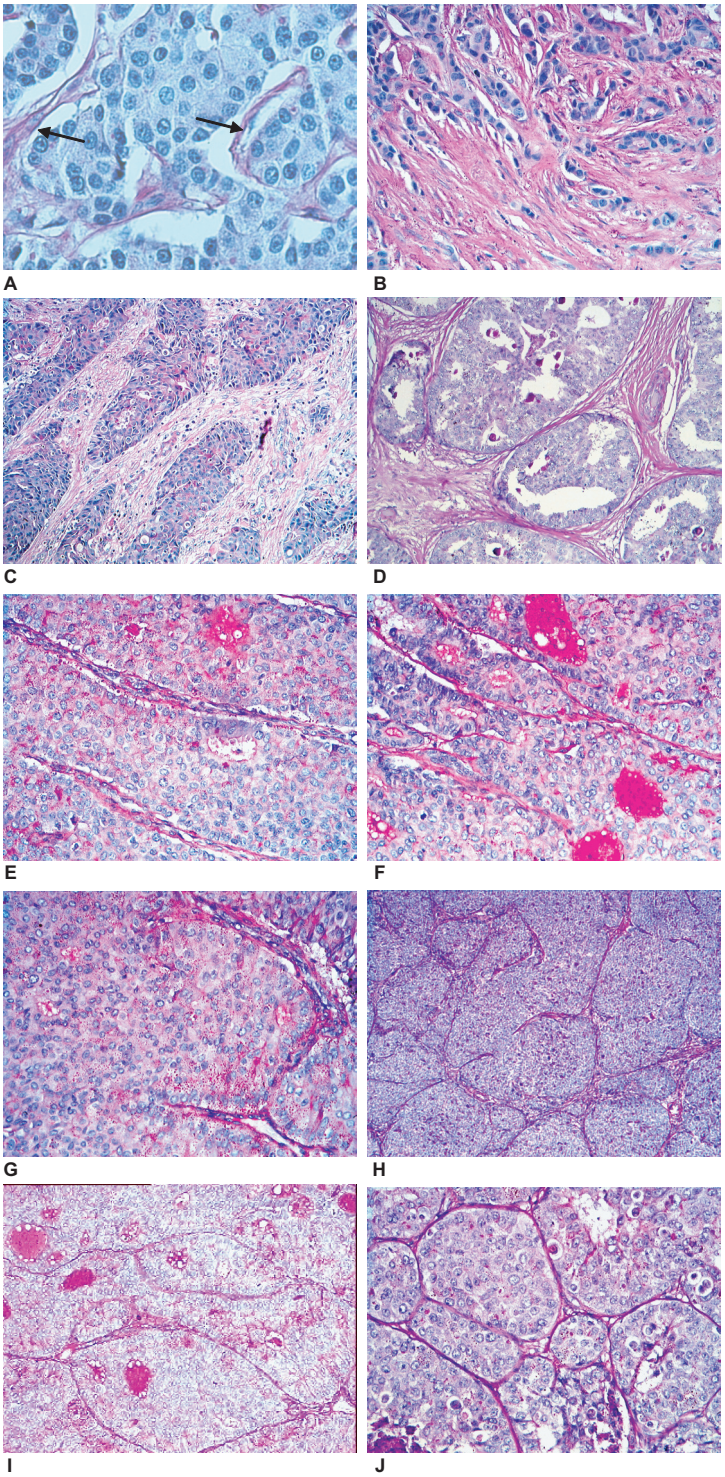
A
B
C
D
E
F
G
H
I
J

Figure 1 **(left) Primary Breast Carcinoma Could Contain a Combination of Different PAS+ Patterns.** Typical patterns are shown by an example. *A*, *small curves of ECM* with total lack of structure around small numbers of tumor cells (arrows) (magnification 400x). *B*, *small cellclusters surrounded by CT*: dominant CT network with breast cancer cells (magnification 200x). *C*, *large cellclusters surrounded by CT*: dominant PAS+ CT network with clusters of breast cancer cells (> 10 cells)(magnification 200x). *D*, *thick circular loops of CT*: thick, circular PAS+ CT layers around clusters of breast cancer cells (>30 cells) (magnification 100x). *E*, *parallel* pattern; straight vessels are arranged parallel to one another without dichotomous branching or cross-linking (magnification 400x). *F*, *parallel with cross-link* pattern: parallel straight vessel are linked to each other in a fashion reminiscent of switching tracks in a rail yard (magnification 400x). *G*, *arcs* are incomplete loops (i.e., the loops that are not closed) (magnification 400x). *H*, *arcs with branching* demonstrate dichotomous branching (magnification 100x). *I*, *loops*: completely closed. The presence of one closed loop is sufficient evidence to record this pattern as present (magnification 200x). 'Arcs with branching' are often founded in 'loops' (magnification 200x). *J*, *network*: Adjacent back-to-back closed loops forming *interconnected loops*.

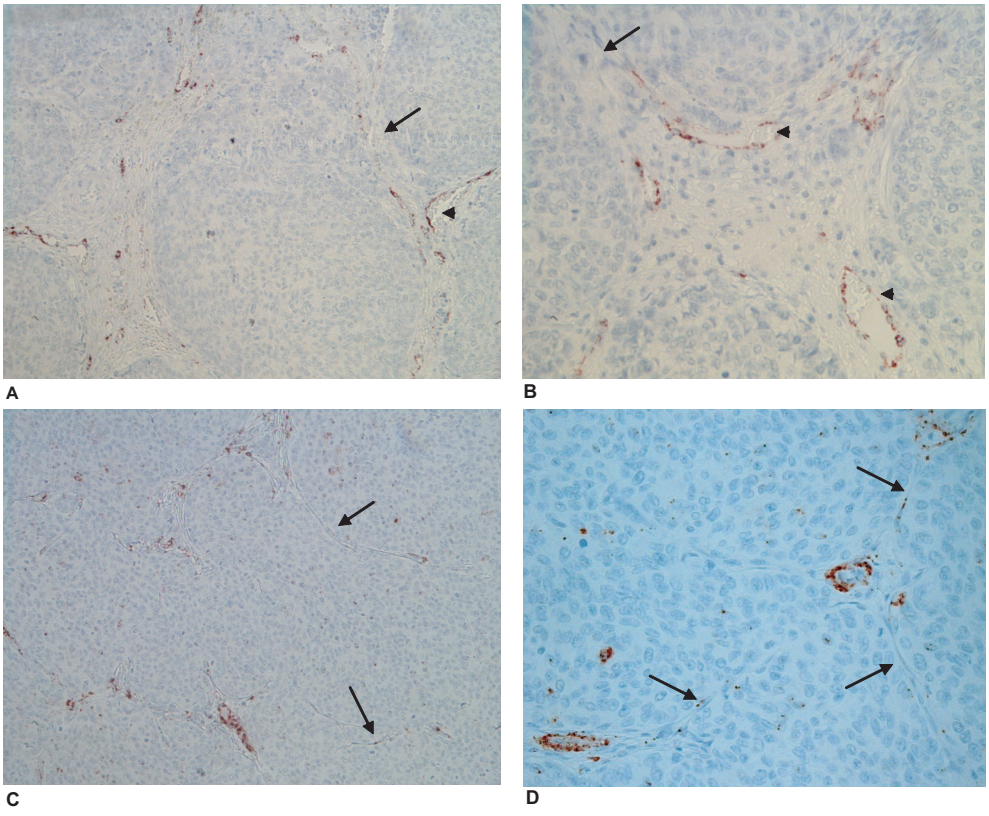

Figure 2 **Vessels in a lymph node metastasis from breast cancer.** *A*, *B*, the tumor is well vascularized as shown by the von Willebrand Factor (vWF)-positive blood vessels, which have erythrocytes inside (arrowheads). Besides the blood vessels, no additional patterns have been stained with the vWF staining (magnifications 100x and 200x, respectively). *C*, *D*, expression of Flt-4 shows staining of vessels. The additional PAS+ patterns (arrows) are not stained with Flt-4 or vWF (magnifications 100x and 200x, respectively).

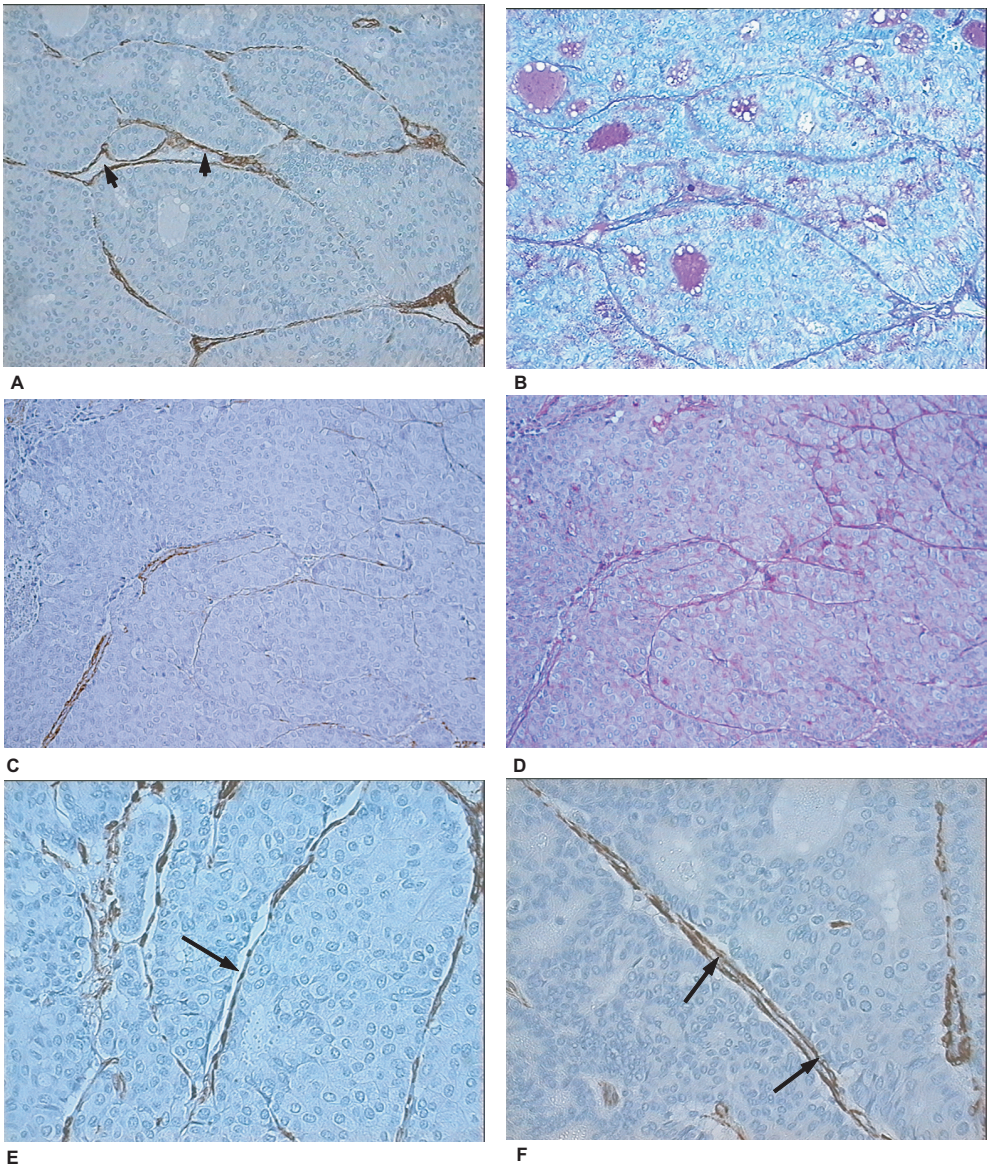

Figure 3 **Expression of Smooth Muscle Actin (SMA)(Compared to a PAS-staining) in a Primary Mammary Carcinoma and Lymph Node Metastasis.** Staining for SMA (*A*, *C*) and the PAS-staining (*B*, *D*) on sequential slides show both the same loops, in primary mamma carcinoma (*A*, *B*) as well as in lymph node metastasis (*C*, *D*). With a higher magnification erythrocytes could be clearly seen (arrowheads, magnification not shown) (magnifications 200x). Both unilateral (*E*) and bilateral (*F*) staining with SMA of the lumen is seen (magnifications 400x).

In contrast, the KM survival curves for patients with positive lymph nodes consisting of PAS+ networks or loops revealed a highly significant shorter period of DFS ($p < 0.0001$ and $p = 0.0002$, respectively) and survival (both p-values < 0.0001) compared to patients lacking these structures (Fig. 5*A,B* and 6*A,B*). All patients with PAS+ arcs or arcs with cross-linking in their positive lymph nodes also had a significant shorter period of DFS ($p = 0.004$ and $p = 0.005$, respectively) and total survival ($p = 0.003$ and $p = 0.0009$) than patients without PAS+ arcs (with cross-linking) (Fig. 5*C,D* and 6*C,D*). There was a trend for patients with lymph node metastases containing PAS+ parallel lanes and PAS+ parallel lanes with cross-linking ($p = 0.07$ and $p = 0.08$, respectively) for a shorter period of DFS (Fig. 5*E,F*). However, the presence of PAS+ parallel lanes (with cross-links) did not give a poor prognosis for total survival (Fig. 6*E,F*). Nevertheless, the presence of any thin PAS+ pattern – including (interconnected) loops, arcs (with branching) and parallel lanes (with cross-links) – in positive lymph nodes is a prognostic indicator for DSF ($p = 0.002$) and, to a lesser extent, for survival ($p = 0.08$) (Fig. 5*G* and 6*G*).

The Cox proportional hazard model using forward selection showed that PAS+ networks in positive lymph nodes and the stage-classification are the two independent risk factors for the occurrence of a distant metastasis (Table 6). Other risk factors were not independently associated with disease free survival, since no other risk factor entered into the Cox model. Furthermore, the presence of a PAS+ networks in positive lymph nodes was the risk factor most strongly associated with poor prognosis.

Discussion

We demonstrate here that, in addition to the tumor blood vessels, different thin PAS+ meshworks may exist in primary breast carcinomas and their lymph node metastases. These PAS+ meshworks are characterized by continuous expression of SMA and patchy expression of CD31. Within these PAS+ meshworks Flt-4+ and vWF+ vessels are embedded.

More importantly, we found that prognosis of clinical outcome is inversely related to the complexity of the PAS+ meshwork in lymph node metastases. Furthermore, the presence of the most complex PAS+ pattern, the PAS+ network, in lymph node metastases from invasive ductal carcinoma of the breast and stage classification of the tumor are the only two independent risk factors associated with the occurrence of a distant metastasis. The presence of a PAS+ network in a positive lymph node is the factor most strongly associated with poor prognosis. In line with previously published studies comparing overall survival and disease free survival in patients that received MRM and BCT as original treatment, the type of treatment was not an independent risk factor for poor prognosis [22-24]. The histological grade was not an independent risk factor, since patients selected in the study had at least one lymph node metastasis and there was, therefore, a bias for a high histological grade. Similarly, the number of positive lymph nodes was not an independent risk factor, since it already entered in the model with the variable stage classification.

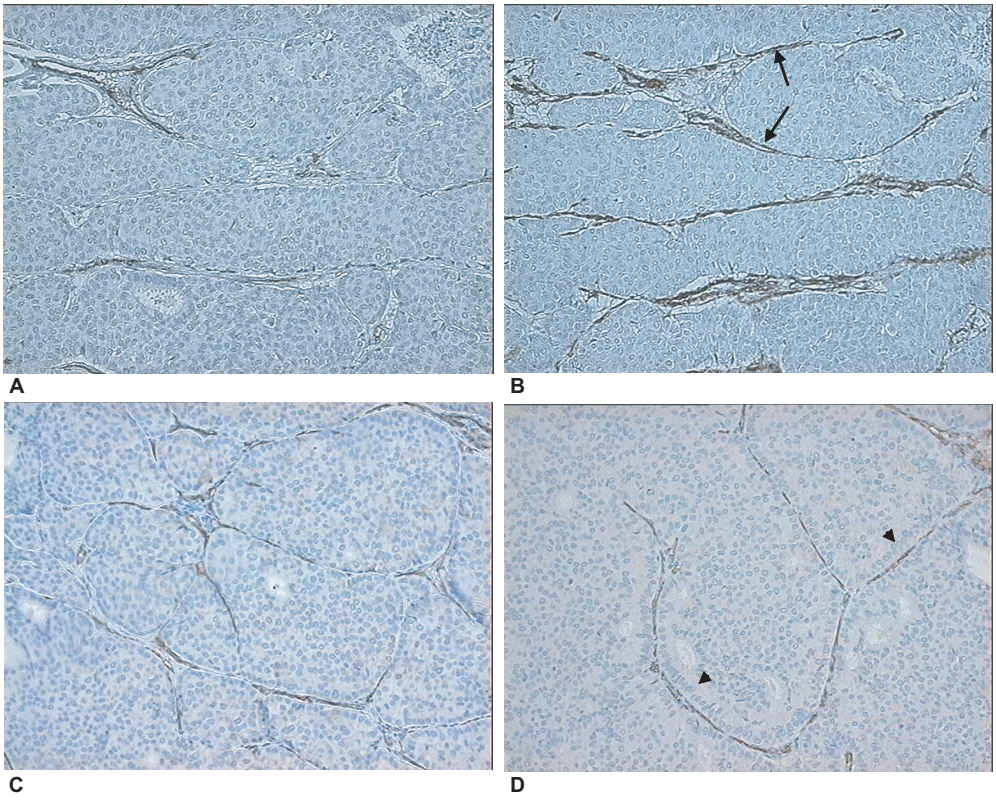

Figure 4 **Expression of CD31 and SMA in Lymph Node Metastasis from a Primary Mammary Carcinoma.** The staining for CD31 (*A*) and SMA (*B*) on sequential slides show co-expression on blood vessels. Additionally, SMA-positive (SMA+) lumina could be seen (arrows). The CD31-positive (CD31+) vessels seems to be connected to each other by the (lumina of) SMA+ framework. *C*, occasionally, however, CD31+ patterns are present alongside the SMA-positive/PAS-positive (SMA+/PAS+) framework. *D*, CD31+ patterns alongside the SMA+/PAS+ framework are also present in the primary mammary carcinoma. Sometimes, breast cancer cells are ordered to the SMA+/PAS+ framework (arrowheads), resembling the manner of normal breast ductal epithelial cells that are polarized to myoepithelium (all magnifications 200x).

Immunohistochemically, these PAS+ meshworks showed continuous expression of SMA (normally expressed by pericytes) and patchy expression of CD31. The presence of lumina in the PAS+ meshwork might be indicative for septa that may facilitate perfusion and/or dissemination of cancer cells. Indeed, tumor cells were frequently present in the lumina, whereas, erythrocytes were occasionally found in these structures.

In 63 % of the patients thin PAS+ patterns were present in both the primary tumors and in their respective lymph nodes. Some tumors may, therefore, have the capability to form such PAS+ patterns, however, none of the PAS+ patterns scored in primary tumors appeared to be of prognostic significance. The non-prognostic value of PAS+ networks in primary

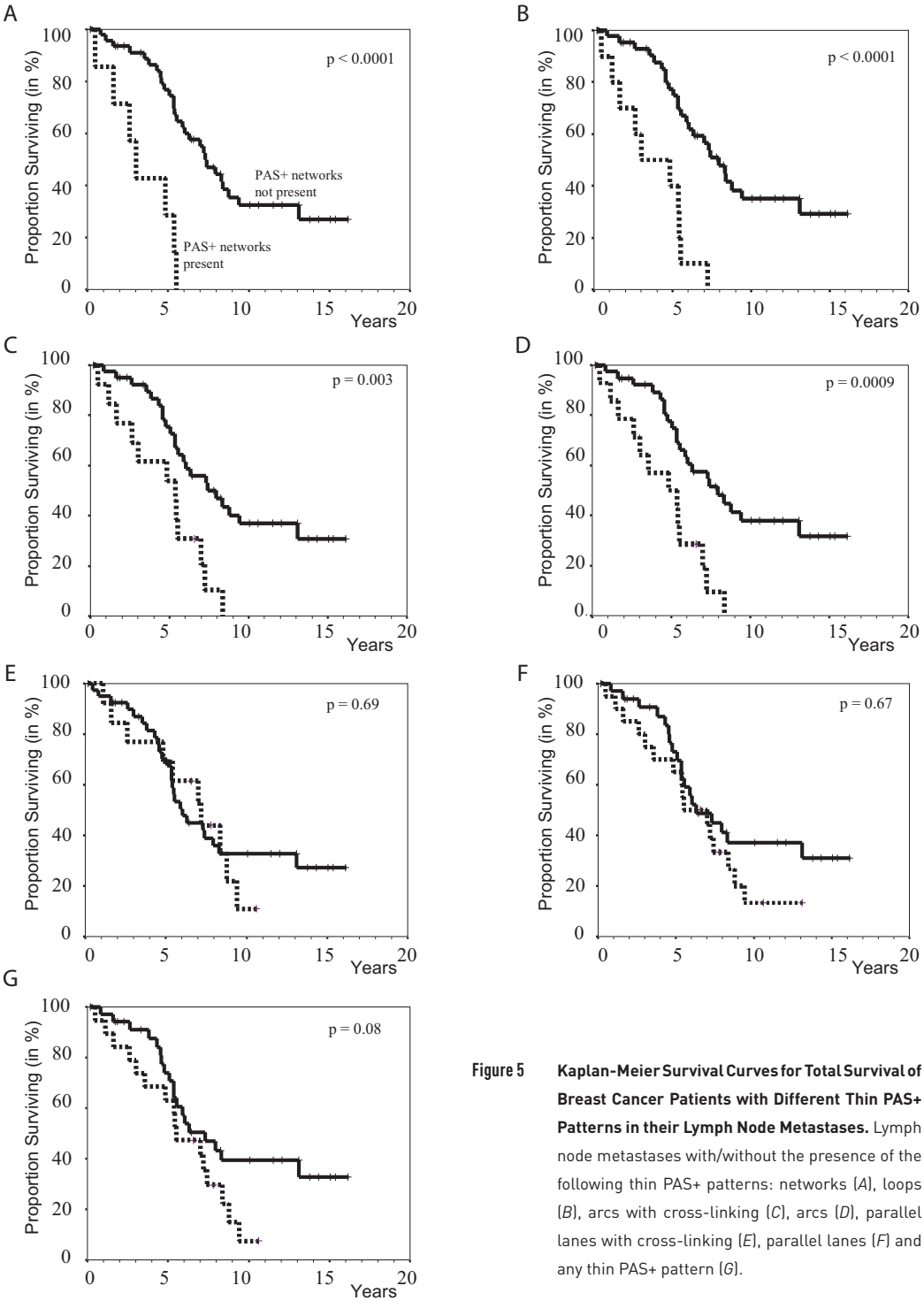

Figure 5 **Kaplan-Meier Survival Curves for Total Survival of Breast Cancer Patients with Different Thin PAS+ Patterns in their Lymph Node Metastases.** Lymph node metastases with/without the presence of the following thin PAS+ patterns: networks (*A*), loops (*B*), arcs with cross-linking (*C*), arcs (*D*), parallel lanes with cross-linking (*E*), parallel lanes (*F*) and any thin PAS+ pattern (*G*).

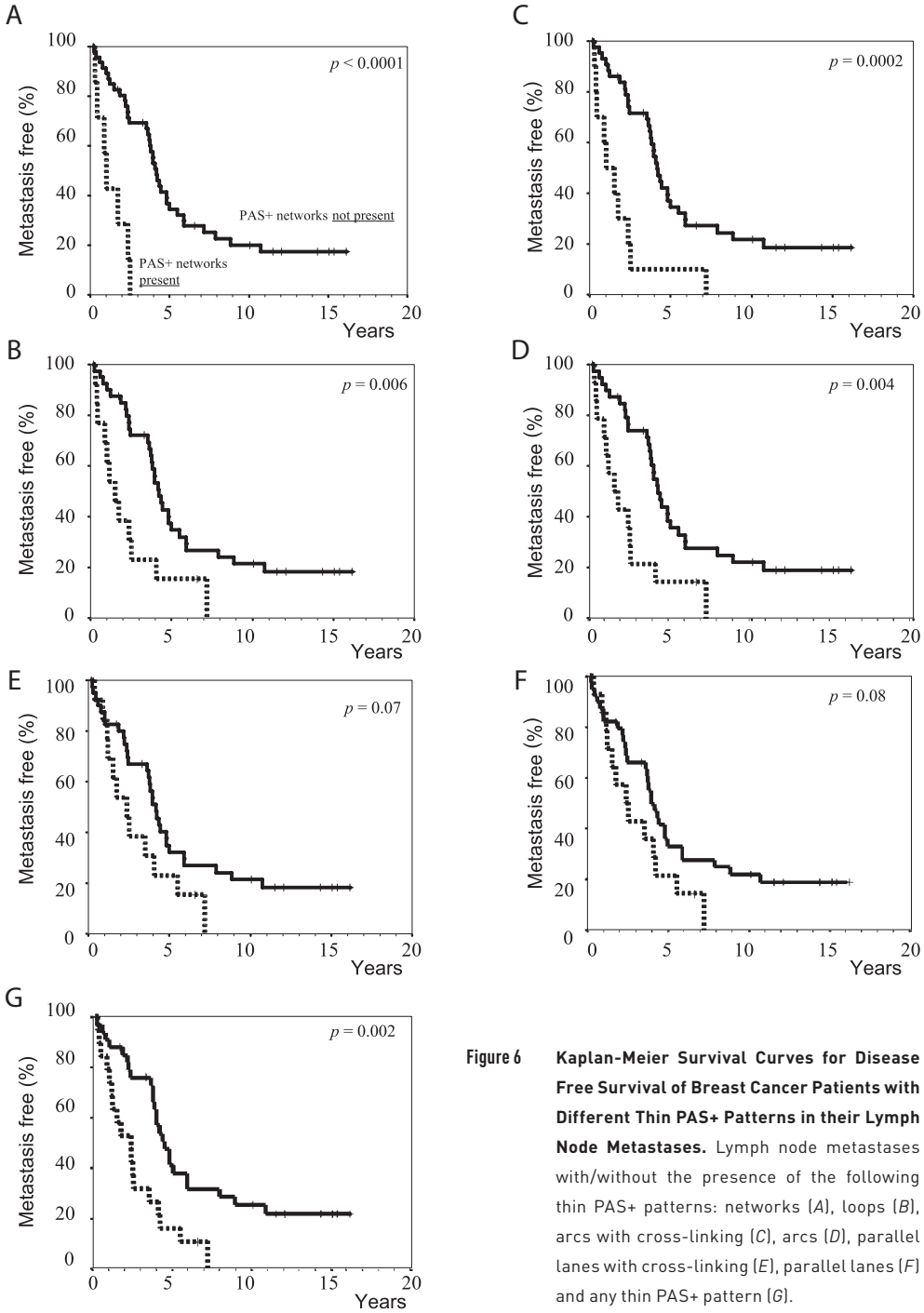

Figure 6 **Kaplan-Meier Survival Curves for Disease Free Survival of Breast Cancer Patients with Different Thin PAS+ Patterns in their Lymph Node Metastases.** Lymph node metastases with/without the presence of the following thin PAS+ patterns: networks (*A*), loops (*B*), arcs with cross-linking (*C*), arcs (*D*), parallel lanes with cross-linking (*E*), parallel lanes (*F*) and any thin PAS+ pattern (*G*).

Jeroen_Buijs_18.indd 86 26-11-2008 10:18:22

tumors can be explained by the co-existence of other PAS+/SMA+ structures in primary tumors or normal breast tissue, that hamper the interpretation. Most probably, myoepithelial cells and myofibroblasts interfere with scoring of the PAS+ patterns in the primary breast cancer. Other apparent inconsistencies, e.g. the association of PAS+ parallel lanes (with cross-links) in lymph nodes with poor prognosis for DFS, but not for total survival, are most likely due to the relatively small number of cases.

It has been well established that malignant breast cancer cells can acquire a mesenchymal phenotype, and transit into a myofibroblast, a process known as epithelial-to-mesenchymal transition (EMT)[25-27]. It is tempting to speculate that tumor cells that align hollow tubular structures are phenotypically distinct from other tumor cells and acquire a fibroblast-like phenotype. Accordingly, the process of epithelial-mesenchymal transition might be a prerequisite for a tumor to form such a network [28]. The generation of such a PAS+ network by genetically deregulated, aggressive tumor cells was termed 'vasculogenic mimicry' (VM) to emphasize their *de novo* generation without participation of endothelial cells and independent of angiogenesis [16,18,29-33]. In VM, the PAS+ interconnected loops are the tumor-lined vessels providing perfusion of erythrocytes. Recent reports suggest that VM also exists in ovarian [34], prostate [28] and breast cancer [29,35]. After establishing an inflammatory breast cancer (IBC) xenograft with VM features [36], Shirakawa and co-workers examined surgically resected breast cancers and classified 7,9 % as containing VM [35]. The existence of VM increased the likelihood of hematogenous spread and gave a poorer prognosis for the patient. However, in this study, erythrocytes were only occasionally detected within the PAS+ network. The PAS+ network may also consist of the PAS+ fluid-conducting spaces without erythrocytes in the form of stromal sheets between nests of tumor cells that could provide nutrition for the tumor cell, and probably facilitate metastasis [11].

In addition, Foss and co-workers provided evidence that PAS+ extracellular septa could be particularly favorable substrates for the in-growth of angiogenic, and possibly lymphatic, vessels [16]. Consequently, tumors that contain these PAS+ structures might be more aggressive, as these structures provide better means for (blood) vessel in-growth than tumors lacking these structures. The lack of continuous flt-4 expression in the PAS+ networks of breast cancer patients may, therefore, indicate that these structures do not entirely represent lymphatic vasculature. Indeed, the differences in distribution of flt-4+ and CD31+ patterns within the PAS+ networks in our tissue specimens from the patients, supports the notion that PAS+ meshworks are complex and consist of multiple types of vasculature (blood vessels, and possibly lymphatics). If the septa consist of two layers of ECM elaborated by opposing layers of tumor cells, the layers could separate, forming channels and laminar openings. Such openings could particularly lead to capillary growth. The patchy expression of the endothelial marker, CD31, is in agreement with this hypothesis. Finally, it has been suggested that the open ends of the growing capillaries could feed blood into the channels, therefore, the presence of erythrocytes in the channels could be explained, and different hypotheses could be reconciled [37].

In conclusion, we show here that the presence of PAS+ networks in lymph node metastases from invasive ductal carcinoma of the breast is one of the two independent risk factors for the occurrence of distant metastases. Moreover, the presence of a PAS+ network in a positive lymph node is the factor most strongly associated with occurrence of a distant metastasis. Therefore, by examining the presence of PAS+ networks in invasive ductal carcinoma of the breast, clinical behavior of this heterogeneous group of patients can be better predicted leading to early more aggressive management. Further research should focus in elucidating the exact nature and origin of the PAS+ network in different carcinomas. The investigation of the – possibly tumor-derived – PAS+ patterns, as observed in breast cancer, can have pathophysiological and therapeutic implications ranging from predisposition to blood-borne spread of tumor cells, to facilitated entry of drugs into tumors, and to efficacy of anti-cancer drugs as anti-angiogenic agents.

Acknowledgment

The authors thank Ronald Brand from the Dept. of Statistics for his advise and comments on the statistical analyses. This work has been supported by the Dutch Cancer Society (Grant nr. RUL 2001-2485).

References

1. Orr RK. The impact of prophylactic axillary node dissection on breast cancer survival--a Bayesian meta-analysis. *Ann Surg Oncol* 1999; 6:109-16.
2. Folkman J. Angiogenesis in cancer, vascular, rheumatoid and other disease. *Nat Med* 1995; 1:27-31.
3. Risau W. Mechanisms of angiogenesis. *Nature* 1997; 386:671-4.
4. Hanahan D, Folkman J. Patterns and emerging mechanisms of the angiogenic switch during tumorigenesis. *Cell* 1996; 86:353-64.
5. Rak J, Kerbel RS. Treating cancer by inhibiting angiogenesis: new hopes and potential pitfalls. *Cancer Metastasis Rev* 1996; 15:231-6.
6. Kumar R, Fidler IJ. Angiogenic molecules and cancer metastasis. *In Vivo* 1998; 12:27-34.
7. de Jong JS, van Diest PJ, Baak JP. Hot spot microvessel density and the mitotic activity index are strong additional prognostic indicators in invasive breast cancer. *Histopathology* 2000; 36:306-12.
8. Engels K, Fox SB, Harris AL. Angiogenesis as a biologic and prognostic indicator in human breast carcinoma. *EXS* 1997; 79:113-56.:113-56.
9. Gasparini G, Harris AL. Clinical importance of the determination of tumor angiogenesis in breast carcinoma: much more than a new prognostic tool. *J Clin Oncol* 1995; 13:765-82.
10. Harris AL, Zhang H, Moghaddam A, Fox S, Scott P, Pattison A *et al*. Breast cancer angiogenesis--new approaches to therapy via antiangiogenesis, hypoxic activated drugs, and vascular targeting. *Breast Cancer Res Treat* 1996; 38:97-108.
11. Clarijs R, Otte-Holler I, Ruiter DJ, de Waal RM. Presence of a fluid-conducting meshwork in xenografted cutaneous and primary human uveal melanoma. *Invest Ophthalmol Vis Sci* 2002; 43:912-8.
12. Folberg R, Pe'er J, Gruman LM, Woolson RF, Jeng G, Montague PR *et al*. The morphologic characteristics of tumor blood vessels as a marker of tumor progression in primary human uveal melanoma: a matched case-control study. *Hum Pathol* 1992; 23:1298-305.

13. Thies A, Mangold U, Moll I, Schumacher U. PAS-positive loops and networks as a prognostic indicator in cutaneous malignant melanoma. *J Pathol* 2001; 195:537-42.
14. Folberg R, Rummelt V, Parys-Van Ginderdeuren R, Hwang T, Woolson RF, Pe'er J *et al*. The prognostic value of tumor blood vessel morphology in primary uveal melanoma. *Ophthalmology* 1993; 100:1389-98.
15. Warso MA, Maniotis AJ, Chen X, Majumdar D, Patel MK, Shilkaitis A *et al*. Prognostic significance of periodic acid-Schiff-positive patterns in primary cutaneous melanoma. *Clin Cancer Res* 2001; 7:473-7.
16. Foss AJ, Alexander RA, Hungerford JL, Harris AL, Cree IA, Lightman S. Reassessment of the PAS patterns in uveal melanoma. *Br J Ophthalmol* 1997; 81:240-6.
17. McLean IW, Keefe KS, Burnier MN. Uveal melanoma. Comparison of the prognostic value of fibrovascular loops, mean of the ten largest nucleoli, cell type, and tumor size. *Ophthalmology* 1997; 104:777-80.
18. Maniotis AJ, Folberg R, Hess A, Seftor EA, Gardner LM, Pe'er J *et al*. Vascular channel formation by human melanoma cells in vivo and in vitro: vasculogenic mimicry. *Am J Pathol* 1999; 155:739-52.
19. van den Broek LJ, van de Vijver MJ. Assessment of problems in diagnostic and research immunohistochemistry associated with epitope instability in stored paraffin sections. *Appl Immunohistochem Molecul Morphol* 2000; 8:316-21.
20. Hazelbag HM, van den Broek LJ, van Dorst EB, Offerhaus GJ, Fleuren GJ, Hogendoorn PC. Immunostaining of chain-specific keratins on formalin-fixed, paraffin-embedded tissues: a comparison of various antigen retrieval systems using microwave heating and proteolytic pre-treatments. *J Histochem Cytochem* 1995; 43:429-37.
21. Valtola R, Salven P, Heikkila P, Taipale J, Joensuu H, Rehn M *et al*. VEGFR-3 and its ligand VEGF-C are associated with angiogenesis in breast cancer. *Am J Pathol* 1999; 154:1381-90.
22. Lee HD, Yoon DS, Koo JY, Suh CO, Jung WH, Oh KK. Breast conserving therapy in stage I & II breast cancer in Korea. *Breast Cancer Res Treat* 1997; 44:193-9.
23. Noguchi M, Yagasaki R, Kawahara F, Minami M, Tsuyama H, Earashi M *et al*. Breast conserving treatment versus modified radical mastectomy in Japanese patients with operable breast cancer. *Int Surg* 1997; 82:289-94.
24. van Tienhoven G, Voogd AC, Peterse JL, Nielsen M, Andersen KW, Mignolet F *et al*. Prognosis after treatment for loco-regional recurrence after mastectomy or breast conserving therapy in two randomised trials (EORTC 10801 and DBCG-82TM). EORTC Breast Cancer Cooperative Group and the Danish Breast Cancer Cooperative Group. *Eur J Cancer* 1999; 35:32-8.
25. Petersen OW, Lind NH, Gudjonsson T, Villadsen R, Ronnov-Jessen L, Bissell MJ. The plasticity of human breast carcinoma cells is more than epithelial to mesenchymal conversion. *Breast Cancer Res* 2001; 3:213-7.
26. Thiery JP. Epithelial-mesenchymal transitions in tumour progression. *Nat Rev Cancer* 2002; 2:442-54.
27. Dandachi N, Hauser-Kronberger C, More E, Wiesener B, Hacker GW, Dietze O *et al*. Co-expression of tenascin-C and vimentin in human breast cancer cells indicates phenotypic transdifferentiation during tumour progression: correlation with histopathological parameters, hormone receptors, and oncoproteins. *J Pathol* 2001; 193:181-9.
28. Sharma N, Seftor RE, Seftor EA, Gruman LM, Heidger PM, Jr., Cohen MB *et al*. Prostatic tumor cell plasticity involves cooperative interactions of distinct phenotypic subpopulations: Role in vasculogenic mimicry. *Prostate* 2002; 50:189-201.
29. Hendrix MJ, Seftor EA, Kirschmann DA, Seftor RE. Molecular biology of breast cancer metastasis. Molecular expression of vascular markers by aggressive breast cancer cells. *Breast Cancer Res* 2000; 2:417-22.
30. McDonald DM, Munn L, Jain RK. Vasculogenic mimicry: how convincing, how novel, and how significant? *Am J Pathol* 2000; 156:383-8.
31. Folberg R, Hendrix MJ, Maniotis AJ. Vasculogenic mimicry and tumor angiogenesis. *Am J Pathol* 2000; 156:361-81.
32. Fausto N. Vasculogenic mimicry in tumors. Fact or artifact? *Am J Pathol* 2000; 156:359.
33. Bissell MJ. Tumor plasticity allows vasculogenic mimicry, a novel form of angiogenic switch. A rose by any other name? *Am J Pathol* 1999; 155:675-9.

34. Sood AK, Seftor EA, Fletcher MS, Gardner LM, Heidger PM, Buller RE *et al*. Molecular determinants of ovarian cancer plasticity. *Am J Pathol* 2001; 158:1279-88.
35. Shirakawa K, Wakasugi H, Heike Y, Watanabe I, Yamada S, Saito K *et al*. Vasculogenic mimicry and pseudo-comedo formation in breast cancer. *Int J Cancer* 2002; 99:821-8.
36. Shirakawa K, Tsuda H, Heike Y, Kato K, Asada R, Inomata M *et al*. Absence of endothelial cells, central necrosis, and fibrosis are associated with aggressive inflammatory breast cancer. *Cancer Res* 2001; 61:445-51.
37. Ruoslahti E. Specialization of tumour vasculature. *Nature Cancer Reviews* 2002; 2:83-90.

Jeroen_Buijs_18.indd 90 26-11-2008 10:18:23

Chapter 3

Optical imaging of cancer metastasis to bone marrow: *a mouse model of minimal residual disease*

Am J Pathol 2002; 160:1143-53

Antoinette Wetterwald [1]
Gabri van der Pluijm [2]
Bianca Sijmons [2]
Jeroen T Buijs [2]
Marcel Karperien [2]
Clemens WGM Löwik [2]
Elsbeth Gautschi [1]
George N Thalmann [1]
Marco G Cecchini [1]

[1] Gene Therapy Laboratory, Department of Clinical Research and Department of Urology, University of Bern, Inselspital, Switzerland

[2] Department of Endocrinology, Leiden University Medical Center, Leiden, Leiden, The Netherlands.

Jeroen_Buijs_18.indd 91 26-11-2008 10:18:23

Abstract

The development of novel anti-cancer strategies requires more sensitive and less invasive methods to detect and monitor *in vivo* minimal residual disease in cancer models. Bone marrow metastases are indirectly detected by radiography as osteolytic and/or osteosclerotic lesions. Marrow micrometastases elude radiographic detection and, therefore, more sensitive methods are needed for their direct identification. Injection of cancer cells into the left cardiac ventricle of mice closely mimics micrometastatic spread. When luciferase-transfected cells are used, whole body bioluminescent reporter imaging (BLI) can detect microscopic bone marrow metastases of ≈0.5 mm^3 volume, a size below the limit where tumors need to induce angiogenesis for further growth. This sensitivity translates into early detection of intra-medullary tumor growth, preceding the appearance of a radiologically evident osteolysis by ≈2 weeks. BLI also enables continuous monitoring in the same animal of growth kinetics for each metastatic site and guides end-point analyses specifically to the bones affected by metastatic growth. This model will accelerate the understanding of the molecular events in metastasis and the evaluation of novel therapies aiming at repressing initial stages of metastatic growth.

Jeroen_Buijs_18.indd 92 26-11-2008 10:18:23

Introduction

Because of the progress made in early detection and surgical treatment of the primary tumor, mortality in cancer patients is increasingly linked to metastatic disease. Bone is the second most common site of metastasis [1] and the frequency of bone metastases at autopsy of cancer patients varies between 60 and 85%, depending on the cancer type [2-4].

Clinical and experimental observations indicate that the hematopoietic marrow, rather than the bone tissue, is the initial site of cancer cell seeding [5]. Indeed, small clusters of cancer cells (= micrometastases) can be detected in a vast proportion of the bone marrow aspirates of subjects affected by a variety of epithelial cancers with no radiological or scintigraphic evidence of bone metastasis at the time of diagnosis and/or surgery of the primary tumor [6,7]. Micrometastases represent the pathophysiological basis of minimal residual disease [8,9] (MRD) that will eventually lead to cancer relapse as overt metastases. However, they cannot be detected by conventional staging methods and are poorly influenced by current treatment [8-10]. Hence, there is a need for alternative therapeutic strategies that should be tested in experimental models able to mimic micrometastatic spread.

Injection of cancer cell lines into the left cardiac ventricle of immunodeficient (*nu/nu*) mice is a widely used animal model of bone/bone marrow metastasis [11,12]. This experimental setting closely resembles the clinical situation of MRD after removal of the primary tumor. However, detection of bone metastasis by radiography [13] makes it not an ideal model of MRD. In fact, radiologically evident osteolytic/osteosclerotic metastases are a late and macroscopic event in the evolution of metastatic bone disease. Thus, the model lacks the sensitivity that would be necessary to dissect the initial processes, such as the "angiogenic switch" [14], essential for tumor progression [15]. Furthermore, the radiological detection of osteolytic and/or osteosclerotic metastases is an indirect measure of the tumor burden. Only a parallel histomorphometric analysis allows the distinction between a therapeutic effect exerted directly on tumor cells or indirectly through inhibition of bone resorption. Therefore, more sensitive methods to detect and monitor directly metastatic growth in bone marrow/bone of whole animals need to be developed.

Expression *in vivo* of reporter genes encoding bioluminescent [16] or fluorescent [17] proteins can be detected externally by sensitive detection systems. Cancer cell lines permanently transfected either with the firefly luciferase (*Luc*) or the green fluorescent protein (GFP) have been used to monitor in living mice local tumor growth [18] and development of metastasis to different organs [17].

We investigated the possibility to apply an equivalent bioluminescent imaging method to visualize *in vivo* the development of bone marrow/bone metastases after injection of luciferase-transfected MDA-MB-231 cells, a human mammary carcinoma cell line [19], into the left cardiac ventricle of immunodeficient (*nu/nu*) mice.

Here we demonstrate that whole-body bioluminescent reporter imaging (BLI) effectively allows sensitive localization and growth monitoring of minimal metastatic deposits in the bone marrow at a stage largely preceding tumor-induced osteolysis.

Materials and Methods

Animals

Female BALB/c *nu/nu* mice were purchased from Iffa Credo (L'Arbresle, France). They were housed in individual ventilated cages under sterile condition according to the Swiss guidelines for the care and use of laboratory animals. Sterile food and water were provided ad libitum. Mice were 5 to 6 weeks old when used for the intracardiac (i.c.) injection of tumor cells. For intraosseous (i.o.), intra-muscle (i.m.) and subcutaneous (s.c.) implantation of tumor cells they were 10-12 weeks old.

For surgical manipulation, mice were anaesthetized by an intra-peritoneal (i.p.) injection of a mixture of Domitor (1mg/kg body weight; Pfizer, Sandwich, UK), Climasol (10mg/kg body weight; Gräub, Bern, Switzerland) and Fentanyl (100μg/kg body weight; University Hospital pharmacy). Mice were recovered from anaesthesia by a s.c. injection of a mixture of the following antidotes: Antisedan (5mg/kg body weight; Pfizer), Sarmasol (1mg/kg body weight; Gräub) and Narcan (2.4mg/kg body weight; Dupont Pharma, Wilmington, DE).

Mice subjected to i.c. injection of tumor cells were sacrificed by CO2 euthanasia at first signs of distress and/or paraplegia. Mice injected s.c., i.m. and/or i.o. with tumor cells were sacrificed immediately after BLI analysis, and those with tumor cells implanted i.o. were sacrificed at the end of the 5-week observation period.

Cell lines

The human mammary carcinoma cell line MDA-MB-231 (MDA-231) was obtained from the American Type Culture Collection (Rockville, MD). A sub-clone inducing invariably bone metastases after i.c. inoculation (bone-seeking clone, MDA-231-B) has been established by sequential cycles of i.c. inoculation of MDA-231 *in vivo* and expansion *in vitro* of the cell population recovered from the resulting bone metastases. Briefly, parental MDA-231 cells ($1x10^5$/100 μl PBS) were injected i.c. in female BALB/c *nu/nu* mice. Development of osteolytic bone metastases was monitored by radiography. When the bone metastases reached the size of ≈2 mm diameter, they were dissected out, cut into small fragments and transferred to 12 well-plates. After 3 days of culture, remnants of the original tissue fragments were removed and each area of cell outgrowth was individually trypsinized with the aid of cloning rings. The individual cell populations resulting from each area of outgrowth were separately expanded by limiting dilution. After expansion, the origin of the clones from the cancer cell population of the original metastases was confirmed by species-specific polymerase chain reaction (PCR) analysis for human ß2-microglobulin, as described earlier [20]. Positive clones only were selected for a new

Jeroen_Buijs_18.indd 94 26-11-2008 10:18:23

cycle of i.c. inoculation *in vivo* and expansion *in vitro* of the cell population recovered from the resulting bone metastases. The MDA-231-B sub-clone was obtained after a total of four of these consecutive cycles. It showed the capacity, after i.c. inoculation, to induce bone metastases, as detected by radiography, in 100% of the animals. For this reason it was selected for the establishment of stable transfectants expressing the luciferase gene.

Cell lines and the explanted fragments of bone metastases were grown in DMEM Medium (Biochrom, Basel, Switzerland) containing 4.5g glucose/l and supplemented with 10% newborn calf serum (Biowhittaker, Verviers, Belgium) and 1% gentamycin. Cells were regularly certified free of mycoplasma contamination.

Establishment of stable transfectants expressing the luciferase reporter gene

A CMV-promoter driven mammalian expression vector for luciferase (CMV-Luc) was generated by cloning a full-length firefly luciferase cDNA[21] into the pcDNA3.1 plasmid (Invitrogen, Breda, Netherlands). MDA-231-B cells were transfected with 1 μg CMV-Luc using fugene-6 (Roche Biochemicals, Almere, Netherlands). Stable transfectants were selected with G418 (800ug/ml; Life Technologies, Basel, Switzerland). Twenty-five different G418-resistant clones were isolated, sub-cloned and tested for luciferase activity. Six clones were found to express luciferase activity. One clone (MDA-231-B/Luc+), expressing the highest levels of luciferase activity (5-12 RLU/μg cell protein) was selected for further experimentation. The clone has been cultured up to 40 passages and, even though in some passages the cells have been propagated in absence of G418 selection, the clone maintains currently the same level of luciferase expression of early passages.

Induction of metastases by intracardiac and intra-venous injection of cancer cells

A single cell suspension of MDA-231-B/Luc+ cells ($1x10^5$/100 μl PBS) was injected into the left heart ventricle according to the method described by Arguello and co-workers.[11] Some animals were injected into the tail vein with an equal number of MDA-231-B/Luc+ cells. The development of metastases was weekly monitored by BLI and radiography. Some of the mice were also imaged 10 minutes and 24 hours after i.c. injection to visualize the early body distribution of MDA-231-B/Luc+cells.

Intraosseous implantation of cancer cells

For direct i.o. implantation of MDA-231-B/Luc+ cells, two holes, distant 4-5 mm from each other and each with a diameter of about 0.35 mm, were drilled through the bone cortex of the upper third of the right tibia with the aid of a dental drill (Hedstroem file, 28mm/30; Maillefer Instruments, Ballaigues, Switzerland). Space in the marrow cavity was created by flushing out the bone marrow of the proximal segment of the bone shaft. The upper hole was sealed by surgical bone wax (Ethicon, Johnson & Johnson, Somerville, NJ) and a single cell suspension of MDA-231-B/Luc+ cells ($1x10^4$/2 μl of PBS) slowly inoculated via a 30-gauge

needle inserted through the lower hole. Finally, the lower hole was sealed with surgical bone wax and the cutaneous wound was sutured. Local tumor development was monitored twice a week by BLI and radiography. This method was adopted to prevent spill of cancer cells from the channel created by the needle and subsequent growth outside the marrow cavity into the surrounding soft tissues during the following period (28 days) of monitoring.

Determination of the lowest cell number detectable in bone

The knee articulation was forced in a flexed position and a 27-gauge needle was inserted through the patellar tendon and guided toward the articular surface of the femur with gentle drilling motion until the bone cortex was perforated.[22] Ten thousand to 1 million MDA-231-B/Luc+ cells in a total volume of 5 μl of PBS were slowly injected into the bone marrow cavity. As control, 1 x 10^4 cells were injected i.m., in the vastus lateralis. As further control, 1 x 10^1, 1 x 10^2, 1 x 10^3 and 1 x 10^4 cells were injected s.c., in the ventral region. A single BLI analysis was performed after 15 minutes. The choice of this less invasive and faster method of cell inoculation was essentially dictated by the necessity to detect bioluminescent emission immediately after cell implantation and by the fact that in this case spill of cancer cells into the soft tissue was less an issue since tumor growth was not followed up.

Bioluminescent reporter imaging (BLI)

An imaging system essentially equivalent to that described by Contag and co-workers [18] was used. The imaging unit consists of an intensified charge-coupled device (CCD)-camera (VIM camera, model C2400-47, Hamamatsu Photonics, Hamamatsu, Japan) fitted to a light-tight chamber (Hamamatsu Photonics) and equipped with a 50 mm/f 1.2 Nikkor lens (Nikon, Küsnacht, Switzerland). The images are generated on an Argus-20 image processor (Hamamatsu Photonics) and transferred via SCSI using a software module (Open*lab*™, Improvision, Coventry, UK) to a computer (Macintosh G4, Apple Computer, Cupertino, CA) and processed by an image analysis software (Open*lab*™, Improvision, Coventry, UK).

For the detection of luciferase expressing cells, mice were anaesthetized as described above, but using half the doses of each sedative. Thirty μl of a 250 mM aqueous solution of luciferin (D-Luciferin Na salt; Molecular Probes, Leiden, Netherlands) were injected i.p. 15 minutes before beginning photon recording. Mice were placed in the light-tight chamber and a grey-scale image of the animal was first recorded with dimmed light. Photon emission was then integrated over a period of 5 minutes and recorded as pseudo-color images. For co-localization of the bioluminescent photon emission on the animal body, grey-scale and pseudo-color images were merged by using the Open*lab*™ imaging software.

Quantification of the bioluminescent signal

The bioluminescent signal was quantified by measuring the amount of highlighted pixels in the area shaped around each site of photon emission with the aid of the Openlab™ imaging software.

Jeroen_Buijs_18.indd 96 26-11-2008 10:18:23

Detection of bone lesions by radiography

Radiographs of the mice, anaesthetized as described above for the BLI analysis, were taken using X-Omat TL films (Kodak, Lausanne, Switzerland).

Immunohistochemistry

The mice injected i.c. MDA-231-B/Luc+ cells were perfused, after sacrifice, with 60 ml of HBSS containing 20U heparin/ml and, then, with 100 ml of 4% paraformaldehyde in Dulbecco's PBS, pH 7.4. Bones that were shown by BLI to be site of bioluminescent emission were selectively excised and further fixed overnight by immersion in fixative at 4°C. After decalcification in EDTA they were processed for paraffin embedding.

Five µm serial sections, after re-hydration and endogenous peroxidase block, were digested for 20 minutes at 37°C with trypsin (0.1% in 25mM Tris, 140 mM NaCl and 10mM CaCl2) for antigen retrieval. Rabbit antibodies (10 µg/ml) against human pan-cytokeratin (Dako, Zug, Switzerland) or control normal rabbit IgG (Jackson ImmunoResearch, La Roche, Switzerland) were followed by biotinylated swine anti-rabbit Ig antibodies (Dako) and streptavidin-biotinylated peroxidase complex (Amersham, Dubendorf, Switzerland). The reaction was developed with 3- amino-9-ethyl-carbazole as chromogen. Sections were slightly counter-stained with hematoxylin. Size measurements of metastatic lesions were performed with the aid of an image analysis software (NIH Image; http://rsb.info.nih.gov/nih-image).

Results

Monitoring in vivo development of metastases after intracardiac and intra-venous injection of cancer cells

In general, within 2 hours from the intracardiac injection of MDA-231-B/Luc+ cells 14 % of the mice died or showed signs of distress, for which they were subjected to euthanasia. The surviving mice all developed bone metastases, as detected by BLI. In contrast, none of the mice (n = 4) injected intra-venously showed either bone or soft tissue metastases during the entire period of observation (4 weeks), as detected both by BLI and radiography.

Ten minutes after i.c. injection of MDA-231-B/Luc+ cells, BLI showed diffuse photon accumulation over the entire animal body, with exclusion of the distal fore- and hind-legs, and of the tail (Fig. 1*A*). Twenty-four hours later photon emission from the same animal was abolished (Fig. 1*B*). However, after 4 weeks BLI could detect distinct areas of photon accumulation, suggestive of metastatic tumor growth, over the hind-legs and over the maxillo-facial region of the same animal (Fig. 1*C*).

First evidence of bioluminescent emission from bones, indicative of bone metastasis, was seen at day 24 after i.c. injection of cancer cells. In all mice (n = 4) discrete photon accumulation was localized over the distal metaphyses of the femurs (Fig. 2*A-D*) and over the

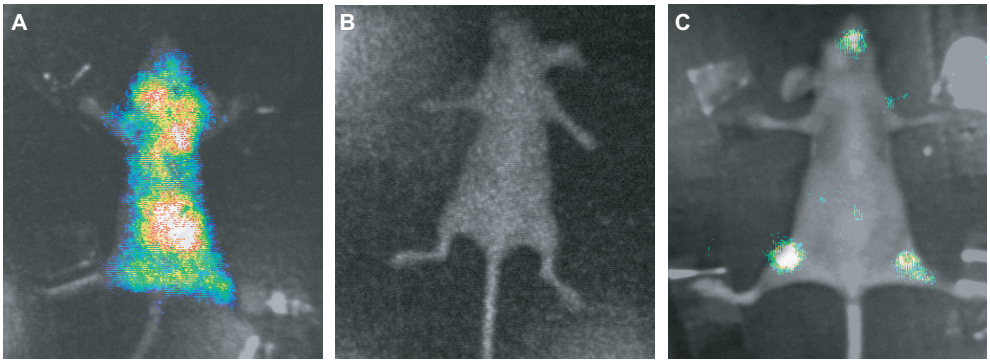

Figure 1 **Fate of MDA-231-B/Luc+ cells injected into the left cardiac ventricle**. Bioluminescent photon emission was externally imaged from the ventral projection of the same mouse 10 minutes (*A*), 24 hours (*B*) and 28 days (*C*) after injection. Signals are displayed as pseudo-color image (blue least intense, white most intense) at a 0-4 bit sensitivity range merged with the gray-scale body image of the mouse.

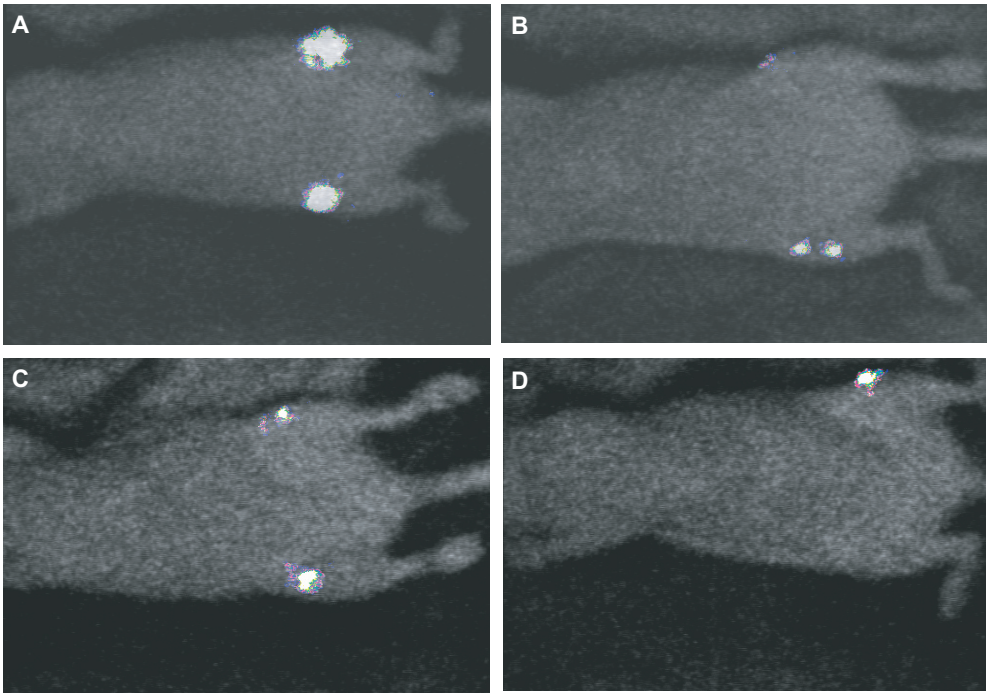

Figure 2 **BLI monitoring *in vivo* the kinetics of bone metastatic growth**. Bioluminescent photon emission was externally imaged 24 days after injection of MDA-231-B/Luc+ cells into the left cardiac ventricle. *A-D*, ventral projections of four different mice. Signals are displayed as pseudo-color image at the most sensitive 0-3 bit range.

Jeroen_Buijs_18.indd 98 26-11-2008 10:18:23

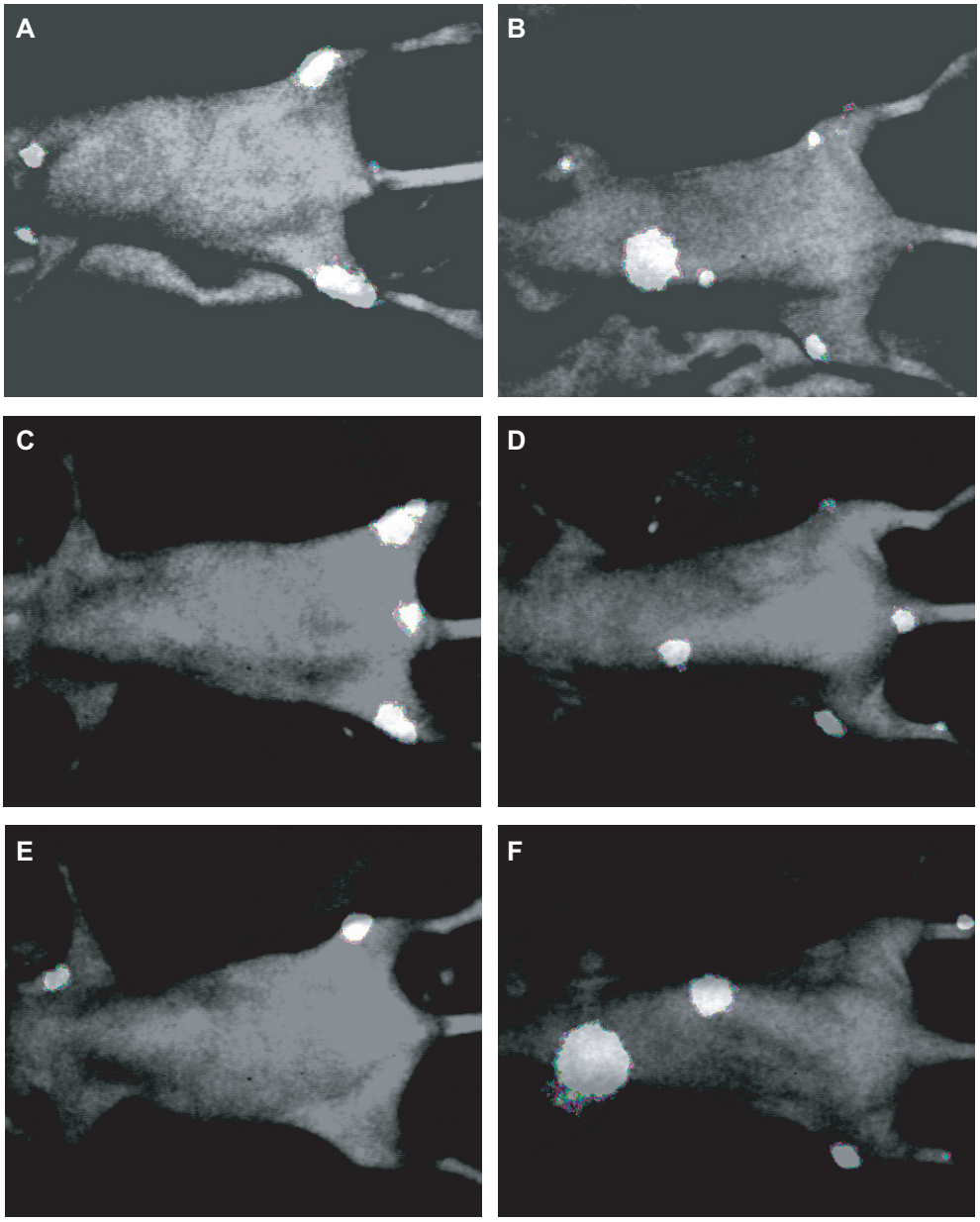

Figure 3 **BLI monitoring *in vivo* the kinetics of bone metastatic growth**. Bioluminescent photon emission was externally imaged 33 days after injection of MDA-231-B/Luc+cells into the left cardiac ventricle. Ventral (*A, C, E*) and dorsal (*B, D, F*) projections of the three mice shown in panels *B, C*, and *D*, respectively, of figure 2. Signals are displayed as pseudo-color image at a 0-5 bit range, less sensitive than that of figure 2, to optimize the anatomical localization.

dorsal projection of the thoracic vertebrae (not shown). In one mouse photons accumulated also over the proximal metaphysis of the tibia (Fig. 2*B*). Whole body radiographs taken at day 25 did not show any sign of osteolysis in any of the bones and, more specifically, in any of the bone locations that were origin of photon emission recorded the previous day (not shown).

The intensity of photon emission at the bone sites described above increased substantially from day 24 to day 33. Furthermore, at day 33, additional bone sites of bioluminescence became apparent (Fig. 3*A-F*). At this time point, the average number of bone metastasis/mouse attained to 6.33 (± 1.45, SEM). However, whole body radiographs taken at the same day showed bone lesions only in 1/3 of the bone sites revealed by photon detection (total 19 versus 6 bone sites, as detected by BLI and radiography, respectively; *n* mice = 3) (not shown). One animal survived until day 38 after i.c. injection of cancer cells. In this mouse an additional bioluminescent site appeared in the region of the sacral vertebrae (Fig. 4*B*). Meanwhile, the signal intensity over all the other bone sites further increased (Fig. 4*A-C*), as compared to day 33. However, the radiographic analysis of the bone lesions at day 38 did not reveal a modification in their number (Fig. 4*D*), as compared to day 33. In all cases the bone lesions were characterized by subtle modifications of the metaphyseal spongiosa due to increased bone remodeling and/or limited areas of osteolysis (Fig. 4*E,F*). At any time point, none of the animals of this series did show photon emission at extra-skeletal locations.

The quantification of the bioluminescent signal localized over the different bone metastatic sites from the time of their first appearance to the time of animal sacrifice (Fig. 4*G*) allowed continuous monitoring *in vivo* of the growth kinetics for each single bone lesion.

Immunohistochemical analysis for human pan-cytokeratin expression confirmed the presence of cancer cells in all the bones that were shown by BLI to be site of bioluminescent emission. One bone metastatic growth was identified both by BLI and radiography as located in the proximal metaphysis of the humerus (Fig. 4*A,D*). The histological and immunohistological analyses showed that cancer cells have extensively invaded the proximal half of the bone marrow cavity of this bone (Fig. 5*A,C*). In contrast, small bone metastases were apparently located by BLI on the distal region of both tibiae (Fig. 3*D,F* and Fig. 4*A-C*), but their presence was not corroborated by radiological signs of increased bone turnover located in the same or in neighboring bones. However, the histological and immunohistochemical analysis of the bones in this region revealed that a single metastatic focus was located in the epiphysis of each calcaneus bone (Fig. 5*B,D*).

MDA-231-B/Luc+ cells were i.c. injected in another series of mice (*n* = 12) to further investigate the potential of this specific bone-seeking clone to metastasize to organs other than bone and to demonstrate the ability of BLI to detect development of soft tissue metastasis. Bone metastases developed in 100% of the mice (12/12; average number of bone metastases/mouse: 5.33 ± 0.78 SEM). Soft tissue metastases were detected by BLI in 33 % of the mice (4/12; average number of soft tissue metastases/mouse: 0.33 ± 0.14 SEM). Lung and brain were the organs affected by the metastatic process in 25% (3/12) and 8% (1/12), respectively, of the mice injected.

Jeroen_Buijs_18.indd 100 26-11-2008 10:18:24

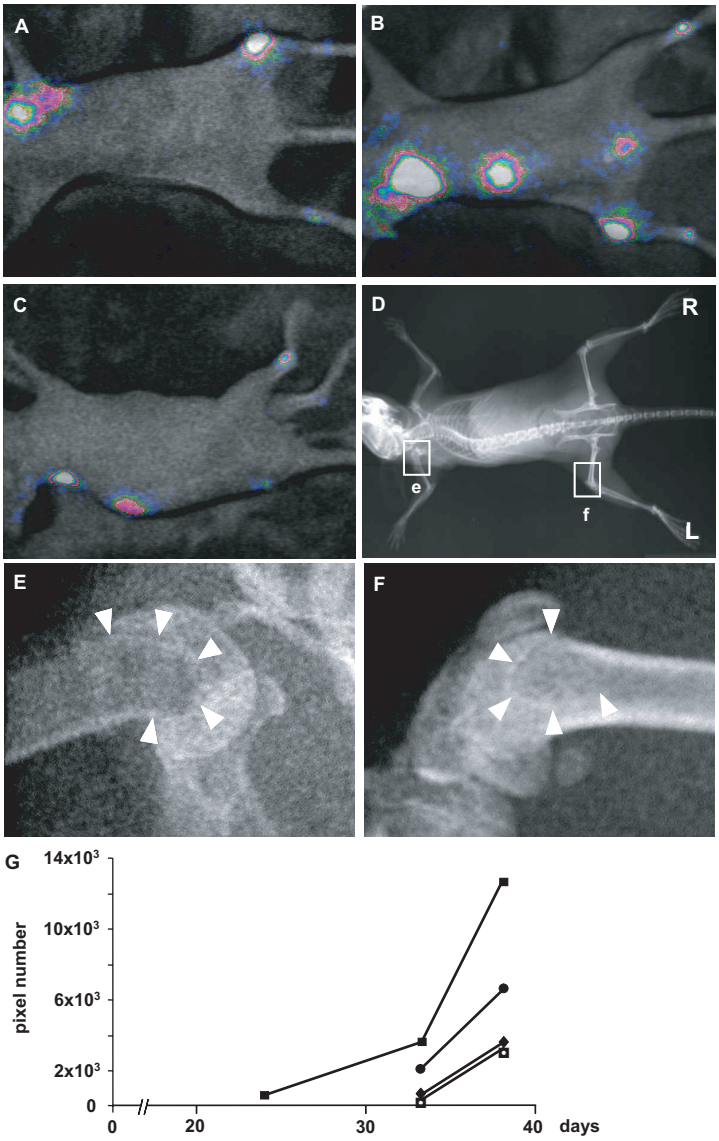

Figure 4 BLI and radiographic monitoring in vivo the kinetics of bone metastatic growth. Bioluminescent photon emission was externally imaged 38 days after injection of MDA-231-B/Luc+ cells into the left cardiac ventricle. Ventral (*A*), dorsal (*B*), and lateral (*C*) projections of the mouse shown in panels E and F of figure 3. Signals are displayed as pseudo-color image at a 0-6 bit range, less sensitive than that of figure 4, to optimize anatomical localization. *D*, whole body radiograph. R = right side, and L = left side of the mouse. The two regions delimited by the rectangular frames (E) on the proximal humerus and (F) on the distal femur are magnified in (*E*) and (*F*), respectively, showing details of the bone density. Arrowheads point at osteosclerotic rims delineating areas of discrete osteolysis. *G*, growth curve obtained by quantification in the same mouse of the bioluminescent signal localized over the left femur(■) at day 24, as shown in figure 2, D, and over the central portion of the spine (●) and the distal regions of the right (◆) and left (◘) tibia at day 33, as shown in figure 3, E and F, and at day 38 (*A, B*).

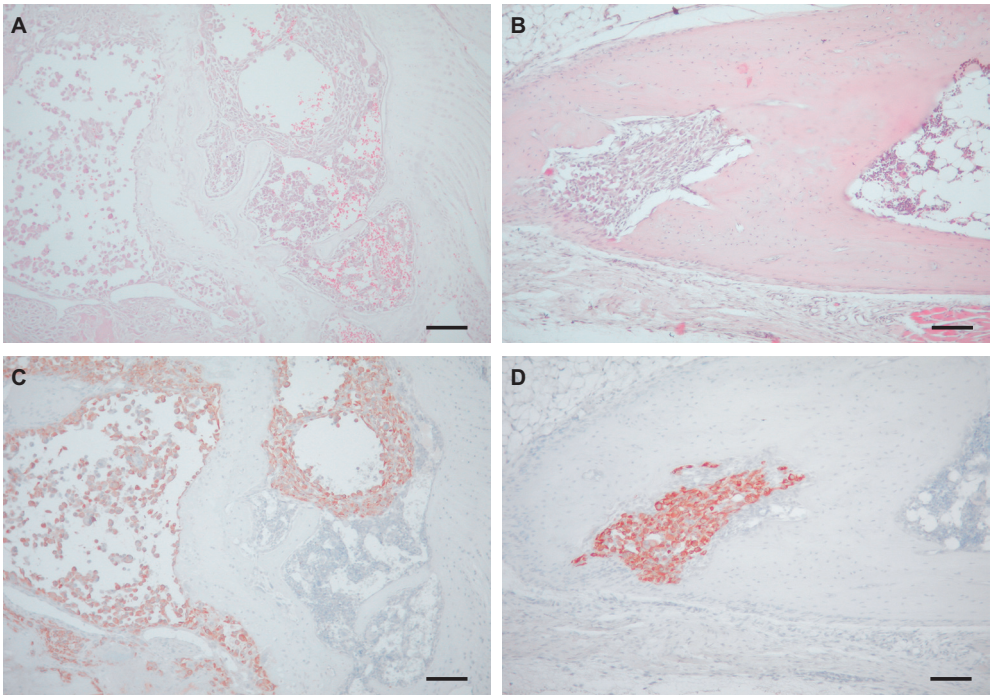

Figure 5 **Histological and immunohistological identification of MDA-231-B/Luc+ cells in two representative sites of metastasis**. Hematoxylin-eosin staining of sections from the left humerus (*A*) and the left calcaneus (*B*). Cytokeratin immunohistochemistry of adjacent sections from the same humerus (*C*) and calcaneus (*D*). Cells immuno-reactive with the anti-human pan-cytokeratin antibody are stained in brownish-red. Bars represent 100 μm.

During the entire experimental period in both series of i.c. inoculated mice none of the bone metastases detected by BLI showed a decline in bioluminescent activity. Furthermore, conventional radiography never detected an osteolytic lesion not showing bioluminescent emission.

Monitoring in vivo tumor growth after intraosseous implantation of cancer cells

Soon after implantation of $1x10^4$ MDA-231-B/Luc+ cells into the tibia marrow cavity, no bioluminescent emission could be detected externally. However, already after 4 days there was a defined, although weak, photon emission localized over the area of implant. The signal on the same area increased progressively and became intense from day 14 (Fig. 6*A*). Nevertheless, radiographs taken at equivalent time points (Fig. 6*B*) showed initial signs of osteolysis only at day 14. The osteolysis in the trabecular bone became clearly evident at day 25, and substantial erosion of the cortical bone was obvious at day 36.

The quantification at different time points of the bioluminescent signal localized over the site of implantation (Fig. 6*C*) allowed continuous monitoring *in vivo* of tumor growth.

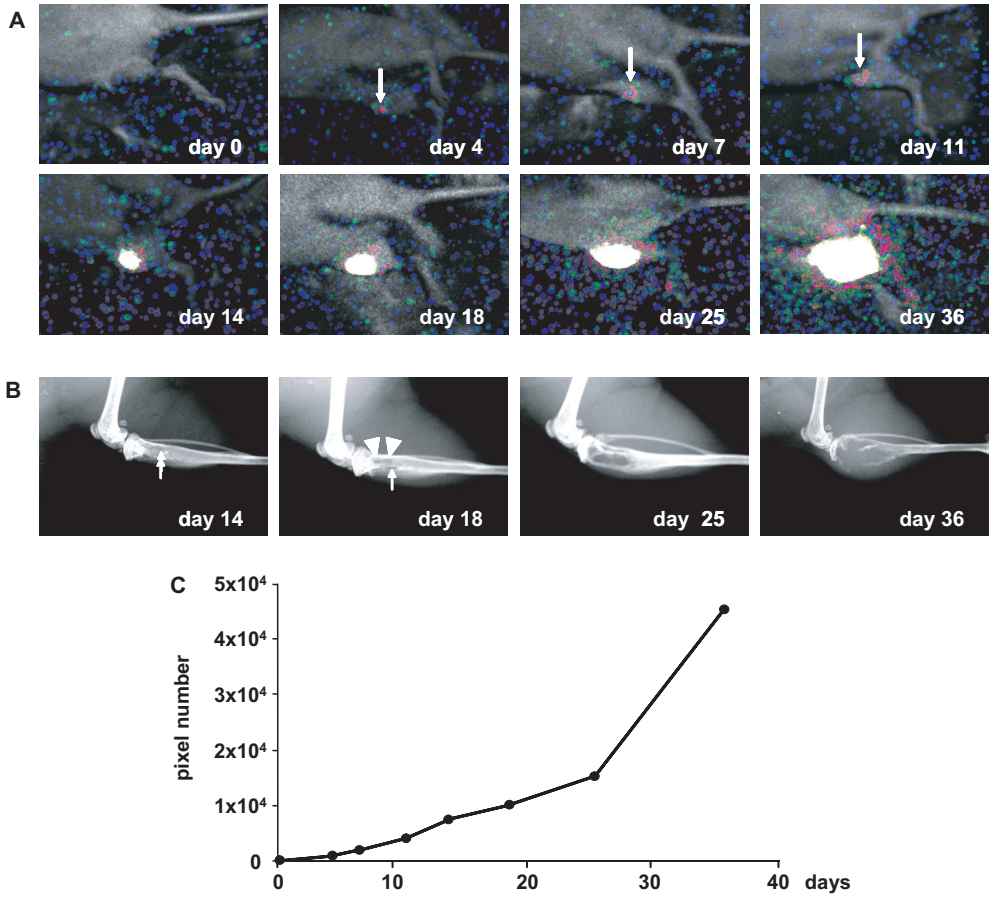

Figure 6 **BLI and radiographic monitoring in vivo the growth kinetics of 2 x 10^4 MDA-231-B/Luc+ cells implanted in the marrow cavity of the right tibia.** *A*, bioluminescent photon emission was recorded immediately (day 0) and at various time points in the 5 weeks following implantation. Signals are displayed as pseudo-color image at the most sensitive 0-3 bit range. Arrow at day 4, 7 and 11 highlights the initial photon accumulation over the area of implantation. *B*, radiographs of the corresponding tibia starting from day 14. Small arrow at day 14 and 18 points at the cortical hole that results from surgical drilling. Arrowheads at day 18 highlight the initial area of osteolysis. *C*, Growth curve obtained by quantification of the bioluminescent signal over the area of implantation during the 5-week recording period.

Determination of the lowest cell number detectable in bone by BLI

Soon after direct inoculation of MDA-231-B/Luc+ cells into the marrow cavity of the femur, BLI could detect a signal from a number of cells as low as 2 x 10^4. However, 1 x 10^4 and 0.1 x 10^4 cells could be detected if injected i.m. and s.c., respectively (not shown). Similarly, microscopic foci of spontaneous bone metastasis could easily be detected. In the specific case shown in figure 5 (*B* and *D*) the three major diameters of the metastatic lesion and the

density of the cancer cells were determined in serial sections comprehensive of the entire extension of the metastatic lesion. Assuming an ellipsoid shape, the total volume of the metastatic lesion resulted of ≈ 0.5 mm^3 volume and the total number of cells contained in it was calculated as ≈ 1.7 x 10^4.

Discussion

This investigation shows for the first time that the i.c. injection of MDA-231-B/Luc+ cancer cells combined to BLI is an ideal model for minimal residual disease (MRD), due to the remarkable sensitivity of the optical imaging in detecting microscopic bone marrow metastases *in vivo*.

The fate of the MDA-231-B/Luc+ cells could already be monitored by BLI immediately following intracardiac injection. The diffuse photon signal imaged over the entire animal body 10 minutes after injection was likely to be emitted by cancer cells not yet extravasated, and the areas of denser emission reflected presumably organs with the highest blood flow. The absence of signal 24 hours later conforms to the already reported rapid clearance and elimination of the majority of i.c. injected cancer cells [23]. Consistently with the elective bone /bone marrow tropism of the parental clone MDA-231-B, the same animal developed exclusively bone metastases within 4 weeks from i.c. injection of MDA-231-B/Luc+ cells. These findings further support the concept that organ specificity of metastases is not due to differences in blood perfusion, but largely depends on local interactions between cancer cells and the organ specific microenvironment [24].

All mice i.c. inoculated with the MDA-231-B sub-clone showed bone metastases, while only 1/4 of them showed soft tissue metastases, as detected by BLI. Thus the MDA-231-B possesses a higher bone-seeking capacity than the parental MDA-231 cell line, shown to induce bone metastases with lower incidence, but with a two-fold higher potential to metastasize to soft tissues [20]. This modified profile of organ distribution of metastases resembles very closely that already reported for another MDA-231 subclone similarly derived from a bone metastasis [25]. In contrast, none of the animals injected intravenously with the MDA-231-B sub-clone did develop either bone or soft tissue metastases. This seems to indicate that the cells are completely cleared by the lung already during the first passage through its circulation, further supporting the rationale for the intracardiac inoculation, as stated in the original description of the method [11]. The absence of metastatic growth in the lung after i.v. injection and the remarkable potential to metastasize to bone marrow after i.c. inoculation may suggest that the MDA-231-B sub-clone has acquired a growth advantage specific for the bone marrow microenvironment. Bone metastases induced by parental MDA-231 cells, when compared to brain and lung metastases, show increased expression of parathyroid hormone-related protein (PTH-rP) [20,25], macrophage colony stimulating factor (M-CSF) and vascular endothelial growth factor (VEGF) –A, -B and –C [20]. All these are

Jeroen_Buijs_18.indd 104 26-11-2008 10:18:29

bone-resorbing or angiogenic cytokines and they may represent the molecular basis for the enhanced osteotropism of bone-seeking clones derived from cancer cell lines [20,25,26].

When compared to the conventional radiographic detection of osteolytic and/or osteosclerotic lesions, BLI offers the important advantage of detecting tumor growth in the marrow cavity much before development of radiologically evident osteolytic and/or osteosclerotic lesions. The early detection is explained by the fact that BLI detects directly tumor burden long before it reaches a critical size able to induce modifications of the local bone remodeling relevant enough to be recognized by radiography. As a consequence, the number of metastatic sites detected by BLI largely exceeds those identified by conventional radiography. It derives a gain in statistical significance and a reduction in the number of animals needed for each experimental group.

Radiography could not detect in any of the animals an osteolytic lesion that did not show also bioluminescent activity. Furthermore, a decline of bioluminescent activity of already developed metastases was never observed. Taken together, these observations indicate that luciferase expression *in vivo*, under non-selective conditions, was stable over the entire experimental period.

BLI could easily image *in vivo* a bone metastatic lesion that at the end-point histological analysis resulted in a tumor of ≈0.5 mm^3 volume, corresponding to ≈1.7x10^4 cells. A similar number of cells could be detected when inoculated directly into the bone marrow cavity. Considering that during the time elapsed between first detection (day 33 after i.c injection of cancer cells) and analysis *ex vivo* (day 38) the spontaneous metastatic lesion has grown, it is likely that BLI can detect bone metastatic growth of even smaller size. Nevertheless, BLI could detect a discrete signal from 1x 10^4 and 0.1x 10^4 cancer cells implanted i.m and s.c., respectively, clearly indicating that intensity of the signal detected by BLI is a function of the tissue composition and depth of the bioluminescent source. This is possibly due to light scattering and quenching by tissue components such as hemoglobin[16,27].

Polymerase chain reaction- (PCR-) based methods also allow sensitive detection and quantification of cancer cell burden in bone/bone marrow [20,28,29]. However, being methods *ex vivo*, they have severe limitations. First, in temporal studies several animal groups need to be sacrificed at different time points. Second, the bone sample is randomly selected and its size necessarily small and inevitably subject to sampling bias. Thus, large numbers of animals per group are needed to reach statistical significance. Third, these methods require disruption of the tissue samples. This precludes the possibility to perform parallel histology-based and gene expression analyses on the same bone sample. In contrast, BLI allows detailed anatomical information, continuous monitoring and precise quantification of bone metastatic growth *in vivo*, consistent reduction in the number of experimental animals and opportunity to perform end-point histological, immunohistological and gene expression analyses guided to the bone(s) specifically affected by metastatic disease.

A similar method of whole body reporter gene imaging able to visualize *in vivo* experimental metastases to bone and soft tissues has been reported [17]. This method utilizes GFP, instead of luciferase, as reporter gene. A possible concern regarding the use of GFP as reporter gene in whole body imaging is the auto-fluorescence generated in animal tissues by external light excitation [16,17]. This background fluorescence may decrease the sensitivity of detection and, thus, delay early identification of bone metastatic foci. The GFP-based whole body imaging could visualize a bone metastatic lesion of about 0.96 mm in diameter at best [17]. At this tumor size the cancer cells may have already induced osteolytic and/or osteosclerotic lesions sufficient to be recognized by radiography. However, the sensitivity of GFP-reporter external imaging was not compared to radiography, and no histological proof of the presence and histomorphometric measurement of the size of the bone metastases were given [17].

All carcinomas, both primary and secondary, when they reach the size of 2-3 mm^3 depend on angiogenesis for further growth [14,15]. The ability of BLI to detect externally bone metastatic foci of even smaller size is extremely relevant in view of the necessity to investigate the pre- and peri-angiogenic phases of metastatic growth.

The model of i.c. injection of *Luc*-transfected cancer cells coupled to BLI detection and continuous monitoring *in vivo* of bone metastases will facilitate studies on the molecular mechanisms involved in early stages of metastatic disease (MRD) and the development of innovative therapeutic strategies.

Acknowledgments

We thank the Department of Clinical Research, University of Bern for the financial and logistic support. This work was supported by grants from the Swiss National Science Foundation Program 37 "Somatic Gene Therapy" (grant 4037-044804), Swiss National Science Foundation (grant 32-57118.99), CaPCURE, and "Stiftung zur Krebsbekämpfung".

References

1. Boring CC, Squires TS, Tong T. Cancer statistics, 1993. *CA Cancer J Clin* 1993; 43:7-26.
2. Jaffe HL. Tumors metastatic to the skeleton. Tumors and tumorous conditions of the bone and joints. Edited by Jaffe HL. Philadelphia, Lea and Febiger, 1968, pp. 589-618.
3. Drew M, Dickinson RB. Osseous complications of malignancy. Clinical cancer medicine, treatment tactics. Edited by Lokich J. Boston, Hall, 1980, pp. 97-124.
4. Thalmann G, Anezinis P, Devoll R, Farach-Carson C, Chung LWK. Experimental approaches to skeletal metastasis of human prostate cancer. Principles and practices of genitourinary oncology. Edited by Raghavan D, Scher HI, Leibel SA, Lange PH. Philadelphia, Lippincott-Raven, 1997, pp 409-16.
5. Willis RA. The spread of tumors in the human body. London, Butterworth, 1973, pp. 229-250.
6. Braun S, Pantel K. Micrometastatic bone marrow involvement: detection and prognostic significance. *Med Oncol* 1999; 16:154-65.
7. McDonnell CO, Hill ADK, McNamara DA, Walsh TN, Bouchier-Hayes DJ. Tumor micrometastases: the influence of angiogenesis. *Eur J Surg Oncol* 2000; 26:105-15.

Jeroen_Buijs_18.indd 106 26-11-2008 10:18:29

8. Hirsch-Ginsberg C: Detection of minimal residual disease: relevance for diagnosis and treatment of human malignancies. *Annu Rev Med* 1998; 49:111-122.
9. Kostler WJ, Brodowicz T, Hejna M, Wiltschke C, Zielinski CC. Detection of minimal residual disease in patients with cancer: a review of techniques, clinical implications, and emerging therapeutic consequences. *Cancer Detect Prev* 2000; 24:376-403.
10. Klein CA. The biology and analysis of single disseminated tumour cells. *Trends Cell Biol* 2000; 10:489-93.
11. Arguello F, Baggs RB, Frantz CN. A murine model of experimental metastasis to bone and bone marrow. Cancer Res 1988; 48:6876-81.
12. Yoneda T, Sasaki A, Mundy GR. Osteolytic bone disease in breast cancer. *Breast Cancer Res Treat* 1994; 32:73-84.
13. Yoneda T. Cellular and molecular basis of preferential metastasis of breast cancer to bone. *J Orthop Sci* 2000, 5:75-81.
14. Hanahan D, Folkman J. Patterns and emerging mechanisms of the angiogenic switch during tumorigenesis. *Cell* 1996, 86:353-364.
15. Carmeliet P, Jain RK. Angiogenesis in cancer and other diseases. *Nature* 2000; 407:249-257.
16. Contag CH, Jenkins D, Contag PR, Negrin RS. Use of reporter genes for optical measurements of neoplastic disease in vivo. *Neoplasia* 2000; 2:41-2.
17. Yang M, Baranov E, Jiang P, Sun FX, Li XM, Li L *et al.* Whole-body optical imaging of green fluorescent protein-expressing tumors and metastases. *Proc Natl Acad Sci USA* 2000; 97:1206-11.
18. Edinger M, Sweeny TJ, Tucker AA, Olomu AB, Negrin RS, Contag CH. Noninvasive assessment of tumor cell proliferation in animal models. *Neoplasia* 1999; 1:303-310.
19. Cailleau R, Yong R. Olive M, Reeves WJ. Breast tumor cell lines from pleural effusions. *J Natl Cancer Inst* 1974; 53:661-74.
20. van der Pluijm G, Sijmons B, Vloedgraven H, Deckers M, Papapoulos SE, Löwik CWGM. Monitoring metastatic behavior of human tumor cells in mice with species-specific polymerase chain reaction: elevated expression of angiogenesis and bone resorption stimulators by breast cancer in bone metastases. *J Bone Miner Res* 2001; 16:1077-91.
21. Nordeen SK. Luciferase reporter gene vectors for analysis of promoters and enhancers. *Biotechniques* 1988; 6:454-58.
22. Wang CW, Chang YW. A model for osseous metastasis of human breast cancer established by intrafemur injection of MDA-MB-435 cells in nude mice. *Anticancer Res* 1997; 17:2471-74.
23. Basse P, Hokland P, Heron I, Hokland M. Fate of tumor cells injected into the left ventricle of heart in Balb/c mice: role of natural killer cells. *J Natl Cancer Inst* 1988; 80:657-65.
24. Fidler IJ. Critical determinants of cancer metastasis: rationale for therapy. *Cancer Chemother Pharmacol* 1999, 43:S3-S10.
25. Yoneda T, Williams PJ, Hiraga T, Niewolna M, Nishimura R: A bone-seeking clone exhibits different biological properties from the MDA-MB-231 parental human breast cancer cells and a brain-seeking clone in vivo and in vitro. *J Bone Miner Res* 2001; 16:1486-95.
26. Koeneman KS, Yeung F, Chung LWK. Osteomimetic properties of prostate cancer cells: a hypothesis supporting the predilection of prostate cancer metastasis and growth in the bone environment. *Prostate* 1999; 39:246-61.
27. Colin M. Haemoglobin interferes with the ex vivo luciferase luminescence assay: consequence for detection of luciferase reporter gene expression *in vivo*. *Gene Ther* 2000; 7:1333-6.
28. Negrin RS, Blume KG. The use of the polymerase chain reaction for the detection of minimal residual disease. *Blood* 1991; 78: 255-8.
29. Sung V, Cattell DA, Bueno JM, Murray A, Zwiebel JA, Aaron AD, Thompson EW. Human breast cancer cell metastasis to long bone and soft organs of nude mice: a quantitative assay. *Clin Exp Metastasis* 1997; 15: 173-83.

Jeroen_Buijs_18.indd 108 26-11-2008 10:18:29

Chapter 4

Interference with the Microenvironment Support Impairs the *De Novo* Formation of Bone Metastasis *In Vivo*

Cancer Res 2005; 65:7682-90.

Gabri van der Pluijm[1]
Ivo Que[1]
Bianca Sijmons[1]
Jeroen T Buijs[1]
Clemens WGM Löwik[1]
Antoinette Wetterwald[2]
George N Thalmann[2]
Socrates E Papapoulos[1]
Marco G Cecchini[2]

[1]Department of Endocrinology,
Leiden University Medical Center,
Leiden, The Netherlands;

[2]Department of Clinical Research and Urology,
Faculty of Medicine,
University of Bern,
Bern, Switzerland

Jeroen_Buijs_18.indd 109 26-11-2008 10:18:30

Abstract

Interference with the microenvironmental growth support is an attractive therapeutic strategy for repressing metastatic tumor growth. Bone is a highly dynamic tissue that is continuously remodelled by bone resorption and subsequent bone formation. Growth factors supporting bone metastatic growth are released especially during bone resorption. Differently from most of the other tissues, drugs that can limit local turnover, namely bisphosphonates (BPs), are available for bone. Thus, we investigated whether pharmacological interference with bone turnover could repress development and growth progression of experimental bone metastasis. Whole body bioluminescent imaging (BLI) was adopted as a validated and reliable method for sensitive detection, monitoring and quantification *in vivo* of the growth progression of bone metastases induced by intracardiac or intraosseous injection of luciferase-transfected breast cancer cells (MDA-231-B/Luc+). Preventive BP-induced reduction of bone turnover, prior to bone colonization by cancer cells, inhibited by a great extent the number of developing bone metastases. Nevertheless, tumor growth in the few, but still developing bone metastases, was affected only transiently. Reduction of bone turnover was also unable to control growth progression of bone metastases, either induced by hematogenous spreading or by intraosseous inoculation, which were already established when BP-treatment was initiated. This, despite a substantial anti-osteolytic effect induced by BPs. Therefore, bone metastatic cancer cells, after an initial growth phase dependent on the interaction with the local stroma, become independent on microenvironmental growth factor support and progress autonomously. Inhibition of bone turnover may represent a useful adjuvant therapy for cancer patients at risk to develop bone metastasis.

Jeroen_Buijs_18.indd 110 26-11-2008 10:18:30

Introduction

Micrometastases, persisting in various tissues of cancer patients after removal of the primary tumor, represent the pathophysiological basis for cancer relapse as overt metastases. Preferential colonization of certain tissues by cancer cells and their subsequent growth are determined by interaction with the tissue-specific microenvironment (Seed & Soil theory) [1,2]. Therefore, pharmacological interference with the microenvironmental growth support, is becoming an attractive therapeutic strategy for repressing metastatic tumor growth [3].

Bone metastases are common in cancer, especially breast and prostate carcinoma. They cause considerable morbidity characterized by severe bone pain and high incidence of skeletal, neurological and hematopoietic complications (hypercalcemia, fracture, spinal cord compression and bone marrow aplasia [4-9]. Evidence from animal studies supports the concept that the rate of bone turnover is directly related to the occurrence and progression of bone metastases [10-13]. Recently, this view has been further substantiated by a clinical study, showing a strong and highly significant association between the rate of bone resorption and incidence of subsequent skeletal complications in breast and prostate cancer patients [14,15].

The skeleton is a highly dynamic tissue that is continuously renewed through the process of bone remodelling. This occurs at multiple sites in the skeleton by temporary structures called 'basic multicellular units' (BMU) [16,17]. The result is the replacement of old bone with new bone, thus maintaining the structural integrity and the mechanical competence of the skeleton throughout adult life. The number and the activity of these BMUs determine the rate of bone turnover [18]. During bone remodelling osteoblasts and osteoclasts, the cellular components of the BMU, secrete paracrine factors that induce chemotaxis and cell adhesion, support cell survival and growth, and stimulate angiogenesis [19,20]. Furthermore, there is experimental evidence showing that growth factors like transforming growth factor-β (TGF-β)are released from the bone matrix and stimulate the secretion of bone active cytokines, which not only enhance bone resorption, but also stimulate further tumor growth ('vicious circle') [19-25].

Taken together the evidence above suggests that pharmacological suppression of bone turnover may not only protect skeletal integrity at the metastatic site and reduce the incidence of skeletal complications, as has been shown with bisphoshonates (BPs), but may also interfere with the local growth support of cancer cells, thus preventing the development and progression of bone metastases. We tested this hypothesis by BP-induced inhibition of bone turnover in animal models of bone metastasis induced by luciferase-expressing human MDA-MB-231 breast cancer cells. Metastatic tumor development and progression was monitored by whole body bioluminescent reporter imaging (BLI) as described earlier [26].

BLI allows spatio-temporal and quantitative analyses of tumor growth and, due to its sensitivity, is ideally suited to evaluate the effectiveness of therapeutic approaches that target both early stages of metastatic development and advanced metastatic disease. BLI

gives detailed information on localization and growth of minimal metastatic deposits in the bone marrow of experimental animals at a stage largely preceding tumor detection by other methods. Simultaneous assessment of bone destruction by morphometrical analyses (radiographs, histomorphometry) and of tumor burden (BLI) allows discrimination between bone sparing effects (inhibition of tumor-induced osteolysis) and interference with tumor progression (viability and growth). Evidence is presented that bone metastatic cancer cells, after an initial stage that is probably necessary to initiate a self-maintaining autocrine growth, become independent from the microenvironmental growth factor support and, thus, expand autonomously, independent of pharmacological reduction of bone turnover.

Materials and Methods

Cell line and culture conditions

MDA-MB-231 (MDA-231), an estrogen independent human breast cancer cell line, was obtained from the American Type Culture Collection (Rockville, MD, USA). A subclone inducing invariably bone metastases after intracardiac inoculation (bone-seeking clone MDA-231-B) has been established by 4 consecutive sequential cycles of intracardiac inoculation of MDA-MB-231 *in vivo* and subsequent expansion *in vitro* of the cell population recovered from the resulting bone metastases as described earlier [26]. MDA-231-B cells were stably transfected with a CMV-promotor driven mammalian expression vector for luciferase, CMV-luc, and one clone with the highest expression of luciferase expression (MDA-231-B/Luc+) was successfully used for *in vivo* optical imaging as described previously [26]. MDA-231-B/Luc+ cells were cultured in Dulbecco's modified Eagle's Medium (DMEM, Gibco-BRL, Breda, the Netherlands) containing 4.5 g of glucose/L and supplemented with 10 % fetal calf serum (Gibco-BRL, Breda, the Netherlands), and 800 µg/ml geneticyne/G418 (Gibco-BRL, Breda, the Netherlands). Cells were regularly certified free of mycoplasma contamination.

All MDA-231-B/Luc+cell cultures were harvested at sub-confluence after being re-fed with fresh medium 24 hours before inoculation preparation. Cell suspensions of MDA-231-B/Luc+(1 x 10^5 cells/100 µl PBS for intracardiac inoculation or 1 x 10^5 cells /10 µl PBS for intraosseous inoculation) were prepared as described previously [26-28].

Animals

Female nude (BALB/c *nu/nu*) mice were purchased from Charles River (L'Arbresle, France). They were housed in individual ventilated cages under sterile condition according to the Dutch guidelines for the care and use of laboratory animals (DEC). Sterile food and water were provided ad libitum. Mice were 6 weeks old when used for the intracardiac or intraosseous inoculation of cancer cells.

For surgical and analytical procedures (intraosseous inoculation, whole body imaging and skeletal radiography) mice were anaesthesised by intraperitoneal injection of a 50 µl

Jeroen_Buijs_18.indd 112 26-11-2008 10:18:30

1:1:1 mixture; Ketamine HCl (Stock solution of 100 mg/ml Nimatek; Vetimex Animal Health B.V., Bladel, The Netherlands.) + Xylazine (2 % Rompun, Bayer AG, Leverkusen, Germany) + PBS (pH 6.8). Intracardiac inoculation of cancer cells was performed under Isofluorane anaesthesia (0.8 L/min, Isofluorane, Air Products, Waddinxveen, The Netherlands) using the Vapex3 system (VetTech Solutions Ltd, United Kingdom). At the end of the experimental period animals were sacrificed by cervical dislocation.

Induction of systemic metastates by intracardiac (i.c.) injection of MDA-231-B/Luc+cells

A single cell suspension of 1 x 10^5 MDA-231-B/Luc+cells /100 µl PBS was injected into the left cardiac ventricle (i.c.) according to the method originally described by Arguello and co-workers [29] and modified for MDA-MB-231 cells by Sasaki and co-workers [30]. The progression of the cancer cell growth was monitored weekly for by optical imaging as described previously [26]. At the same time points, osteolytic bone metastases were monitored by radiographs and analyzed as published earlier [26-28]. After the experimental period, the animals were sacrificed, and selected long bones site of cancer metastasis dissected and processed for further histomorphometric and immunohistochemical analysis (see below).

Intraosseous inoculation (i.o.) of MDA-231-B/Luc+cells

A single cell suspension of MDA-231-B/Luc+cells was injected into the right tibiae as described previously [26-28]. In brief, two holes, 4 to 5 mm apart and each with a diameter of ~ 0.35 mm, were drilled through the bone cortex of the upper right tibia with the aid of a dental drill. Space in the bone marrow was created by flushing out the bone marrow from the proximal end of the shaft. The upper hole was sealed by surgical wax and 1 x 10^5 MDA-231-B/Luc+cells per 10 µl PBS were slowly inoculated via a 30-gauge needle through the lower hole. Finally the lower hole was sealed with surgical wax and the cutaneous wound was sutured. The progression of cancer cell growth was monitored weekly by optical imaging as described previously (see below). At the same time points, osteolytic bone metastases were monitored by radiographs and analyzed as described previously [26-28]. After the experimental period the animals were sacrificed, the tibia site of intraosseous inoculation dissected and processed for further histomorphometrical and immunohistochemical analysis (see below).

Bioluminescent reporter imaging (BLI) and quantification of the bioluminescent signal

Whole body optical imaging of tumors induced by the luciferase-expressing human breast cancer cell line MDA-MB-231, inoculated either i.o. or i.c, was performed as described earlier [26]. After intra-peritoneal administration of 2 mg D-luciferin (Perbio Science Nederland B.V., Etten-Leur, The Netherlands), the animals were immediately transferred to a light-tight chamber and reference gray-scale body-surface images were taken using a intensified charged-coupled device (CCD) camera (C2400-77AH-01, Hamamatsu Photonics K.K.,

Japan) fitted with a 25 mm/0.95 f (optical aperture) objective (Schneider Optik, Kreuznanch, Germany). Five minutes after administration of D-luciferin, photon emission was integrated for a period of 3 minutes and processed using an Argus 20 image processor and M4314 image intensifier (Hamamatsu). Gray-scale images and bioluminescent images were superimposed using OpenLab software (Improvision, Coventry, UK). The relative light intensity was visualized by pseudocolors. Analyses for each metastatic site were performed after definition of the region of interest (= ROI, Openlab software) and quantified as described previously [26]. Values are expressed as relative light units (RLU).

Radiographical Analyses

After intraosseous or intracardiac inoculation of MDA-231-B/Luc+breast cancer cells into 6-week-old nude mice the formation of osteolytic lesions of the in the skeleton was assessed by radiography (Kodak X-OMAT TL film, Eastman Kodak Company, Rochester NY) using a Hewlett Packard X-ray system Faxitron 43805 as described previously [27,28]. Osteolytic areas were measured using NIH-Image 1.62b7 software as described earlier [27,28].

Histomorphometry, Histochemistry and Immunohistochemistry

Dissected long bones were fixed in 4 % paraformaldehyde (pH 6.8), decalcified as described previously and processed for paraffin embedding [27,28]. Longitudinal sections (5 μm) were cut through the sagittal plane of the tibiae containing tumors induced by the i.o. inoculation of MDA-231-B/Luc+cells. Sections were either submitted to Goldner staining or histochemical staining for tartrate resistant acid phospahtase (TRAcP) as described previously [27,28].

Histomorphometric measurements of tumor burden were performed on central sections through the tumor (largest tumor area). Tumor growth in bone could be readily identified by cytokeratin staining alone or in combination with HE staining. Total tumor area, as an estimate of total tumor burden, was measured by image analysis using NIH-Image 1.62b7 Image Analyses Software as described previously by us [27,28]. Subsequently, a distinction was made between the total tumor burden and intra- and extraosseous tumor burden. For this the digital image of the total tumor area was subdivided into an area delimited by the bone cortex or, were this has been partially resorbed as a result of the tumor-induced osteolysis, by a virtual line joining the remnants of the bone cortex, to define 'intraosseous' tumor growth. In addition, extraosseous tumor growth was defined as extramedullary growth of cancer cells (tumor cells growing surrounding the bone cortex or its remnants).

Histomorphometric measurements of trabecular bone volumes were performed after Goldner staining on the same central sections as used for tumor burden measurements (see above). Trabecular bone volume (TBV) was estimated in the proximal tibia by measuring the total area of trabecular structures in an area 0-2 mm distal to the capillary invasion front of the growth plate. TBV is expressed as percentage of the total area that was covered by trabeculae.

Jeroen_Buijs_18.indd 114 26-11-2008 10:18:30

Bisphosphonate treatment

Treatment protocols to establish the effects of olpadronate on the generation and progression of systemic bone metastases induced by i.c. injection of MDA-231-B/Luc+cells were performed according to the following two schemes (Fig. 1):

Preventive protocol: effect of long-term BP treatment on '*de novo*' generation and growth of systemic bone metastases (Fig. 1*A*). Beginning from two days prior to inoculation of MDA-231-B/Luc+cells the mice were treated by daily s.c. injections with 1.6 μM olpadronate/kg/day for the whole duration of the *in vivo* study (48 days). The generation and progression of bone metastases was monitored by BLI and radiography at day 7, 14, 21, 28, 33, 39 and 46. After 48 days of BP treatment (= day 46 from i.c. injection of cancer cells) the animals were sacrificed.

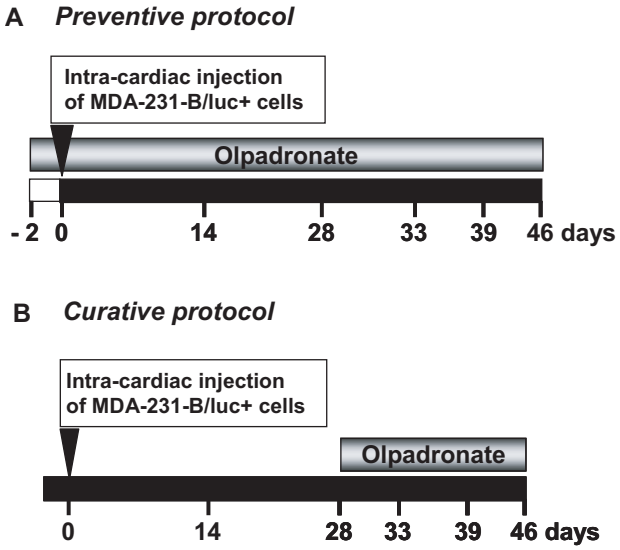

Figure 1 **Preventive and curative protocols for bisphosphonate (BP) treatment in a heart injection model of bone metastasis.** *A*, in the preventive protocol, 4-week-old female BALB/c *nu/nu* mice were treated with 1.6 μM/kg/day olpadronate for two days prior to inoculation of cancer cells. Subsequently 10^5 MDA-231-B/Luc+cells were inoculated into the left cardiac ventricle and the animals were treated by daily s.c. injections with 1.6 μM/kg/d of olpadronate for the duration of the experiment. The formation of bone metastases (and quantification of individual metastasis) was monitored and quantified weekly by whole body bioluminescent reporter imaging (BLI). In the same animals, the formation of osteolytic lesions was followed by radiography. *B*, in the curative protocol, 10^5 MDA-231-B/Luc+cells were inoculated into the left cardiac of ventricle 4-week-old female BALB/c *nu/nu*. Animals were monitored weekly to assess the formation of distant metastases and osteolysis (BLI, radiography). Starting from 28 days after cancer cell inoculation, the animals were equally distributed into two experimental groups and they were given either 1.6 μM/kg/day olpadronate or vehicle. Subsequently the progression of bone metastasis was monitored by BLI and radiography at day 5, 11 and 18. After 18 days of BP treatment (= day 46 from intracardiac injection) the animals were sacrificed.

Curative protocol: effect of short-term BP treatment on growth of established bone metastases (Fig. 1*B*). The presence of established bone metastases was verified by BLI and radiography. 28 days after i.c. injection of MDA-231-B/Luc+cells the animals were equally distributed into two experimental groups based on a comparable bone metastatic tumor burden/mouse, as detected by BLI. Subsequently, to one experimental group 1.6 μM/kg/day olpadronate was given, while to the other vehicle was administered (0.9% NaCl) for the following 18 days. The progression of bone metastasis was monitored by BLI and radiography at day 5, 11 and 18. After 18 days of BP treatment (= day 46 from i.c. inoculation of cancer cells) the animals were sacrificed.

To investigate the effect of BP on tumor development and osteolysis subsequent to intraosseous inoculation of MDA-231-B/Luc+cells, beginning from day 3 after inoculation (day of inoculation = day 0) the animals were treated for a period of 40 days by daily subcutaneous (s.c.) injections of BP dissolved in 0.9 % NaCl (50 μl volume) at the following doses: 16 μM/kg/d pamidronate, 1.6 μM/kg/d olpadronate. These doses were shown previously to complete inhibit osteoclastic bone resorption *in vivo* (31, 32). After this treatment period the animals were sacrificed. Alternatively, in order to achieve constantly elevated blood levels of BP during the entire period of treatment, 16 μM/kg/day of olpadronate dissolved in 0.9 % NaCl, a dose of ten fold higher than the maximal resorption-inhibitory dose *in vivo*, was continuously infused by osmotic minipumps (200 μl, 0.25 μl/hr, model 2004; Alzet Scientific products, Alza Corporation, Mountain View, CA) over a period of 28 days, beginning from day 0 after i.o. inoculation of MDA-231-B/Luc+cells. Osmotic minipumps filled with vehicle solution (0.9% NaCl in water) were implanted in a control group. The animals were sacrificed at the end of the treatment period.

BP effect on the expression of luciferase in MDA-231-B/Luc+cells

To exclude putative bisphosphonate effects on luciferase expression by MDA-231-B/Luc+cells, the breast cancer cells were cultured in the continuous presence of bisphosphonates for up to 48 hours. Continuous treatment of MDA-231-B/Luc+cells with a dose range of bisphosphonates (10-4 – 10-8 M for 24 and 48 hours) did not affect functional expression of the luciferase gene in MDA-231-B/Luc+cells *in vitro* as measured in luciferase assays and semi-quantitative PCR (results not shown).

Statistical Analysis

All data are represented as mean ± s.e.m. for animal studies and mean ± SD for histomorphometrical analyses. Statistical evaluation was carried out by ANOVA or two-tailed Student's t-test.

Results

Effect of BP treatment on the *'de novo'* generation and progression of systemic bone metastases ('Preventive' protocol).

In this experiment we investigated whether pharmacological inhibition of bone turnover prior to inoculation of cancer cells, and continued for the duration of the entire experiment, could prevent the initiation and maintenance of a positive interaction between the bone microenvironment and cancer cells. For this purpose olpadronate was given two days prior to inoculation of MDA-231-B/Luc+cells into the left cardiac ventricle and continued throughout the entire duration of the experiment (48 days) (Fig. 1).

Consistently with our previous findings [26] BLI showed that MDA-231-B/Luc+cells metastasize exclusively to the skeleton. At the end of the experimental period (day 47) olpadronate treatment decreased significantly the number of bone metastases per animal, as detected by BLI, by about 70% (Fig. 2*A*). Radiographic analysis in the same animals showed, from day 40 onwards, almost no osteolytic bone lesions in BP-treated animals as compared to control (Fig. 2*B*).

During the early experimental period olpadronate treatment significantly delayed the progression of the bone metastases, detected by BLI as total tumor burden per animal, (Fig. 2*C*, day 26-33), and tumor burden for each bone metastatic site (Fig. 2*D*, day 26-40). However, this effect was only transient and at later stages both the total burden per mouse (Fig. 2*C*, day 40-47) and the tumor burden per bone metastatic site (Fig. 2*D*, day 47) in the olpadronate treated animals became equivalent to those of the vehicle-treated animals.

Effect of BP treatment on growth of established bone metastases ('Curative' protocol).

In this experiment we investigated the effect of pharmacological inhibition of bone turnover on the bone microenvironmental growth support for cancer metastases that are already in an advanced stage of progression. For this purpose, daily s.c. administration of olpadronate (1.6 μM/kg/d for 18 days) was initiated when bone metastases had already developed (day 28) following i.c. injection of MDA 231-B/Luc+ cells (Fig. 1*B*).

As in the previous experiment MDA-231-B/Luc+cells metastasized exclusively to the skeleton. Olpadronate treatment did not affect the number of bone metastases detected by BLI (Fig. 3A), but significantly reduced at the end of treatment period (day 18) the number of osteolytic lesions per mouse as assessed by radiography (Fig. 3*B*). A discrepancy between BLI and radiography in the number of bone metastases detected in control and olpadronate treated animals can be noticed (Fig. 3*A,B*).

Olpadronate treatment transiently affected (day 5), although not significantly, total tumor burden per animal, as detected by BLI (Fig. 3*C*). However, at later time points tumor growth was not further affected by olpadronate (Fig. 3*C*) and at the end of the experiment it even enhanced significantly tumor burden per bone metastatic lesion (Fig. 3*C,D*).

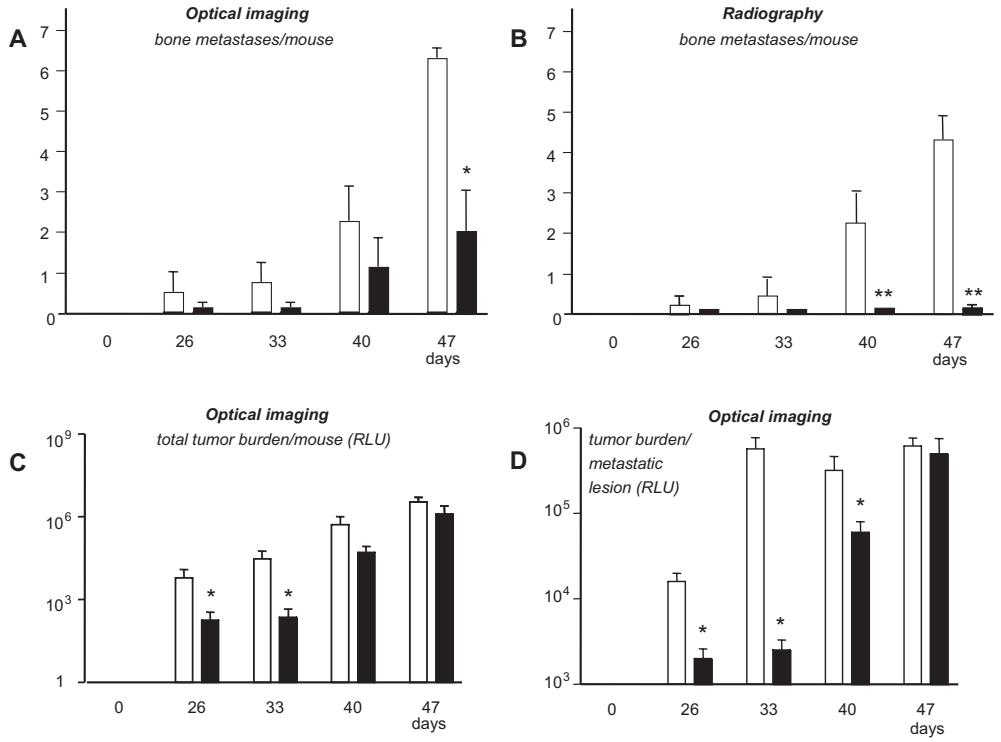

Figure 2 **Prevention of bone metastasis formation by the BP Olpadronate after inoculation of MDA-231-B/Luc+into the left cardiac ventricle of nude mice ('Preventive protocol').** Olpadronate (or vehicle) was given two days prior to inoculation of MDA-231-B/Luc+cells into the left cardiac ventricle and continued for the duration of the experiment (1.6 μM/kg/d for 48 days). Distribution and growth of MDA-231-B/Luc+cells was monitored weekly by BLI and radiography. Under both experimental conditions, MDA-231-B/Luc+cells metastasize exclusively to the skeleton. *A*, number of bone metastases per mouse determined by BLI. *B*, number of bone metastases per mouse determined by radiographical analysis. *C*, Total tumor burden per mouse (BLI). *D*, tumor burden per bone metastatic lesion (BLI). BLI measurements (C and D) are expressed relative light units (RLU). Open bars and closed bars represent Vehicle-treated and olpadronate-treated animals respectively. Values are expressed as means ± s.e.m., n=8. * $p \leq 0.05$, ** $p \leq 0.001$.

As shown in a representative radiograph of an olpadronate treated animal (Fig. 4*A*), there is minimal osteolysis in the left proximal tibia and proximal humerus. However, the photon emission detected by BLI of the same bone areas (Fig. 4*B*) indicates that these bones are site of metastatic growth of MDA-231-B/Luc+cells. Due to the limited intraosseous space, most of this growth seems to have taken place in the soft tissues surrounding bone, as revealed on the radiograph by the tumor shadow present especially around the left humerus (Fig. 4).

Effect of BP-treatment on intraosseous growth of breast cancer cells.

To investigate in more detail the cellular events during inhibition of bone turnover, progression and growth of cancer cells was analyzed in a model of tumor growth in the bone marrow. For

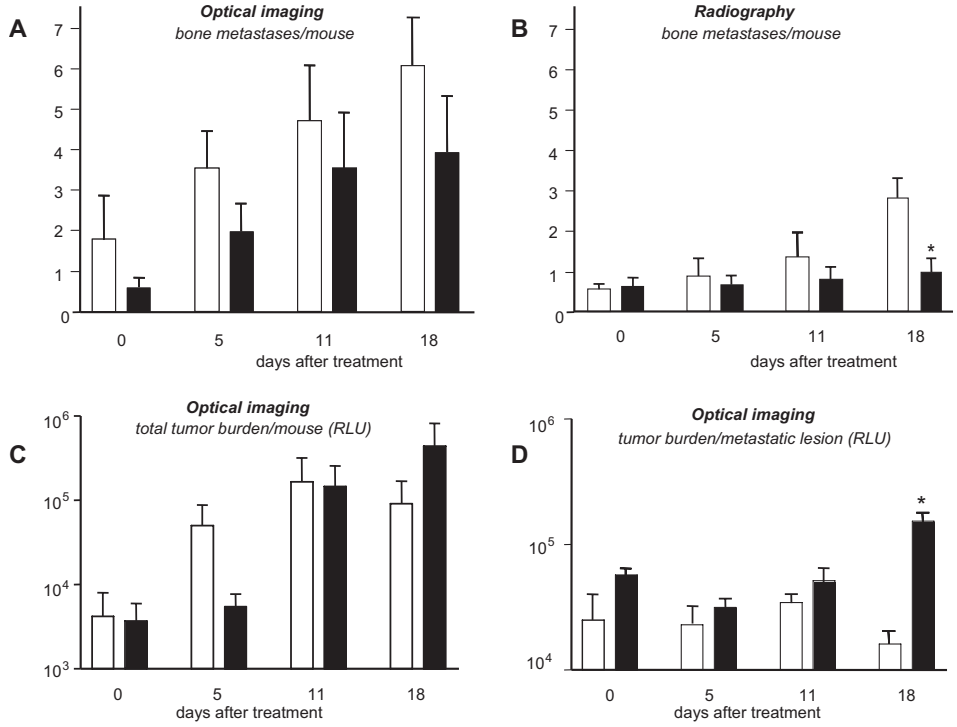

Figure 3 **Effects of olpadronate treatment on existing bone metastases, induced by inoculation of MDA-231-B/Luc+into the left cardiac ventricle of nude mice according to the 'Curative protocol' (see figure 1 B).** Daily s.c. administration of olpadronate (1.6 μM/kg/d for 18 days), was initiated when bone metastases had already developed (day 28) following i.c. injection of MDA 231-B/luc+ cells. The fate and growth of MDA-231-B/Luc+cells were monitored weekly by BLI and radiography. Under both experimental conditions, MDA-231-B/Luc+cells metastasize exclusively to the skeleton. *A*, number of bone metastases per mouse determined by BLI. *B*, number of bone metastases per mouse determined by radiographical analysis. *C*, total tumor burden per mouse (BLI). *D*, tumor burden per bone metastatic lesion (BLI). BLI measurements (figures 2 C and D) are expressed relative light units (RLU). Open bars and closed bars represent Vehicle-treated and olpadronate-treated animals respectively. Values are expressed as means ± s.e.m., n=8. * $p \leq 0.05$.

this purpose MDA-231-B/Luc+cells were inoculated directly into the tibiae of nude mice [26-28], which were then treated by daily s.c. injections with olpadronate or pamidronate.

Continuous BP treatment did not significantly affect growth of the cancer cells as determined by BLI (Fig. 5A,*C*). As expected, both BPs strongly and significantly inhibited the development of radiologically evident osteolytic lesions (Fig. 5*B,C*). Histomorphometric analysis (Fig. 5*D*) confirmed that BPs inhibited cancer-induced bone destruction leading to a significant increase in trabecular bone area associated with a significant decrease in TRAcP+ resorbing osteoclasts at the bone surface (Table 1). As a consequence of this bone sparing effect of BP treatment, the intra-bone tumor burden was significantly decreased, although it was clear that the cancer cells were filling completely the bone marrow spaces

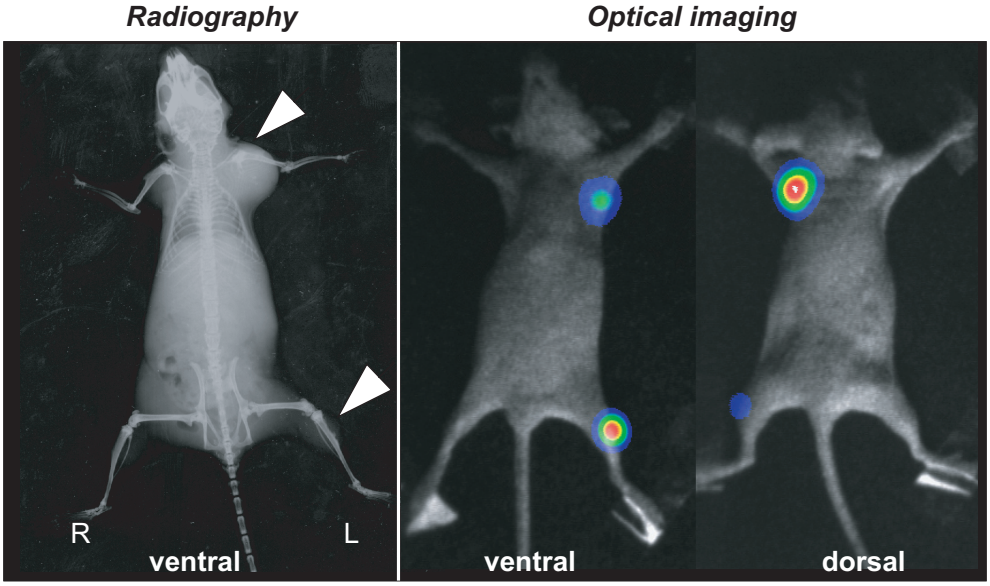

Figure 4 **Representative radiograph and bioluminescent images of an olpadronate treated mouse according to the Curative protocol (18 days of treatment, day 46, see figure 3).** Osteolysis is minimal in the left proximal tibia and proximal humerus (left panel, arrows). However, the photon emission spectra detected by BLI of the same bone areas (central and right panel) indicate that these bones are the site of metastatic growth of MDA-231-B/Luc+cells. Due to the limited intraosseous space, most of this growth seems to have taken place in the soft tissues surrounding bone, as revealed on the radiograph by the tumor shadow present especially around the left humerus.

(Fig. 5*D*). In contrast to the intraosseous tumor burden, no significant inhibition of the overall tumor burden (= intraosseous and in surrounding soft tissues) was observed (Fig. 5*D*), which is in line with the optical imaging data presented in figures 5*A* and *C*.

Table 1 Effects of bisphosphonate treatment on osteoclast numbers at the bone surface of MDA-231-B/Luc+breast cancer cells growing in tibiae of 6-week-old female nude mice.

	No. osteoclast/mm bone surface, mean (SD)	P
Vehicle treated	22 (4)	-
Pamidronate 1.6 µmol/kg/d	5 (1)	< 0.01
Olpadronate 1.6 µmol/kg/d	4 (2)	< 0.01

Note: n = 5 per experimental group. Ps represent bisphosphonate treated vs. vehicle treated animals.

Previously it was found that the intensity of the signal detected by BLI is a function of the tissue composition and depth of the bioluminescent source [33,34]. There is the possibility that changes in the tissue type invaded by the tumor growth and/or representation of bone

tissue, with consequent differences in light penetration and light scattering between the experimental groups (vehicle vs. BP), may have generated artifactual results in determining tumor burden by BLI. To exclude this, the treatment/control ratios of the tumor burden values obtained by BLI and histomorphometrical analyses were compared. No differences in ratios between these two measurement methods were found (0.98±0.16 and 1.17±0.22 treatment/control ratios for pamidronate and olpadronate respectively). This correlation indicates that potential differences in quenching and/or light scattering by bone cannot account for the observed lack of *in vivo* growth inhibitory effects during BP treatment, and confirms the reliability of BLI as method to quantify tumor burden.

Taken together, these results clearly show that BP, despite a significant decrease in intraosseous tumor burden due to their bone-sparing effect, do not affect tumor growth rate, but merely modify the direction of tumor growth. As a result cancer cells invade more conspicuously the soft tissues (muscle, tendon and connective tissue) surrounding the long bones.

To ensure constant delivery of a dose of BP sufficient to inhibit the high bone turnover of rapidly growing animals in a further experiment, olpadronate was administered by osmotic mini-pumps. In line with the data obtained after s.c. administration with BP in the same intraosseous tumor model (Fig. 5*A,C,D*), continuous high dose olpadronate treatment did not affect the tumor growth as detected by BLI (Fig. 5*E*). As expected, continuous olpadronate treatment strongly and significantly inhibited tumor-induced osteolysis, as detected by radiography (Fig. 5*F*). Histomorphometric analysis confirmed these effects of olpadronate by showing a significantincrease in bone volume, a decrease in intra-bone tumor volume, and no significant effect on total tumor burden (Table 2).

Table 2 Histomorphometric analysis of TBV (%), intraosseous tumor volume (mm2), and total tumor volume (mm2) of MDA-231-B/Luc+breast cancer cells growing in tibiae of 6-week-old female nude mice.

	Vehicle, mean (SD)	Olpadronate, mean (SD)	P
TBV	3 (2)	13 (3)	< 0.05
Intra-bone tumor burden	16 (4)	8 (1)	< 0.05
Total tumor volume	39 (6)	25 (6)	n.s.

Note: Olpadronate (or vehicle) was released at a high dose by osmotic mini-pumps (16 µmol/kg/d, 24 hours/d) for 28 days. n = 5, n.s. = not significant.

Discussion

Interference with the microenvironmental growth support is currently being evaluated as a therapeutic strategy for the treatment of metastatic disease. Bone metastasis is a paradigm of the interactions that take place at the tumor-stroma interface [1,2] and evidence from

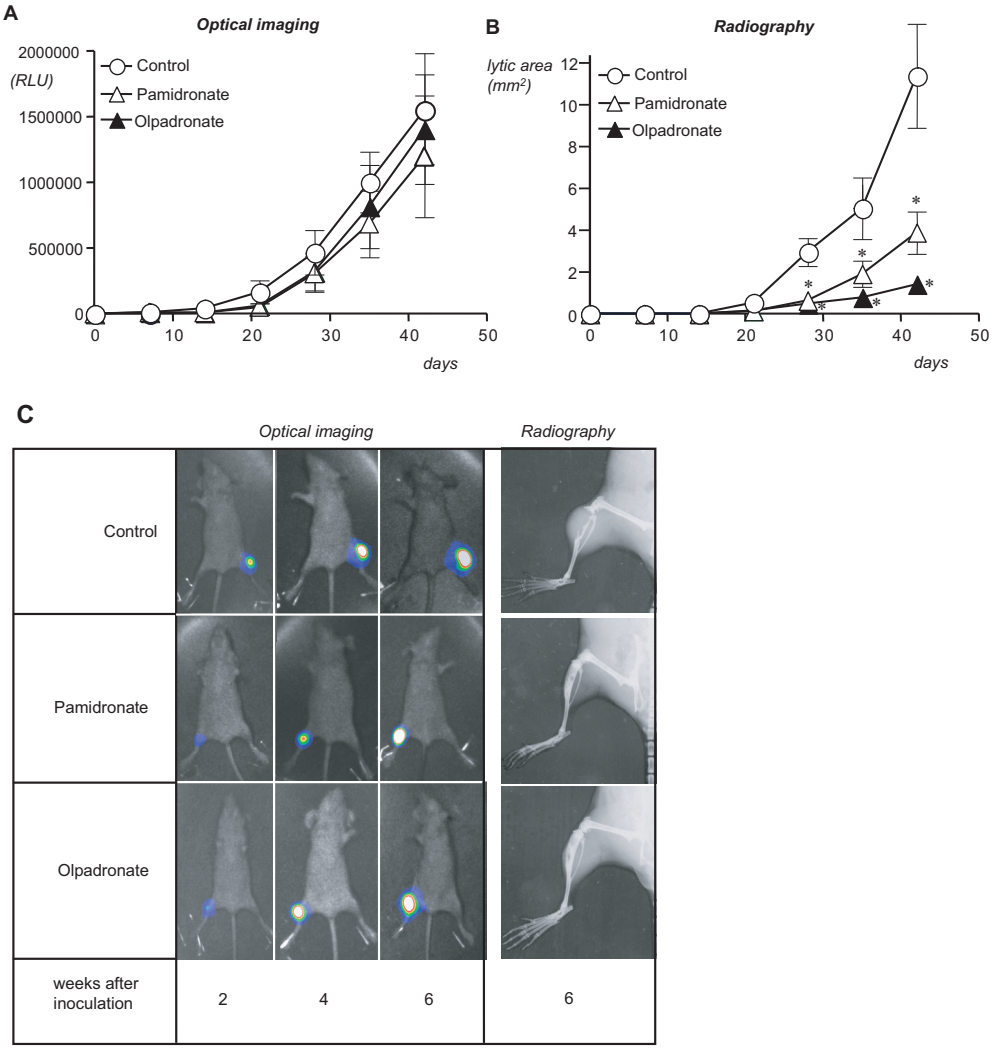

Figure 5 **Effects of BP treatment on tumor growth of MDA-231-B/Luc+ breast cancer cells (BLI+histology) and osteolysis (radiography) in tibiae of 6-week-old female nude mice.** MDA-231-B/Luc+cells were inoculated directly into the left tibia of nude mice, which were subsequently treated by daily s.c. injections with 1.6 μM/kg/d olpadronate (closed triangles), 16 μM/kg/d pamidronate (open triangles) or vehicle (open circles). *A*, growth of breast cancer cells in the bone marrow cavity measured by BLI (RLU). *B*, development of osteolytic areas due to tumor-induced bone destruction as assessed radiographically (lytic area, mm^2). *C*, representative animals of each experimental groups (BLI, radiography). *D*, histomorphometric analysis of intra-bone tumor burden, trabecular bone volumes and total tumor burden (= total of intra-bone + extramedullary tumor burden). *E*, continuous release of high dose of Olpadronate by osmotic mini-pumps (16 μM/kg/d, 24 hours/day) on intra bone tumor growth as detected by BLI. *F*, continuous release of high dose of Olpadronate by osmotic mini-pumps (16 μM/kg/d, 24 hours/day) on development of osteolytic lesions as assessed radiographically (mm^2). Values are expressed as means ± s.d., n = 5, * $p \leq 0.05$.

Jeroen_Buijs_18.indd 122 26-11-2008 10:18:32

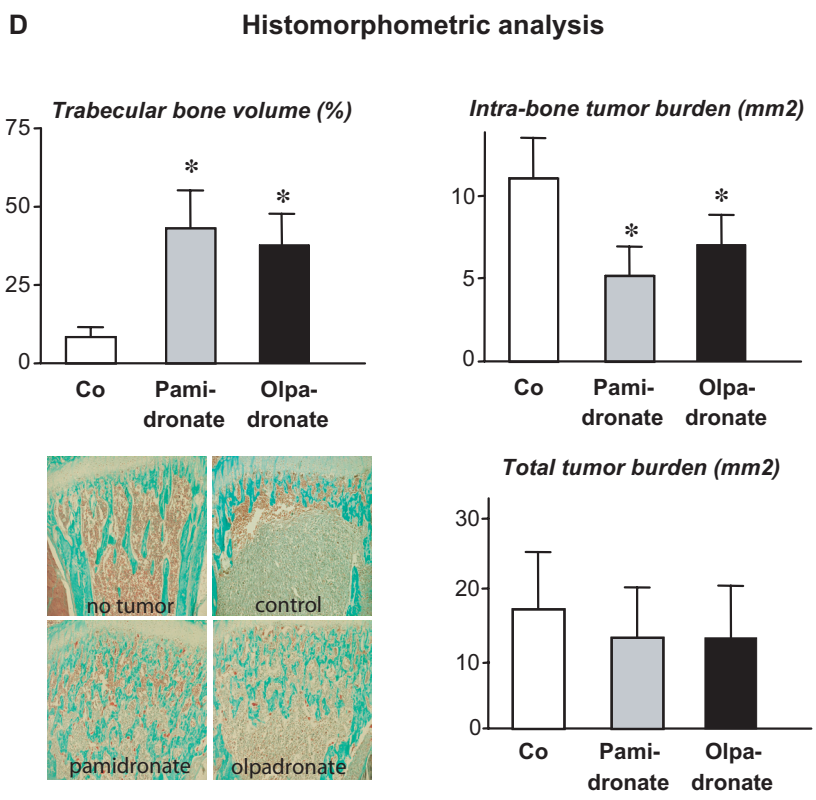
D
Histomorphometric analysis
Trabecular bone volume (%)
75
50
25
0
Co
Pami-dronate
Olpa-dronate
Intra-bone tumor burden (mm2)
10
5
0
Co
Pami-dronate
Olpa-dronate
no tumor
control
pamidronate
olpadronate
Total tumor burden (mm2)
30
20
10
0
Co
Pami-dronate
Olpa-dronate

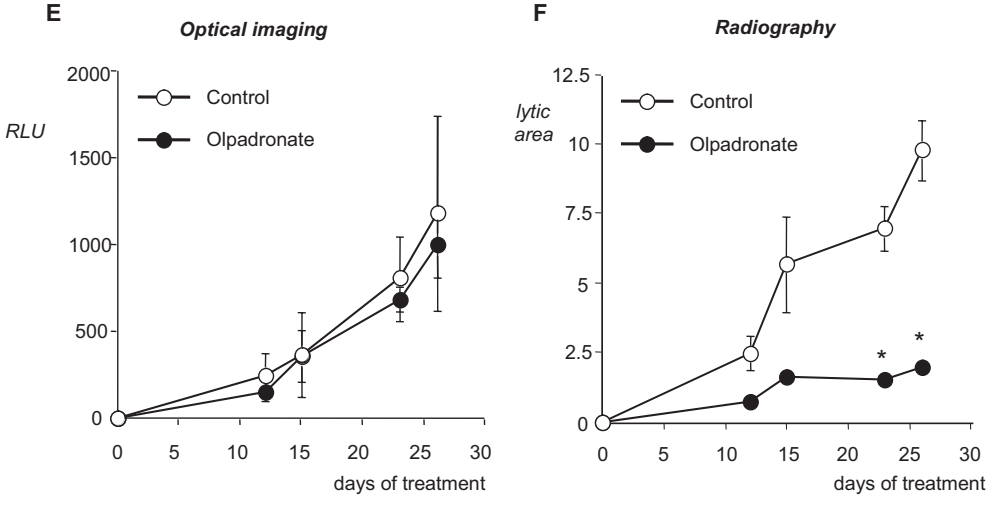
E
Optical imaging
RLU
2000
1500
1000
500
0
Control
Olpadronate
0
5
10
15
20
25
30
days of treatment
F
Radiography
lytic area
12.5
10
7.5
5
2.5
0
Control
Olpadronate
0
5
10
15
20
25
30
days of treatment

animal and clinical studies support the notion that bone turnover, particularly bone resorption, contributes substantially to initiation and maintanance of local tumor growth through release of growth factors and bone resorbing cytokines ('vicious cycle'). Differently from other tissues, bone turnover can be reduced by pharmacological means and, thus, animal models of bone metastasis offer the unique opportunity to test *in vivo* the therapeutic efficacy of the interference with the tumor-stroma interface.

In this study we investigated whether inhibition of bone turnover by BP administration could prevent the development of bone metastases and/or repress tumor growth in already developed bone metastases. Our results show unequivocally that inhibition of bone turnover by BPs, prior to the establishment of a micrometastatic spreading induced by intracardiac inoculation of breast cancer cells ('Preventive' protocol), reduces by a great extent, although not completely, the development of bone metastases as detected by BLI. Although not significant, a tendency toward this effect is also present when BP are administered later, after the establishment of a micrometastatic spreading ('Curative' protocol), when some bone metastases had already been generated, but a residual number had still to develop. In this case, the limited entity of this residual number and, thus, the low statistical power, may explain the lack of significance.

The dose of olpadronate given (1.6 µmol/kg body weight/day) has been shown previously to efficiently inhibit bone resorption *in vivo* [32], but in the present study, it did not prevent the formation of bone metastases by >70%. This level of inhibition is consistent with the observation that in the experimental animal not more than 70% of the bone resorption can be inhibited by high dose of BPs [35]. Possibly, this persistently low level of bone resorption is sufficient to provide growth support to a minimal number of micrometastatic foci.

Although preventive BP-inhibition of bone turnover precludes to a great extent the generation of bone metastases from experimentally-induced micrometastatic spread of breast cancer cells, the progression of tumor growth in the small number of still developing metastases, as detected by BLI, is significantly reduced only during early stages. A similar trend is also seen when BP are administered according to the 'Curative protocol' to mice with already developed bone metastases. However, at later stages, bone metastatic growth is even accelerated, leading to a significant increase of tumor burden per metastatic lesion in the 'Curative protocol' after 18 days of BP treatment. This result is in line with earlier observations by others demonstrating that BP treatment, despite preserving trabecular bone, does not inhibit bone metastatic growth, and may even increase skeletal tumor burden [36]. This suggests that bone metastatic growth, once it is initiated and reaches a critical mass, proceeds independently of the bone microenvironmental growth support and is self-maintained by autocrine mechanisms.

The lack of effect by interference with the microenvironmental support on growth progression of already developed bone metastases was corroborated in a further experiment in which bone tumors were induced by intraosseous inoculation of breast cancer cells. Also

Jeroen_Buijs_18.indd 124 26-11-2008 10:18:33

in this case continuous inhibition of bone resorption, achieved by BP administered either s.c. or by sustained high dose release, did not affect tumor growth. Concomitant with BLI, radiographic and histomorphometric analysis could even better dissect the known BP bone sparing effect from an effect on tumor growth that may result either directly from these compounds or indirectly from the inhibition of bone turnover. In fact, histomorphometry revealed that, although the tumor mass confined within the bone marrow cavity was decreased as effect of the reduced intra-medullary space made available by persisting bone trabeculae, the total tumor mass was compensated by growth of cancer cells forced to invade the soft tissues (muscle, tendon and connective tissue) surrounding the bone cortex. Bone tissue may partially segregate the cancer cells within the medullary cavity and prevent them from invading the surrounding soft tissues. Instead, upon inhibition of bone resorption, the invasive growth is most likely forced to modify its direction from intra-medullary to extramedullary. It is important to note that MDA-MB-231 breast cancer cells have been shown to be able to migrate from bone marrow to periosteal surfaces [26], probably through vascular channels thus providing an opening to the periosteum and bone surrounding tissues.

Previous studies investigating the effect of BP-induced inhibition of bone resorption/turnover on bone metastatic growth in comparable animal models have shown contradictory results [30,36-40]. BPs have been reported to reduce the tumor burden in established bone metastases, but not in soft tissue and visceral metastases. This effect seemed to be mediated by induction of apoptosis in the cancer cells [30,37]. Treatment with BP, given prior to the development of evident metastasis, resulted in a marked reduction of the number of bone metastases [30,38-40]. However, in another preventive study it has been reported that BP treatment resulted in an increased tumor burden in the developing bone metastases, but not in visceral metastases [38]. In most of these investigations tumor burden has been quantified indirectly by measuring the osteolytic area on bone radiographs.

The difference between BLI and radiography in the number of bone metastastic foci detected either in the BP- or in the vehicle-treated animals is consistent with our previous report [26] and corroborates further the higher sensitivity, reliability and statistical power of the BLI method. BLI provides a direct indication of tumor viability and growth, while radiography does not detect actual tumor burden, but reveals only osteolysis, which is an indirect, late and inconsistent sign of the presence of a tumor [26]. In fact, determination of the osteolytic area depends not only on tumor cell mass, but also on the ability of the cancer cells to secrete bone-resorbing cytokines. Obviously, this consideration is especially true when bone resorption is pharmacologically inhibited. Furthermore, the determination of the osteolytic area does not take in account extension of the tumor burden in the surrounding soft tissues.

From the considerations above it should be concluded that the determination of the osteolytic area is invalid as a measurement of bone tumor mass. Therefore, the results of previous studies, based exclusively on this method, should be reconsidered. Only histo-

morphometry could avoid the latter pitfall. However, when a parallel histomorphometric analysis was performed, only intraosseous tumor burden was measured. Only one study assessed this analysis to the neighboring tissues. In the latter paper, BP-induced inhibition of bone resorption restrained only intraosseous tumor growth, while increasing tumor burden in the soft tissues [30]. This effect is perfectly in line with the results presented here with both histomorphometry and BLI, a much more reliable and sensitive method for monitoring tumor burden *in vivo*.

In vitro, BPs have been reported to exert direct anti-proliferative and pro-apoptotic effects on cancer cells [41-43], to interfere with cancer cell adhesion to bone matrix proteins [44,45], to inhibit matrix metalloproteinases [46,47], and to diminish cancer cell migration and invasion [48,49]. The results shown here exclude that BP may have a direct cytostatic effect *in vivo*.

Collectively, the results obtained in this investigation substantiate the concept that interference with the bone microenvironmental growth support, namely through inhibition of bone resorption/turnover, may be of therapeutic relevance for inhibiting early developmental steps of bone metastasis. However, they seem to exclude that the same strategy could repress progression of overt bone metastases and, also, that BPs may exert an effect on cancer cell growth, either directly by induction of apoptosis or indirectly by inhibition of angiogenesis.

How can the therapeutic effect of inhibition of bone resorption/turnover on early stages of bone metastasis development be explained? Bone remodelling does not occur throughout the entire bone surface, but takes place at microscopic patches of bone resorption and subsequent bone formation, called basic multicellular units (BMUs). The number and the activity of these BMUs determine the rate of bone turnover. Osteoblasts and osteoclasts, the cellular components in an active BMU, secrete and/or release from bone matrix cytokines, like TGF-β and IGF-1, which physiologically modulate the biology of bone cells. However, they can also act as paracrine growth factors for neighboring cancer cells that may have colonized bone marrow [19,22-25,28,50-55]. Consequently, local growth factor release by an active BMU in close proximity of a bone marrow micrometastasis may evoke the growth and invasive potential of the cancer cells, ultimately leading to the development of a macrometastasis (Fig. 6). We hypothesize that the probability for a bone marrow micrometastasis of becoming a clinically evident bone metastasis should be related to the chance that micrometastatic cancer cells extravasate in the proximity of an active BMU. In contrast, cancer cells extravasating near to a non-remodelling, 'resting' bone surface will persist as 'dormant', and eventually become apoptotic. Accordingly, a higher number and density of active BMUs (high bone turnover rate) should favour the probability that bone marrow micrometastases 'home' near active BMUs. This may explain the clinical and experimental evidence showing an association between high bone turnover rate and the preferential development of hematogenous metastases at sites of active bone remodelling [14,15]. Conversely, a preventive inhibition of bone turnover, e.g., by BP, prior to the generation of a self-maintaining, autocrine

Jeroen_Buijs_18.indd 126 26-11-2008 10:18:33

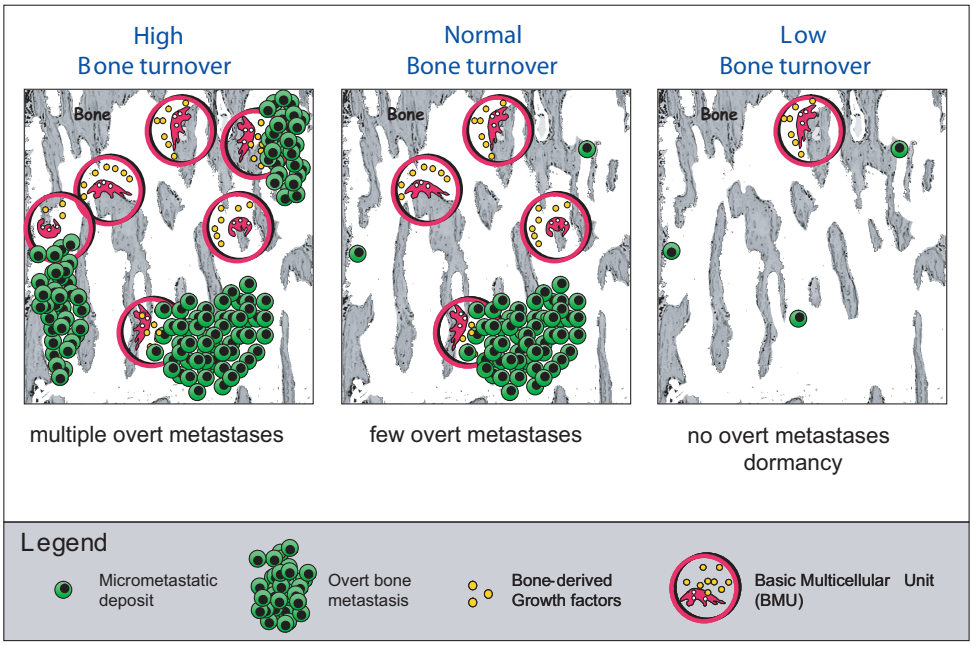

Figure 6 ***Hypothesis regarding the importance of bone turnover rate and the therapeutic relevance for inhibiting early developmental steps of bone metastasis.*** Bone turnover takes place at microscopic patches of bone resorption and subsequent bone formation, called basic multicellular units (BMUs). The number and the activity of these BMUs determine the rate of bone turnover. Osteoblasts and osteoclasts, the cellular components of an active BMU, secrete cytokines from bone matrix, which can act as paracrine growth factors for neighboring cancer cells that may have colonized bone marrow (micrometastatic deposits). Consequently, local growth factor release by an active BMU in close proximity of a bone marrow micrometastasis may evoke the growth and invasive potential of the cancer cells, ultimately leading to the development of an overt bone metastases. Interference with the bone microenvironmental growth support through inhibition of bone resorption/turnover (for instance by BPs), may be of therapeutic relevance for inhibiting early developmental steps of bone metastasis. However, cancer cell growth of overt bone metastases during treatment with BPs is not affected. The probability of a bone marrow micrometastasis to become clinically evident bone metastasis may thus be related to the chance that micro-metastatic cancer cells extravasate in the proximity of an active BMU. In contrast, cancer cells extravasating near to a non-remodelling, 'resting' bone surface will persist as 'dormant', and eventually become apoptotic. Preventive inhibition of bone turnover, e.g., by BPs, prior the generation of a self-maintaining, autocrine cancer cell growth, may arrest the 'vicious cycle' underlying the initial growth support by the BMU and, ultimately, frustrate the development of clinically evident macrometastasis.

cancer cell growth, may arrest the 'vicious cycle' underlying the initial growth support by the BMU and, ultimately, frustrate the development of clinically evident macrometastasis.

Assessment of the bone turnover status may lead to a better identification and stratification of the cancer patients at risk to develop bone metastases. Cancer patients, probably harboring micrometastasis in the bone marrow at the moment of diagnosis and/or surgery, but with high bone turnover rate, either basal (e.g., induced by menopause) or subsequent to surgical or chemical sex steroid deprivation, may benefit from a prophylactic, BP-induced reduction of the bone turnover rate.

Acknowledgments

We thank the department of Endocrinology, Leiden University Medical Center (Leiden, the Netherlands) and the department of Clinical Research, Faculty of Medicine, University of Bern (Bern, Switzerland), for the financial and logistic support. This study was supported by grants from the Dutch Cancer Society (KWF, RUL 2001-2485), Royal Netherlands Academy of Arts and Sciences, the Swiss National Science Foundation (Grant Nr. 32-57118.99) and the Bernische Krebsliga (project 'From the Bench to Bedside – Prevention, Detection and Treatment of Micrometastases').

References

1. Paget S. The distribution of secondary growths in cancer of the breast. *Lancet* 1889; 1:571-3.
2. Fidler IJ. The pathogenesis of cancer metastasis: The seed and soil hypothesis revisited. *Nature Reviews Cancer* 2003; 3: 453-8.
3. Liotta LA, Kohn EC. The microenvironment of the tumour-host interface. *Nature 2001*; 411: 375-9.
4. Coleman RE, Rubens RD. 3(Amino-1,1-hydroxypropylidene) bisphosphonate (APD) for hypercalcaemia of breast cancer. *Br J Cancer* 1987; 56:465-9.
5. Powles T, Paterson S, Kanis JA, McCloskey E, Ashley S, Tidy A *et al*. Randomized, placebo-controlled trial of clodronate in patients with primary operable breast cancer. *J Clin Oncol* 2002, 20:3219-24.
6. Elte JW, Bijvoet OL, Cleton FJ, van Oosterom AT, Sleeboom HP. Osteolytic bone metastases in breast carcinoma pathogenesis, morbidity and bisphosphonate treatment. *Eur J Cancer Clin Oncol* 1986; 22:493-500.
7. van Holten-Verzantvoort AT, Bijvoet OL, Cleton FJ, Hermans J, Kroon HM, Harinck HI *et al.* Reduced morbidity from skeletal metastases in breast cancer patients during long-term bisphosphonate (APD) treatment. *Lancet* 1987; 2:983-5.
8. Coleman RE Skeletal complications of malignancy. *Cancer* 1997; 80:1588-94.
9. Eaton CL, Coleman RE Pathophysiology of bone metastases from prostate cancer and the role of bisphosphonates in treatment. *Cancer Treat Rev* 2003; 29:189-98.
10. Krempien B, Diel IJ, Jöckle-Kretz B, Büchele R, Andre L. The Walker Carcinomasarcoma 256 as an experimental model of bone metastasis. Influence of skeletal metabolism on the development of bone metastases. *Verh Dtsch Ges Pathol* 1984; 68:211-16.
11. Arguello F, Baggs RB, Graves BT, Harwell SE, Cohen HJ, Frantz CN. Effect of IL-1 on experimental bone/bone-marrow metastases. *Int J Cancer* 1992; 52: 802-07.
12. Kostenuik PJ, Singh G, Suyama KL, Orr FW, Stimulation of bone resorption results in a selective increase in the growth rate of spontaneously metastatic Walker 256 cancer cells in bone. *Clin Exp Metastasis* 1992; 10:411-418.

13. Schneider A, Kalikin LM, Mattos AC, Keller ET, Pienta KJ, McCauley LK. Increased bone turnover facilitates prostate cancer metastasis to the skeleton. *The IVth international Conference on Cancer-Induced Bone Disease* 2003. San Antonio, Tx. December, 7-9. Abstract 41.
14. Brown JE, Thomson CS, Ellis SP, Gutcher SA, Purohit OP, Coleman RE. Bone resorption predicts for skeletal complications in metastatic bone disease. *Br J Cancer* 2003; 89:2031-37.
15. Costa L, Demers LM, Gouveia-Oliveira A, Schaller J, Costa EB, de Moura MC *et al.* Prospective evaluation of the peptide-bound collagen type I cross-links N-telopeptide and C-telopeptide in predicting bone metastases status. *J Clin Oncol* 2002; 20:850-6.
16. Hattner R, Epker BN, Frost HM. Suggested sequential mode of control of changes in cell behaviour in adult bone remodelling. *Nature* 1965; 206:489-90.
17. Eriksen EF, Axelrod DW Melsen F. *Bone histomorphometry*, p. 3-12. New York: Raven Press, 1994.
18. Mundy GR, Chen D, Oyajobi BO Bone remodelling. In: F. M.J. (ed.), *Primer on the metabolic bone diseases and disorders of mineral metabolism*, 5th edition, pp. 46-58. Washington: American Society for Bone and Mineral Research, 2003.
19. Mundy GR. Metastasis to bone: causes, consequences and therapeutic opportunities. *Nat Rev Cancer* 2002; 2:584-93.
20. Roodman GD Mechanisms of bone metastasis. *N Engl J Med* 2004; 350:1655-64.
21. Mundy GR, Yoneda T. Mechanisms of bone metastasis. In: G. Singh (ed.), *Bone metastasis – mechanisms and pathophysiology*, pp. 1-16. Heidelberg: Springer,.
22. Yin JJ, Selander K, Chirgwin JM Dallas M, Grubbs BG, Wieser *et al.* TGF-beta signaling blockade inhibits PTHrP secretion by breast cancer cells and bone metastases development. *J Clin Invest* 1999; 103:197-06.
23. Guise TA, Yin JJ, Taylor SD, Kumagai Y, Dallas M, Boyce BF *et al.* Evidence for a causal role of parathyroid hormone-related protein in the pathogenesis of human breast cancer-mediated osteolysis. *J Clin Invest* 1996; 98:1544-49.
24. Thomas RJ, Guise TA, Yin JJ, Elliott J, Horwood NJ, Martin TJ *et al.* Breast cancer cells interact with osteoblasts to support osteoclast formation. *Endocrinology*, 140: 4451-4458, 1999.
25. Guise TA, Chirgwin JM. Transforming growth factor-beta in osteolytic breast cancer bone metastases. *Clin Orthop* 2003; S32-38.
26. Wetterwald A, van der Pluijm G, Que I, Sijmons B, Buijs J, Karperien M *et al.* Optical imaging of cancer metastasis to bone marrow: a mouse model of minimal residual disease. *Am J Pathol* 2002; 160:1143-53.
27. van der Pluijm G, Sijmons B, Vloedgraven H, van der Bent C, Drijfhout *et al.* Urokinase-receptor/integrin complexes are functionally involved in adhesion and progression of human breast cancer *in vivo. Am J Pathol* 2001; 159:971-82.
28. van der Pluijm G, Sijmons B, Vloedgraven H, Deckers M, Papapoulos S, Lowik C. Monitoring metastatic behavior of human tumor cells in mice with species-specific polymerase chain reaction: elevated expression of angiogenesis and bone resorption stimulators by breast cancer in bone metastases. *J Bone Miner Res* 2001; 16:1077-91.
29. Arguello F, Baggs RB, Frantz CN. A murine model of experimental metastasis to bone and bone marrow. *Cancer Res* 1988; 48:6876-81.
30. Sasaki A, Boyce BF, Story B, Wright KR, Chapman M, Boyce R *et al.* Bisphosphonate risedronate reduces metastatic human breast cancer burden in bone in nude mice. *Cancer Res* 1995; 55:3551-57.
31. Reitsma PH, Bijvoet OL, Verlinden-Ooms H, van der Wee-Pals LJ. Kinetic studies of bone and mineral metabolism during treatment with (3-amino-1-hydroxypropylidene)-1,1-bisphosphonate (APD) in rats. *Calcif Tissue Int* 1980; 32:145-57.
32. Papapoulos SE, Hoekman K, Lowik CW, Vermeij P, Bijvoet OL. Application of an *in vitro* model and a clinical protocol in the assessment of the potency of a new bisphosphonate. *J Bone Miner Res* 1989, 4:775-81.
33. Contag CH, Contag PR, Mullins JI, Spilman SD, Stevenson DK, Benaron DA. Photonic detection of bacterial pathogens in living hosts. *Mol Microbiol* 1995; 18:593-603.
34. Contag CH, Spilman SD, Contag PR, Oshiro M, Eames B, Dennery P *et al.* Visualizing gene expression in living mammals using a bioluminescent reporter. *Photochem Photobiol* 1997; 66:523-31.

35. Antic VN, Fleisch H, Muhlbauer RC. Effect of bisphosphonates on the increase in bone resorption induced by a low calcium diet. *Calcif Tissue Int* 1996; 58:443-448.
36. Kostenuik PJ, Orr FW, Suyama K, Singh, G. Increased growth rate and tumor burden of spontaneously metastatic Walker 256 cancer cells in the skeleton of bisphosphonate-treated rats. *Cancer Res* 1993; 53: 5452-57.
37. Hiraga T, Williams PJ, Mundy GR, Yoneda T. The bisphosphonate ibandronate promotes apoptosis in MDA-MB-231 human breast cancer cells in bone metastases. *Cancer Res* 2001, 61:4418-24.
38. Krempien B, Manegold C. Prophylactic treatment of skeletal metastases, tumor induced osteolysis, and hypercalcemia in rats with the bisphosphonate Cl2MBP. *Cancer* 1993, 72: 91-8.
39. Krempien B, Wingen F, Eichmann T, Müller M, Schmähl D. Protective effect of a prophylactic treatment with the bisphosphonate 3-amino-1-hydroxypropane-1,1 bisphosphonic acid on the development of tumor osteopahthies in rat: experimental studies with the Walker Carcinosarcoma 256. *Oncology* 1988; 45:41-6.
40. Hall DG, Stoica G. Effect of the bisphosphonate risedronate on bone metastases in a rat mammary adenocarcinoma model system. *J Bone Miner Res* 1994, 9:221-230.
41. Shipman CM, Rogers MJ, Apperley JF, Russell RG, Croucher PI. Bisphosphonates induce apoptosis in human myeloma cell lines: a novel anti-tumour activity. *Br J Hematol* 1997; 98:665-72.
42. Senaratne SG, Pirianov G, Mansi JL, Arnett TR, Colston KW. Bisphosphonates induce apoptosis in human breast cancer cell lines. *Br J Cancer* 2000; 82:1459-68.
43. Lee MV, Fong EM, Singer FR, Guenette RS. Bisphosphonate treatment inhibits the growth of prostate cancer cells. *Cancer Res* 2001; 61: 2602-8.
44. Boissier S, Magnetto S, Frappart L, Cuzin B, Ebetino FH, Delmas PD *et al.* Bisphosphonates inhibit prostate and breast carcinoma cell adhesion to unmineralized and mineralized bone extracellular matrices. *Cancer Res* 1997; 57:3890-4.
45. van der Pluijm G, Vloedgraven H, van Beek E, van der Wee-Pals L, Lowik C, Papapoulos S. Bisphosphonates inhibit the adhesion of breast cancer cells to bone matrices *in vitro*. *J Clin Invest* 1996; 98:698-705.
46. Heikkila P, Teronen O, Moilanen M, Konttinen YT, Hanemaaijer R, Laitinen M *et al*. Bisphosphonates inhibit stromelysin-1 (MMP-3), matrix metalloelastase (MMP-12), collagenase-3 (MMP-13) and enamelysin (MMP-20), but not urokinase-type plasminogen activator, and diminish invasion and migration of human malignant and endothelial cell lines. *Anticancer Drugs* 2002; 13:245-54.
47. Teronen O, Heikkila P, Konttinen YT, Laitinen M, Salo T, Hanemaaijer R *et al.* MMP inhibition and downregulation by bisphosphonates. *Ann N Y Acad Sci* 1999; 878: 453-465.
48. Boissier, S., Ferreras, M., Peyruchaud, O., Magnetto, S., Ebetino, F. H., Colombel, M., Delmas, P., Delaisse, J. M., and Clezardin, P. Bisphosphonates inhibit breast and prostate carcinoma cell invasion, an early event in the formation of bone metastases. *Cancer Res* 2002; 60: 2949-2954.
49. Virtanen SS, Vaananen HK, Harkonen PL, Lakkakorpi PT Alendronate inhibits invasion of PC-3 prostate cancer cells by affecting the mevalonate pathway. *Cancer Res* 2002, 62: 2708-2714.
50. Yin JJ, Mohammad KS, Kakonen SM, Harris S, Wu-Wong JR, Wessale JL *et al.* A causal role for endothelin-1 in the pathogenesis of osteoblastic bone metastases. *Proc Natl Acad Sci U S A* 2003, 100: 10954-10959.
51. Lange PH, Vessella RL. Mechanisms, hypotheses and questions regarding prostate cancer micrometastases to bone. *Cancer Metastasis Rev* 1999; 17: 331-336.
52. Kang Y, Siegel PM, Shu W, Drobnjak M, Kakonen SM, Cordon-Cardo C *et al.* A multigenic program mediating breast cancer metastasis to bone. *Cancer Cell* 2003; 3: 537-549.
53. Guise TA, Yin JJ, Mohammad KS. Role of endothelin-1 in osteoblastic bone metastases. *Cancer* 2003; 97:779-84.
54. Roodman GD. Role of stromal-derived cytokines and growth factors in bone metastasis. *Cancer* 2003; 97: 733-738.

Jeroen_Buijs_18.indd 130 26-11-2008 10:18:36

55. Cooper CR, Chay CH, Gendernalik JD, Lee HL, Bhatia J, Taichman RS *et al.* Stromal factors involved in prostate carcinoma metastasis to bone. *Cancer* 2003; 97: 739-747.

Jeroen_Buijs_18.indd 132 26-11-2008 10:18:36

Chapter 5

Inhibition of Bone Resorption and Growth of Breast Cancer in the Bone Microenvironment

Bone 2008, in press

Jeroen T Buijs[1]
Ivo Que[1]
Clemens WGM Löwik[1]
Socrates E Papapoulos[1]
Gabri van der Pluijm[1,2]

Departments of UrologyEndocrinology[1]
and Urology[2],
Leiden University Medical Center, Leiden,
The Netherlands

Jeroen_Buijs_18.indd 133 26-11-2008 10:18:36

Abstract

Breast cancer frequently metastasizes to bone, where tumor cells induce osteoclasts to locally destroy bone. During bone resorption, growth factors are locally released that may support bone metastatic growth. Differently from most other tissues, drugs that can limit local turnover are available for bone.

We examined the hypothesis that inhibition of bone resorption by two different mechanisms may also affect the growth of cancer cells in bone. For this, we have tested the effects of high doses of osteoprotegerin (OPG) and zoledronic acid (ZOL), the most potent bisphosphonate available, on progression of breast cancer cells in the bone microenvironment using whole body bioluminescent imaging (BLI).

Both treatments significantly inhibited the development of radiographically detectable osteolytic lesions. Histological examination corroborated the radiographic findings, showing that both treatments preserved the integrity of bone trabeculae and prevented bone destruction, (significantly higher trabecular bone volumes vs. vehicle). However, whereas practically no TRAcP-positive osteoclasts were observed in tibiae preparations of animals treated with Fc-OPG, TRAcP-positive osteoclasts were still present in the animals treated with ZOL. Intra-bone tumor burden was reduced upon ZOL and Fc-OPG treatment. Although there appeared to be a trend for less overall total tumor burden upon treatment with both compounds, this was not significant as assessed by BLI and histomorphometrical analysis due to the extramedullary growth of cancer cells which was not affected by these treatments.

Collectively, anti-resorptive agents with different mechanisms of actions — ZOL and FcOPG — significantly reduced cancer-induced osteolysis and intraosseous tumor burden, but failed to restrain local tumor growth. However, interference with the bone microenvironmental growth support could still be of therapeutic relevance when given to patients early in the course of bone metastatic disease.

Jeroen_Buijs_18.indd 134 26-11-2008 10:18:36

Introduction

Micrometastases persisting in various tissues of cancer patients after removal of the primary tumor represent the pathophysiological basis for cancer relapse as overt metastases. The survival of these cells and the development of metastases depend on the growth support provided by the microenvironment and the ability of cancer cells to adapt to this environment [1-3]. Bone provides a favorable microenvironment for the survival and growth of certain common cancers, including breast cancer which metastasizes frequently to the skeleton and causes significant morbidity and deterioration of life [4-6].

Studies in animal models of bone metastases strongly suggest that the rate of bone turnover enhances the occurrence and progression of metastases in the bone-bone marrow microenvironment [7-9]. These findings are supported by clinical studies which showed a significant association between the rate of bone resorption, assessed by biochemical markers of bone remodeling, and disease progression in the skeleton [10,11]. It was, therefore, hypothesized that suppression of bone resorption by agents that inhibit the formation and/or activity of the osteoclasts may not only protect skeletal integrity in metastatic disease but may also affect local tumor growth.

Previous studies of animal models with bone metastasis from breast cancer treated with bisphosphonates showed that reduction of bone turnover prior to bone colonization by cancer cells, could significantly reduce the number and progression of bone metastases [12-15]. However, when bisphosphonates were given to animals with established bone metastases they did not consistently affect the growth potential of the breast cancer cells in the bone microenvironment, despite a substantial anti-osteolytic effect [12,13]. There are several potential explanations for these findings: tumor growth response is related to the magnitude of suppression of bone resorption and, hence, the potency, and/or the dose (dosing regimen) of the bisphosphonates given; the fundamental mechanism of inhibition of bone resorption by the bisphosphonates; the initial growth phase of cancer cells in bone is dependent upon the interaction with the bone microenvironment, but eventually becomes independent of the bone microenvironent and can progress autonomously [13,50]. To address these questions we assessed the effects of very high doses of the most potent bisphosphonate currently available, zoledronic acid (ZOL), and we compared these to the effects of osteoprotegerin (Fc-OPG), that inhibits bone resorption by a different mechanism of action, in an experimental model of intra-tibial injection of human breast cancer cells.

MATERIALS & METHODS

Cell lines and culture conditions

The luciferase expressing bone-seeking clone MDA-MB-231 (MDA-231)-B/Luc+ was cultured as previously described [16,17]. Cell suspensions of MDA-231-B/Luc+(1.0 x 10^5 cells /10 µl PBS) were prepared for intraosseous injection as described previously [13,17].

Animals

Female nude (BALB/c *nu/nu*) mice were purchased from Charles River (L'Arbresle, France) and were used for the studies with human MDA-231-B/Luc+breast cancer cells.

Mice were housed in individual ventilated cages under sterile condition. Sterile food and water were provided *ad libitum*. Mice were 6 weeks old when used for intraosseous inoculation of cancer cells. Animal experiments were approved by the local committee for animal health, ethics and research of Leiden University and carried out in accordance with European Communities Council Directive 86/609/EEC.

For surgical and analytical procedures (intraosseous inoculation, BLI, radiography) mice were anesthetized by intraperitoneal injection of a 50 µl 1:1:1 mixture; Ketamine HCl (Stock solution of 100 mg/ml Nimatek; Vetimex Animal Health B.V., Bladel, The Netherlands) + Xylazine (2 % Rompun, Bayer AG, Leverkusen, Germany) + PBS (pH 6.8). Intracardiac inoculation of cancer cells was performed under Isofluorane anesthesia (0.8 L/min, Isofluorane, Air Products, Waddinxveen, The Netherlands) using the Vapex3 system (VetTech Solutions Ltd, United Kingdom). At the end of the experimental period animals were sacrificed by cervical dislocation.

Histomorphometry, Histochemistry and Immunohistochemistry

Dissected long bones were fixed in 4 % paraformaldehyde (pH 6.8), decalcified as described previously and processed for paraffin embedding [16,18]. Five micrometer longitudinal sections were cut through the sagittal plane of the tibiae containing tumors induced by the intra-bone inoculation of MDA-231-B/Luc+cells. Sections were either submitted to Goldner staining or histochemical staining for Tartrate Resistant Acid Phosphatase (TRAcP) as described previously [13].

Histomorphometric analysis of tumor burden was performed on central sections through the tumor (largest tumor area) as described previously [13]. Subsequently, a distinction was made between intraosseous and extramedullary tumor burden. For this, the digital image of the total tumor area was subdivided into an area delimited by the bone cortex or, were this has been partially resorbed as a result of the tumor-induced osteolysis, by a virtual line joining the remnants of the bone cortex, to define 'intraosseous' tumor growth. Evidently, the intraosseous, or intra-bone, tumor burden was critically selected between the bone trabeculae. Accordingly, the extramedullary tumor growth was defined as tumor cells growing surrounding the bone cortex or its remnants.

Histomorphometric measurements of trabecular bone volumes were performed after Goldner staining on the same central sections as used for tumor burden measurements. Trabecular bone volume (TBV) was estimated in the proximal tibia by measuring the total area of trabecular structures in an area 0-2 mm distal to the capillary invasion front of the growth plate. TBV is expressed as percentage of the total area that was covered by trabeculae.

Jeroen_Buijs_18.indd 136 26-11-2008 10:18:37

Statistical Analyses

All data are represented as means ± SE. Statistical evaluation was carried out by ANOVA using post-hoc of LSD.

RESULTS

Effect of ZOL and Fc-OPG on bone destruction

Compared to vehicle treatment, both treatments inhibited significantly the development of radiographically detectable osteolytic lesions (Fig. 1). There was no significant difference between the two treatment groups, but Fc-OPG prevented completely the development of radiographically evident osteolytic lesions.

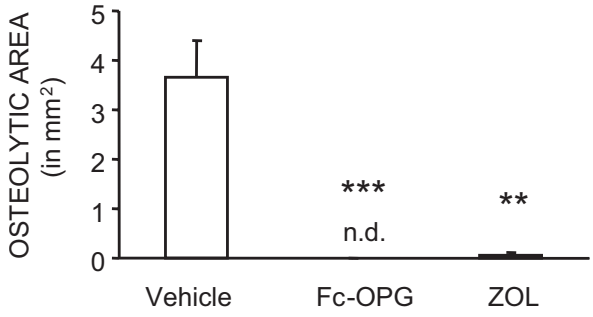

Figure 1 **Radiographically evident osteolytic lesions after 42 days of experimental treatment with Fc-OPG or ZOL.** n.d. = not detected; ** p <0.01, *** p < 0.001 compared to vehicle.

Histological examination of tibiae inoculated with tumor cells corroborated the radiographic findings (Fig. 2*A*). In vehicle-treated animals trabecular bone was destroyed and was replaced by tumor. In contrast, treatment with either ZOL or Fc-OPG preserved the integrity of bone trabeculae and prevented bone destruction (Fig. 2). In addition, trabecular bone volume (TBV) was similar between the two actively treated groups and significantly higher than in animals treated with vehicle alone (Fig. 2*B*).

The effect of both ZOL and Fc-OPG on bone destruction was due to their action on bone resorption as evidenced by the significant decrease in TRAcP-positive (TRAcP+) osteoclasts (Fig. 3). However, whereas practically no TRAcP+ cells were observed in tibiae preparations of animals treated with Fc-OPG, such cells were still present in the animals treated with ZOL (Fig. 3*B*). Though, in the ZOL-treated animals, many of the TRAcP+ osteoclasts that are still present are not tightly attached to the bone surface and represent non-active osteoclasts not capable of resorbing bone (Fig. 3*A*). This discrepancy between the effects on osteoclasts of the two agents is probably due to their different mechanisms of actions. Fc-OPG inhibits the formation and activity of osteoclasts whereas ZOL acts primarily on mature osteoclasts and

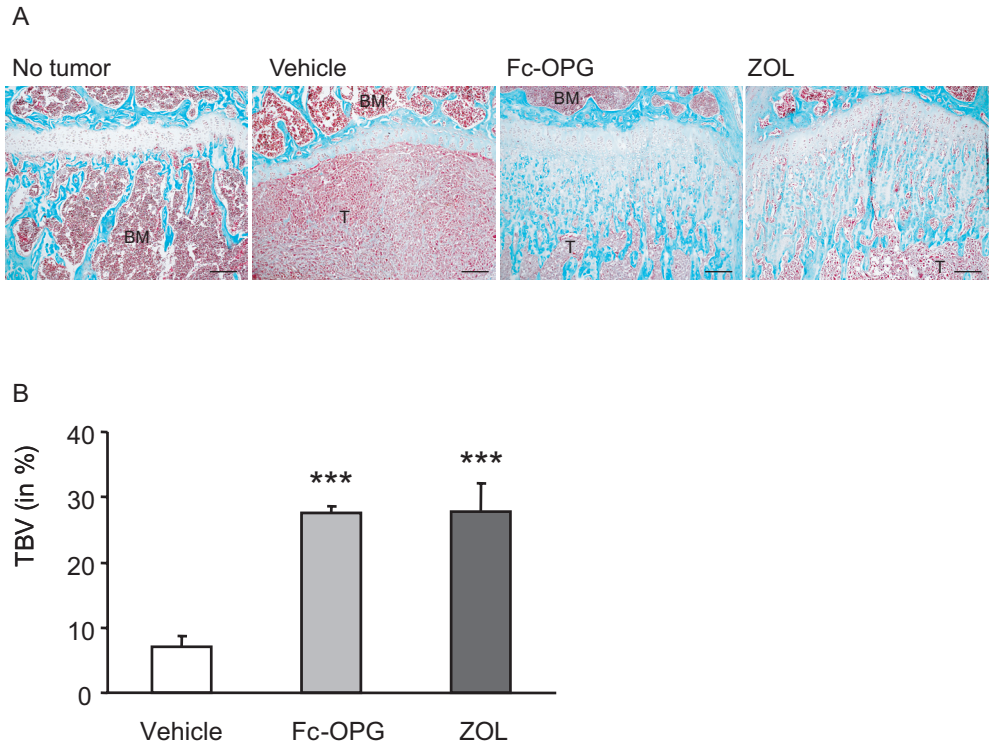

Figure 2 **Effects of Fc-OPG and ZOL treatment on bone trabeculae as shown by Goldner staining.** *A,* Fc-OPG and ZOL treatment inhibited cancer-induced bone destruction leading to a significant increase in trabecular bone area when compared with vehicle treated animals. Scalebars = 100µm; BM = bone marrow; T = tumor. *B,* trabecular bone volume (TBV) was significantly increased by Fc-OPG and ZOL treatment to a comparable extent when compared with vehicle treatment as determined by histomorphometric analysis. *** p <0.001 compared to vehicle.

increases their rate of apoptosis. Therefore, the TRAcP+ cells persisting in the ZOL treatment group are probably non-functioning osteoclasts, as shown previously [20-22].

Effect of ZOL and Fc-OPG on tumor growth

A. ZOL and Fc-OPG did not decrease the total tumor growth in the hindlimb assessed by BLI. Representative examples of animals treated with vehicle, ZOL or Fc-OPG are shown in figure 4*A* and the overall results of treatment are depicted in figure 4*B*. Although there appeared to be a trend for less tumor burden with both active treatments at the end of the experiment, this was not significantly different from vehicle-treated animals.

B. Histologically, the intra-bone tumor burden was significantly decreased with both treatments (Fig. 5*B*), but cancer cells were still present in bone marrow spaces (Figs. 2*A*, 3*A* and 5*A*). In contrast, extramedullary growth of cancer cells was not affected (Fig. 5*B*).

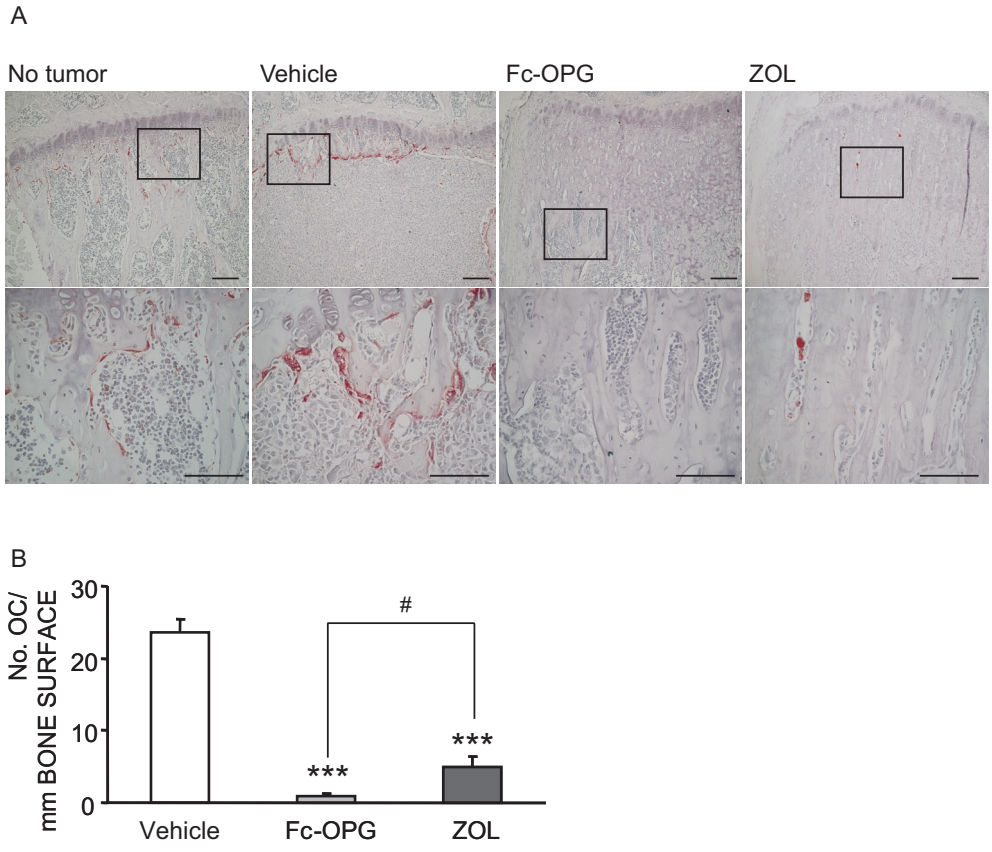

Figure 3 **TRAcP staining to examine osteoclast numbers.** Osteoclasts were stained red with TRAcP staining. *A,* in the ZOL treated animals, many of the TRAcP+ osteoclasts that are still present are not tightly attached to the bone surface and represent non-active osteoclasts not capable of resorbing bone. In the Fc-OPG group the osteoclasts were almost totally eradicated. Selected areas in the figures at the top are enlarged in the figures at the bottom. Scalebars are 50µm (figures at the top) and 80µm (figures at the bottom). *B,* both Fc-OPG and ZOL treatment significantly reduced the number of osteoclasts compared to vehicle treatment. In addition, Fc-OPG treatment resulted in a superior deletion of osteoclasts when compared to ZOL treatment. *** $p < 0.001$ compared to vehicle; # $p < 0.05$.

The overall tumor burden (combined intra-bone and extramedullary growth) decreased, but not significantly so, which is full agreement with the BLI data.

DISCUSSION

In this study we tested the hypothesis that suppression of bone resorption could reduce the growth and progression of breast cancer cells in the bone microenvironment. For this we have used a mouse model of intra-tibial injection of cancer cells as a model for late events

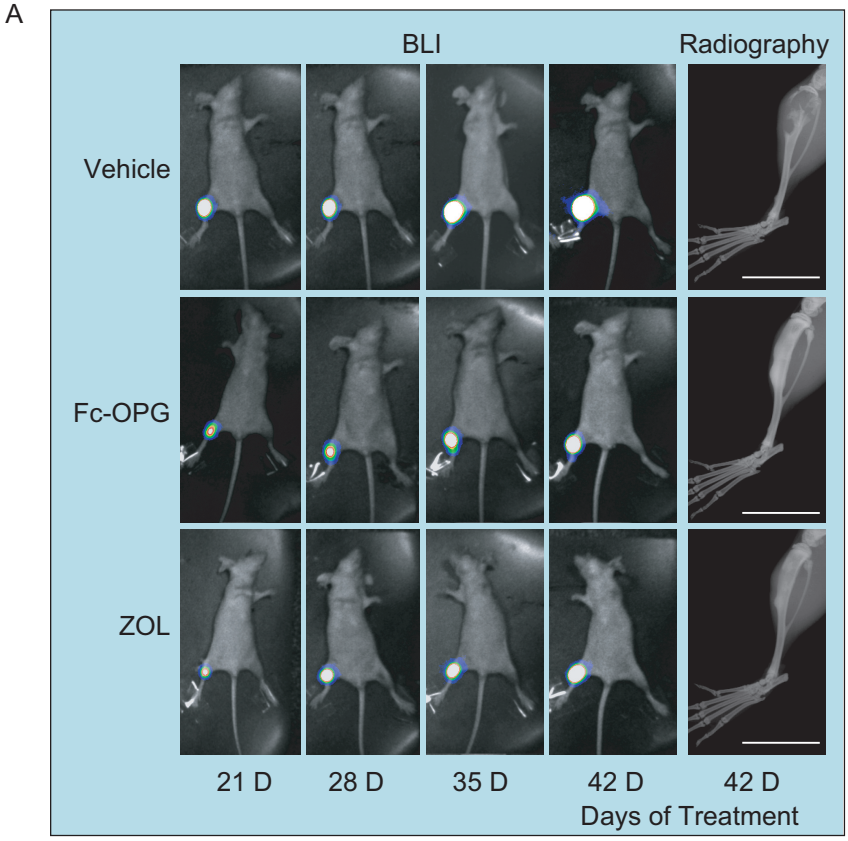

Figure 4 **Tumor growth as detected by bioluminescent imaging.** *A*, representative examples of Fc-OPG and ZOL treated mice with intraosseous tumor growth and tumor-induced bone destruction as detected by bioluminescent imaging (BLI) and radiography. Scale bars in X-rays: 10 mm. *B*, tumor burden as measured by BLI and quantified in 10^5 relative light units (RLU).

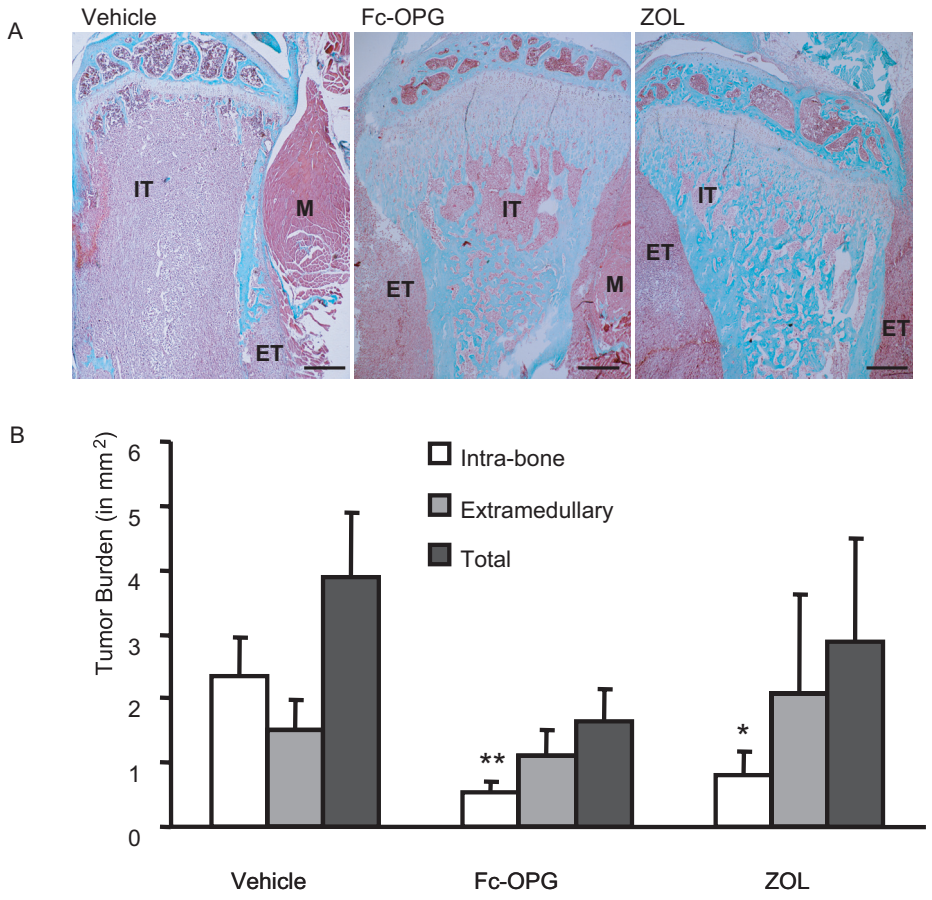

Figure 5 **Effects of Fc-OPG and ZOL treatment on intra-bone and extramedullary tumor growth in tibiae as assessed by histomorhphogical analysis.** *A*, goldner staining showing intra-bone tumor growth (IT), extramedullary tumor growth (ET), and muscle tissue (M). Scale bars: 200 µm. *B*, ** p <0.01 and * p <0.05 compared to vehicle.

in the bone metastatic process. This *in vivo* model, therefore, does not represent earlier stages of bone metastasis (e.g., bone homing), but is ideally suited to monitor the effects of bone resorption inhibitors on the growth of cancer cells in the bone microenvironment. Our results show that the two very potent agents used, ZOL and Fc-OPG, significantly reduce intra-bone tumor burden (as measured by histology). Despite a marked effect on tumor-induced bone resorption and intra-bone tumor burden, ZOL and Fc-OPG failed to reduce the total tumor burden which included extramedullary growth.

Interference with the microenvironmental growth support has been proposed as an attractive strategy for decreasing metastatic tumor growth [23]. Bone is a dynamic tissue that is continuously remodeled by bone resorption and subsequent bone formation [24]. Animal

and human studies have shown that high bone remodeling promotes the formation of bone metastases [8-10,13] through the release of factors from bone matrix that support metastatic growth in the bone marrow [1,25].

Differently from other tissues, agents that specifically decrease bone resorption and remodeling are available and are used clinically or experimentally for the protection of bone destruction by metastases from different primary tumors [26-30]. The question is whether local growth and spread of metastases in bone can also be decreased during this process. To provide an answer to this question, in the present proof-of-concept study we aimed to suppress bone resorption maximally with doses of agents that specifically and effectively inhibit and osteoclast-induced bone resorption.

Bisphosphonates are used extensively in the management of patients with bone metastases [27,29-31]. They suppress bone resorption and reduce significantly the frequency of skeletal-related events [31-34]. Of the currently available bisphosphonates, ZOL is the most potent inhibitor of bone resorption *in vitro* and *in vivo* [21,34] and it has also been reported to induce apoptosis of tumor cells *in vitro* [35-37]. We, therefore, used high doses of ZOL to examine the relation between suppression of bone resorption and local progression of breast cancer cell growth. As expected and previously reported [22,38], ZOL reduced markedly tumor-induced osteolysis, as shown radiographically and histologically, through its effects on osteoclasts. TRAcP+ cells were not totally eradicated but those still persisting were probably inactive apoptotic osteoclasts, as has been previously shown in studies with different bisphosphonates [20,22]. Intraosseous tumor burden was reduced, however, the total tumor burden (intrabone and extramedullary) still progressed and although at the end of the experiment this appeared less compared to controls, the difference was not significant. It should be noted that the dosing regimen we used seems unlikely to be responsible for the observed effects as daily and and once-weekly administration of ZOL has been reported to have similar effects on tumor growth in a different model of bone metastasis [50].

ZOL, as all potent nitrogen-containing bisphosphonates, acts primarily on mature osteoclasts and decreases their activity and life-span [21,39]. To exclude the possibility that for an effect on tumor growth all stages of osteoclastogenesis leading to increased bone resorption need to be optimally suppressed, we also treated animals with Fc-OPG. OPG is the natural inhibitor of RANK ligand (RANKL) [40-42], an essential factor for the formation and activity of osteoclasts [43,44]. Fc-OPG has been shown in animal models to strongly inhibit cancer-induced osteolysis [45-47] and to suppress bone resorption in patients with bone metastases from breast cancer [28]. In our study, Fc-OPG suppressed markedly bone resorption, protected the integrity of bone trabeculae and prevented the development of osteolytic lesions. These effects were due to its actions on osteoclast formation and activity as evidenced by the nearly complete eradication of TRAcP+ cells in bone from treated animals. Furthermore, as was also the case with ZOL, intraosseous tumor burden was significantly reduced. Since there was not an effect of Fc-OPG on extramedullary tumor burden, the total tumor

Jeroen_Buijs_18.indd 142 26-11-2008 10:18:43

burden (sum of intraosseous and extramedullary) still progressed, and although throughout the entire experiment this appeared less compared to controls, the difference was not significant.

It should be noted that with both ZOL and Fc-OPG the intra-bone tumor burden diminished considerably as shown in histological sections of the tibiae. This is, at least in part, due to the increase in trabecular bone volume and concomitant decrease in bone marrow volume where tumor cells could reside. In other words, even if tumor cells completely fill bone marrow spaces, the relative intra-bone tumor volume would be less in ZOL and Fc-OPG-treated animals compared to vehicle-treated animals. In fact, space limitations within the bone marrow may direct invasive growth towards the extramedullary.

If we had, thus, confined our assessment of tumor growth strictly within the bone we could have arrived to the wrong conclusion about an effect on tumor growth. This underlines the importance of careful dissection of the tumor-containing bones in such a way that the invaded surrounding soft tissue is not removed. It is important to note that the growth of MDA-231 breast cancer cell outside the bone collar in the surrounding soft tissue was also observed in our previous studies with olpadronate [13] and those of Sasaki and co-workers with risedronate and other BPs [12,15]. In these studies, a bone metastasis model of injection of tumor cells into the left heart ventricle was used, rather than direct injection into bone. Therefore, tumor cells invading the surrounding soft tissue can not fully be explained by a potential artefact of the model of direct injection into bone. In this respect, it is also important to note that MDA-231 cancer cells can migrate from the bone marrow to periosteal surfaces through vascular channels [13].

Zheng and co-workers showed that curative OPG treatment significantly inhibited tumor growth in the bone environment, as assessed by histology [48]. In fact, tumor areas for OPG and vehicle treated mice were comparable to our data. Furthermore, OPG treatment inhibited proliferation and stimulated apoptosis of cancer cells in the bones. Another study, in which tumor cells were injected into the left heart ventricle, showed that curative low and high dose OPG treatment inhibited tumor growth in bone, and that only high dose OPG increased tumor cell apoptosis [49].

So, bone resorption inhibitors could affect tumor progression in bone by decreasing the bone marrow volume where tumor cells could reside, and by stimulating apoptosis and inhibiting proliferation of cancer cells. However, our data demonstrate that tumor progression into extramedullary spaces is not affected by those treatments. In addition, ZOL and Fc-OPG do not have a major impact on overall tumor burden under the experimental conditions described here. Therefore the results of our experiments do not provide support for the notion that suppression of bone resorption in already established metastatic disease in bone arrest tumor growth and progression, despite its inhibitory effects on intra-bone tumor volume. These data favor the hypothesis that metastatic cancer cells in bone after an initial growth phase that depends on their interaction with the bone marrow stroma

and extracellular bone matrix, become increasingly independent of microenvironmental growth factor support and progress autonomously [13]. At this stage, for skeletal protection and arrest of further tumor growth, anti-resorptive agents should probably be combined with compounds with different mechanism of action on the metastatic cascade such as, for example, cytostatics or anti-angiogenic factors.

The important, and clinically relevant question, that still needs to be addressed is whether suppression of bone resorption early in the course of metastatic disease and while cancer cells are still dormant may prevent the development of macrometastases. Animal studies with bone resorption inhibitors given before the colonization of bone by cancer cells strongly suggest that this can be feasible [13-15]. Therefore, this issue needs to be addressed in properly designed clinical studies.

Acknowledgments

We thank Dr. William C. Dougall for helpful suggestions and critical review during the preparation of the manuscript. This work was supported by Dutch Cancer Society grant RUL 2001-2485 and Amgen Inc. Thousand Oaks, CA 91320, USA.

References

1. Mundy GR. Metastasis to bone: causes, consequences and therapeutic opportunities. *Nat Rev Cancer* 2002; 2:584-93.
2. Paget S. The distribution of secondary growths in cancer of the breast. *Lancet* 1889; 1:571-3.
3. Clines GA, Guise TA. Hypercalcaemia of malignancy and basic research on mechanisms responsible for osteolytic and osteoblastic metastasis to bone. *Endocr Relat Cancer* 2005; 12:549-83.
4. Coleman RE. Skeletal complications of malignancy. *Cancer* 1997; 80:1588-94.
5. Jemal A, Siegel R, Ward E, Murray T, Xu J, Smigal C *et al*. Cancer statistics, 2006. *CA Cancer J Clin* 2006; 56:106-30.
6. Mercadante S. Malignant bone pain: pathophysiology and treatment. *Pain* 1997; 69:1-18.
7. Arguello F, Baggs RB, Graves BT, Harwell SE, Cohen HJ, Frantz CN. Effect of IL-1 on experimental bone/bone-marrow metastases. *Int J Cancer* 1992; 52:802-7.
8. Kostenuik PJ, Singh G, Suyama KL, Orr FW. Stimulation of bone resorption results in a selective increase in the growth rate of spontaneously metastatic Walker 256 cancer cells in bone. *Clin Exp Metastasis* 1992; 10:411-8.
9. Schneider A, Kalikin LM, Mattos AC, Keller ET, Allen MJ, Pienta KJ *et al*. Bone turnover mediates preferential localization of prostate cancer in the skeleton. *Endocrinology* 2005; 146:1727-36.
10. Brown JE, Cook RJ, Major P, Lipton A, Saad F, Smith M *et al*. Bone turnover markers as predictors of skeletal complications in prostate cancer, lung cancer, and other solid tumors. *J Natl Cancer Inst* 2005; 97:59-69.
11. Costa L, Demers LM, Gouveia-Oliveira A, Schaller J, Costa EB, de Moura MC *et al*. Prospective evaluation of the peptide-bound collagen type I cross-links N-telopeptide and C-telopeptide in predicting bone metastases status. *J Clin Oncol* 2002; 20:850-6.
12. Sasaki A, Boyce BF, Story B, Wright KR, Chapman M, Boyce R *et al*. Bisphosphonate risedronate reduces metastatic human breast cancer burden in bone in nude mice. *Cancer Res* 1995; 55:3551-7.

Jeroen_Buijs_18.indd 144 26-11-2008 10:18:43

13. van der Pluijm G, Que I, Sijmons B, Buijs JT, Lowik CW, Wetterwald A *et al*. Interference with the microenvironmental support impairs the de novo formation of bone metastases in vivo. *Cancer Res* 2005; 65:7682-90.
14. Hiraga T, Williams PJ, Ueda A, Tamura D, Yoneda T. Zoledronic acid inhibits visceral metastases in the 4T1/luc mouse breast cancer model. *Clin Cancer Res* 2004; 10:4559-67.
15. Sasaki A, Kitamura K, Alcalde RE, Tanaka T, Suzuki A, Etoh Y *et al*. Effect of a newly developed bisphosphonate, YH529, on osteolytic bone metastases in nude mice. *Int J Cancer* 1998; 77:279-85.
16. van der Pluijm G, Sijmons B, Vloedgraven H, Deckers M, Papapoulos S, Lowik C. Monitoring metastatic behavior of human tumor cells in mice with species-specific polymerase chain reaction: elevated expression of angiogenesis and bone resorption stimulators by breast cancer in bone metastases. *J Bone Miner Res* 2001; 16:1077-91.
17. Wetterwald A, van der Pluijm G, Que I, Sijmons B, Buijs J, Karperien M *et al*. Optical imaging of cancer metastasis to bone marrow: a mouse model of minimal residual disease. *Am J Pathol* 2002; 160:1143-53.
18. van der Pluijm G, Sijmons B, Vloedgraven H, van der Bent C, Drijfhout JW, Verheijen J *et al*. Urokinase-receptor/integrin complexes are functionally involved in adhesion and progression of human breast cancer in vivo. *Am J Pathol* 2001; 159:971-82.
19. Morony S, Capparelli C, Lee R, Shimamoto G, Boone T, Lacey DL *et al*. A chimeric form of osteoprotegerin inhibits hypercalcemia and bone resorption induced by IL-1beta, TNF-alpha, PTH, PTHrP, and 1, 25(OH)2D3. *J Bone Miner Res* 1999; 14:1478-85.
20. Alakangas A, Selander K, Mulari M, Halleen J, Lehenkari P, Monkkonen J *et al*. Alendronate disturbs vesicular trafficking in osteoclasts. *Calcif Tissue Int* 2002; 70:40-7.
21. Dunford JE, Thompson K, Coxon FP, Luckman SP, Hahn FM, Poulter CD *et al*. Structure-activity relationships for inhibition of farnesyl diphosphate synthase in vitro and inhibition of bone resorption in vivo by nitrogen-containing bisphosphonates. *J Pharmacol Exp Ther* 2001; 296:235-42.
22. Mundy GR, Yoneda T, Hiraga T. Preclinical studies with zoledronic acid and other bisphosphonates: impact on the bone microenvironment. *Semin Oncol* 2001; 28:35-44.
23. Liotta LA, Kohn EC. The microenvironment of the tumour-host interface. *Nature* 2001; 411:375-9.
24. Hill PA. Bone remodelling. *Br J Orthod* 1998; 25:101-7.
25. Guise TA, Mundy GR. Cancer and bone. *Endocr Rev* 1998; 19:18-54.
26. Vaananen K. Mechanism of osteoclast mediated bone resorption--rationale for the design of new therapeutics. *Adv Drug Deliv Rev* 2005; 57:959-71.
27. Michaelson MD, Smith MR. Bisphosphonates for treatment and prevention of bone metastases. *J Clin Oncol* 2005; 23:8219-24.
28. Body JJ, Greipp P, Coleman RE, Facon T, Geurs F, Fermand JP *et al*. A phase I study of AMGN-0007, a recombinant osteoprotegerin construct, in patients with multiple myeloma or breast carcinoma related bone metastases. *Cancer* 2003; 97:887-92.
29. Coleman RE. Bisphosphonates in breast cancer. *Ann Oncol* 2005; 16:687-95.
30. Elte JW, Bijvoet OL, Cleton FJ, van Oosterom AT, Sleeboom HP. Osteolytic bone metastases in breast carcinoma pathogenesis, morbidity and bisphosphonate treatment. *Eur J Cancer Clin Oncol* 1986; 22:493-500.
31. Lipton A, Theriault RL, Hortobagyi GN, Simeone J, Knight RD, Mellars K *et al*. Pamidronate prevents skeletal complications and is effective palliative treatment in women with breast carcinoma and osteolytic bone metastases: long term follow-up of two randomized, placebo-controlled trials. *Cancer* 2000; 88:1082-90.
32. Body JJ, Diel IJ, Lichinitser MR, Kreuser ED, Dornoff W, Gorbunova VA *et al*. Intravenous ibandronate reduces the incidence of skeletal complications in patients with breast cancer and bone metastases. *Ann Oncol* 2003; 14:1399-405.
33. Powles T, Paterson A, McCloskey E, Schein P, Scheffler B, Tidy A *et al*. Reduction in bone relapse and improved survival with oral clodronate for adjuvant treatment of operable breast cancer [ISRCTN83688026]. *Breast Cancer Res* 2006; 8:R13.
34. Rosen LS, Gordon DH, Dugan W, Jr., Major P, Eisenberg PD, Provencher L *et al*. Zoledronic acid is superior to pamidronate for the treatment of bone metastases in breast carcinoma patients with at least one osteolytic lesion. *Cancer* 2004; 100:36-43.

35. Senaratne SG, Pirianov G, Mansi JL, Arnett TR, Colston KW. Bisphosphonates induce apoptosis in human breast cancer cell lines. *Br J Cancer* 2000; 82:1459-68.
36. Jagdev SP, Coleman RE, Shipman CM, Rostami H, Croucher PI. The bisphosphonate, zoledronic acid, induces apoptosis of breast cancer cells: evidence for synergy with paclitaxel. *Br J Cancer* 2001; 84:1126-34.
37. Fromigue O, Lagneaux L, Body JJ. Bisphosphonates induce breast cancer cell death in vitro. *J Bone Miner Res* 2000; 15:2211-21.
38. Peyruchaud O, Winding B, Pecheur I, Serre CM, Delmas P, Clezardin P. Early detection of bone metastases in a murine model using fluorescent human breast cancer cells: application to the use of the bisphosphonate zoledronic acid in the treatment of osteolytic lesions. *J Bone Miner Res* 2001; 16:2027-34.
39. Hughes DE, Wright KR, Uy HL, Sasaki A, Yoneda T, Roodman GD *et al*. Bisphosphonates promote apoptosis in murine osteoclasts in vitro and in vivo. *J Bone Miner Res* 1995; 10:1478-87.
40. Simonet WS, Lacey DL, Dunstan CR, Kelley M, Chang MS, Luthy R *et al*. Osteoprotegerin: a novel secreted protein involved in the regulation of bone density. *Cell* 1997; 89:309-19.
41. Yasuda H, Shima N, Nakagawa N, Yamaguchi K, Kinosaki M, Mochizuki S *et al*. Osteoclast differentiation factor is a ligand for osteoprotegerin/osteoclastogenesis-inhibitory factor and is identical to TRANCE/RANKL. *Proc Natl Acad Sci U S A* 1998; 95:3597-602.
42. Khosla S. Minireview: the OPG/RANKL/RANK system. *Endocrinology* 2001; 142:5050-5.
43. Theoleyre S, Wittrant Y, Tat SK, Fortun Y, Redini F, Heymann D. The molecular triad OPG/RANK/RANKL: involvement in the orchestration of pathophysiological bone remodeling. *Cytokine Growth Factor Rev* 2004; 15:457-75.
44. Blair JM, Zhou H, Seibel MJ, Dunstan CR. Mechanisms of disease: roles of OPG, RANKL and RANK in the pathophysiology of skeletal metastasis. *Nat Clin Pract Oncol* 2006; 3:41-9.
45. Croucher PI, Shipman CM, Van Camp B, Vanderkerken K. Bisphosphonates and osteoprotegerin as inhibitors of myeloma bone disease. *Cancer* 2003; 97:818-24.
46. Morony S, Capparelli C, Sarosi I, Lacey DL, Dunstan CR, Kostenuik PJ. Osteoprotegerin inhibits osteolysis and decreases skeletal tumor burden in syngeneic and nude mouse models of experimental bone metastasis. *Cancer Res* 2001; 61:4432-6.
47. Morony S, Warmington K, Adamu S, Asuncion F, Geng Z, Grisanti M *et al*. The inhibition of RANKL causes greater suppression of bone resorption and hypercalcemia compared with bisphosphonates in two models of humoral hypercalcemia of malignancy. *Endocrinology* 2005; 146:3235-43.
48. Zheng Y, Zhou H, Brennan K, Blair JM, Modzelewski JR, Seibel MJ *et al*. Inhibition of bone resorption, rather than direct cytotoxicity, mediates the anti-tumour actions of ibandronate and osteoprotegerin in a murine model of breast cancer bone metastasis. *Bone* 2007; 40:471-8.
49. Canon JR, Roudier M, Bryant R, Morony S, Stolina M, Kostenuik PJ *et al*. Inhibition of RANKL blocks skeletal tumor progression and improves survival in a mouse model of breast cancer bone metastasis. *Clin Exp Metastasis* 2007; 25:119-29.
50. Daubine F, Le Gall C, Gasser J, Green J, Clezardin P. Antitumor effects of clinical dosing regimens of bisphosphonates in experimental breast cancer bone metastasis. J Natl Cancer Inst 2007;99:322-30.

Jeroen_Buijs_18.indd 146 26-11-2008 10:18:44

Chapter 6

Bone Morphogenetic Protein 7 in the Development and Treatment of Bone Metastases from Breast Cancer

Cancer Res 2007; 67:8742-51

Jeroen T Buijs[1],
Nico V Henriquez[1],
Petra GM van Overveld[2], Geertje van der Horst[2],
Ivo Que[1], Ruth Schwaninger[5],
Cyrill Rentsch[5], Peter ten Dijke[3],
Anne-Marie Cleton-Jansen[4],
Keltouma Driouch[6], Rosette Lidereau[6],
Richard Bachelier[7], Slobodan Vukicevic[8],
Philippe Clézardin[7], Socrates E Papapoulos[1],
Marco G Cecchini[5], Clemens WGM Löwik[1],
Gabri van der Pluijm[1,2]

Departments of Endocrinology[1], Urology[2],
Molecular Cell Biology[3] and Pathology[4],
Leiden University
Medical Center, Leiden, The Netherlands;
[5]Department of Clinical Research and Urology,
University of Bern, Bern, Switzerland;
[6]Centre René Huguenin and Institut National
de la Sante et de la Recherche Medicale,
Research Unit 735, St.Cloud, France;
[7]Institut National de la Sante et de la
Recherche Medicale, Research Unit 664, Laennec;
School of Medicine, Lyon, France;
[8]Department of Anatomy,
School of Medicine, Zagreb, Croatia

Jeroen_Buijs_18.indd 147 26-11-2008 10:18:44

Abstract

Bone Morphogenetic Protein 7 (BMP7) counteracts physiologic epithelial-to-mesenchymal transition (EMT), a process that is indicative of epithelial plasticity. Since EMT is involved in cancer we investigated whether BMP7 plays a role in prostate cancer growth and metastasis.

In this study we show that decreased BMP7 expression in primary breast cancer is significantly associated with the formation of clinically overt bone metastases in patients with ≥ 10 years follow-up. In line with these clinical observations, BMP7 expression is inversely related to tumorigenicity and invasive behavior of human breast cancer cell lines. Moreover, BMP7 decreased the expression of vimentin, a mesenchymal marker associated with invasiveness and poor prognosis, in human MDA-MB-231-B/Luc+ breast cancer cells under basal and TGF-ß stimulated conditions. In addition, exogenous addition of BMP7 to TGF-ß stimulated MDA-MB-231 cells inhibited Smad-mediated TGF-ß signaling. Furthermore, in a well-established bone metastasis model using whole body bioluminescent reporter imaging, stable overexpression of BMP7 in MDA-MB-231 cells inhibited *de novo* formation and progression of osteolytic bone metastases and, hence, their metastatic capability. In line with these observations, daily intra-venous administration of BMP7 (100 µg/kg/day) significantly inhibited orthotopic and intra-bone growth of MDA-MB-231-B/Luc+ cells in nude mice.

Our data suggest that decreased BMP7 expression during carcinogenesis in the human breast contributes to the acquisition of a bone metastatic phenotype. Since exogenous BMP7 can still counteract the breast cancer growth at the primary site and in bone, BMP7 may represent a novel therapeutic molecule for repression of local and bone metastatic growth of breast cancer.

Jeroen_Buijs_18.indd 148 26-11-2008 10:18:44

Introduction

Approximately 90% of cancer deaths result from the local invasion and distant metastasis of tumor cells [1]. Better understanding of the process of metastasis is, therefore, urgently needed. Increased motility and invasiveness of breast cancer cells is reminiscent of the epithelial-to-mesenchymal transition (EMT) that occurs during embryonic development [2,3]. This transition to a more mesenchymal, motile cellular phenotype is the result of a complex physiological process that includes dissolution of adherens junctions, loss of cell polarity, a change to spindle-like cell morphology, cytoskeletal reorganization, increased cell motility, loss of epithelial markers and induction of mesenchymal marker [2,4]. Increased vimentin expression and perturbation of E-cadherin-mediated cell adhesion appear as hallmarks of this process [4-8]. However, in organogenesis 'mesenchymal' cells may possess remarkable plasticity and can eventually, regain a fully differentiated epithelial phenotype via a mesenchymal-to-epithelial transition (MET) [9-11].

Members of the transforming growth factor ß (TGF-ß) superfamily, which include bone morphogenetic proteins (BMPs), are involved in the control of many different biological processes including cell proliferation, differentiation, apoptosis and regulation of invasiveness [12-14]. In normal and non-malignant epithelial cells TGF-ß is a potent growth inhibitor [15,16]. However, different types of carcinomas often escape this tumor-suppressing activity and become refractile to growth inhibition [15,16]. Even more, TGF-ß can also potentiate tumorigenesis and contribute to the progression and invasiveness of various carcinomas [8,17,18]. Accordingly, it has been shown that a blockade of TGF-ß (signaling) inhibits tumor cell viability, migration, and metastasis [19], including the formation of bone metastases [20,21]. The homodimeric protein bone morphogenetic protein 7 (BMP7) induces MET in normal and non-transformed cells [14,22]. For instance, during kidney development, BMP7 is essential for the condensation and epithelialization of the metanephric mesenchyme in the kidney, resulting in the formation of the tubular epithelium [9-11,14]. Furthermore, BMP7 appears to be involved in the preservation of the epithelial phenotype [23,24], decreases fibrogenesis [23-25], and causes repression of inflammation [26,27].

In this study, we present a crosstalk between BMP7 and TGF-ß signaling in the regulation of EMT in breast cancer and identified BMP7 as a potential therapy for metastatic bone disease.

Materials and Methods

Cell line and Culture Conditions

The human breast cancer cell lines MDA-MB-231 (MDA-231), T47D and ZR-75-1 (ATCC, Rockville, USA) were cultured in DMEM (Gibco-BRL, Breda, The Netherlands) containing 4.5 g of glucose/L for MDA-231 or RPMI (ATCC, Rockville, USA) for T47D and ZR-75-1, supplemented

with 10% FCS (Gibco-BRL, Breda, The Netherlands), 100 units/ml penicillin and 50 µg/ml streptomycin (Life Technologies, Invitrogen, Breda, The Netherlands). Culture medium for T47D was supplemented with 6,5 µg/ml insulin (Sigma Chemical Co., St. Louis, MO, USA), and in culture medium for MDA-231-B/Luc+, a bone-seeking and luciferase expressing subclone from MDA-231 [28], 800 µg/ml geneticin/G418 (Gibco-BRL, Breda, The Netherlands) was added. MCF10A [29] and its fully malignant derivate MCF10CA1a [30] (Barbara Ann Karmanos Cancer Institute, Detroit, MI, USA) were cultured as described previously [30]. All cell lines were grown in a humidified incubator at 37°C and 5% CO2. Mycoplasma contamination was regularly tested by PCR, but never detected.

Putative BMP7 effects on luciferase expression by MDA-231-B/Luc+cells have been tested and excluded (data not shown).

Generation of isogenic BMP7-overexpressing cell lines using targeted integration

MDA-231 cells that display an unique predilection for bone (MDA-231-BO2 [31]) were selected to generate a stable cell line that overexpresses BMP7. Stable cell lines were generated using the Flp-In system (Invitrogen, Breda, The Netherlands) according to manufacturer's protocol [32]. In short, a MDA-231-BO2-Flp-in host cell line (MDA-231-BO2-Frt11) was generated by stable introduction of a single copy of a Flp-Recombinase target (FRT) site as an integral part of an antibiotic resistancy gene in the genome of these cells. Subsequently, a luciferase expressing subclone (MDA-231-BO2-Frt11/Luc+) was generated as described previously [28]. This clone was used for the generation of isogenic stable cell lines by transient co-transfection of an FRT-targeting vector and a Flp-recombinase expression vector. The FRT-targeting vector was either a pcDNA5/FRT vector (Invitrogen, Breda, The Netherlands) expressing Green Fluorescent Protein (GFP) (control) or BMP7 (target gene) under the control of the CMV promotor. Due to Flp-mediated recombination at the genomic FRT-site, this targeting vector was incorporated in the genome. Simultaneously, a shift in antibiotic resistancy was introduced allowing positive selection for integrants in the genomic FRT-site only and negative selection for random integrants in one single step [32]. This method allows the generation of isogenic stable cell lines, which only differ in sequence inserted in the genomic FRT site, thereby eliminating the need for clonal selection. It is important to note that both the MDA-231-BO2-Frt11 and MDA-231-BO2-Frt11/Luc+ cell line were validated for *in vivo* bone metastasis formation.

Patients

We retrospectively analyzed tumor tissue from 67 primary unilateral non-metastatic ductal breast carcinomas excised from women treated at Centre René Huguenin, St. Cloud, France from 1980 to 1994. The samples were examined histologically for the presence of tumor cells. A tumor sample was considered suitable if the proportion of tumor cells was more than 70%. Immediately after surgery, the tumor samples were stored in liquid nitrogen until RNA extraction.

Jeroen_Buijs_18.indd 150 26-11-2008 10:18:44

Standard prognostic factors are presented in Table 1. All patients were treated by hormone therapy only after surgery. The patients had physical examinations and routine chest radiography every 3 months for the first 2 years, followed by annual examination (mammograms). The median follow-up was 11.2 years (range 1.5-20.3y). 35 Patients were without relapse (≥ 10 years of follow-up), 17 patients developed exclusively visceral metastases (liver and/or lung) and 15 patients developed exclusively bone metastases. Immunohistochemical validation was performed on fixed, paraffin-embedded tissue sections from primary breast tumor specimens (8/67).

Table 1 Characteristics of the 67 breast tumors from patients with and without relapse.

	Total population (%)	Number of patients with relapse (%)	P-values
Total	67 (100)	32 (47.8)	
Histological grade §			
I+II	48 (71.6)	22 (45.8)	n.s
III	17 (28.4)	10 (58.8)	
Lymph node status			
Node-negative	13 (19.4)	1 (7.7)	P=0.0072
Node-positive 1-3	34 (50.7)	18 (52.9)	
Node-positive >3	20 (29.9)	13 (65)	
Clinical tumor size			
≤30mm	25 (37.3)	7 (28)	P=0.040
>30mm	42 (62.7)	25 (59.5)	
Estrogen receptor status			
Negative	9 (13.4)	4 (44.4)	n.s.
Positive	58 (86.6)	28 (48.3)	
Relapses			
+	32 (15 with bone mets)		
-	35		

§ Scarff Bloom Richardson classification, n.s. = not significant.

Enzyme-linked immunosorbent assay (ELISA) for human BMP7

Levels of BMP7 in conditioned media were measured with a commercially available specific ELISA kit using sandwich enzyme immunoassay technique (R&D systems, Abingdon, United Kingdom). Cells were routinely cultured for 4 days.

Real-Time RT-PCR

Total RNA was extracted with the RNeasy Midi kit (Qiagen, Venlo, The Netherlands) from *in vitro* cultured cells at 70-80% confluence. Reverse transcription was performed with random primers in the presence of RNase inhibitor (Roche Diagnostics, Rotkreuz, Switzerland). Quantitative real-time RT-PCR (qPCR) was performed using commercially obtained exon-specific primers for BMP7, E-cadherin, vimentin, and ß-actin (primer catalog numbers:

Hs 002333477 m1, Hs 00170423 m1, Hs 00185584 m1 and Hs 99999903 m1, respectively; Applied Biosystems, Rotkreuz, Switzerland) on an ABI Prism 7700 sequence detection system (Applied Biosystems, Rotkreuz, Switzerland). All experiments were performed in duplo on 4 different samples. For BMP7 mRNA detection in patients, qPCR (incl. thermal cycling conditions) was performed as described previously [33]. Each sample was normalized on the basis of its TATA box-binding protein (TBP) content. Primers used: BMP7 fwd ATG GCC AAC GTG GCA GAG AA, BMP7 rev CAG CCC AGG TCT CGG AAG CT, TBP fwd TGC ACA GGA GCC AAG AGT GAA and TBP rev CAC ATC ACA GCT CCC CAC CA. All qPCR values were normalized using the comparative method of Livak and Schmittger [34].

Western Blot

Cells were seeded in 6-wells plates at a density of 20.000/cm^2 in DMEM with 0.1% Fetal Clone II (FCII; HyClone, Perbio Science Nederland B.V., Etten-Leur, The Netherlands) for MDA-231-B/Luc+. After 18 hours, cells were stimulated with recombinant human mature BMP7 (rhBMP7) [35] (0.5 mg batches, Creative Biomolecules, Hopkinton, MA, USA; rhBMP7 was freshly dissolved to a stock solution – 1 mg/ml in 20 mM acetate buffer with 5 % mannitol, pH 4.5 – and was obtained from Dr. Vukicevic) and/or porcine TGF-ß2 (R&D systems, Uithoorn, The Netherlands). After an additional 48 hours, cells were lysed and collected in 250 µl lysisbuffer (20 nM Tris pH 7.5; 20% glycerol; 400 mM KCl; 1 nM DTT; aprotinin (1/1000) and Roche protease inhibitor mix) followed by one or two rounds of freeze/thawing, and used for Western Blot analysis as described earlier [36]. Rabbit polyclonal antibodies α-vimentin (diluted 1:500; ab7783, Abcam, Cambridge, UK) and α-E-cadherin (diluted 1:500; sc-7870, Santa Cruz Biotechnologies, Tebu-bio, Heerhugowaard, The Netherlands), and a mouse monoclonal antibody α-beta-actin (clone AC-15, Sigma–Aldrich, Zwijndrecht, The Netherlands) were used as primary antibodies.

Cells Grown on Chamber Slides

MDA-231-B/Luc+cells were seeded at a density 20.000/cm^2 in DMEM with 0.1% FCII in 8 chamber slides (Falcon, Becton Dickinson, Etten-Leur, The Netherlands), and growth factors were added after 18 hours. After 30 hours, cells were dried for 5 minutes and fixed with 3.7% paraformaldehyde (pH 6.8) (Merck, VWR, Amsterdam, The Netherlands) in PBS for 10 minutes and stained for vimentin as described for tissues, with the exception of the antigen retrieval step (see section 'histomorphometry, histochemistry and immunohistochemistry'). Images were acquired using a color charged-coupled device (CCD) camera mounted on a Nikon Eclips 610 microscope at a twenty-fold magnification. Subsequently, cells were scored double-blind for positive vimentin staining from four randomly chosen fields by two investigators (J.B. and P.v.O.).

Jeroen_Buijs_18.indd 152 26-11-2008 10:18:44

Transient transfections and transcription reporter assays

MDA-231 cells were seeded at a density 7.500 cells /cm^2 in DMEM with 10% FCII in 24-well plates. On the subsequent day, cells were transiently transfected with 1µg of the indicated constructs using FuGENE 6 (Roche, Mannheim, Germany) transfection reagent following manufacturer's protocol. To correct for transfection efficacy, 100 ng of renilla luciferase (pRL-CMV; Promega, Madison, WI, USA or pRL-CAGGS, Promega, Madison, WI, USA) was co-transfected. On day 3, cells were serum starved for 24 hours before stimulation with TGF-ß and/or BMP7 for a duration of 30 hours. On day 5, luciferase activities were quantified using Dual Luciferase Assay (Promega, Madison, WI, USA) [37]. Firefly luciferase activity was corrected for renilla luciferase activity. The experiments were performed in four fold and repeated at least twice. Values are expressed as means ± s.e.m.

Luciferase Reporter Gene Constructs

For intracellular signaling of TGF-ß the *CAGA-luciferase* construct, consisting of 12 Smad3/Smad4 binding sequences (CAGA boxes) and the luciferase-coding sequence was used. The CAGA boxes confer TGF-ß stimulation to a heterologous promoter reporter construct, whose activity depends on binding of activated Smad3/Smad4 transcription factor complexes [37].
The *BRE-luciferase* construct, that is based on the mouse Id1 promoter, was used to study the presence and functionality of BMP-receptors [38].

Proliferation Assay

Cells were seeded in 96-wells plates at a density of 4.000/cm^2. 18 Hours after MDA-231-B/Luc+cells were seeded, cells were stimulated with 500 ng/ml BMP7 for 72 hours. Proliferation was measured with the CellTiter 96 Aqueous Non-Radioactive Cell Proliferation Assay (Promega, Madison, WI, USA) according to manufacturer's protocol.

Animals

Female nude mice (BALB/c *nu/nu*) were purchased from Charles River (L'Arbresle, France). Animals were housed in individual ventilated cages under sterile condition, and sterile food and water were provided *ad libitum*. Animal experiments were approved by the local committee for animal health, ethics and research of Leiden University and carried out in accordance with European Communities Council Directive 86/609/EEC. For surgical and analytical procedures mice were anaesthetized by intra-peritoneal injection of a 50 µl 1:1:1 mixture; Ketamine HCl (Stock solution of 100 mg/ml Nimatek; Vetimex Animal Health B.V., Bladel, The Netherlands.) + Xylazine (2% Rompun, Bayer AG, Leverkusen, Germany) + PBS (pH 6.8). At the end of the experimental period animals were sacrificed by cervical dislocation.

Animal Models

All cells were harvested at 70-80% confluence after changing to geneticin-free medium 24 hours before inoculation.

For tumor growth in the bone marrow, single cell suspensions 2.5 x 10^5 MDA-231-B/Luc+cells/ 10 µl PBS were injected into the right tibiae of 6-week old mice as described previously [28,39].

Three days after intraosseous (i.o.) inoculation of MDA-231-B/Luc+cells the animals were equally distributed into three experimental groups based on a comparable tumor burden/mouse, as detected by whole body bioluminescent reporter imaging (BLI). From this time point (day 0), and during a subsequent period of 24 days, all animals received vehicle or rhBMP7 (10 µg/kg/day or 100 µg/kg/day) treatment by tail vein injection. The progression of intraosseous growth was monitored by BLI at day 3, 10, 17 and 24 and by radiography at day 17 and 2 [28,39].

6-Weeks old mice were also i.o. inoculated (1.0 x 10^5 cells/ 10 µl PBS) with either MDA-231-BO2-Frt11(GFP)/Luc+ cells (n=8) or MDA-231-BO2-Frt11(BMP7)/Luc+ cells (n = 5). The progression was monitored by BLI weekly and by radiography at the end of the experiment (day 28) [28,39].

For orthotopic tumor growth, single-cell suspensions of 1.0 x 10^6 MDA-231-B/Luc+cells/ 10 µl PBS were inoculated via a 0.5 ml U-100 insulin needle (29G ½, BD Micro-Fine, Becton Dickinson, Etten-Leur, The Netherlands) into the mammary fat pads of 7-week old mice. Animals were equally distributed into two experimental groups based on a comparable tumor burden/mouse, as detected by BLI. From this time point (day 0), all animals were given vehicle or BMP7 (100 µg/kg/day) treatment by tail vein injection. Subsequently, the progression of orthotopically growing tumors was monitored weekly by BLI [28,39].

4.5-Weeks old nude mice were inoculated (5,0 x 10^5 cells/ 100 µl PBS) in the tail artery with either MDA-231-BO2-Frt11(GFP)/Luc+ cells (n=13) or MDA-231-BO2-Frt11(BMP7)/Luc+ cells (n=8), as described earlier [31]. The progression was monitored by BLI weekly and by radiography at the end of the experiment (day 28) [28,39].

After the experimental periods, mice were sacrificed by cervical dislocation.

Mammary fat pads and tibiae with tumors were dissected and processed for further histomorphometrical and immunohistochemical analysis (see below).

Whole Body Bioluminescent Reporter Imaging of Isogenic BMP7- and GFP-Overexpressing Cell lines

In animals that were inoculated with either MDA-231-BO2-Frt11(GFP)/Luc+ or MDA-231-BO2-Frt11(BMP7)/Luc+, the luciferase activity was visualized through imaging of whole bodies with an intensified-charge-coupled device (I-CCD) video camera of the *in vivo* Imaging System (IVIS 100, Xenogen, Alameda, CA, USA). The animals were anesthetized using the isofluorane anesthesia system (XGI-8, Xenogen), and injected intra-peritoneally with 2 mg D-luciferin sodium salt (Synchem OHG, Felsberg/Altenburg, Germany) dissolved in

Jeroen_Buijs_18.indd 154 26-11-2008 10:18:44

PBS. Animals were kept anesthetized, and measurements were performed 5 min after the injection of D-luciferin. Bioluminescence imaging was acquired with a 15-cm FOV, a medium binning factor, and exposure times of 10–60 s. Imaging data were analyzed by using the program living image (Xenogen, Alameda, CA, USA). Values are expressed as relative light units (RLU) in photons/sec.

Radiographical Analysis

Radiographic analyses of osteolytic lesions were assessed by radiography (Kodak X-OMAT TL film, Eastman Kodak Company, Rochester NY) using a Hewlett Packard X-ray system Faxitron 43805, and quantified using NIH-Image 1.62b7 software as described earlier [39].

Histomorphometry, Histochemistry and Immunohistochemistry

After orthotopic tumors and bone metastasis were fixed in 3.7% paraformaldehyde (pH 6.8) in PBS and processed, they were submitted to Goldner staining, staining for tartrate-resistant acid phosphatase (TRAcP), H&E staining or immunohistochemical staining as described previously [39,40]. Histomorphometric measurements of tumor burden were performed on central sections through the tumor (largest tumor area). Tumor growth in bone could be readily identified by pancytokeratin staining alone or in combination with H&E staining. Total tumor areas, as an estimate of total tumor burden, was measured by image analysis using NIH-Image 1.62b7 image analyses software as described previously [39]. Subsequently, a distinction was made between the total tumor burden and the intraosseous and extraosseous tumor burden as described previously [39].

The following rabbit polyclonal antibodies were used at a concentration of 10 µg/ml: α-human pan-cytokeratin (DAKO, Heverlee, Belgium), α-human vimentin (ab7783, Abcam, Cambridge, UK), α-human BMP7 (2854ab, directed against pro-domain of BMP7, obtained from Dr.Vukicevic) [35,41], α-phosphorylated Smad1 (PS1) [42] and normal rabbit IgG (Jackson Immuno Research, Cambridgeshire, UK) antibodies as negative control. Goat α-rabbit IgG (DAKO, Heverlee, Belgium) was used as secondary antibody. For antigen retrieval, slides were treated for 10 minutes at 37°C with 5 µg/ml proteinase K (Gibco-BRL, Breda, The Netherlands). To quantify PS1 and TRAcP staining, three histological sections per mouse (n=8) were acquired using a color CCD camera mounted on a Nikon Eclipse 610 microscope at a twenty-fold magnification. Subsequently, the number of cells that stained positive was scored single-blind by two investigators (G.v.d.P. and P.v.O.).

BMP7 staining on patient material was performed similarly, except that 5% normal goat serum (Jackson Immuno Research, Cambridgeshire, UK)/ 0.5% Boehringer Milk Powder (Boehringer Mannheim, Mannheim, Germany)/ TTBS was used instead of 0.5% Boehringer Milk Powder/ TTBS for incubation and first antibody dilution, and 0.01 M citrate buffer (pH 6.0) (7 minutes at 98°C) was used as antigen retrieval step, unless stated otherwise.

Jeroen_Buijs_18.indd 155 26-11-2008 10:18:44

Statistical Analysis

Survival rates were determined using the log-rank test. Since BMP7 mRNA levels in patients did not follow a Gaussian distribution, (a) the mRNA levels in each subgroup of samples were characterized by their median values and ranges, rather than their mean values and coefficients of variation, and (b) relationships between the molecular markers and clinical and histological parameters were tested using the non-parametric Mann-Whitney *U* test. Other data are represented as mean ± s.e.m.. *In vivo* tumor growth was measured by general linear model with repeated measurements using a LSD *post-hoc* test when applicable. Other statistical evaluations were carried out by ANOVA using a LSD *post-hoc* test when applicable.

Results

BMP7 Expression in Human Primary Breast Cancer and Formation of Distant Metastasis

BMP7 mRNA expression levels in primary breast tumors developing bone or visceral metastases were not significantly different from breast cancer patient without relapse (column 2 vs. 1, Table 2), and there was no significant difference observed that patients with primary breast tumors developing bone metastases had lower BMP7 mRNA expression levels (p = 0.13; column 3 vs. 1, Table 2) than patients without relapse. However, BMP7 mRNA expression levels in primary breast tumors developing bone metastases were significantly lower when compared to primary breast tumors developing visceral (lung and/or liver) metastases (p = 0.027; column 3 vs. 4, Table 2).

Table 2 **BMP7 mRNA expression levels in human primary breast carcinomas as detected by qPCR.** Median (range) of mRNA levels

1	2	3	4
Breast tumor without metastasis (n=35)	**Breast tumor with metastasis (n=32)**	**Breast tumor with bone metastasis (n=15)**	**Breast tumor with visceral metastasis (n=17)**
1.0 (0.03 - 85.92)	0.83 (0.01 - 11.43) #	0.48 (0.01 - 3.71)	1.40 (0.17 - 11.43) *

#, n.s. (column 1 vs. 2); *, p = 0.027 (column 3 vs. 4)

In patient matched normal ducts of the breast, apical BMP7 staining could be observed (Fig. 1, *upper panels*). Staining intensity of BMP7 protein in primary breast cancer specimens was in accordance with BMP7 mRNA levels (Fig. 1, middle panels). Adult kidney were used as positive (Fig. 1, *left bottom panel*) and negative (Fig. 1, *right bottom panel*) control.

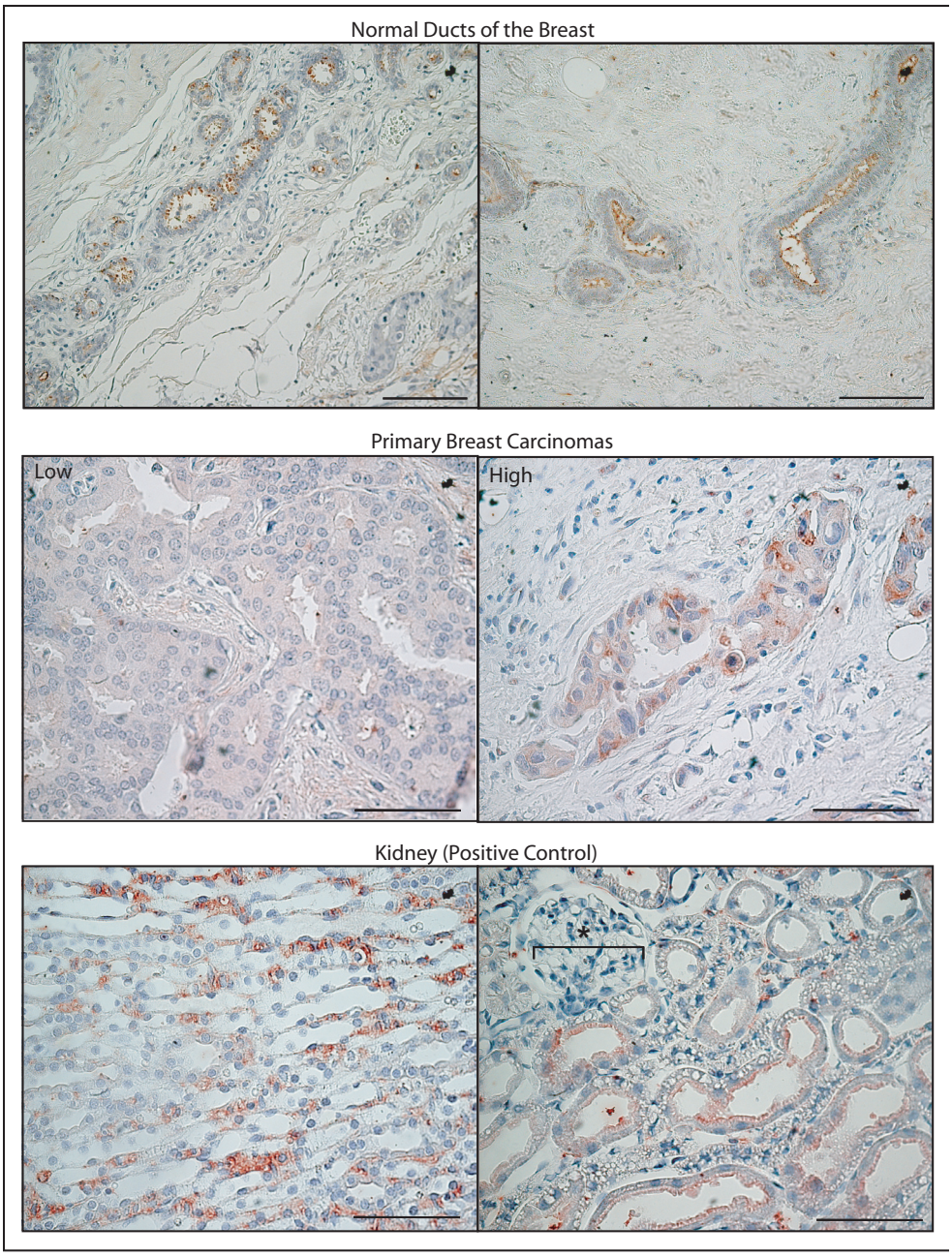

Figure 1 **BMP7 mRNA expression levels and BMP7 immunolocalization in human primary breast cancer.** BMP7 immunolocalization. Upper panels, normal ducts of the breast (Pronase (0.1% for 10 minutes at 37°C, Roche) was used as antigen retrieval step). Immunolocalization of BMP7 in primary breast tumors with low (left middle panel) and high (right middle panel) levels of BMP7 mRNA (0.09 and 16.11, respectively). Rat kidney: medullary rays were used as a positive (left bottom panel) and glomeruli (as indicated by *) as negative control (right bottom panel). Adjacent to the negative glomerulus, convulated tubuli stained positive for BMP7. Scale bars in upper left panel 80 µm, scale bars in other panels 50 µm.

Tumorigenicity and BMP7 Expression *In Vitro*

We investigated whether BMP7 expression in human breast cancer cell lines is associated with tumorigenic and metastatic potential. The six cell lines examined in this study have progressively greater tumorigenic and metastatic potential when arranged in the following order: MCF10A (normal breast epithelial cells), ZR-75-1, T47D, MCF10CA1a, MDA-231 and MDA-231-B/Luc+, where MCF10CA1a, MDA-231 and its derivate MDA-231-B/Luc+are highly tumorigenic and metastatic. This arrangement of the cell lines inversely correlates with the expression of BMP7 (Fig. 2*A*). E-cadherin/vimentin expression ratios, indicative of epithelial phenotype, are also inversely related to BMP7 expression (Fig. 2*A*), suggesting that acquisition of an invasive phenotype coincides with decreased BMP7 expression.

Immunohistochemical staining of MDA-231-B/Luc+cells for vimentin demonstrated a heterogeneous population with 22% vimentin positive (Vim+) cells (Fig. 2*B*). Stimulation with BMP7 significantly decreased the percentage of Vim+ cells (5%; $p = 0.038$ versus control), while stimulation with TGF-ß significantly increased the percentage of Vim+ cells (49%; $p = 0.002$ versus control). This increase in vimentin expression by TGF-ß could be blocked completely by co-incubation of BMP7 (12% Vim+ cells; $p < 0.001$ versus TGF-ß treated cells). These results were further confirmed by Western Blotting (Fig. 2*C*).

Next we tested whether BMP7 acts on MDA-231 cells to inhibit the acquisition of an invasive, mesenchymal phenotype by antagonizing Smad-dependent TGF-ß signaling.

The presence of functionally active TGF-ß receptor complexes, particularly ALK5, in MDA-231 cells was demonstrated by the dose-dependent activation of the CAGA-luciferase reporter, whose activity depends on activated Smad3/4 transcription factor complexes (Fig. 2*D*). Addition of BMP7 to TGF-ß-stimulated MDA-231 cells significantly inhibited the TGF-ß-driven CAGA-luciferase activity ($p < 0.001$).

Addition of BMP7, but not TGF-ß, stimulated BRE4-luciferase activity, indicating the presence of functioning, activated type I BMP-receptor complexes in MDA-231 cells (Fig. 2*D*). TGF-ß antagonizes BMP7 induced BRE-luciferase activity ($p < 0.001$).

It is important to note that BMP7 did not affect proliferation of MDA-231-B/Luc+cells *in vitro* using different cell culture conditions (1% FCS and 10% FCS; Suppl. Fig. 1).

BMP7 overexpression and Experimental Bone Metastasis

As detected with ELISA, overexpression of BMP7 in MDA-231 cells (MDA-231-BO2-Frt11(BMP7)/Luc+) resulted in substantial secretion of BMP7 protein in the medium, 6.55 ng BMP7 protein/ 1E6 cells/ day. In contrast, BMP7 protein was not detectable in the control cell line (MDA-231-BO2-Frt11(GFP)/Luc+), < 0.03 ng BMP7 protein/ 1E6 cells/ day.

Overexpression of BMP7 in MDA-231 cells (MDA-231-BO2-Frt11(BMP7)/Luc+) significantly inhibited both the intra-bone growth ($p = 0.034$), osteolytic area ($p = 0.007$), and extraosseous extension ($p = 0.042$) when compared to control (MDA-231-BO2-Frt11(GFP)/Luc+) (Fig. 3*A*). Moreover, in an experimental model of bone metastasis using tail inoculation of breast can-

Jeroen_Buijs_18.indd 158 26-11-2008 10:18:48

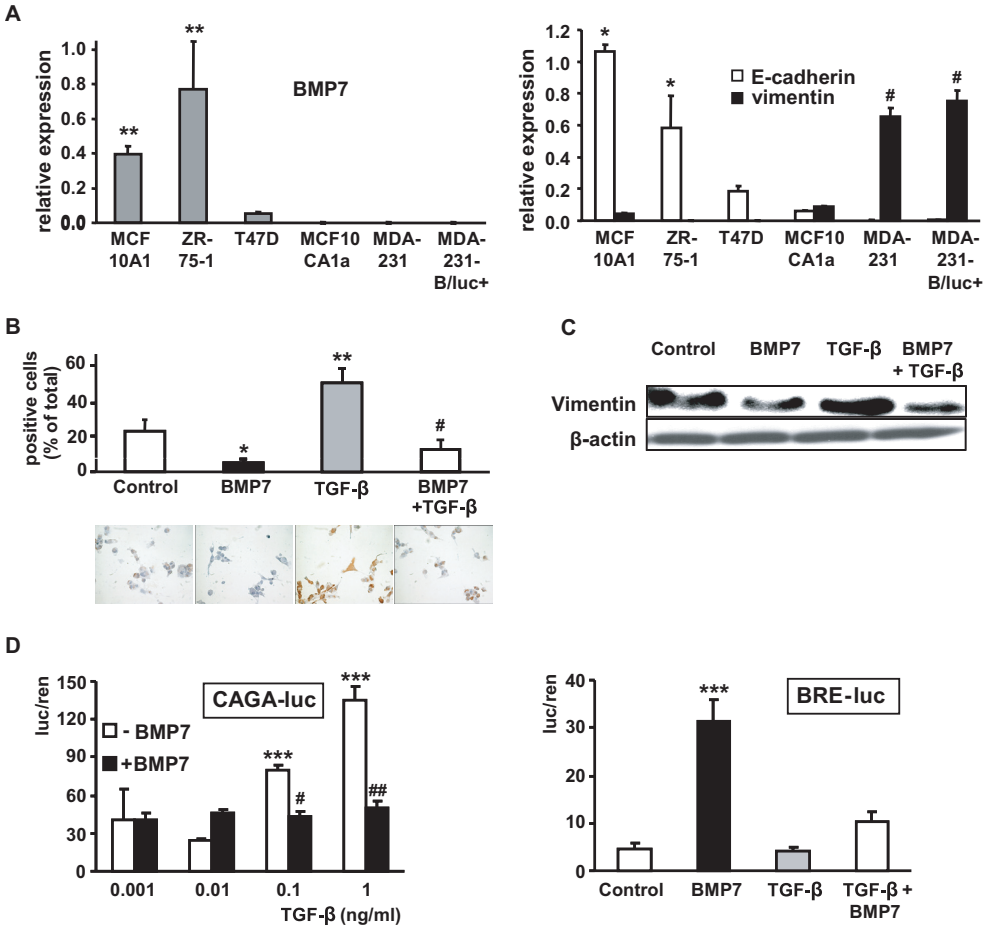

Figure 2 **E-cadherin and vimentin expression in breast cancer cell lines.** *A*, BMP7, E-cadherin and vimentin mRNA expression in human breast cancer cell lines with increasing tumorigenic and metastatic potential (left to right) as detected by qPCR. E-cadherin expression in MDA-231 and MDA-231-B/Luc+cells, vimentin expression in T47D and ZR-75-1 cells, and BMP7 expression in MCF10CA1a, MDA-231 and MDA-231-B/Luc+cells were just above detection level. ** $p < 0.01$ versus BMP7 expression in T47D, MCF10CA1a, MDA-231 and MDA-231-B/Luc+cell lines. * $p < 0.05$ versus E-cadherin expression in all other cell lines; # $p < 0.01$ MDA-231 cell lines versus the other cell lines; Expression values are normalised to ß-actin (BMP7/10^3 ß-actin). *B*, vimentin immunolocalization of MDA-231-B/Luc+cells after incubation with 1 µg/ml BMP7 in the presence or absence of 10 ng/ml TGF-ß. Representative examples are shown. *C*, expression of vimentin by MDA-231-B/Luc+cells after incubation with 1 µg/ml BMP7 in the presence or absence of 10 ng/ml TGF-ß as detected by Western Blotting. * $p < 0.05$ and ** $p < 0.01$ versus control, # $p < 0.001$ versus TGF-ß, n.s. = not significant. *D*, MDA-231 cells were transiently transfected with the CAGA-luciferase reporter (left panel) and the BRE-luciferase reporter (right panel) constructs. The presence of functionally active TGF-ß receptor complexes was demonstrated with stimulation of the CAGA-luc reporter by TGF-ß (*** $p < 0.001$ vs. all other conditions). Addition of BMP7 (500 ng/ml) to TGF-ß-stimulated MDA-231 cells significantly (# $p < 0.01$, ## $p < 0.001$) inhibited TGF-ß-driven CAGA-luc activity. Values are normalized to renilla (CAGA-luc/10^5 pRL-CAGGS). Value vehicle treated is 16.1 ± 1.1. BMP7 (200 ng/ml), but not TGF-ß (5 ng/ml), induces BRE-luc actvity, indicating the presence and functionality of BMP-receptors in MDA-231 cells. *** $p < 0.001$ vs. all other conditions; values are normalized to renilla (BRE4-luc/10^{-1} pRL-CMV).

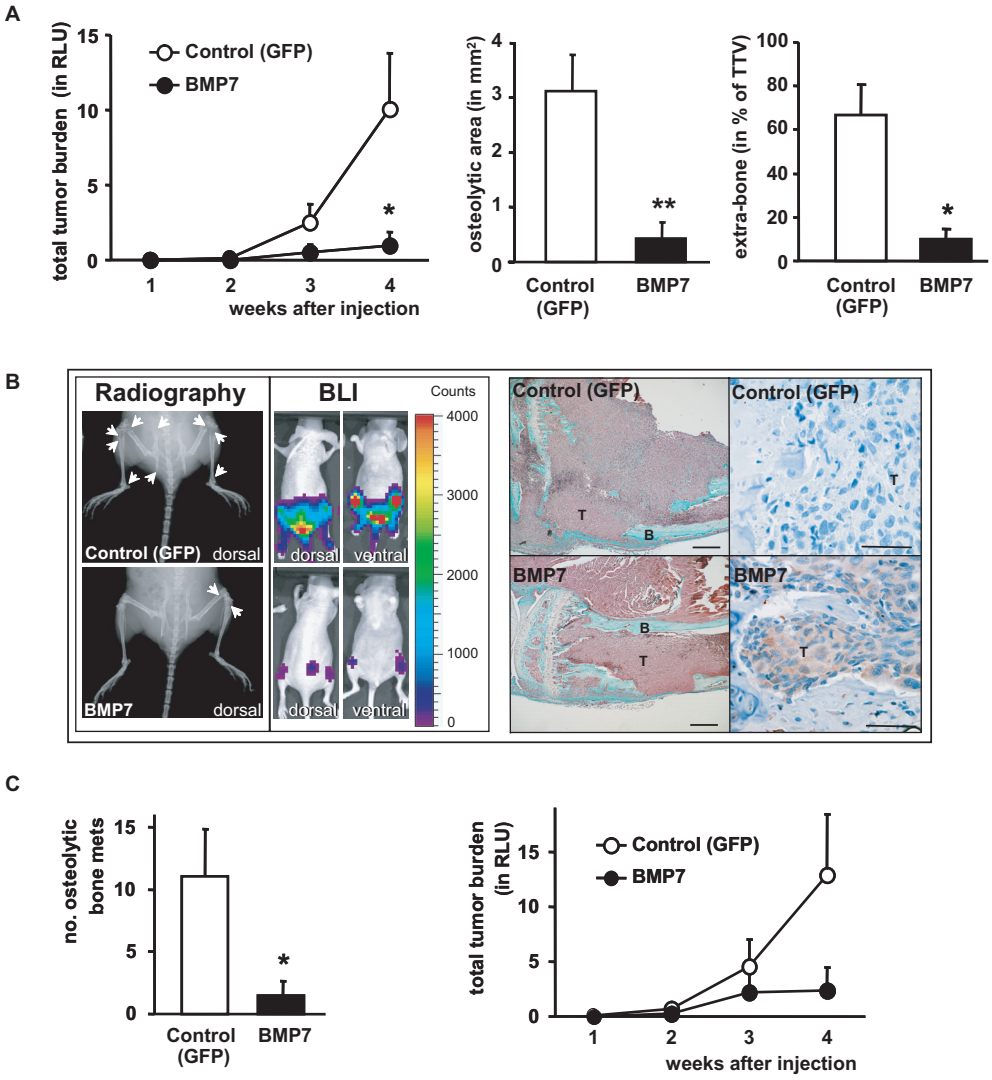

Figure 3 **Bone metastatic and intra-bone growth of MDA-231 cells expressing BMP7.** *A*, in an experimental model of intraosseous implantation of breast cancer cells, stable BMP7 overexpression inhibited osteolysis as detected by radiographical analysis, total tumor burden as measured by BLI (RLU: 10^6 photons/sec), and extraosseous tumor volume determined as the percentage of total tumor volume (TTV) that has started to grow extramedullary. *B*, experimental model of bone metastasis formation after tail inoculation of breast cancer cells, from which representative examples of radiography, BLI, Goldner staining (scale bars 200 µm) and BMP7 immunolocalization (scale bars 50 µm) (from left to right) are shown. Arrows indicate osteolytic lesions; T = tumor; B = bone. *C*, in the experimental bone metastasis model stable BMP7 overexpression inhibited de novo formation of osteolytic bone metatases (per mouse) as detected by radiographical analysis, and total tumor burden (per mouse) as measured by BLI (RLU: 10^6 photons/sec). * $p < 0.05$ and ** $p < 0.01$ versus control (GFP).

Jeroen_Buijs_18.indd 160 26-11-2008 10:18:50

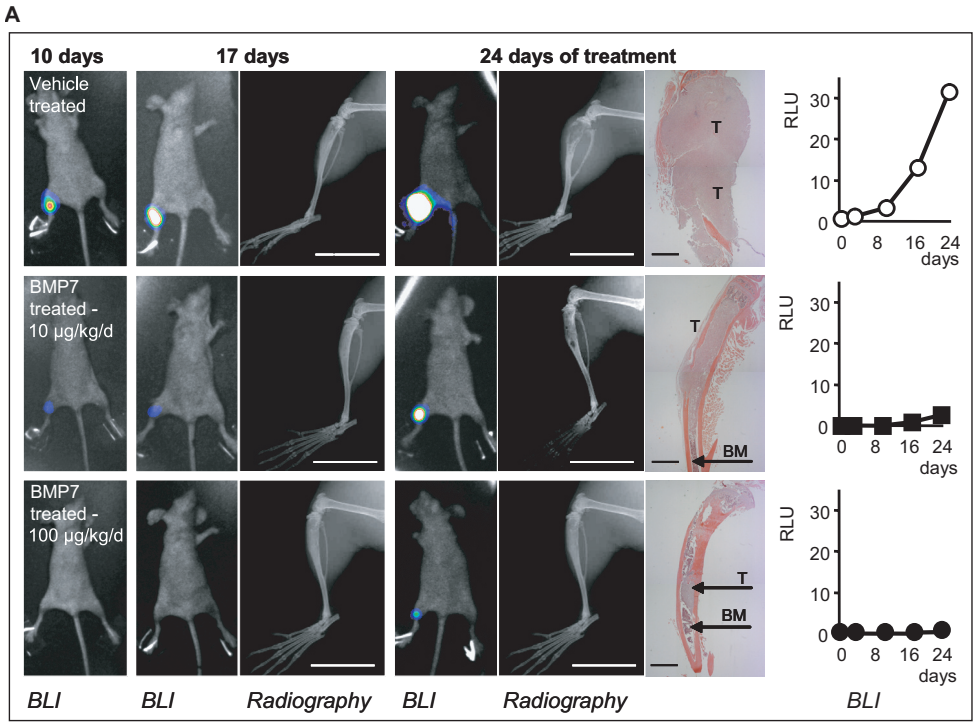

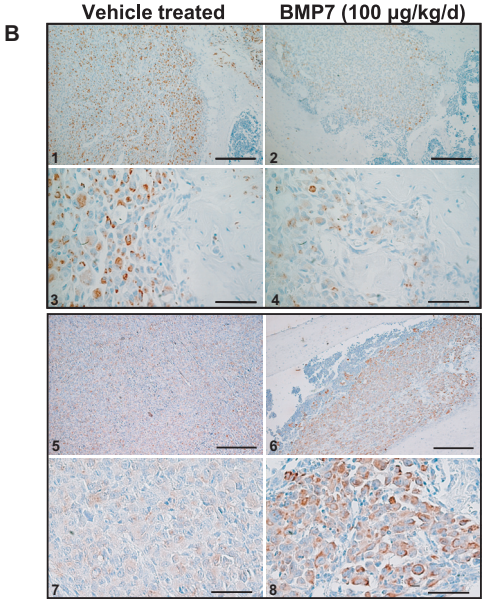

Figure 4 **Representative examples of BMP7 treatment and intra-bone growth of MDA-231-B/Luc+cells.** *A*, intra-bone growth of tumor cells and tumor-induced osteolysis (BLI, radiography and histology). In the graphs, BLI is quantified in relative light units (RLU) (10^5 photons/sec). Scale bars in X-rays: 10 mm; scale bars in histological sections: 1 mm. T = tumor, BM = bone marrow. *B*, expression of vimentin (1-4) and pan-cytokeratin (5-8) in MDA-231-B/Luc+cells growing in bone marrow after vehicle (1,2,5,6) and 100 µg/kg/d BMP7 (3,4,7,8) treatment. Scale bars in 1,2,5,6: 150 µm, scale bars in 3,4,7,8: 40 µm.

cer cells, overexpression of BMP7 in MDA-231 cells (MDA-231-BO2-Frt11(BMP7)/Luc+) was shown to significantly inhibit the number of osteolytic lesions (p = 0.025; Fig. 3*B,C*). In line with the ELISA data described above, overexpression of BMP7 protein in tumor cells was also detected in histological sections in bone metastasis from MDA-231 cells overexpressing BMP7 (MDA-231-BO2-Frt11(BMP7)/Luc+), but not in the GFP-control cell line (Fig. 3*B*). In addition, a trend was noticed for less overall total tumor burden as detected by BLI (p = 0.10; Fig. 3C). Furthermore, it is important to note that BMP7 overexpression did not affect the growth rate *in vitro* (doubling time MDA-231-BO2-Frt11(BMP7)/Luc+ cells: 21.0hr, vs. MDA-231-BO2-Frt11(GFP)/Luc+ cells: 20.9hr).

Experimental BMP7 Treatment

Fig. 4 depicts a representative example from each experimental group (vehicle treatment, 10 µg/kg/day BMP7 or 100 µg/kg/day BMP7) showing different *in vivo* imaging methods (BLI, radiography, histology) that have been used to detect MDA-231-B/Luc+breast cancer cells growing in bone. Breast cancer growth in bone and the formation of osteolytic lesions was strongly inhibited, particularly in the high dose BMP7 group (100 µg/kg/day BMP7) (Fig. 4*A*). Markedly, mice receiving 100 µg/kg/day BMP7 had tumors that express higher levels of cytokeratins and lower levels of vimentin when compared to vehicle treated mice (Fig. 4*B*). The number of strong cytokeratin-positive cells was increased by 25% upon BMP7 treatment. This indicates that BMP7 treatment provokes a more epithelial-like phenotype.

In the vehicle treated group, the tumor burden increased strongly over time (Fig. 5*A*). Tumor growth in mice receiving 10 µg/kg/day BMP7 was not significantly different from vehicle treated animals, whereas 100 µg/kg/day BMP7 strongly and significantly inhibited tumor progression (p = 0.038; Fig. 5*A*). This result was confirmed by histomorphometric analysis of total tumor burden (p = 0.049; Fig. 6*A*). In addition, no significant difference was observed in extraosseous tumor volume upon BMP7 treatment (100 µg/kg/day) (p = 0.15; Fig. 5*A*). Furthermore, radiographic analysis of the tibiae revealed that mice receiving 100 µg/kg/day BMP7 show significantly smaller bone lesions (p = 0.046), although number of osteoclasts per mm bone cortex appeared not to be different at the end of the experiment (p = 0.528; Fig. 5*B*). Systemic administration of BMP7 for the duration of the experiment can directly act on MDA-231-B/Luc+bone metastatic cells as visualized by significantly enhanced nuclear staining for phospho-Smad1 when compared to vehicle treated animals (p = 0.0097; Fig. 5*C*).

Next, we studied the effects of BMP7 treatment on the growth of MDA-231-B/Luc+cells that were orthotopically implanted into the mammary fat pads of nude mice (Fig. 6*A-C*). Fig. 6*B* depicts a representative example from both experimental groups (vehicle and 100 µg/kg/day BMP7) as detected by BLI and histomorphometry. Tumor growth of the orthotopically implanted breast cancer cells in mice receiving 100 µg/kg/day BMP7 was significantly inhibited versus vehicle treated animals (p = 0.049; Fig. 6*C*).

Jeroen_Buijs_18.indd 162 26-11-2008 10:18:55

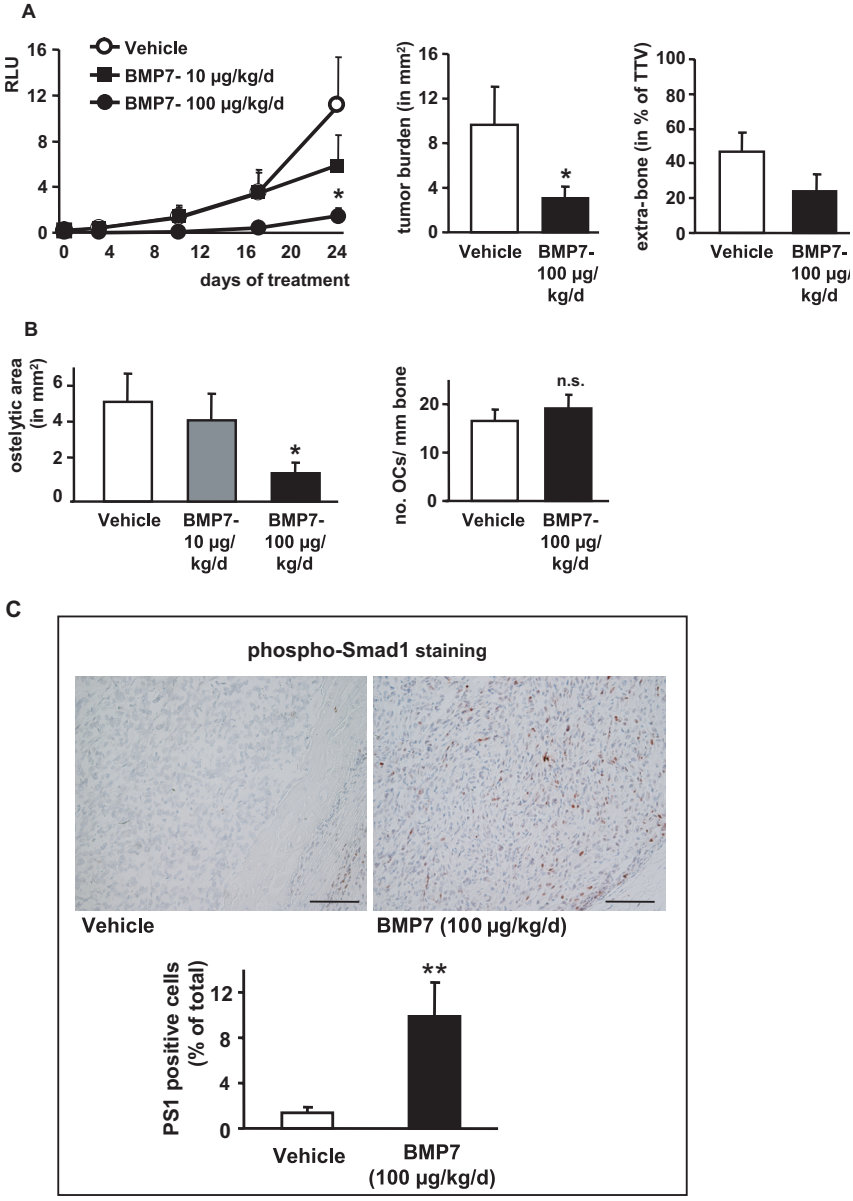

Figure 5 **Effects of BMP7 treatment on intra-bone tumor growth, osteolysis and BMP7 signalling of MDA-231-B/Luc+cells.** *A*, tumor burden as measured by BLI (RLU: 10^5 photons/sec) and histomorphometric analysis, and the extraosseous tumor volume determined as the percentage of total tumor volume (TTV) that has started to grow extramedullary. *B*, radiographical analysis of tumor-induced osteolysis in tibia at the end of the experimental treatment (24 days)(left), and number of osteoclasts (OCs) per mm bone cortex (right). *C*, phospho-Smad1 positive cells in the tumor at the end of the experimental treatment. The animals were either vehicle or BMP7 treated 6 hours prior explantation and fixation of the tibiae. Scale bars: 80 µm, * $p < 0.05$ and ** $p < 0.01$ versus vehicle.

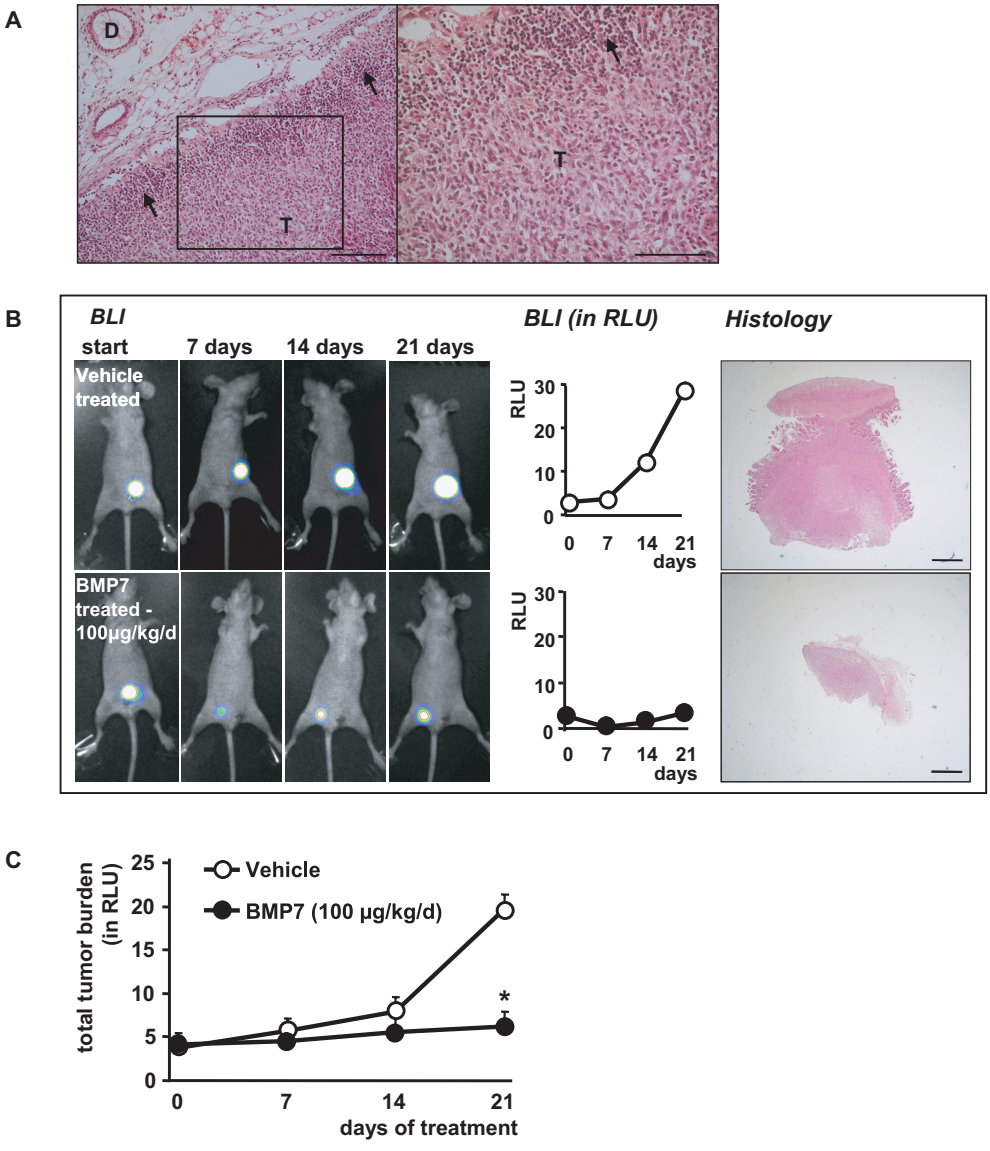

Figure 6 **BMP7 treatment and growth of MDA-231-B/Luc+cells in mammary fat pads.** *A*, orthotopically implanted MDA-231-B/Luc+cells have formed a tumor located in the mammary fat pad as shown by Hematoxylin & Eosin staining. The figure on the right is a magnification from the box in the left figure. Lymphocytic infiltrates (indicated by arrows) in tumors could be observed. Scale bar: 80 µm (left figure) and 50 µm (right figure); D = mammary duct, T = tumor. *B*, representative examples for BLI and HE staining are shown. BLI is quantified in RLU (10^5 photons/sec), scale bars: 500 µm. (C) Tumor burden is measured by BLI (RLU: 10^5 photons/sec). * $p < 0.05$ versus vehicle.

Discussion

While BMP7 has been proposed as a marker of differentiation in normal and breast cancer cells [43], the role of BMP7 in breast cancer progression has remained largely elusive [43-45]. In this report novel evidence is provided for a role of BMP7 in breast cancer development and bone metastases. We describe here that BMP7 expression in patients with primary breast tumors exclusively developing bone metastases is significantly lower than in primary breast tumors developing exclusively visceral (lung and/or liver) metastases. These clinical findings suggest that decreased BMP7 expression may confer a bone metastatic potential to human breast cancer cells. Normal ducts of the breast display strong apical BMP7 protein expression. BMP7 protein expression in patient-matched lymph node metastases was low or absent, and as a consequence, generally lower than in normal ducts and primary breast carcinomas (J.T.Buijs, unpublished observations). Strikingly, BMP7 appears to be expressed predominantly in tumor cells in the solid tumor area rather than in migratory tumor cells outside this area [43], indicating that low BMP7 expression may support the acquisition of a more migratory invasive phenotype.

It has been well-established that the process of epithelial-to-mesenchymal transition (EMT) provides mechanisms for breast epithelial cells to overcome physical constraints imposed on them by intercellular junctions and adopt a motile phenotype [3,8,46]. It is becoming increasingly clear that this local invasive process, representing initial stages of the metastatic cascade during carcinogenesis, is adapted from the remarkable epithelial plasticity (EMT) that occurs during embryonic development and postnatal tissue maintenance [2,47]. In many cancers, TGF-ß is a pro-tumorigenic factor that stimulates 'oncogenic' EMT [8,17,18]. In contrast, BMP7 is a strong inducer of the reverse process (MET) during embryonic development [9-11,14] and in renal fibroblasts [22]. Moreover, BMP7 can inhibit TGF-ß-induced fibrosis [25], and counteracts TGF-ß-induced EMT in normal renal epithelial cells [24].

We show here that BMP7 mRNA expression is inversely related to tumorigenicity and invasive behavior of human breast cancer cell lines. Functional studies reveal that BMP7 overexpression by breast cancer cells inhibits *de novo* formation of osteolytic bone metastases, and hence, the metastatic capability of breast cancer cells in our *in vivo* bone metastasis model. Furthermore, BMP7 overexpression significantly inhibited tumor growth in bone. In keeping with these functional data, daily systemic administration of BMP7 strongly and significantly impairs both the orthotopic and intraosseous growth of human MDA-231-B/Luc+breast cancer cells in nude mice.

Our *in vitro* studies reveal for the first time that BMP7 is a potent inhibitor of TGF-ß-induced EMT in MDA-MB-231 cancer cells. In these cells, BMP7 is able of counteracting Smad-dependent TGF-ß signaling. These actions of BMP7 may be of critical importance and could explain the observed beneficial effects of experimental BMP7 treatment on orthotopic growth and skeletal metastasis. In this context it is important to note that inactive TGF-ß is

concentrated and stored in high amounts in extracellular bone matrix, and can be released and activated by osteoclastic resorption. Activated bone matrix-derived TGF-ß may act as a paracrine growth factor for neighboring osteolytic cancer cells that may have colonized the bone marrow [21,40,48]. Our *in vivo* data further support this notion since BMP7 antagonizes TGF-ß signaling routes in human breast cancer cells that are metastatic to the skeleton. We hypothesize that the activation process of micrometastases in bone marrow may bear similarities to EMT that occurs at the primary site in various epithelial cancers and during ontogeny [49].

BMP7, however, could not restore E-cadherin expression in MDA-231-B/Luc+cells. Recent observations support the notion that hypermethylation of the E-cadherin promoter in MDA-MB-231 cells is involved in E-cadherin expression [6]. Apparently, BMP7 can not overcome this epigenetic effect.

It is important to note that comparable data have been obtained in clinical samples of prostate cancer [50] and uveal melanoma [51]. Moreover, in human prostate cancer we recently observed that BMP7 antagonizes TGF-ß induced EMT concomitant with an induction of E-cadherin expression [50].

Collectively, our data suggest that BMP7 regulates epithelial homeostasis in the human mammary gland by preserving the epithelial phenotype. Decreased BMP7 expression during breast cancer progression may, therefore, contribute to the acquisition of a bone metastatic phenotype. Furthermore, exogenous BMP7 can still inhibit breast cancer growth at the primary site and in bone marrow. Therefore, BMP7 may represent a novel therapeutic molecule for repression of local and bone metastatic growth of human breast cancer.

Acknowledgments

This work was supported by grants from Dutch Cancer Society (KWF project RUL-2001-2485) and European Sixth Framework Programme, MetaBre, FP6-503049).

References

1. Sporn MB. The war on cancer. *Lancet* 1996; 347:1377-81.
2. Thiery JP. Epithelial-mesenchymal transitions in development and pathologies. *Curr Opin Cell Biol* 2003; 15:740-6.
3. Hay ED. An overview of epithelio-mesenchymal transformation. *Acta Anat (Basel)* 1995; 154:8-20.
4. Grunert S, Jechlinger M, Beug H. Diverse cellular and molecular mechanisms contribute to epithelial plasticity and metastasis. *Nat Rev Mol Cell Biol* 2003; 4:657-65.
5. Dandachi N, Hauser-Kronberger C, More E, Wiesener B, Hacker GW, Dietze O *et al*. Co-expression of tenascin-C and vimentin in human breast cancer cells indicates phenotypic transdifferentiation during tumour progression: correlation with histopathological parameters, hormone receptors, and oncoproteins. *J Pathol* 2001; 193:181-9.

6. Lombaerts M, van Wezel T, Philippo K, Dierssen JW, Zimmerman RM, Oosting J *et al*. E-cadherin transcriptional downregulation by promoter methylation but not mutation is related to epithelial-to-mesenchymal transition in breast cancer cell lines. *Br J Cancer* 2006; 94:661-71.
7. Siitonen SM, Kononen JT, Helin HJ, Rantala IS, Holli KA, Isola JJ. Reduced E-cadherin expression is associated with invasiveness and unfavorable prognosis in breast cancer. *Am J Clin Pathol* 1996; 105:394-402.
8. Thiery JP. Epithelial-mesenchymal transitions in tumour progression. *Nat Rev Cancer* 2002; 2:442-54.
9. Dudley AT, Lyons KM, Robertson EJ. A requirement for bone morphogenetic protein-7 during development of the mammalian kidney and eye. *Genes Dev* 1995; 9:2795-807.
10. Luo G, Hofmann C, Bronckers AL, Sohocki M, Bradley A, Karsenty G. BMP-7 is an inducer of nephrogenesis, and is also required for eye development and skeletal patterning. *Genes Dev* 1995; 9:2808-20.
11. Vukicevic S, Kopp JB, Luyten FP, Sampath TK. Induction of nephrogenic mesenchyme by osteogenic protein 1 (bone morphogenetic protein 7). *Proc Natl Acad Sci U S A* 1996; 93:9021-6.
12. Ducy P, Karsenty G. The family of bone morphogenetic proteins. *Kidney Int* 2000; 57:2207-14.
13. Itoh S, Itoh F, Goumans MJ, Ten Dijke P. Signaling of transforming growth factor-beta family members through Smad proteins. *Eur J Biochem* 2000; 267:6954-67.
14. Simic P, Vukicevic S. Bone morphogenetic proteins in development and homeostasis of kidney. *Cytokine Growth Factor Rev* 2005; 16:299-308.
15. Oft M, Peli J, Rudaz C, Schwarz H, Beug H, Reichmann E. TGF-beta1 and Ha-Ras collaborate in modulating the phenotypic plasticity and invasiveness of epithelial tumor cells. *Genes Dev* 1996; 10:2462-77.
16. Roberts AB, Wakefield LM. The two faces of transforming growth factor beta in carcinogenesis. *Proc Natl Acad Sci U S A* 2003; 100:8621-3.
17. Peinado H, Quintanilla M, Cano A. Transforming growth factor beta-1 induces snail transcription factor in epithelial cell lines: mechanisms for epithelial mesenchymal transitions. *J Biol Chem* 2003; 278:21113-23.
18. Piek E, Moustakas A, Kurisaki A, Heldin CH, Ten Dijke P. TGF-(beta) type I receptor/ALK-5 and Smad proteins mediate epithelial to mesenchymal transdifferentiation in NMuMG breast epithelial cells. *J Cell Sci* 1999; 112:4557-68.
19. Yingling JM, Blanchard KL, Sawyer JS. Development of TGF-beta signalling inhibitors for cancer therapy. *Nat Rev Drug Discov* 2004; 3:1011-22.
20. Deckers M, van Dinther M, Buijs J, Que I, Lowik C, van der Pluijm G *et al*. The tumor suppressor Smad4 is required for transforming growth factor beta-induced epithelial to mesenchymal transition and bone metastasis of breast cancer cells. *Cancer Res* 2006; 66:2202-9.
21. Yin JJ, Selander K, Chirgwin JM, Dallas M, Grubbs BG, Wieser R *et al*. TGF-beta signaling blockade inhibits PTHrP secretion by breast cancer cells and bone metastases development. *J Clin Invest* 1999; 103:197-206.
22. Zeisberg M, Shah AA, Kalluri R. Bone morphogenic protein-7 induces mesenchymal to epithelial transition in adult renal fibroblasts and facilitates regeneration of injured kidney. *J Biol Chem* 2005; 280:8094-100.
23. Hruska KA, Guo G, Wozniak M, Martin D, Miller S, Liapis H *et al*. Osteogenic protein-1 prevents renal fibrogenesis associated with ureteral obstruction. *Am J Physiol Renal Physiol* 2000; 279:F130-F143.
24. Zeisberg M, Hanai J, Sugimoto H, Mammoto T, Charytan D, Strutz F *et al*. BMP-7 counteracts TGF-beta1-induced epithelial-to-mesenchymal transition and reverses chronic renal injury. *Nat Med* 2003; 9:964-8.
25. Wang S, Hirschberg R. BMP7 antagonizes TGF-beta -dependent fibrogenesis in mesangial cells. *Am J Physiol Renal Physiol* 2003; 284:F1006-F1013.
26. Gould SE, Day M, Jones SS, Dorai H. BMP-7 regulates chemokine, cytokine, and hemodynamic gene expression in proximal tubule cells. *Kidney Int* 2002; 61:51-60.

27. Li T, Surendran K, Zawaideh MA, Mathew S, Hruska KA. Bone morphogenetic protein 7: a novel treatment for chronic renal and bone disease. *Curr Opin Nephrol Hypertens* 2004; 13:417-22.
28. Wetterwald A, van der Pluijm G, Que I, Sijmons B, Buijs J, Karperien M *et al*. Optical imaging of cancer metastasis to bone marrow: a mouse model of minimal residual disease. *Am J Pathol* 2002; 160:1143-53.
29. Soule HD, Maloney TM, Wolman SR, Peterson WD, Jr., Brenz R, McGrath CM *et al*. Isolation and characterization of a spontaneously immortalized human breast epithelial cell line, MCF-10. *Cancer Res* 1990; 50:6075-86.
30. Santner SJ, Dawson PJ, Tait L, Soule HD, Eliason J, Mohamed AN *et al*. Malignant MCF10CA1 cell lines derived from premalignant human breast epithelial MCF10AT cells. *Breast Cancer Res Treat* 2001; 65:101-10.
31. Peyruchaud O, Winding B, Pecheur I, Serre CM, Delmas P, Clezardin P. Early detection of bone metastases in a murine model using fluorescent human breast cancer cells: application to the use of the bisphosphonate zoledronic acid in the treatment of osteolytic lesions. *J Bone Miner Res* 2001; 16:2027-34.
32. Notting IC, Buijs JT, Que I, Mintardjo RE, van der HG, Karperien M *et al*. Whole-body bioluminescent imaging of human uveal melanoma in a new mouse model of local tumor growth and metastasis. *Invest Ophthalmol Vis Sci* 2005; 46:1581-7.
33. Bieche I, Parfait B, Le Doussal V, Olivi M, Rio MC, Lidereau R *et al*. Identification of CGA as a novel estrogen receptor-responsive gene in breast cancer: an outstanding candidate marker to predict the response to endocrine therapy. *Cancer Res* 2001; 61:1652-8.
34. Livak KJ, Schmittgen TD. Analysis of relative gene expression data using real-time quantitative PCR and the 2(-Delta Delta C(T)) Method. *Methods* 2001; 25:402-8.
35. Jones WK, Richmond EA, White K, Sasak H, Kusmik W, Smart J *et al*. Osteogenic protein-1 (OP-1) expression and processing in Chinese hamster ovary cells: isolation of a soluble complex containing the mature and pro-domains of OP-1. *Growth Factors* 1994; 11:215-25.
36. Deckers MM, Karperien M, van der Bent C, Yamashita T, Papapoulos SE, Lowik CW. Expression of vascular endothelial growth factors and their receptors during osteoblast differentiation. *Endocrinology* 2000; 141:1667-74.
37. Dennler S, Itoh S, Vivien D, Ten Dijke P, Huet S, Gauthier JM. Direct binding of Smad3 and Smad4 to critical TGF beta-inducible elements in the promoter of human plasminogen activator inhibitor-type 1 gene. *EMBO J* 1998; 17:3091-100.
38. Korchynskyi O, Ten Dijke P. Identification and functional characterization of distinct critically important bone morphogenetic protein-specific response elements in the Id1 promoter. *J Biol Chem* 2002; 277:4883-91.
39. van der Pluijm G, Que I, Sijmons B, Buijs JT, Lowik CW, Wetterwald A *et al*. Interference with the microenvironmental support impairs the de novo formation of bone metastases in vivo. *Cancer Res* 2005; 65:7682-90.
40. van der Pluijm G, Sijmons B, Vloedgraven H, Deckers M, Papapoulos S, Lowik C. Monitoring metastatic behavior of human tumor cells in mice with species-specific polymerase chain reaction: elevated expression of angiogenesis and bone resorption stimulators by breast cancer in bone metastases. *J Bone Miner Res* 2001; 16:1077-91.
41. Chubinskaya S, Merrihew C, Cs-Szabo G, Mollenhauer J, McCartney J, Rueger DC *et al*. Human articular chondrocytes express osteogenic protein-1. *J Histochem Cytochem* 2000; 48:239-50.
42. Persson U, Izumi H, Souchelnytskyi S, Itoh S, Grimsby S, Engstrom U *et al*. The L45 loop in type I receptors for TGF-beta family members is a critical determinant in specifying Smad isoform activation. *FEBS Lett* 1998; 434:83-7.
43. Schwalbe M, Sanger J, Eggers R, Naumann A, Schmidt A, Hoffken K *et al*. Differential expression and regulation of bone morphogenetic protein 7 in breast cancer. *Int J Oncol* 2003; 23:89-95.
44. Alarmo EL, Rauta J, Kauraniemi P, Karhu R, Kuukasjarvi T, Kallioniemi A. Bone morphogenetic protein 7 is widely overexpressed in primary breast cancer. *Genes Chromosomes Cancer* 2006; 45:411-9.

Jeroen_Buijs_18.indd 168 26-11-2008 10:18:58

45. Bobinac D, Maric I, Zoricic S, Spanjol J, Dordevic G, Mustac E *et al*. Expression of bone morphogenetic proteins in human metastatic prostate and breast cancer. *Croat Med J* 2005; 46:389-96.
46. Vincent-Salomon A, Thiery JP. Host microenvironment in breast cancer development: epithelial-mesenchymal transition in breast cancer development. *Breast Cancer Res* 2003; 5:101-6.
47. Savagner P, Kusewitt DF, Carver EA, Magnino F, Choi C, Gridley T *et al*. Developmental transcription factor slug is required for effective re-epithelialization by adult keratinocytes. *J Cell Physiol* 2005; 202:858-66.
48. Mundy GR. Metastasis to bone: causes, consequences and therapeutic opportunities. *Nat Rev Cancer* 2002; 2:584-93.
49. Bryden AA, Freemont AJ, Clarke NW, George NJ. Paradoxical expression of E-cadherin in prostatic bone metastases. *BJU Int* 1999; 84:1032-4.
50. Buijs JT, Rentsch CA, van der Horst G, van Overveld PGM, Wetterwald A, Schwaninger R *et al*. BMP7, a Putative Regulator of Epithelial Homeostasis in the Human Prostate, is a Potent Inhibitor of Prostate Cancer Bone Metastasis In Vivo. *Am J Pathol* 2007; 171:1047-57.
51. Notting I, Buijs J, Mintardjo R, van der Horst G, Vukicevic S, Lowik C *et al*. Bone morphogenetic protein 7 inhibits tumor growth of human uveal melanoma in vivo. *Invest Ophthalmol Vis Sci* 2007; 48:4882-9.

Jeroen_Buijs_18.indd 170 26-11-2008 10:18:58

Chapter 7

BMP7, a Putative Regulator of Epithelial Homeostasis in the Human Prostate, is a Potent Inhibitor of Prostate Cancer Bone Metastasis *In Vivo*

Am J Pathol 2007; 171:1047-57

Jeroen T Buijs*[1,2], Cyrill A Rentsch*[4], Geertje van der Horst[2], Petra GM van Overveld[2], Antoinette Wetterwald[4], Ruth Schwaninger[4], Niek V Henriquez[1], Peter ten Dijke[3], Fran Borovecki[5], Regula Markwalder[4], George N Thalmann[4], Socrates E Papapoulos[1], Rob CM Pelger[4], Slobodan Vukicevic[5], Marco G Cecchini[4], Clemens WGM Löwik[2], Gabri van der Pluijm[1,2]

* both authors contributed equally

Departments of Endocrinology[1], Urology[2], Molecular Cell Biology[3], Leiden University Medical Center, Leiden, The Netherlands; [4]Department of Clinical Research and Urology, University of Bern, Bern, Switzerland; [5]Dept. of Anatomy, School of Medicine, Zagreb, Croatia

Jeroen_Buijs_18.indd 171 26-11-2008 10:18:58

Abstract

Bone Morphogenic Protein 7 (BMP7) counteracts physiologic epithelial-to-mesenchymal transition (EMT), a process that is indicative of epithelial plasticity. Since EMT is involved in cancer we investigated whether BMP7 plays a role in prostate cancer growth and metastasis.

BMP7 expression in laser micro-dissected primary human prostate cancer tissue was strongly down-regulated compared to normal prostate luminal epithelium. Furthermore, BMP7 expression in prostate cancer cell lines was inversely related to their tumorigenic and metastatic potential *in vivo* and significantly correlated to E-cadherin/vimentin ratios. Exogenous addition of BMP7 to human prostate cancer cells dose-dependently inhibited TGF-ß induced activation of nuclear Smad-2/3 via ALK5 and induced E-cadherin expression. Moreover, BMP7-induced activation of nuclear Smad1/4/8 signaling transduced via BMPR-1A receptors was synergistally stimulated in the presence of TGF-ß, a growth factor that is enriched in the bone microenvironment.

Daily BMP7 administration to nude mice inhibited the growth of cancer cells in bone. In contrast, no significant growth inhibitory effect of BMP7 was observed in intra-prostatic xenografts. Collectively, our observations suggest that BMP7 controls and preserves the epithelial phenotype in the human prostate, underscoring a decisive role of the tumor microenvironment in mediating the therapeutic response of BMP7. BMP7 can still counteract the EMT process in the metastatic tumor, positioning BMP7 as a novel therapeutic molecule for treatment of metastatic bone disease.

Jeroen_Buijs_18.indd 172 26-11-2008 10:18:58

Introduction

The phenotypic changes of increased motility and invasiveness of carcinoma cells are reminiscent of the epithelial-to-mesenchymal transition (EMT) that occurs during embryonic development and morphogenesis [1-3].

During EMT epithelial cell layers lose polarity and cell-cell contact, undergo a dramatic remodeling of the cytoskeleton, express mesenchymal components and manifest a migratory phenotype by resolving cell-matrix contacts and digesting adjacent basal lamina [4,5]. Whereas in the developing embryo EMT is a prerequisite for the formation of various tissues and organs, EMT in postnatal life is required for repair and remodeling of numerous tissues or organs [1,6].

Plasticity resulting from cells shifting between epithelial and mesenchymal phenotypes is discernible either by EMT or the reverse process of mesenchymal-to-epithelial transition (MET) [2]. Both processes have emerged as a fundamental principle for reprogramming of gene transcription and as a major determinant of stem cell fate in development and in adult tissue homeostasis. The process of EMT is currently considered a potential mechanism of the disease progression in malignant and fibrotic disorders [1].

An example of the latter is the persistence of a pathogenic insult of the kidney that causes disruption of the tubular basement membrane and eventually may lead to renal fibrosis due to transition of tubular epithelial cells into a migratory, mesenchymal phenotype (EMT-derived fibroblasts in the interstitium) [6].

In epithelial cells TGF-ß has been identified as one of the main inducers of EMT during development and in fibrotic disorders [5-10], while another member of the TGF-ß superfamily, bone morphogenetic protein 7 (BMP7) alias osteogenic protein-1 (OP-1), is involved in the maintenance of the epithelial phenotype by induction of MET [11-14]. Zeisberg and co workers demonstrated that BMP7 was capable of counteracting TGF-ß-induced EMT and could reverse chronic renal injury [13,14].

Prostate cancer is the second most frequently diagnosed cancer and the second leading cause of cancer death in the Western male population. Evidence is mounting that during carcinogenesis developing prostate cancer cells acquire mesenchymal (and even osteoblastic) characteristics and migratory features concomitant with a loss of epithelial characteristics like E-cadherin expression [15,16]. In cancer progression, "oncogenic" EMT refers to clusters of malignant cells that loose epithelial characteristics and acquire self-sustained migratory and highly invasive phenotypes [5]. We hypothesized that the Gleason histological grading of prostate cancer parallels EMT starting from "well-differentiated" cells with well-defined boundaries that still resemble healthy prostate epithelium (Gleason patterns 1 and 2), via infiltrative cancer cells with less-defined boundaries with extensions into adjacent non-neoplastic prostate tissue (Gleason pattern 3), towards "poorly-differentiated" highly migratory prostate cancer cells that have lost many epithelial characteristics and have acquired an invasive, metastatic and mesenchymal phenotype (Gleason patterns 4 and 5).

Jeroen_Buijs_18.indd 173 26-11-2008 10:18:58

Several defects in the canonical TGF-ß signaling pathway have been reported in prostate cancer [17,18] and may contribute to the development and progression of prostate cancer as alterations in TGF-ß and TGF-ß-receptor II expression are associated with poor clinical outcome [19]. A growing number of *in vivo* studies demonstrate that inhibitors of TGF-ß or TGF-ß-receptors may reduce the metastatic and/or invasive properties of a variety of experimental cancers by preventing EMT pathways [5,20,21], thus underscoring the importance of TGF-ß in oncogenic EMT associated with cancer progression.

This study was designed to investigate whether tumorigenicity and invasive behavior is associated with modulated BMP7 expression in clinical prostate cancer specimens and in human prostate cancer cell lines with different tumorigenic potential. Furthermore, we studied if systemic administration of BMP7 affects the growth of human prostate cancer cells in orthotopic tumor and bone metastasis models by whole body bioluminescent imaging (BLI). We present evidence for cross talk between BMP7 and TGF-ß signalling in the regulation of EMT in prostate cancer and we identified BMP7 as a potential therapy for metastatic bone disease.

Materials and Methods

Tissue Sampling

Radical prostatectomy specimens were obtained at the department of Urology of the University of Bern, Switzerland. Written informed consent was obtained from all patients and tissue sampling was approved by the local ethical committee. Within 15 minutes from surgical excision, samples of prostate cancer tissue or non-cancerous tissue of the prostate were taken and either snap-frozen or immersed in RNAlater (Qiagen, Basel, Switzerland) [22]. Tissue adjacent to the respective samples was processed for paraffin embedding and served as histological control. Histological diagnosis and grading were performed by a pathologist (R.M.).

Laser Capture Microdissection (LCM)

Six µm cryo-sections were treated according to the HistoGene LCM Frozen Section staining Kit (Arcturus, Bucher Biotech, Basel, Switzerland) [22,23]. The P.A.L.M. Micro-Beam system (P.A.L.M. Microlaser Technologies, Bernried, Germany) was used to excise approximately thousand pure epithelial cells of non-cancerous prostate (NP) and prostate cancer (PC) tissue in each prostate. Total RNA was extracted with the Pico Pure RNA Isolation Kit (Arcturus).

Real-Time PCR Analysis

Total RNA (see above) was reverse transcribed using random primers in presence of RNase inhibitor (Roche Diagnostics, Rotkreuz, Switzerland). Real-time PCR was performed with

Jeroen_Buijs_18.indd 174 26-11-2008 10:18:58

exon specific primers for human BMP7 (Hs_002333477_m1), GAPDH (Hs_99999905_m1) E-cadherin (Hs 00170423 m1), Vimentin (Hs_00185584_m1), and β-actin (Hs_99999903_m1) (primer catalogue Applied Biosystems, Rotkreuz, Switzerland) on an ABI Prism 7700 Sequence Detection System (Applied Biosystems). The resulting values were normalized to GAPDH or β-actin. Semi-quantitative PCR was performed on samples of experimentally-induced bone metastases from PC-3M-Pro4 after intracardiac inoculation into nude mice using the following exon-specific and human-specific BMP primers [22,24].

Cell lines and culture conditions

The human prostate cancer cell lines PC-3 (ATCC Number CRL-1435, ATCC-LGC Promochem, Molsheim Cedex, France) and PC-3M-Pro4 were grown in DMEM+ 10% FCS (Bio-Wittaker, Verviers, Belgium). The PC-3M-Pro4 cells were generated from PC-3M cells, by injecting PC-3M cells into athymic mouse prostates and selecting for variants with increasing metastatic potential by several rounds of re-injecting cells from xenograft tumors back into the mouse prostate [25,26]. The human prostate cancer cell line LNCaP and LNCaP-derived cell lines C4-2 and C4-2B4 [27,28] were grown in T-Medium.

Cells at 70%-80% confluence were used for RNA extraction using an RNeasy Midi RNA extraction kit (Qiagen). Quantitative real-time PCR analysis was performed as described above.

Human PC-3M-Pro4 prostate cancer cells were stably transfected with a CMV-promoter driven mammalian expression vector for luciferase, CMV-luc, and one clone with the highest expression of luciferase expression (PC-3M-Pro4/Luc+) was successfully used for *in vivo* whole body bioluminescent reporter imaging (BLI) [29,30,32]. PC-3M-Pro4/Luc+ were cultured in DMEM+10% FCS and 800 µg/ml geneticyne/G418 (Gibco-BRL, Breda, the Netherlands). Cells were regularly certified free of mycoplasma contamination.

For intraosseous or orthotopic inoculation cell suspensions of PC-3M-Pro4/Luc+ (1 x 10^5 cells /10 µl PBS) were prepared [29-32].

Animals

Male nude (BALB/c *nu/nu)* mice were purchased from Charles River (L'Arbresle, France). Mice were housed in individual ventilated cages under sterile condition according to the Dutch guidelines for the care and use of laboratory animals (DEC 4077). For surgical and analytical procedures were performed mice were anaesthetized [29,31,32].

Intraosseous inoculation of PC-3M-Pro4/Luc+ cells

A single cell suspension of PC-3M-Pro4/Luc+ cells was injected into the right tibiae [29-32]. The progression of cancer cell growth was monitored weekly by BLI. After the experimental period the animals were sacrificed, the tibia dissected and processed for further histomorphometrical and immunohistochemical analysis (see below).

Inoculation of PC-3M-Pro4/Luc+ into the mouse prostate (orthotopic implantation)

A single cell suspension of 1 x 10^5 PC-3M-Pro4/Luc+ cells/10 µl PBS was surgically inoculated into the prostate of anaesthesized 6-week-old male nude mice. The cutaneous wound was sutured. The progression of cancer cell growth was monitored weekly by BLI. Subsequently the animals were treated daily with 100 µg/kg/d BMP7 or vehicle solution. After the experimental period the animals were sacrificed. Directly after removal of the mouse prostate, BLI images were taken of the animals to establish the number of locoregional lymph node metastases. Tissues dissected and processed for further histomorphometrical and immunohistochemical analysis (see below).

Induction of systemic metastases by intracardiac injection of PC-3M-Pro4/Luc+ cells

A single cell suspension of 1 x 10^5 PC-3M-Pro4/Luc+ cells /100 µl PBS was injected into the left cardiac ventricle and cancer cell growth was monitored weekly by BLI and radiography [29-32]. Daily BMP7 treatment started 2 days prior to inoculation of the cancer cells until the end of the experiment.

BMP7 treatment and prostate cancer growth *in vivo*

Human BMP7 was obtained from Dr. Vukicevic. BMP7 was expressed, purified and lyophilized [33]. When used, BMP7 was freshly dissolved to a stock solution containing 1 mg/ml in 20 mM acetate buffer with 5 % mannitol, pH 4.5. BMP7 (20 µl) or vehicle solution (20 µl, 20 mM acetate buffer with 5 % mannitol) was administered daily into the tail veins of mice for 21-23 days (100 µg/kg/d human BMP7).

Whole body bioluminescent reporter imaging (BLI) and quantification of the bioluminescent signal

BLI of tumors induced by the luciferase-expressing human prostate cancer cell lines was performed [29,32]. Analyses for each metastatic site were performed after definition of the region of interest and quantified [32]. Values are expressed as relative light units (RLU).

Histomorphometry, Histochemistry and Immunohistochemistry (IHC)

Five micrometer paraffin sections of patient-matched normal prostate and prostate cancer tissue were rehydrated, and a rabbit polyclonal antibody against BMP7 pro-domain was applied at a dilution of 1:100. Rabbit IgG (Jackson ImmunoResearch, La Roche, Switzerland) served as negative control. A species-specific biotinylated anti-IgG antibody followed by streptavidin/alkaline phosphatase conjugate (Amersham Biosciences) were used as the detection system. 3-Amino-9-ethyl-carbazole (AEC, Sigma, Buchs, Switzerland) served as chromogen (Sigma, Buchs, Switzerland).

Dissected tissues from animal studies were fixed in 4 % paraformaldehyde (pH 6.8), decalcified (only bones) as described previously and processed for paraffin embedding, sectioning and staining [31] with PS1 antibodies directed against phosphorylated-Smad1 [34,35].

Immuno-blotting

Crude cell lysates (10 µg/lane) loaded were separated on SDS-polyacrylamide gels and blotted on Hybond-P membranes (Amersham Biosciences). E-Cadherin mAb (5µg/ml) and a monoclonal mouse anti-actin antibody (1:5000) were used as primary antibodies. Binding was detected with a peroxidase-labeled anti-mouse secondary antibody (Amersham Biosciences) and the ECL Advanced chemiluminescence substrate (Amersham) using the VersaDoc imaging system and QuantityOne imaging software (Bio-Rad).

Human BMP7 ELISA

PC-3M-Pro4 cells, and a clone stably transfected to overexpress rhBMP7, were seeded in a 6-wells plate (120.000 cells/ml) and conditioned medium was harvested and analysed for BMP7 protein synthesis by ELISA after 4 days of culture according to the manufacturer's protocol (R&D systems).

Transient transfections and transcription reporter assays

Transient transfections and transcription reporter assays were performed and values expressed as luciferase intensities (relative light units or RLU) [36]. The experiments were performed in four fold and repeated at least twice. Values are expressed as means ± s.e.m. Incubation time with TGF-ß or BMP7 was performed for 30 hours.

Luciferase Reporter Gene Constructs

For intracellular signaling of TGF-ß the CAGA-luciferase construct, consisting of 12 Smad3/Smad4 binding sequences (CAGA boxes) and the luciferase-coding sequence was used. The CAGA boxes confer TGF-ß, but not BMP-stimulation to a heterologous promoter reporter construct [37].

The BRE4-luciferase construct, that is based on the mouse Id1 promoter, was used to study the presence and functionality of BMP-receptors [37]. Signaling of BMP to stimulate the expression of BRE4-luciferase is transduced by BMPR-IA and mediated by Smad1, Smad4 and Smad5, which form a complex with this reporter construct [38].

The SBE4 construct consists of 4 Smad Binding Elements (SBEs) in the promoter of the JunB gene, an immediate early gene that is potently induced by TGF-ß, activin, and bone morphogenetic proteins [39].

The E-cadherin promoter-luciferase construct is based on the upstream fragment (positions -178 to +92). The pGL3-E-cadherin promoter plasmid [40] was a kind gift from Dr. Antonio Garcia de Herreros.

Statistical Analysis

The paired t-test was performed for statistical evaluation of patient matched mRNA expression and the unpaired t-test for comparison of mRNA expression in bulk and laser captured tissue

using GraphPad Prism Version 3 (GraphPad Software Inc., USA). Data are presented as mean ± s.e.m. ANOVA was performed for statistical evaluation of whole body BLI data and reporter-luciferase assays. A p-value equal or superior to 0.05 was considered as non-significant.

Results

BMP7 mRNA Expression in Radical Prostatectomy Specimens

Samples of prostate cancer tissue (PC) and internal controls from the same patient (non-cancerous tissues of the prostate, NP) were obtained after radical prostatectomy and BMP7 mRNA was measured by real-time PCR.

In bulk tissue BMP7 mRNA expression was generally lower than in whole tissue specimens of non-cancerous prostate (11/16, mean decrease 26 %), a non significant difference (Fig. 1*A,C*; P=0.1). However, the multi-focal nature of prostate cancer and the coexistence of epithelial and stromal tissues may cross-contaminate and dilute cell-specific gene expression analyzed in bulk tissue specimens. Therefore, we next collected pure populations of >1000 prostate cancer cells and patient-matched non-cancerous prostate epithelial cells by laser capture microdissection (LCM) from 14 patients. In 93% of those cancer cell samples BMP7 mRNA was strongly under-expressed when compared to patient-matched non-cancerous epithelial cells (13/14, mean decrease 70%, P=0.0019; Fig. 1*B,D*). Comparison of the BMP7 mRNA expression in non-cancerous prostate either derived from bulk tissue or from laser captured epithelial cells revealed a 9.4 x higher expression in the epithelial compartment alone than in bulk tissue. BMP7 expression in laser captured prostate cancer was also (2.8 x) higher when compared to bulk prostate cancer tissue, but these differences were less pronounced. These data strongly suggest that BMP7 is expressed mainly in the epithelial compartment of the prostate gland, particularly in the glandular epithelium.

Immunohistochemical analyses were performed for BMP7 on primary prostate cancer specimens and non-cancerous tissue adjacent to the respective samples which served as a histological control. Histological diagnosis and grading were performed by a certified pathologist (R.M.). BMP7 immunoreactivity was present in the cytoplasm of the luminal cell layer of the normal acinar epithelium in samples of non-cancerous prostate tissue, while hardly any BMP7 could be detected in basal cells (Fig. 1*E,F*). In addition, BMP7 protein expression was also found in the prostate stromal compartment and blood vessels. In contrast, prostate cancer cells showed lack of BMP7 immunoreactivity (Fig. 1*G,H*).

Our LCM and IHC data reveal that BMP7 expression is enriched in non-cancerous prostate epithelium compared to prostate cancer cells in the same patients, suggesting that BMP7 down-regulation may facilitate prostate carcinogenesis, dissemination and/or metastasis. Moreover, BMP7 expression (ratio PC/NP) appeared inversely correlated to Gleason patterns but the distribution of patients for each pattern were too small to reach statistical significance (results not shown).

Jeroen_Buijs_18.indd 178 26-11-2008 10:18:59

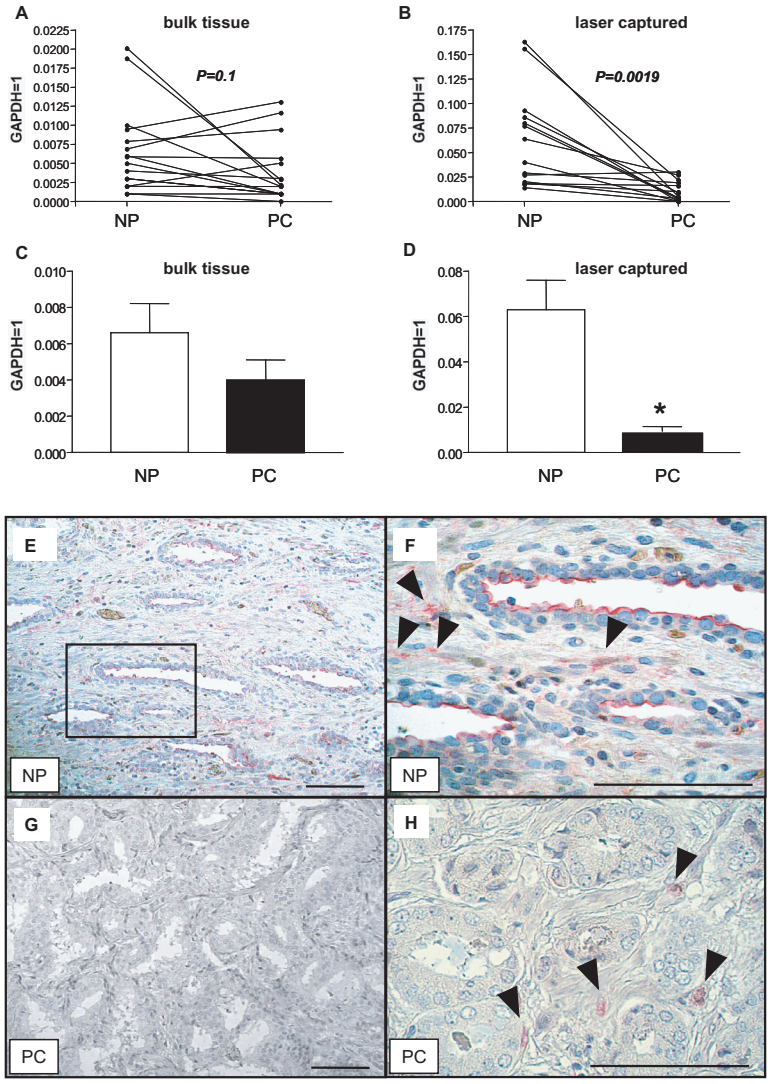

Figure 1 **BMP7 mRNA expression in non-cancerous prostate epithelium (NP) and prostate cancer cells (PC) of radical prostatectomy specimens.** *A*, BMP7 mRNA expression in patient matched specimens consisting predominantly of NP and PC tissue (n=16, P=0.1, paired t-test). *B*, BMP7 mRNA expression in NP and neoplastic epithelial cells isolated by LCM (PC) (n=14, P=0.0019, paired t-test). *C*, mean BMP7 mRNA expression values ± s.e.m. in bulk tissue in NP and PC both normalized to GAPDH (P=0.1, paired t-test). *D*, mean BMP7 mRNA expression values ± s.e.m. in microdissected non cancerous epithelium (NP) and neoplastic epithelium (PC) both normalized to GAPDH (P=0.0019, paired t-test). BMP7 mAb immuno-reactivity and in clinical specimens of NP (E,F) and PC (G,H). *E*, boxed area is magnified in *F*, BMP7 immuno-reactivity was detected in the apical cytoplasm of the luminal cell layer of the normal acinar epithelium and parts of stroma (arrowhead), but weak or no staining of the basal cells was found. *G, H*, prostate cancer cells lack BMP7 immuno-reactivity, whereas BMP7 was still detectable in parts of the stroma (arrowhead). Bars = 100 µm.

BMP7 mRNA Expression in Prostate Cancer Cell Lines

We further investigated whether BMP7 expression in prostate cancer cell lines was associated with tumorigenicity, metastatic potential and EMT degree. The prostate cell lines examined have progressively greater tumorigenic and metastatic potential in the following order: LNCaP, C4-2, C4-2B4, PC-3, PC-3M-Pro4. This arrangement of cell lines also parallels the gradual loss of expression of epithelial markers (E-cadherin epithelial marker) and acquisition of mesenchymal characteristics (Fig. 2*A*). Vimentin is a characteristic marker for the mesenchymal phenotype of cancer cells and enhanced vimentin expression was previously found in motile prostate cell lines and in poorly differentiated and metastatic prostate carcinoma [41]. In line with these observations we found that vimentin expression increased with tumorigenicity and that E-cadherin/vimentin ratios decreased with augmented invasiveness and aggressiveness (Fig. 2*A*).

BMP7 mRNA levels in prostate cancer cell lines strongly correlated to E-cadherin/vimentin ratio (Fig. 2*A,B*) whereas no association was observed for other BMPs (results not shown) [24]. The highly tumorigenic and metastatic human prostate cancer cell line PC-3 and its derivative PC-3M-Pro4 did not show detectable BMP7 mRNA expression (Fig. 2*B*) and protein synthesis *in vitro* (human specific BMP7 ELISA; all < 10 pg/ml hBMP7, n=4). The lack of BMP7 expression by PC-3M-Pro4 cells *in vitro* was confirmed *in vivo* in bone metastases (Fig. 2*D*), suggesting that the bone microenvironment is unable to induce BMP7 expression in the metastatic cancer cells. In contrast, the LNCaP, C4-2, and C4-2B4 cell lines, characterized by a much lower tumorigenic and metastatic potential, showed substantial expression of BMP7 mRNA (Fig. 2*B*). E-cadherin/vimentin ratio together with BMP7 expression, therefore, decreased with increasing tumorigenic potential and a strong correlation exists between BMP7 expression and E-cadherin/vimentin ratio (R^2=0.98, p=0.0015, Fig. 2*C*).

BMP7 Treatment of Bone Metastasis and Orthotopic Prostate Cancer Growth *In Vivo*

To test whether the observed decrease of BMP7 expression during prostate cancer progression may contribute to the acquisition of an invasive metastatic phenotype, we investigated if systemic administration of rhBMP7 affected the growth of human prostate cancer cells in orthotopic tumor and bone metastasis animal models by whole body bioluminescent reporter imaging (BLI) of human PC-3M-Pro4/Luc+ cells.

Three days after intra-bone inoculation of PC-3M-Pro4/Luc+ cells into the tibiae of BALB/c *nu/nu* mice, the animals were treated daily via tail i.v. injections of 100 µg/kg rhBMP7 or a vehicle solution and growth of prostate cancer cells was monitored weekly by BLI and radiography. Administration of BMP7 for the duration of the experiment resulted in a significant and sustained inhibition of tumor cell growth and tumor-induced osteolysis in bone marrow (Fig. 3*A-C*). Systemic administration of BMP7 directly acts on bone-residing PC-3M-Pro4/Luc+ tumor cells as visualized by nuclear staining for Phospho-Smad1 while this is significantly lower in vehicle–treated animals (Fig. 3*D*). Inoculation of PC-3M-Pro4/

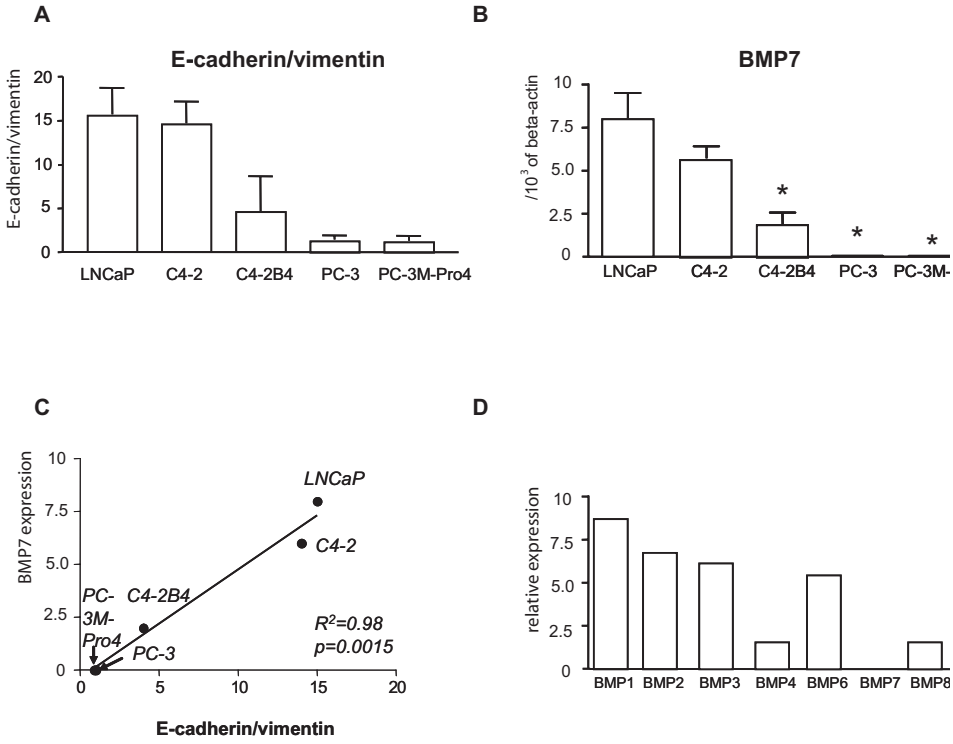

Figure 2 **mRNA expression levels of E-cadherin, vimentin and BMPs in prostate cancer cell lines with different tumorigenic potential** *in vitro* **and in experimentally-induced bone metastases.** *A*, E-cadherin/vimentin ratios in prostate cancer cell lines. *B*, BMP7 mRNA expression in prostate cancer cell lines. *C*, correlation between E-cadherin/vimentin ratio and BMP7 mRNA expression in prostate cancer cell lines with different tumorigenic potential (R^2=0.98, P=0.0015). *D*, Relative BMP mRNA expression levels in an experimentally-induced bone metastasis from PC-3M-Pro4 cells in nude mice (β2-μglobulin was used for normalization as described previously [31]). All panels: mRNA levels (± SEM) were quantified by real-time RT-PCR.

Luc+ cells into the left cardiac ventricle of nude mice resulted in the formation of multiple bone metastases [29-32]. Continuous daily treatment with BMP7 did not significantly inhibited the number of bone metastases, despite a tendency toward a decrease. However, the average tumor burden per bone lesion was significantly decreased upon BMP7 treatment (Fig. 3*E*).

Our data therefore suggest that BMP7 inhibits the growth of bone metastases by human prostate cancer cells in nude mice. In contrast to its inhibitory effect on bone metastases, BMP7 treatment of orthotopically implanted PC-3M-Pro4/Luc+ cells did not alter tumor growth (Fig. 4*A*). After removal of the prostate containing the orthotopically growing tumor, multiple loco-regional lymph nodes harbored bioluminescent PC-3M-Pro4/Luc+ cells (Fig.

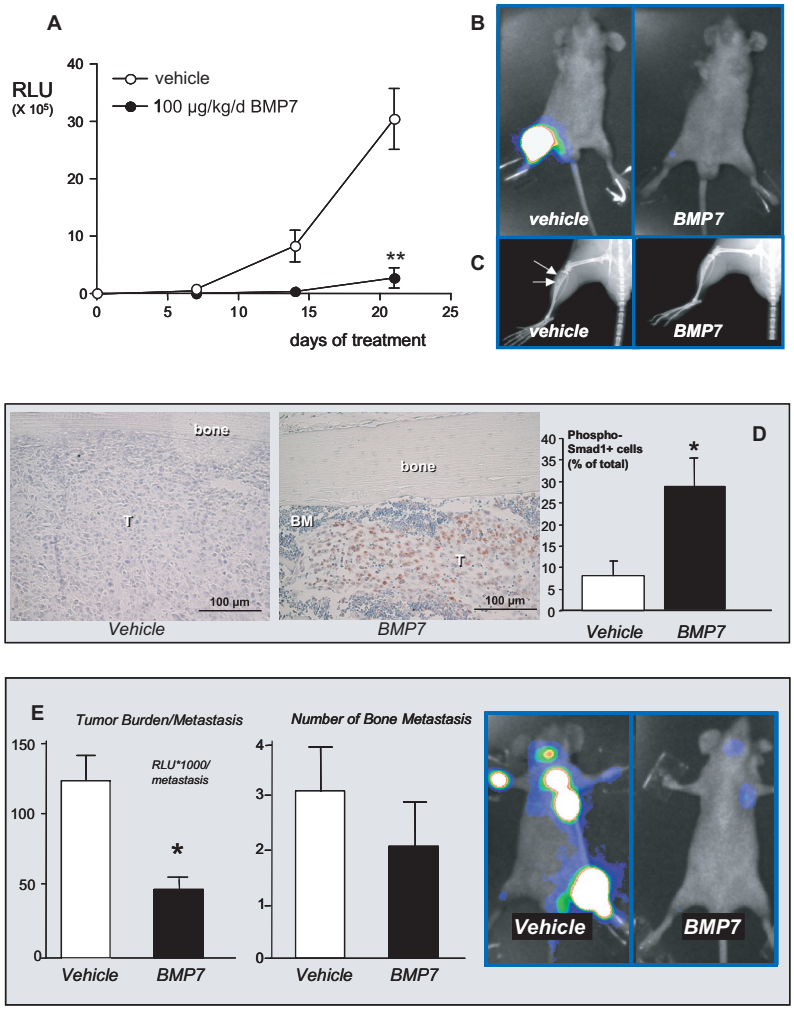

Figure 3 **Effects of systemic administration of 100 µg/kg/d rhBMP7 on the growth of human prostate cancer cells in bone marrow and bone metastasis** *in vivo* **after intraosseous transplantation or intracardiac inoculation of human PC-3M-Pro4/Luc+ cells using whole body bioluminescent reporter imaging.** *A*, BMP7 treatment of PC-3M-Pro4/Luc+ cells growing in bone marrow of nude mice as monitored by BLI. *B*, representative examples of bioluminescent photon emission in a vehicle and BMP7 treated animal at day 21. *C*, representative radiographs at day 21 after intraosseous transplantion of PC-3M-Pro4/Luc+ cells growing in bone marrow (arrows indicate bone lesions in tibiae of nude mice). *D*, immunohistochemical analyses of phosho-Smad1localization at day 21 after intraosseous transplantation of PC-3M-Pro4/Luc+ cells growing in bone marrow. The animals were either vehicle treated (upper left panel) or treated with rhBMP7 (upper right panel) 6 hours prior to explantation and fixation of the tibiae. The number of phosphoSmad1 positive cells in the BMP7 treated group are increased significantly. *E*, effect of BMP7 treatment on the formation and growth of bone metastases by PC-3M-Pro4/Luc+ in nude mice as monitored by BLI (tumor burden, number of bone metastases, representative examples of BLI at day 19). BLI was performed once weekly starting at day 0 after intraosseous implantation or intracardiac inoculation of the prostate cancer cells and quantified in relative light units (RLU) ± s.e.m. n=8 for each experimental group for intraosseous transplantation experiment (A-D); n=10 for intracardiac inoculation (E). Values are expressed as means ± s.e.m. *p<0.05, **p<0.001 (ANOVA)

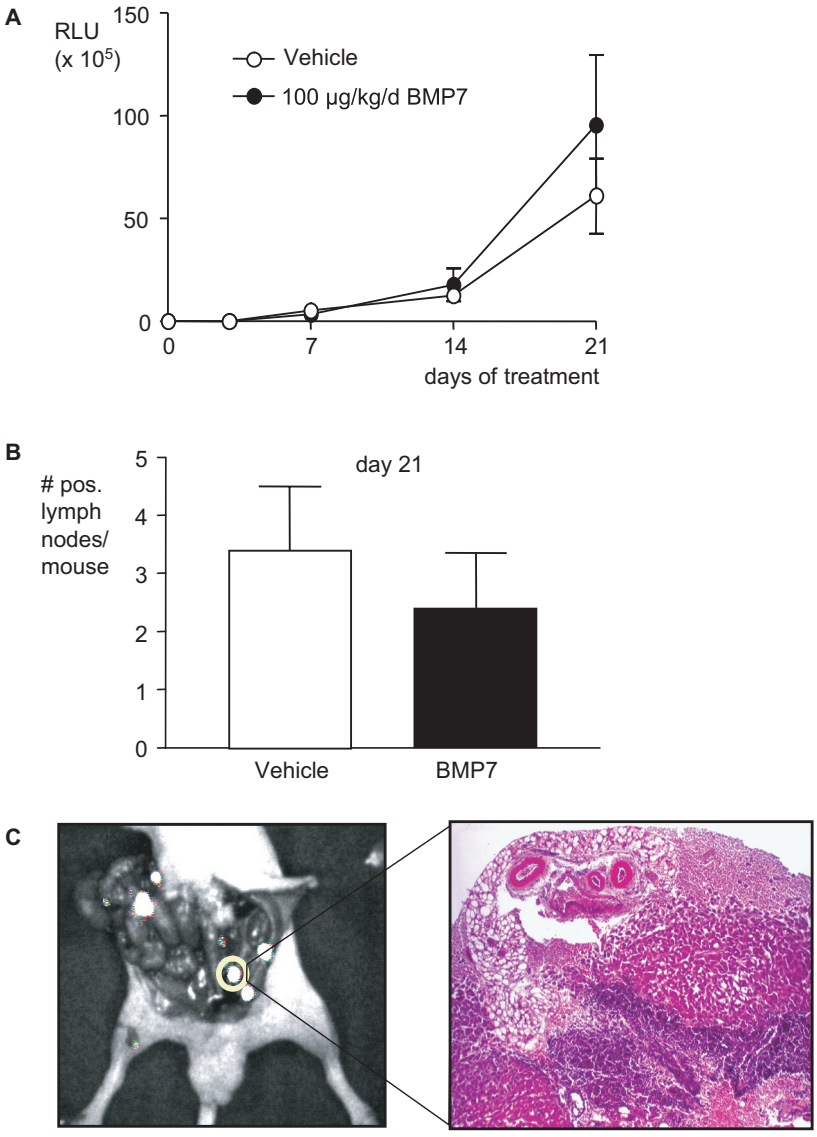

Figure 4 **Effects of systemic administration of 100 µg/kg/d rhBMP7 on intra-prostatic growth of human PC-3M-Pro4/Luc+ cells and formation of loco-regional lymph node metastases nude mice.** *A*, tumor take of PC-3M-Pro4/Luc+ cells growing in prostate upon treatment with vehicle solution or 100 µg/kg/d rhBMP7 as monitored by BLI. *B*, number of affected lymph nodes in nude mice after 21 days as detected by BLI. *C*, representative example of bioluminescent photon emission of a mouse with multiple loco-regional lymph node metastases 21 days after intra-prostatic inoculation of PC-3M-Pro4/Luc+ cells. The mouse prostate was removed prior to bioluminescent reporter imaging to obtain sensitive measurements of affected lymph nodes (panel B). The presence of micrometastatic deposits in lymph nodes was confirmed by HE-staining. BLI was performed at least once weekly starting at day 0 after intra-prostatic implantation of the prostate cancer cells and quantified in Relative light units (RLU) ± s.e.m. n=8 for each experimental group. Values are expressed as means ± s.e.m. (ANOVA).

4*B*). Administration of BMP7, however, did not result in decreased formation of locoregional lymph node metastases (Fig. 4*C*).

BMP7 and Epithelial-to-Mesenchymal Transition in Prostate Cancer Cells

Next we tested whether BMP7 acts on human PC-3M-Pro4 prostate cancer cells to inhibit the acquistion of an invasive, mesenchymal phenotype by antagonizing Smad-dependent TGF-ß signaling. For this, we first studied the functionality of both TGF-ß and BMP receptors in PC-3M-Pro4 prostate cancer cells. Challenging PC-3M-Pro4/Luc+ cells by both BMP7 and TGF-ß, that were transiently transfected with SBE4-luciferase, resulted in a significant induction of reporter expression (Fig. 5*A*). This indicates that functional TGF-ß and BMP receptors are present in these cells, thus confirming our earlier observations [22,24]. Exogenous addition of BMP7, but not of TGF-ß, strongly stimulated BRE4-luciferase activity in PC-3M-Pro4 cells and indicated the presence of functioning, activated type I BMP-receptor complexes in these prostate cancer cells (Fig. 5*B*). Strikingly, when BMP7 and TGF-ß were given simultaneously, BRE4-luciferase activity was significantly stimulated in a synergistic manner (Fig. 5*B*).

The presence of functionally active TGF-ß receptor complexes, particularly ALK5 (TGF-ß type I receptor), in PC-3M-Pro4 cells was demonstrated by the CAGA-luciferase reporter. The CAGA boxes confer TGF-ß, but not BMP, stimulation to the promoter reporter constructs in PC-3M-Pro4 cells in a dose-dependent manner (Fig. 5 *C,D*). Addition of BMP7 to TGF-ß-stimulated PC-3M-Pro4 cells dose-dependently inhibited TGF-ß-driven CAGA-luciferase activity. This suggests that BMP7 counteracts TGF-ß-induced nuclear activation of Smad3/4 (Fig. 5*C,D*) in human prostate cancer cells, whereas TGF-ß can stimulate BRE4-luciferase only in the presence of BMP7 (Fig. 5*B*).

The observed anti-tumor effects of BMP7 *in vivo* may, therefore, be caused by inhibition of TGF-ß mediated growth stimulatory responses in bone metastasis. This may be particularly true for the bone microenvironment since bone is a storehouse for TGF-ß and it has been shown that activated TGF-ß is released from bone matrix by bone-resorbing osteoclasts [29,31,32,42,43].

The expression level of E-cadherin appears to be inversely related with prostate cancer grade and its loss considered a hall mark of EMT [23,44,45]. Recombinant human BMP7 dose-dependently induced E-cadherin promoter activity (> 150% at 1 µg/ml BMP7, $p<0.01$) while TGF-ß had no effect (Fig. 6*A*). Strikingly, E-cadherin promoter activity was stimulated in a synergistic, dose-dependent and significant manner by BMP7 in the presence of TGF-ß (Fig. 6*B*, 350%). In line with this observation, Western blot analysis revealed that E-cadherin/vimentin ratio at the protein level was strongly up-regulated under these circumstances (Fig. 6*C*). These data, therefore, suggest that BMP7 can counteract the acquisition of an invasive, metastatic phenotype by re-expressing the key epithelial marker E-cadherin, that is an absolute requirement for epithelial integrity by decreasing cell motility, invasion and migration.

Jeroen_Buijs_18.indd 184 26-11-2008 10:19:02

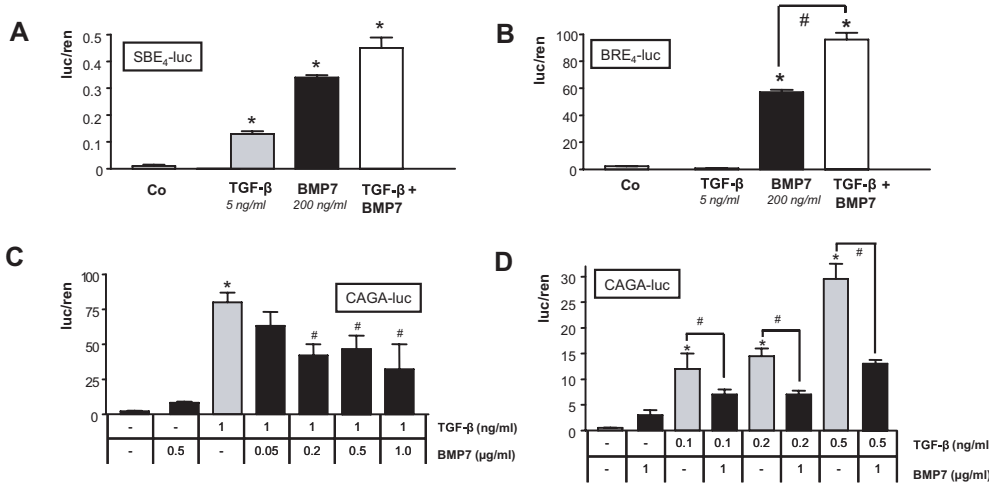

Figure 5 **The effects of BMP7 on gene promoter luciferase constructs in human PC-3M-Pro4 prostate cancer cells.** *A*, challenge of the SBE4 construct, demonstrates the presence of functional BMP7 and TGF-ß receptors (Smad-mediated signaling). *B*, BMP7, but not TGF-ß, induces BRE4-luciferase actvity, indicating the presence and functionality of BMP-receptors. Signaling of BMP to stimulate the expression of BRE4-luciferase is transduced by BMPR-IA and mediated by Smad1, Smad4 and Smad5, both of which form a complex with this reporter construct. Strikingly signaling of BMP7 to stimulate BRE4-luciferase is significantly enhanced when co-incubated in the presence of TGF-ß. *C,D,* the presence of functionally active TGF-ß receptor complexes, particularly ALK5 (TGF-ß type I receptor), in PC-3M-Pro4 cells was demonstrated by the CAGA-luciferase reporter, whose activity depends on binding of activated Smad3/Smad4 transcription factor complexes. The CAGA boxes confer TGF-ß, but not BMP, stimulation to the promoter reporter constructs. Addition of BMP7 to TGF-ß-stimulated PC-3M-Pro4 cells dose-dependently inhibited TGF-ß-driven CAGA-luciferase activity. All panels: * p < 0,01 vs. Co; # p < 0,01 vs. TGF-ß

When TGF-ß was added to PC-3M-Pro4/Luc+ cells the intermediate filament and mesenchymal marker vimentin was redistributed in the prostate cancer cells (Fig. 6*D*). This TGF-ß-induced vimentin expression and cellular redistribution was completely abolished by BMP7 (Fig. 6*D*).

Discussion

In this report novel evidence is provided for the importance of BMP7 (and TGF-ß) in the development of an epithelial cancer and metastastic behavior with prostate cancer as a model. Our clinical findings suggest that decreased BMP7 expression is implicated in

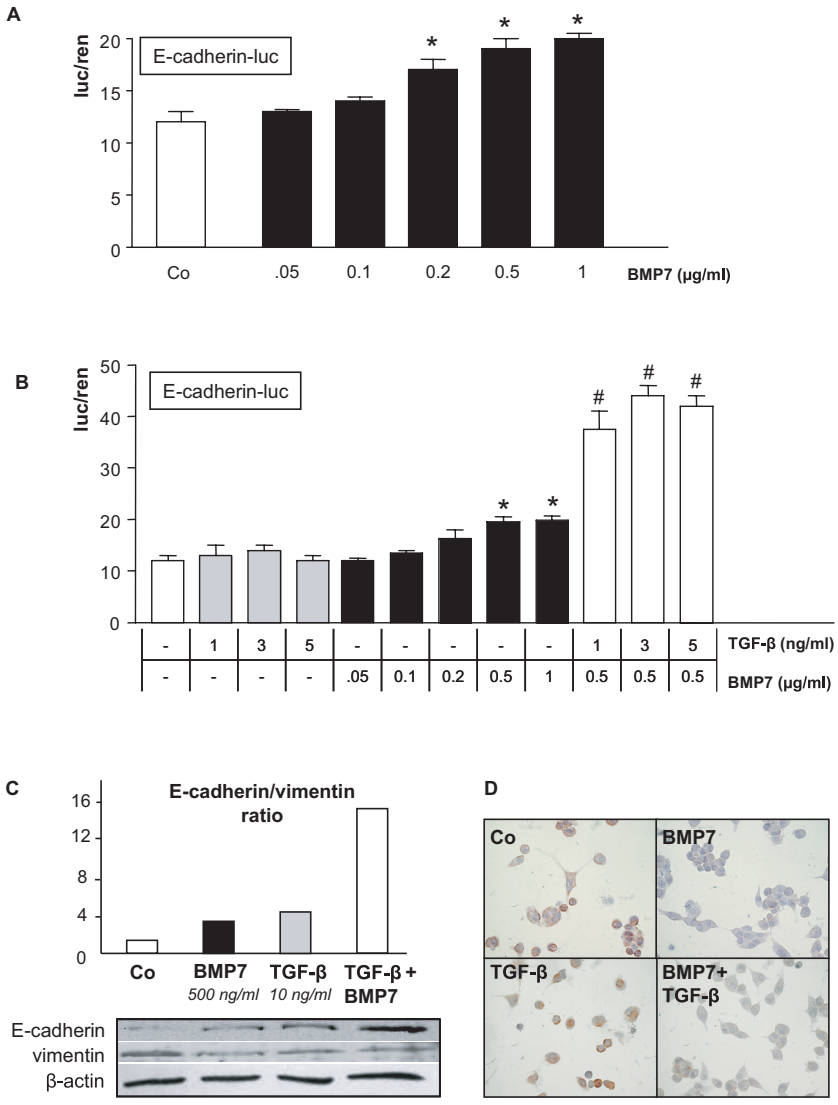

Figure 6 **The effects of BMP7 on E-cadherin promoter luciferase constructs,and protein expression of E-cadherin/vimentin in human PC-3M-Pro4 prostate cancer cells.** *A,B,* BMP7 induces a dose-dependent and significant increase in E-cadherin promoter-luciferase construct activity (* p<0.05 vs. Co; # p<0.01 vs. BMP7 aloneCo). E-cadherin promoter activity is significantly and synergistically enhanced when BMP7 and TGF-ß were coincubated (P<0.05 vs BMP7 alone). *C,* E-cadherin and vimentin protein expression in PC-3M-Pro4 cells in the presence or absence of rhBMP7 and/or TGF-ß for 48 hours as determined by immuno-blotting. Treatment of PC-3M-Pro4 cells with 0.5 µg/ml rhBMP7 in the presence of TGF-ß induces protein expression of E-cadherin. Values are expressed as E-cadherin/Vimentin ratio. *D,* vimentin mAb immuno-reactivity of cultured PC-3M-Pro4 cells. In the presence of BMP7 the TGF-ß–induced vimentin expression and cellular redistribution was completely abolished. Values are expressed as means ± s.d. (n=4, ANOVA).

human prostate cancer and we postulate a role for BMP7 in controlling epithelial homeostasis of the prostate gland. In line with these clinical findings experimental treatment of bone metastases from human prostate cancer *in vivo* position BMP7 as a good candidate for the treatment of skeletal metastasis from prostate cancer.

Members of the TGF-ß superfamily play crucial roles in embryonic development, certain fibrotic diseases, inflammation and cancer. Although TGF-ß inhibits the proliferation of normal prostate cells and functions as a tumor suppressor in early tumorigenesis, it acts as a tumor promoter in later stages of tumor progression and mediates oncogenic EMT [2,5,10,17,46-49,63]. Prostate cancers often grow in a variety of growth patterns, that are classified by Gleason histological grading. Prostate cancer classification according to this "gold standard" is predictive of disease status and also seems to parallel EMT. Laser capture micro-dissection of prostate epithelium/cancer was used because the epithelial compartment in the normal prostate represents only a small percentage (~5%) of the entire organ. Furthermore, infiltrative prostate cancer patterns vary among individual cases. The latter can lead to misinterpretation of epithelium-specific gene expression among the various clinical specimens. By comparing pure populations of laser-captured cancer cells and non-cancerous epithelial cells from the same patient we observed significant and consistent BMP7 mRNA under-expression in invasive primary prostate carcinoma. In contrast, BMP7 mRNA expression in bulk tissue specimens of non-cancerous prostate and prostate cancer tissue showed only a tendency toward under-expression in prostate cancer. Our observations support concerns that high throughput RNA expression analysis performed on bulk tissue samples, either on primary tumors or its metastases, may not detect differences in relevant gene expression restricted to the epithelial or mesenchymal compartment [22]. Clearly, LCM is preferred to establish putative changes in gene expression repertories in both epithelial and stromal compartments.

Emerging evidence from a variety of tumors suggests that the effects of BMPs (and TGF-ß) are cell specific and could be either pro-tumorigenic or anti-tumorigenic [48]. For instance, BMP7 was shown to either counteract EMT by inducing MET, to induce EMT or to have no effect [2,4,10,49,50]. In the non-cancerous human prostate, expression of BMP7 protein was restricted mainly to the glandular epithelium, whereas primary prostate cancers show low or undetectable BMP7 protein expression. It also appeared that BMP7 expression is negatively correlated to Gleason score (data not shown) but the number of patients per Gleason pattern were too small for statistical analysis. Clearly more LCM and real-time PCR analysis are warranted to address this issue.

In line with these clinical observations, the level of BMP7 expression in tested prostate cancer cell lines correlated with an epithelial phenotype and appears, therefore, inversely related to their tumorigenic and metastatic potential *in vivo*.

Daily systemic administration of recombinant BMP7 did not affect the growth of orthopically implanted PC-3M-Pro4/Luc+ prostate cancer cells and subsequent formation of

lymph node metastasis in nude mice. However, the growth of micrometastatic deposits from human PC-3M-Pro4/Luc+ prostate cancer cells in bone marrow was inhibited significantly, whereas the process of bone marrow colonization per sé appeared unaffected. Our findings suggest, therefore, that the tumor microenvironment is an important determinant of the therapeutic response to BMP7.

Our *in vitro* studies reveal for the first time that BMP7 is a potent inhibitor of TGF-ß-induced EMT in PC-3M-Pro4 prostate cancer cells. In these cells, BMP7 counteracts TGF-ß-induced activation of Smad3/4 signaling. BMP7 induced a dose-dependent expression of E-cadherin that led to an overall increase in E-cadherin/vimentin ratio as an established indicator of less-malignant and more epithelial phenotype. Surprisingly, we observed that these BMP7-mediated effects were synergistically enhanced by co-incubation with TGF-ß at both transcriptional and protein levels. These actions of BMP7 may be of critical importance for explaining the successful experimental treatment of skeletal metastasis and intra-bone growth. In this context it is important to note that TGF-ß, which is concentrated in high inactive amounts in bone matrix, can be released and activated by osteoclastic resorption. TGF-ß may act as paracrine growth factors for neighboring cancer cells that may have colonized the bone marrow [31,32,42,43]. Compelling evidence suggests that the formation of micrometastatic deposits in bone marrow and subsequent development into clinically overt (macro)metastasis are critically dependent on the tumor-bone (marrow) interactions, in particular bone remodeling [32,43,51]. Although little is known regarding the impact of bone (marrow) stromal cells in prostate cancer bone metastasis, it can be argued that the production and release of specific growth factors, CSFs and cytokines like Wnts, that are critically important for the maintenance of the hematopoietic stem cells niche (and that regulate hematopoiesis), may also be essential for colonization, survival and growth of cancer cells. Interestingly, TGF-ß/BMPs and other pathways like wingless/Wnt, Notch, Hedgehog, appear not only to be involved in bone development/homeostasis and hematopoiesis but also in prostate cancer initiation and progression [2,8,52-55]. Our *in vitro* and *in vivo* data further support the notion BMP7 can antagonize TGF-ß signaling routes in human prostate cancer cells that are metastatic to the skeleton.

EMT provides mechanisms for prostate epithelial cells to overcome physical constraints imposed on them by intercellular junctions and adopt a motile phenotype. We hypothesize that the activation process of micrometastases in bone marrow may bear similarities to EMT that occurs at the primary site in various epithelial cancers and during ontogeny. TGF-ß/BMPs and their signaling molecules, have been implicated in the cellular plasticity that occurs during organogenesis, tissue repair/remodeling and carcinogenesis where cells can shift between epithelial and mesenchymal phenotypes [1,2]. EMT/MET can thus be viewed as a prime example of such cell plasticity. Considering the importance of TGF-ß superfamily in bone metastasis [42], our findings suggest that the efficacy of BMP7 in the experimental treatment of bone metastases is interfering with recapitulation of such cell plasticity of bone

Jeroen_Buijs_18.indd 188 26-11-2008 10:19:03

marrow micrometastatic cancer cells, particularly the acquisition of an invasive phenotype by (TGF-ß-driven?) EMT. Clinical studies also seem to underline the cellular plasticity of prostate cancer during dissemination and bone metastasis [56,57]. The transition from a well-differentiated epithelial phenotype to an invasive mesenchymal phenotype may, of course, involve molecular mechanisms other than those described here (reviewed in [58]). Other studies have provided evidence that motility and invasiveness can be enhanced without inducing a complete conversion of cellular identity [58]. After migrating to new organ or tissue territories, metastatic prostate cancer cells can regain epithelial morphology by a phenomenon known as MET and re-establish E-cadherin expression and epithelial junctions [56-58]. The observed reversion to an epithelial morphology in prostate cancer seems possible even at bone metastatic sites [56-58] and is in full agreement with our *in vitro* and *in vivo* data presented here. Furthermore, previous studies demonstrated cellular plasticity of human prostate cancer cells (PC-3 cells), particularly the EMT/MET interconversion induced by different culture conditions (monolayer vs. 3D cultures) [59].

In many prostate cancer patients, micrometastatic deposits may already exist in bone marrow after removal of the primary tumor that cannot be identified at the time of diagnosis (minimal residual disease). Whole body BLI of luciferase-expressing human prostate cancer cells revealed that growth of micrometastatic deposits in bone marrow are significantly inhibited by systemic administration of BMP7. Similar observations were made by us for other epithelial cancers, including breast cancer [62,63]. Interestingly, recent data suggest that BMPs can inhibit the tumorigenic potential of human brain tumor-initiating cells, mediated via a significant reduction in the stem-like, tumor-initiating precursors [60]. Accumulating evidence suggests that cancer stem cells with tumor-initiating potential exist in human prostate cancer [61]. Although speculative at present, the observed therapeutic effects of BMP7 described here may be mediated, at least in part, by prostate cancer cells with tumor-initiating (and metastastic) potential. Studies are currently on-going to address these important issues.

In conclusion, our data suggest that BMP7 controls the epithelial homeostasis in the human prostate gland by preserving the epithelial phenotype. Loss of BMP7 expression during prostate cancer progression could stimulate the TGF-ß stimulated EMT and, thus, contribute to the acquisition of an invasive phenotype. However, exogenous BMP7 can still counteract the EMT process in the metastatic tumor, thus underscoring tumor plasticity, but its therapeutic response may be determined by the microenvironment. Therefore, BMP7 may represent a novel therapeutic molecule for repression of systemic prostate cancer progression.

Acknowledgments

This work was supported by grants from the European Commission (PRIMA/504587 and MetaBre LSHC-CT-2004-503049), the Dutch Cancer Society (RUL-2001-2485 and UL-2004-3028), the Swiss National Foundation (Grant Nr. 3200-068409.72), and the Bernische Krebsliga (project: From the Benchside to Bedside – Prevention, Detection and Treatment of Micrometastases), and from the Genera Foundation.

References

1. Thiery JP. Epithelial-mesenchymal transitions in development and pathologies. *Curr Opin Cell Biol* 2003; 15:740-6.
2. Prindull G. Hypothesis: cell plasticity, linking embryonal stem cells to adult stem cell reservoirs and metastatic cancer cells? *Exp Hematol*, 2005; 33:738-46.
3. Huber MA, Kraut N, Beug H. Molecular mechanisms for epithelial-mesenchymal transition during tumor progression. *Curr Opin Cell Biol* 2005; 17:548-58.
4. Piek E, Moustakas A, Kurisaki A, Heldin CH, ten Dijke P. TGF-(beta) type I receptor/ALK-5 and Smad proteins mediate epithelial to mesenchymal transdifferentiation in NMuMG breast epithelial cells. *J Cell Sci* 1999; 112(Pt24): 4557-68.
5. Zavadil J, Bottinger EP. TGF-beta and epithelial-to-mesenchymal transitions. *Oncogene* 2005; 24:5764-74.
6. Kalluri R, Neilson EG. Epithelial-mesenchymal transition and its implications for fibrosis. *J Clin Invest* 2003; 112:1776-84.
7. Bottinger EP, Bitzer M. TGF-beta signaling in renal disease. *J Am Soc Nephrol* 2002; 13:2600-10.
8. Zavadil J, Cermak L, Soto-Nieves N, Bottinger EP. Integration of TGF-beta/Smad and Jagged1/Notch signalling in epithelial-to-mesenchymal transition. *Embo J* 2004; 23:1155-65.
9. Zeisberg M, Kalluri R. The role of epithelial-to-mesenchymal transition in renal fibrosis. *J Mol Med* 2004; 82: 175-81.
10. Valcourt U, Kowanetz M, Niimi H, Heldin CH, Moustakas A. TGF--beta and the Smad signaling pathway support transcriptomic reprogramming during epithelial-mesenchymal cell transition. *Mol Biol Cell* 2005; 16:1987-2002.
11. Vukicevic S, Latin V, Chen P, Batorsky R, Reddi AH, Sampath TK. Localization of osteogenic protein-1 (bone morphogenetic protein-7) during human embryonic development: high affinity binding to basement membranes. *Biochem Biophys Res Commun* 1994, 198: 693-700.
12. Jena N, Martin-Seisdedos C, McCue P, Croce CM: BMP7 null mutation in mice: developmental defects in skeleton, kidney, and eye. *Exp Cell Res* 1997; 230:28-37.
13. Zeisberg M, Hanai J, Sugimoto H, Mammoto T, Charytan D, Strutz F, Kalluri R. BMP-7 counteracts TGF-beta1-induced epithelial-to-mesenchymal transition and reverses chronic renal injury. *Nat Med* 2003; 9:964-68.
14. Zeisberg M, Shah AA, Kalluri R. Bone morphogenic protein-7 induces mesenchymal to epithelial transition in adult renal fibroblasts and facilitates regeneration of injured kidney. *J Biol Chem* 2005; 280: 8094-100.
15. Dunsmuir WD, Gillett CE, Meyer LC, Young MP, Corbishley C, Eeles RA, *et al*. Molecular markers for predicting prostate cancer stage and survival. *BJU Int* 2000, 86: 869-78.
16. Richmond PJ, Karayiannakis AJ, Nagafuchi A, Kaisary AV, Pignatelli M. Aberrant E-cadherin and alpha-catenin expression in prostate cancer: correlation with patient survival. *Cancer Res 1997*; 57:3189-93.
17. Bello-DeOcampo D, Tindall DJ. TGF-betal/Smad signaling in prostate cancer. *Curr Drug Targets* 2003; 4:197-207.
18. Horvath LG, Henshall SM, Kench JG, Turner JJ, Golovsky D, Brenner PC *et al*. Loss of BMP2, Smad8, and Smad4 expression in prostate cancer progression. *Prostate* 2004; 59:234-42.

Jeroen_Buijs_18.indd 190 26-11-2008 10:19:03

19. Wikstrom P, Stattin P, Franck-Lissbrant I, Damber JE, Bergh A. Transforming growth factor beta1 is associated with angiogenesis, metastasis, and poor clinical outcome in prostate cancer. *Prostate* 1998; 37:19-29.
20. Dumont N, Arteaga CL. Targeting the TGF-beta signaling network in human neoplasia. *Cancer Cell* 2003; 3:531-36.
21. Yingling JM, Blanchard KL, Sawyer JS. Development of TGF-beta signalling inhibitors for cancer therapy. *Nat Rev Drug Discov* 2004; 3: 1011-22.
22. Rentsch CA, Cecchini MG, Schwaninger R, Germann M, Markwalder R, Heller M *et al.* Differential expression of TGF-beta-stimulated clone 22 in normal prostate and prostate cancer. *Int J Cancer* 2006; 118:899-906.
23. Rubin MA, Mucci NR, Figurski J, Fecko A, Pienta KJ, Day ML. E-cadherin expression in prostate cancer: a broad survey using high-density tissue microarray technology. *Hum Pathol* 2001; 32:690-97.
24. Schwaninger R, Rentsch CA, Wetterwald A, van der Horst G, van Bezooijen RL, van der Pluijm G *et al.* Lack of noggin expression by cancer cells is a determinant of the osteoblast response in bone metastases. *Am J Pathol* 2007; 170:160-75.
25. Sobel RE, Sadar MD. Cell lines in prostate cancer research: A compendium of old and new lines-Part I. *J Urology* 2005; 173:342-59.
26. Pettaway CA, Pathak S, Greene G, Ramirez E, Wilson MR, Killion JJ *et al.* Selection of highly metastatic variants of different human prostate carcinomas using orthotopic implantation in nude mice. *Cancer Res* 1996, 2:1627-36.
27. Wu TT, Sikes RA, Cui Q, Thalmann GN, Kao C, Murphy CF, Yang H *et al*. Establishing human prostate cancer cell xenografts in bone: induction of osteoblastic reaction by prostate-specific antigen-producing tumors in athymic and SCID/bg mice using LNCaP and lineage-derived metastatic sublines. *Int J Cancer* 1998; 77:887-94.
28. Thalmann GN, Anezinis PE, Chang SM, Zhau HE, Kim EE, Hopwood VL *et al.* Androgen-independent cancer progression and bone metastasis in LNCaP model of human prostate cancer. *Cancer Res* 1994; 54:2577-81.
29. Wetterwald A, van der Pluijm G, Que I, Sijmons B, Buijs J, Karperien M, *et al.* Optical imaging of cancer metastasis to bone marrow: a mouse model of minimal residual disease. *Am J Pathol* 2002; 160:1143-53.
30. Papapoulos SE, Hamdy NAT, van der Pluijm G. Bisphosphonates in the management of prostate carcinoma metastatic to the skeleton. *Cancer* 2000; 88:3047-53.
31. van der Pluijm G, Sijmons B, Vloedgraven H, Deckers M, Papapoulos S, Lowik C. Monitoring metastatic behavior of human tumor cells in mice with species-specific polymerase chain reaction: elevated expression of angiogenesis and bone resorption stimulators by breast cancer in bone metastases. *J Bone Miner Res* 2001; 16:1077-91.
32. van der Pluijm G, Que I, Sijmons B, Buijs JT, Lowik CWGM, Wetterwald A *et al.* Interference with the microenvironmental support impairs the *de novo* formation of bone metastases in vivo. *Cancer Res* 2005; 65:7682-90.
33. Jones WK, Richmond EA, White K, Sasak H, Kusmik W, Smart J *et al.* Osteogenic protein-1 (OP-1) expression and processing in Chinese hamster ovary cells: isolation of a soluble complex containing the mature and pro-domains of OP-1. *Growth Factors* 1994; 11:215-25.
34. Persson U, Izumi H, Souchelnytskyi S, Itoh S, Grimsby S, Engstrom U *et al*. The L45 loop in type I receptors for TGF-beta family members is a critical determinant in specifying Smad isoform activation. *FEBS Lett* 1998; 434:83-7.
35. Rosendahl A, Pardali E, Speletas M, ten Dijke P, Heldin CH, Sideras P. Activation of bone morphogenetic protein/Smad signaling in bronchial epithelial cells during airway inflammation. *Am J Respir Cell Mol Biol* 2002; 27:160-9.
36. Goumans MJ, Valdimarsdottir G, Itoh S, Rosendahl A, Sideras P, ten Dijke P. Balancing the activation state of the endothelium via two distinct TGF-beta type I receptors. *Embo J* 2002; 21:1743-53.
37. Dennler S, Itoh S, Vivien D, ten Dijke P, Huet S, Gauthier JM. Direct binding of Smad3 and Smad4 to critical TGF-beta-inducible elements in the promoter of human plasminogen activator inhibitor-type 1 gene. *Embo J* 1998; 17:3091-100.

38. Korchynskyi O, ten Dijke P. Identification and functional characterization of distinct critically important bone morphogenetic protein-specific response elements in the Id1 promoter. *J Biol Chem* 2002, 277: 4883-91.
39. Jonk LJ, Itoh S, Heldin CH, ten Dijke P, Kruijer W. Identification and functional characterization of a Smad binding element (SBE) in the JunB promoter that acts as a transforming growth factor-beta, activin, and bone morphogenetic protein-inducible enhancer. *J Biol Chem* 1998; 273:21145-52.
40. Batlle E, Sancho E, Franci C, Dominguez D, Monfar M, Baulida J *et al.* The transcription factor snail is a repressor of E-cadherin gene expression in epithelial tumour cells. *Nat Cell Biol* 2000; 2:84-8.
41. Lang SH, Hyde C, Reid IN, Hitchcock IS, Hart CA, Bryden AA *et al.* Enhanced expression of vimentin in motile prostate cell lines and in poorly differentiated and metastatic prostate carcinoma. *Prostate* 2002; 52:253-263.
42. Yin JJ, Selander K, Chirgwin JM, Dallas M, Grubbs BG, Wieser R *et al.* TGF-beta signaling blockade inhibits PTHrP secretion by breast cancer cells and bone metastases development. *J Clin Invest* 1999; 103:197-206.
43. Mundy GR. Metastasis to bone: causes, consequences and therapeutic opportunities. *Nat Rev Cancer* 2002; 2:584-93.
44. Umbas R, Isaacs WB, Bringuier PP, Schaafsma HE, Karthaus HF, Oosterhof GO *et al.* Decreased E-cadherin expression is associated with poor prognosis in patients with prostate cancer. *Cancer Res* 1994, 54:3929-33.
45. Tomita K, van Bokhoven A, van Leenders GJ, Ruijter ET, Jansen CF, Bussemakers MJ *et al.* Cadherin switching in human prostate cancer progression. *Cancer Res* 2000; 60:3650-54.
46. Tang B, de Castro K, Barnes HE, Parks WT, Stewart L, Bottinger EP *et al.* Loss of responsiveness to transforming growth factor beta induces malignant transformation of nontumorigenic rat prostate epithelial cells. *Cancer Res* 1999; 59:4834-42.
47. Wakefield LM, Roberts AB. TGF-beta signaling: positive and negative effects on tumorigenesis. *Curr Opin Genet Dev* 2002; 12:22-9.
48. Tu WH, Thomas TZ, Masumori N, Bhowmick NA, Gorska AE, Shyr Y *et al.* The loss of TGF-beta signaling promotes prostate cancer metastasis. *Neoplasia* 2003, 5:267-77.
49. Yang S, Zhong C, Frenkel B, Reddi AH, Roy-Burman P. Diverse biological effect and Smad signaling of bone morphogenetic protein 7 in prostate tumor cells. *Cancer Res* 2005; 65:5769-77.
50. Danielpour D. Functions and regulation of transforming growth factor-beta (TGF-beta) in the prostate. *Eur J Cancer* 2005; 41:846-857.
51. Schneider A, Kalikin LM, Mattos AC, Keller ET, Allen MJ, Pienta KJ *et al.* Bone turnover mediates preferential localization of prostate cancer in the skeleton. *Endocrinology* 2005;146:1727-36.
52. Chen G, Shukeir N, Potti A, Sircar K, Aprikian A, Goltzman D *et al.* Up-regulation of Wnt-1 and beta-catenin production in patients with advanced metastatic prostate carcinoma: potential pathogenetic and prognostic implications. *Cancer* 2004; 101:1345-56.
53. Huang HC, Klein PS. Interactions between BMP and Wnt signaling pathways in mammalian cancers. *Cancer Biol Ther* 2004, 3:676-78.
54. Grego-Bessa J, Diez J, Timmerman L, de la Pompa JL. Notch and epithelial-mesenchyme transition in development and tumor progression: another turn of the screw. *Cell Cycle* 2004; 3:718-21.
55. Karhadkar SS, Bova GS, Abdallah N, Dhara S, Gardner D, Maitra A *et al.*. Hedgehog signalling in prostate regeneration, neoplasia and metastasis. *Nature* 2004; 431:707-12.
56. Bryden AA, Freemont AJ, Clarke NW, George NJ. Paradoxical expression of E-cadherin in prostatic bone metastases. *BJU Int* 1999; 84:1032-1034.
57. Bryden AA, Hoyland JA, Freemont AJ, Clarke NW, Schembri Wismayer D, George NJ. E-cadherin and beta-catenin are down-regulated in prostatic bone metastases. *BJU Int* 2002, 89:400-3.
58. Christiansen JJ, Rajasekaran AK. Reassessing epithelial to mesenchymal transition as a prerequisite for carcinoma invasion and metastasis. *Cancer Res* 2006; 66: 8319-26.

Jeroen_Buijs_18.indd 192 26-11-2008 10:19:03

59. Lang SH, Sharrard RM, Stark M, Villette JM, Maitland NJ. Prostate epithelial cell lines form spheroids with evidence of glandular differentiation in three-dimensional Matrigel cultures. *Br J Cancer* 2001; 85:590-99.
60. Piccirillo SGM, Reynolds BA, Zanetti N, Lamorte G, Binda E, Broggi G *et al.* Bone morphogenetic proteins inhibit the tumorigenic potential of brain tumour-initiating cells. *Nature* 2006; 444:761-5.
61. Collins AT, Berry PA, Hyde C, Stower MJ, Maitland NJ. Prospective identification of tumorigenic prostate cancer stem cells. *Cancer Res* 2005; 65:10946-51.
62 Buijs JT, Henriquez NV, van Overveld PG, van der Horst G, Que I, Schwaninger R, Rentsch C, Ten Dijke P, Cleton-Jansen AM, Driouch K, Lidereau R, Bachelier R, Vukicevic S, Clézardin P, Papapoulos SE, Cecchini MG, Löwik CW, van der Pluijm G. Bone Morphogenetic Protein 7 in the Development and Treatment of Bone Metastases from Breast Cancer. *Cancer Res* 2007; 67:8742-51.
63 Notting IC, Buijs JT, Mintardjo R, van der Horst G, Vukicevic S, Löwik CWGM, Schalij-Delfos N, Keunen J, van der Pluijm G. Bone Morphogenetic Protein 7 inhibits tumor growth of uveal melanoma *Invest Ophthalmol Vis Sci* 2007 48:4882-9.

Jeroen_Buijs_18.indd 194 26-11-2008 10:19:03

Chapter 8

General Discussion

Jeroen_Buijs_18.indd 195 26-11-2008 10:19:04

Jeroen_Buijs_18.indd 196 26-11-2008 10:19:04

The skeleton is one of the most commonly affected organs in metastatic disease, and it is a major cause of morbidity, characterized by severe pain and high incidence of fractures, spinal cord compression and bone marrow aplasia requiring hospitalization. However, only a restricted number of solid cancers, especially those of the breast and prostate, are responsible for the majority of the bone metastases [1-4]. Despite the high frequency of skeletal metastases, the molecular mechanisms underlying the predisposition for tumors to colonize bone are poorly understood and treatment options are often unsatisfactory. Therefore, the focus of this thesis is to better understand the processes that contribute to the formation of distant metastasis (**chapter 2**), particularly to bone (**chapter 4–7**), as well as to explore new treatment strategies with conventional (**chapter 4** and **5**) and novel therapeutic molecules (**chapter 6** and **7**) using new and better animal models (**chapter 3–7**).

PAS+ Structures as Predictor of Clinical Outcome in Breast Cancer Patients

Although current clinicopathologic parameters are widely used to predict outcome, the clinical behavior of prostate and breast cancer can still be quite different [5]. In order to improve breast and prostate cancer management, better and reliable markers are needed that can distinguish patients with good and poor prognosis.

In **chapter 2**, we demonstrate that, in addition to the tumor blood vessels, different thin periodic acid-Schiff-positive (PAS+) meshworks may exist in invasive ductal carcinoma (IDC) of the breast and their lymph node metastases. More importantly, the complexity of the PAS+ meshwork in the lymph node metastases was related to poor prognosis. Moreover, we found that the presence of the most complex thin PAS+ pattern — the PAS+ network — in lymph node metastases and stage classification of the tumor were the only two independent risk factors associated with the occurrence of a distant metastasis. Additionally, the presence of a PAS+ network in a positive lymph node is the factor most strongly associated with poor prognosis.

Immunohistochemically, these PAS+ meshworks showed continuous expression of SMA and patchy expression of CD31. The presence of lumina in the PAS+ meshwork might be indicative for septa that may facilitate perfusion and/or dissemination of cancer cells. Indeed, tumor cells were frequently present in the lumina, whereas, erythrocytes were only occasionally found in these structures.

In 63 % of the patients, thin PAS+ patterns were present in both the primary tumors and in their respective lymph node metastases. Some tumors may, therefore, have the capability to form such PAS+ patterns; however, none of the thin PAS+ patterns scored in primary tumors appeared to be of prognostic significance. The non-prognostic value of these patterns in primary tumors can be explained by the coexistence of other PAS+/SMA+ structures in primary tumors or normal breast tissue, that hamper the interpretation. Most probably, myoepithelial cells and myofibroblasts interfere with scoring of the PAS+ patterns in the primary breast cancer.

Foss and co-workers provided evidence that PAS+ extracellular septa could be particularly favorable substrates for the in-growth of angiogenic, and possibly lymphatic, vessels [6]. Consequently, tumors that contain these PAS+ structures might be more aggressive, as these structures provide better means for (blood) vessel in-growth than tumors lacking these structures. The lack of continuous flt-4 (alias VEGFR-3) expression in the PAS+ networks of breast cancer patients may, therefore, indicate that these structures do not entirely represent lymphatic vasculature. Indeed, the differences in distribution of flt-4+ and CD31+ patterns within the PAS+ networks in our tissue specimens from the patients, support the notion that PAS+ meshworks are complex and consist of multiple types of vasculature (blood vessels, and possibly lymphatics). If the septa consist of two layers of ECM elaborated by opposing layers of tumor cells, the layers could separate, forming channels and laminar openings. Such openings could particularly lead to capillary growth. The patchy expression of the endothelial marker, CD31, is in agreement with this hypothesis. Finally, it has been suggested that the open ends of the growing capillaries could feed blood into the channels. This may explain the presence of erythrocytes in the channels, reconciling different hypotheses [7].

In both uveal and cutaneous melanoma the presence of networks that stain positive with PAS has also been described [8-11] and was shown to be of prognostic significance as well [11-13]. These cancers could also generate such PAS+ networks *in vitro* without participation of endothelial cells and thus independent of angiogenesis. This was termed 'vasculogenic mimicry' (VM) to emphasize their *de novo* generation [6,14-19]. In VM, the PAS+ interconnected loops are the tumor-lined vessels that might be perfused indicated by the presence of erythrocytes. Tumor cells that form the PAS+ loops express a variety of endothelial markers, such as VE-cadherin. It was reported that vasculogenic mimicry may also exist in ovarian [20], prostate [21] and inflammatory breast cancer [14,22]. It is tempting to speculate that tumor cells that align hollow tubular structures are phenotypically distinct from other tumor cells due to epithelial cell plasticity. Accordingly, epithelial cell plasticity might be a prerequisite for a tumor to form such a network [21]. The absence of expression of VE-cadherin, an endothelial marker that was shown to be a crucial molecule for melanoma VM [23], in both the MDA-MB-231 (MDA-231) and PC-3M-Pro4 cell lines (unpublished results), makes it less likely that VM is also present in our models.

Although the exact nature and origin of the PAS+ network in different carcinomas remains to be elucidated, the presence of PAS+ patterns, at least in breast cancer (**chapter 2**), uveal and cutaneous melanoma [11-13], is a strong and independent risk factor for the occurrence of a distant metastasis. Therefore, by examining IDC patients for the presence of PAS+ networks in their lymph node metastases, the clinical behavior of this heterogeneous group of breast cancer patients can be better predicted, which may ultimately lead to improved management of the disease.

Jeroen_Buijs_18.indd 198 26-11-2008 10:19:04

A Mouse Model of Bone Metastasis using Bioluminescent Imaging

Animal models have become important tools to study the molecular mechanisms that are involved in the formation of bone metastases, and have adequately served as pre-clinical models to test new drug compounds and strategies. The formation of bone metastases after injection of breast cancer cells into the left cardiac ventricle of immunodeficient (*nu/nu*) mice, has been one of the most widely used model of bone metastasis [24-26]. This experimental setting closely resembles the clinical situation of *minimal residual disease* (MRD) after removal of the primary tumor. However, radiographic analysis for detection of experimentally-induced bone metastases is far from ideal. Firstly, radiologically evident osteolytic/osteosclerotic metastases are a late and macroscopic event in the evolution of metastatic bone disease. Thus, radiography lacks the sensitivity that would be necessary to investigate initial processes, such as the 'angiogenic switch', which may be critical for tumor progression [27]. Secondly, radiography does not detect actual tumor burden but reveals only changes in bone mineral density, which is an indirect, late, and inconsistent sign of the presence of a tumor. In fact, determination of an osteolytic area depends on the ability of the cancer cells to secrete bone-resorbing cytokines rather than on tumor mass itself. Furthermore, the determination of the osteolytic area does not take into account the extension of the tumor burden in the surrounding soft tissues. Therefore, more sensitive and direct methods of detecting bone metastatic growth in experimental animals are needed.

As described in **chapter 3**, we are now able to directly monitor the distribution and growth of luciferase-transfected cancer cells in intact animals using whole-body bioluminescent reporter imaging (BLI). BLI is based upon photon signals emitted by luciferase-expressing cancer cells after addition of the substrate luciferin, and provides a direct indication of tumor viability and growth. In comparison with the indirect detection using radiography, the BLI method yields higher sensitivity, reliability, and statistical power. The remarkable sensitivity of the optical imaging in detecting microscopic bone marrow (BM) metastases allows the detection of bone micrometastatic deposits of 0.5 mm^3 volume, preceding the appearance of radiological evident osteolysis by ~2 weeks. In fact, newer optical imaging modalities with even better resolution have already been developed. In **chapters 4–7**, BLI was used both to study the molecular mechanisms in bone metastasis, as well as to develop and evaluate conventional and novel treatments.

Treatment of Bone Metastases with Bone Resorption Inhibitors

Interference with the microenvironmental growth support has been proposed as an attractive strategy for decreasing metastatic tumor growth [28]. Bone is a dynamic tissue that is continuously remodeled by bone resorption and subsequent bone formation [29]. Animal and human studies have shown that increased bone remodeling promotes the formation of bone

metastases through the release of factors from bone matrix that support metastatic growth in the BM [30,31]. Differently from other tissues, agents that specifically interfere with the tumor microenvironment are available for bone and bisphosphonates (BPs) are used clinically for the protection of bone destruction by metastases from different primary tumors [32-36].

In **chapter 4**, we have shown that treatment with clinically relevant doses of BPs before the establishment of micrometastases (preventive protocol) reduced the number of developing bone metastases by ~70%. This level of inhibition is consistent with the observation that in the experimental animal not more than 70% of the bone resorption can be inhibited by high doses of BPs [37]. Possibly, this persistently low level of bone resorption is sufficient to provide growth support to a minimal number of micrometastatic foci. BP treatment also inhibited the early progression of tumor growth in the small number of still developing metastases. However, at later stages, when bone metastases have already developed, BP treatment did not inhibit tumor growth.

So, when BPs were given to animals with established bone metastases they did not inhibit the growth of breast cancer cells in the bone microenvironment, despite a substantial anti-osteolytic effect. There are at least three hypotheses to explain these data, the lack of tumor growth response was due 1) to the magnitude of suppression of bone resorption and, hence, the potency of the BPs given, 2) to the mechanism of inhibition of bone resorption by the BPs, or 3) that the initial growth phase of cancer cells in bone is dependent upon the interaction with the bone microenvironment, but eventually becomes independent of the bone microenvironment and can progress autonomously.

To address these issues, we used an experimental model of intraosseous growth and compared the effects of very high doses of the most potent BP currently available [38,39], zoledronic acid (ZOL), with the effects of osteoprotegerin (Fc-OPG), which inhibits bone resorption by a different mechanism of action (**chapter 5**). As expected, both Fc-OPG and ZOL treatment markedly suppressed bone resorption, protected the integrity of bone trabeculae and prevented the development of osteolytic lesions. Intraosseous tumor burden was reduced, however, the total tumor burden (intra-bone and extramedullary) still progressed. Although at the end of the experiment the total tumor burden in treated groups appeared less compared to controls, this difference was not significant.

Previous studies of the effects of BPs on bone metastatic breast cancer growth in animal models have shown contradictory results. BPs were reported to reduce the tumor burden in established bone metastases but not in soft tissue and visceral metastases. This effect seemed to be mediated by induction of apoptosis of the cancer cells [25,40]. Treatment with BP, given before the development of evident metastasis, resulted in a marked reduction of the number of bone metastases [25,41,42]. However, another preventive study showed that BP treatment resulted in an increased tumor burden in the developing bone metastases but not in visceral metastases [43]. In these investigations tumor burden has been quantified by indirect measurements of the tumor-induced osteolytic area on bone radiographs and end-stage

Jeroen_Buijs_18.indd 200 26-11-2008 10:19:04

histology. In contrast, BLI allowed us to detect the total tumor burden directly and more sensitive, yielding more reliable data. Our BLI data favor the hypothesis that metastatic cancer cells in bone — after an initial growth phase that depends on their interaction with the BM stroma and extracellular bone matrix — become increasingly independent of microenvironmental growth factor support and is self-maintained by autocrine mechanisms.

How can the therapeutic effect of inhibition of bone resorption/turnover on early stages of bone metastasis development be explained? Bone remodeling does not occur throughout the entire bone surface but takes place at microscopic patches of bone resorption and subsequent bone formation. The number and activity of so-called basic multicellular units (BMUs) determine the rate of bone turnover. We hypothesize that the probability that a micrometastasis becomes a clinically evident bone metastasis should be related to the chance that metastasis-initiating cells (MICs) are in close proximity with an active BMU. MICs may extravasate near active BMUs, or dormant MICs may encounter active BMUs. In either case, a higher number of active BMUs (high bone turnover rate) increases the probability that MICs come in close proximity of active BMUs. This hypothesis is substantiated by clinical data demonstrating that high bone turnover in cancer patients with metastatic bone disease is associated with skeletal-related events, disease progression and death [44-47], and by experimental evidence showing that high bone turnover is causally associated with establishment and progression of bone metastases [31,48]. Accordingly, inhibition of bone turnover before the generation of a self-maintaining, autocrine cancer cell growth may arrest the vicious cycle underlying the initial growth support by the BMU and ultimately prevent the outgrowth of a micrometastasis into an overt bone metastasis.

Based on our preclinical data (**chapter 4**) and that of others, one may predict that BP therapy as adjuvant treatment in breast cancer patients decreases the risk of formation of new bone metastases. However, clinical studies have shown mixed results with regard to the development of new bone metastases. Clodronate as adjuvant therapy significantly reduced [49], non-significantly reduced [50], or did not reduce [51,52] the development of new bone metastases. Nevertheless, the largest reported randomized controlled study to date of BP use in patients with breast cancer demonstrated that clodronate significantly improved bone relapse-free survival [52,53]. Results from the National Surgical Adjuvant Breast and Bowel Project B34 trial, an even larger randomized placebo-controlled trial of clodronate versus placebo in women with early-stage breast cancer who have received standard adjuvant systemic therapy, are awaited.

Although current clinicopathologic parameters are widely used to predict clinical outcome, the clinical behavior of breast (and prostate) cancer can still be quite different. Therefore, more specific and more reliable markers that can distinguish between patients with high and low risk for bone metastasis formation are needed, and may become the rationale to start adjuvant BP treatment even before the onset of bone metastatic disease.

At present, the most promising approaches that may lead to a better identification and stratification of the cancer patients at risk to develop bone metastases are the 1) assessment of bone turnover status, 2) use of microarray technology, and 3) detection of disseminating tumor cells (DTCs) in BM (and blood).

Although high bone turnover rate in bone metastatic cancer patients is associated with bone disease progression [45-47], to date, it has not been specifically addressed whether high bone turnover in non-metastatic cancer patients is associated with subsequent formation of new bone metastases. Interestingly, many cancer patients with a resected primary tumor display a high bone turnover rate, which is either induced at a basal level (e.g., induced by menopause) or induced after surgical or chemical gender steroid deprivation. Especially these patients — who probably harbor micrometastatic MICs in the BM at the moment of diagnosis and/or surgery — may benefit from prophylactic bone resorption inhibition by BPs.

Microarray analysis is a new and promising technique that may also identify which patients are at increased risk for developing bone metastases. Using this technology, Kang and co-workers generated a 122-gene bone metastasis signature by comparing gene expression among sublines of the human breast cancer cell line, MDA-231, that are highly vs. weakly metastatic to bone in nude mice [54]. Moreover, Woelfle and co-workers reported a 73–gene signature capable of identifying lymph node-negative patients with or without BM micrometastasis [55]. Furthermore, Smid and co-workers have studied lymph node-negative primary breast cancer and reported a putative molecular signature capable of predicting metastatic recurrence to bone vs. recurrence elsewhere in the body [56]. A 31-gene signature was selected to predict which patients developed bone metastases with 100% sensitivity and 50% specificity. The low specificity may reflect that microarray analysis only describes global mRNA obtained from the tumor, whereas all genes that are necessary to metastasize to bone have to be coordinately expressed in an individual tumor cell. Surprisingly, genes that were previously identified to promote bone metastasis such as IL-8 [57], PTHrP [58] and αvβ3 [59], were not members within any of these bone signatures. Although the bone signatures from Kang and Smid display a common increase in the FGFR-p42/44 MAPK pathway, it is still disappointing that just one single gene (*BENE*) is shared between any two of the three signatures. Besides differences in experimental approaches and patient population selected, the lack of overlap may also be reflected by the low reproducibility between studies using microarray technology. This was demonstrated by the comparison of two studies which both generated a gene signature capable to predict distant metastasis in lymph node negative breast cancer patients [60,61]. Although both studies included a similar number and type of patients, had comparable experimental design, and used similar statistical methods of validation, the resulting 70 and 76 gene predictors overlapped only by three genes.

Another approach to predict which patients are at high risk to develop a bone metastasis is to screen BM for the presence of DTCs. Although not only true MICs might be identified,

Jeroen_Buijs_18.indd 202 26-11-2008 10:19:04

the presence of DTCs in BM at time of diagnosis is significantly associated with the formation of distant metastases, particularly to bone [62,63].

In conclusion, these different approaches are very promising and may lead to a better stratification of patients at high risk for the *de novo* formation of bone metastasis, and therefore, may become the rationale to start adjuvant BP treatment even before the onset of bone metastatic disease. However, these approaches need first to be extensively validated in large confirmatory studies by independent groups.

BMP7 in Progression and Metastasis in Osteotropic Cancers

The increased motility and invasiveness of cancer cells are reminiscent of the epithelial-to-mesenchymal transition (EMT) that occurs during embryonic development [64]. The EMT is associated with decreased expression of epithelial markers such as E-cadherin, and increased expression of mesenchymal markers such as vimentin. By signaling through the Smad mediators, transforming growth factor (TGF)-ß is a well-known inducer of EMT in both embryogenesis and its' counterpart in cancer progression. However, in organogenesis, 'mesenchymal' cells may possess remarkable plasticity and may regain a fully differentiated phenotype via a mesenchymal-to-epithelial transition (MET) under the influence of bone morphogenetic protein (BMP) 7 [65-67]. Under pathologic conditions, particularly in malignant disease, the role of BMP7 has remained largely elusive.

Expression of BMPs during Cancer Progression

In **chapter 6** and **7**, we described that BMP7 expression in breast and prostate cancer cell lines *in vitro* correlated with expression of E-cadherin, and inversely correlated with aggressiveness and expression of vimentin. In addition, human prostate cancer cells from the primary tumor had a decreased BMP7 expression when compared with matched non-carcinogenic prostate epithelium as assessed by laser-microdissection and immunohistochemical staining. Overall, BMP6 is overexpressed in aggressive prostate cancer when compared with normal prostate tissue [68-70], and BMP2, BMP4, [70] and BMP7 (**chapter 7**) are expressed predominantly in normal prostate tissue, and their expression tends to be lower or absent during progression of prostate cancer (reviewed in [71]). In this regard, it should be mentioned that it seems to have become a general misconception that BMP7 was found to be significantly increased in prostate cancer bone metastases. This is probably due to the misleading title "Increased expression of BMP7 in bone metastatic prostate cancer" of an article [72], in which BMP7 mRNA expression levels in bone metastatic prostate cancer from autopsies were only found to be significantly increased when compared to non-tumor bearing bone, not when compared to primary tumor. Therefore, this first needs to be further investigated, including immunohistochemical staining for BMP7 on autopsy material.

BMP7 expression in prostate cells is regulated by androgens because orchidectomy decreased BMP7 expression [73], while testosterone and dihydrotestosterone increased it [74] (Fig. 1). These observations are in line with our data, showing that BMP7 expression is reduced in prostate cancer cell lines that are androgen-insensitive. These data, consequently, raise the question that evolution of prostate cancer to metastatic dissemination after hormonal therapy may be linked to the loss of androgen-induced BMP7 expression

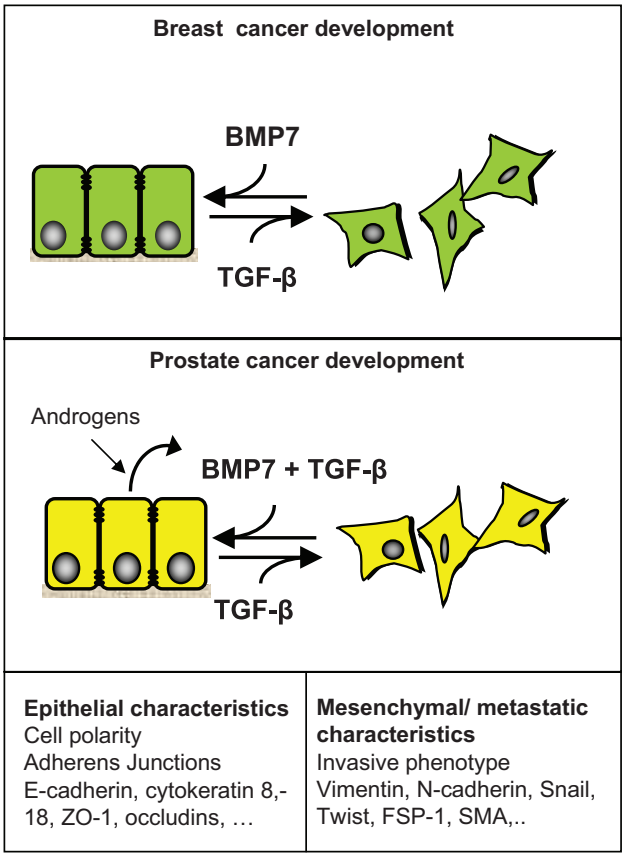

Figure 1 **Role of BMP7 in cancer progression.** Top: In breast cancer, TGF-ß and BMP7 exert opposing effects. Whereas TGF-ß induces epithelial-to-mesenchymal (EMT), BMP7 induces the opposite process of mesenchymal-to-epithelial transition (MET). Bottem: Similarly, BMP7 induces MET, and TGF-ß induces EMT in prostate cancer cells. Remarkably, BMP7 induces MET more prominently in the presence of TGF-ß in prostate cancer cells. In the prostate gland, androgens stimulate the production of BMP7 by prostate epithelial cells. In the later stage of the disease, BMP7 ceases to act on cancer cells, potentially because of the loss of androgen-induced production of BMP7 after anti-androgen therapy. Subsequently, TGF-ß alone induces EMT, including repression of E-cadherin expression and stimulation of the acquisition of an invasive phenotype. Consequently, the cancer cells with an acquired metastatic potential can disseminate through the bloodstream to other organs, including bones.

Jeroen_Buijs_18.indd 204 26-11-2008 10:19:04

and loss of epithelial phenotype maintenance. In other words, androgen deprivation therapy may directly result in perturbation of the epithelial homeostasis.

The expression of different BMPs in breast cancer progression is less well-studied, and only a very limited number of studies have explored the consequences of BMP signaling on patient outcome. In ductal breast cancer patients, BMP2 expression did not affect the overall or relapse-free survival [75], whereas overexpression of BMP receptor IB associated with poor prognosis in estrogen receptor (ER)-positive breast cancer [76]. In 170 breast cancer patients with IDC, Schwalbe and co-workers observed that expression of BMP7 protein was highly associated with ER and progesterone receptor (PR) levels. Using a tissue microarray (TMA), we confirmed indeed that expression of BMP7 in 520 breast cancer patients was associated with ER + PR levels (manuscript in preparation). To follow up on these findings, we are currently investigating whether treatment with the hormones estrogen and progesterone regulates BMP7 gene expression in breast cancer as well (manuscript in preparation). Furthermore, our TMA data did not show an association between BMP7 expression in primary tumor and (disease free) survival or metastatic pattern. This seeming discrepancy with the data that BMP7 mRNA was associated with formation of bone metastasis (**chapter 6**), may be explained by the findings from Alarmo and co-workers who showed that there is no significant correlation between BMP7 copy number, BMP7 mRNA and BMP7 protein levels [77]. This is substantiated by the fact that invasive lobular carcinoma (ILC) of the breast expressed elevated levels of BMP7 protein when compared to IDC, even though an increase in *BMP7* gene copy number was found in IDC, but not in ILC [77]. The observation that regulating the recruitment of histone deacetylase HDAC2 to the BMP7 promoter region acts as a regulatory mechanism to control BMP7 expression [78], suggests that the lack of association between BMP7 copy number and BMP7 mRNA may be due to epigenetic regulation. Moreover, the lack of correlation between BMP7 mRNA and protein expression levels could be a result of the stability of mRNA or protein. The 3'UTR of BMP7 mRNA is very long, which is a characteristic that has been linked to mRNA stability [79]. Subsequently, translation could occur from very few copies of mRNA. The involvement of microRNAs — non-coding small RNAs that primarily function as gene regulators [80] — on regulating BMP7 mRNA has not been addressed to date, but the presence of such microRNAs may greatly influence BMP7 mRNA stability. In addition, BMPs are synthesized as pre-proteins, which are modified to mature BMPs by pro-domain cleavage, and are subsequently secreted. Pro-domains are known to affect the stability of the BMP protein [81]. Taken together, it is likely that both mRNA and protein processing are involved in the regulation of BMP7 expression levels.

Although the finding from Alarmo and co-workers that BMP7 expression was lost from most of the local recurrences as compared with the corresponding primary tumor [82] is in agreement with our data, the observation that BMP7 protein levels in primary breast cancer are associated with the formation of bone metastases [82], is not. In contrast to Schwalbe and our findings, Alarmo and co-workers did not find an association between BMP7 and ER or

PR [82]. They explained this discrepancy by differences in tumor materials and classification of immunohistochemical staining results. Surprisingly, only 37% of primary IDC and 57% of primary ILC were classified as being positive for BMP7, while in an earlier study the same authors showed that the majority (71.4%) of 91 breast cancer patients (IDC+ILC) showed strong BMP7 staining, whereas moderate staining was observed in the rest of the cases [77]. Even though they performed an additional antigen retrieval step, one would not expect that BMP7 staining was detected exclusively in the cytoplasm, when an earlier study showed exclusive nuclear staining in primary breast cancer cells using the same antibody (sc-9305; D.Bobinac, personal communication).

Using tissue micro arrays containing malignant primary skin melanomas [83] or primary renal carcinomas [84], BMP7 was associated with poor and good prognosis, respectively. This apparent contradiction underlines once more the heterogeneous effects that specific BMPs can exert on different cell types.

BMP7, Cellular Function and Signaling

BMPs have a well-known role in osteogenesis by inducing differentiation of cells from the osteoblast lineage and enhancing osteoblast activity [85,86]. For example, BMP7 has the ability to enhance osteoblast activity, partly by inducing VEGF expression [87]. Therefore, BMPs have also been implicated in the sclerotic phenotype of bone metastases. Noggin is a BMP antagonist and inhibits BMP2, -4, -6, -7 signaling by binding BMP ligands [88]. Indeed, overexpression of Noggin in osteosclerotic prostate cancer cell lines significantly decreased the osteoblastic response *in vivo*, but tumor burden was not affected [89,90]. In contrast, overexpression of Noggin in the osteolytic prostate cancer cell line PC-3 significantly inhibited the expansion of the lesion *in vivo* [91]. In this and other studies, particularly BMP2 and BMP6 stimulated migration and invasion of prostate cancer cells, while BMP4 and BMP7 had no or almost no effect [89,91,92]. Direct experimental evidence that a specific BMP could affect the osteoblastic response was provided when neutralizing BMP6 antibodies inhibited, besides intra-bone tumor growth, the blastic response [92]. Taken together, the inhibitory effects of Noggin on cancer progression are most probably mediated by antagonizing the pro-tumorigenic effects of BMP2 and BMP6, rather than antagonizing BMP4 or BMP7.

Many different BMP7-induced biological effects are known, but they are mostly cell type-dependent as well as dose-dependent. In prostate cancer, addition of BMP7 to *in vitro* cultured cells has resulted, so far, in at least three different kinds of responses, affecting 1) proliferation, 2) apoptosis, and 3) cellular plasticity (Fig. 2*A*)[93-97].

Although under normal culture conditions — 10% fetal calf serum (FCS) in culture medium — BMP7 did not affect proliferation of PC-3 cells, BMP7 could inhibit the proliferation of the LNCaP, PC-3 and DU 145 cells under culture conditions of 1% FCS [94]. The observed G1-arrest was most likely caused by BMP7 induced up-regulation of the cyclin-dependent kinase inhibi-

Jeroen_Buijs_18.indd 206 26-11-2008 10:19:04

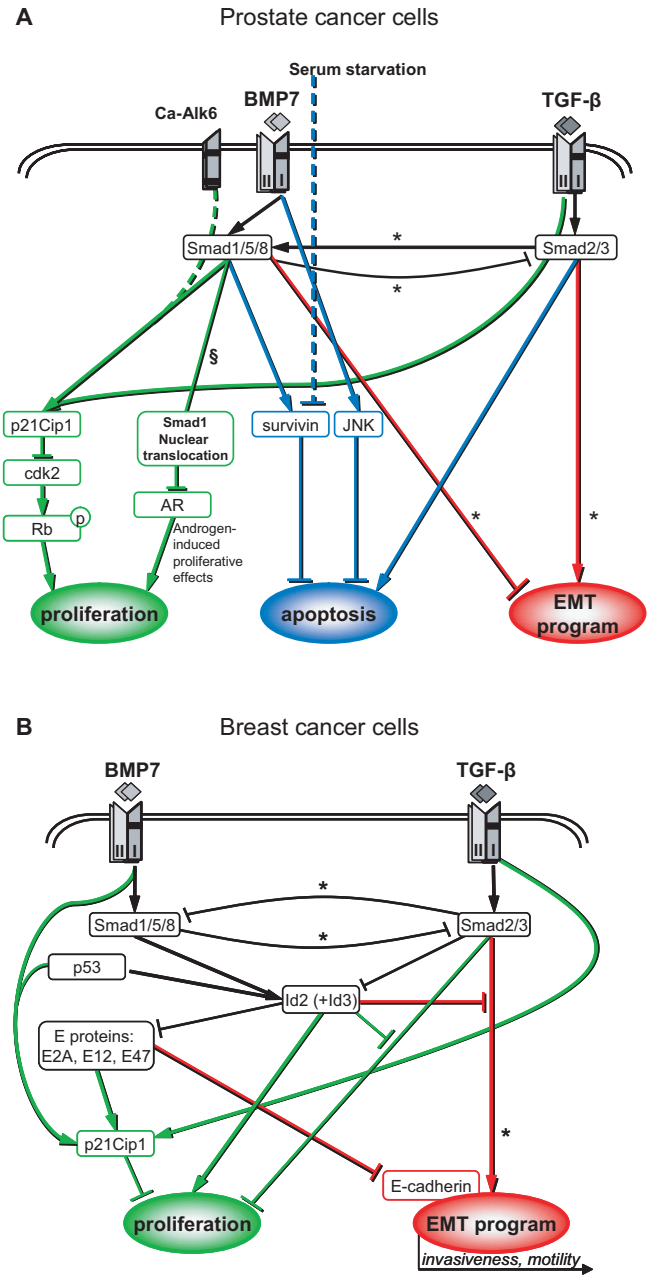

Figure 2 **BMP7-induced intracellular signaling cascades described in prostate (A) and breast (B) cancer cells, regulating cellular processes, such as proliferation, apoptosis and epithelial plasticity.** In addition, a very limited scheme for intracellular TGF-ß signaling is depicted . *, signaling pathway described in this thesis; §, described for BMP signaling; based on data from [93-96](A) and [115,116](B).

tor (CDKI) p21CIP1/WAF1 [94], as was also demonstrated for BMP2 and BMP4 in LNCaP cells [98]. Interestingly, BMP7 induced a concentration-dependent biphasic effect on the proliferation of LNCaP in the absence of exogenous androgen. While higher concentrations of BMP7 inhibited proliferation of LNCaP cells, lower concentrations of BMP7 stimulated the proliferation in the absence of androgen [94]. At yet another FCS concentration (0.5% FCS), the anti-proliferative effect of BMP7 was only detected in the cell line representing a benign prostatic epithelial hyperplasia (BPH-1), but not in the invasive PC-3 and DU 145 cells [97].

In keeping with the findings that BMP signaling can exert anti-proliferative effects, Kim and co-workers demonstrated that transfection of a dominant negative type II BMP receptor (BMPRII) into PC-3M cells (a PC-3 subclone), resulted in a growth rate 10 times higher than that of control cells in the murine tumor model [99]. In addition, the introduction of the constitutively active ALK6 (BMPRIB) in PC-3 cells resulted in the inhibition of cell proliferation *in vitro* as well as inhibition of tumor growth after subcutaneous injection [94].

In the second type of response, BMP7 protected prostate cancer cells from stress-induced apoptosis. Yang and co-workers have shown that BMP7 inhibited serum starved-induced apoptosis in LNCaP and C4-2B cells [96]. In the C4-2B cells, this was mediated via both Smad5-dependent upregulation of Survivin and Smad-independent activation of the JNK pathway.

Finally, the third type of described responses to BMP7 is related to cell plasticity. It has long been recognized that TGF-ß can induce morphologic conversion, invasiveness, and migration in epithelial cells, collectively referred to as an EMT [64]. BMP7, however, was shown to induce the opposite process, the mesenchymal-to-epithelial transition (MET) in renal epithelial cells [100,101]. In **chapter 7**, we demonstrate that BMP7 induce MET in prostate cancer cells, as demonstrated by induced E-cadherin promoter activity and E-cadherin protein expression, and concomitant inhibition of vimentin expression. Therefore, we hypothesize that BMP7 expressed in normal epithelial cells induces E-cadherin expression and contributes to maintenance of an epithelial state, whereas loss of BMP7 during cancer progression may result in EMT and metastasis (Fig. 1). In prostate cancer cells, the effects of BMP7 could be further potentiated by addition of TGF-ß (Fig. 3). The synergistic actions of BMP7 and TGF-ß were not detected in any other epithelial cell line studied so far and may be cell-specific for reasons that remain to be explained.

In contrast, Yang and co-workers showed that BMP7, but not TGF-ß, stimulated EMT in PC-3 cells [97]. However, in addition to our *in vitro*, *in vivo*, and clinical data, a protective role for BMP7 is substantiated by data obtained in numerous studies that showed that 1) loss of BMP7 increases the invasive and migratory properties of prostate cancer cells [102], 2) BMP7 is downregulated in recurrent prostate cancer [74], and 3) that BMP receptors are frequently lost during prostate cancer progression [99,103]. Interestingly, the accessory type III receptor endoglin was shown to decrease prostate cancer cell migration and invasion through activation of ALK2–Smad1 pathway [104]. This is in total agreement with earlier data, which showed

Jeroen_Buijs_18.indd 208 26-11-2008 10:19:04

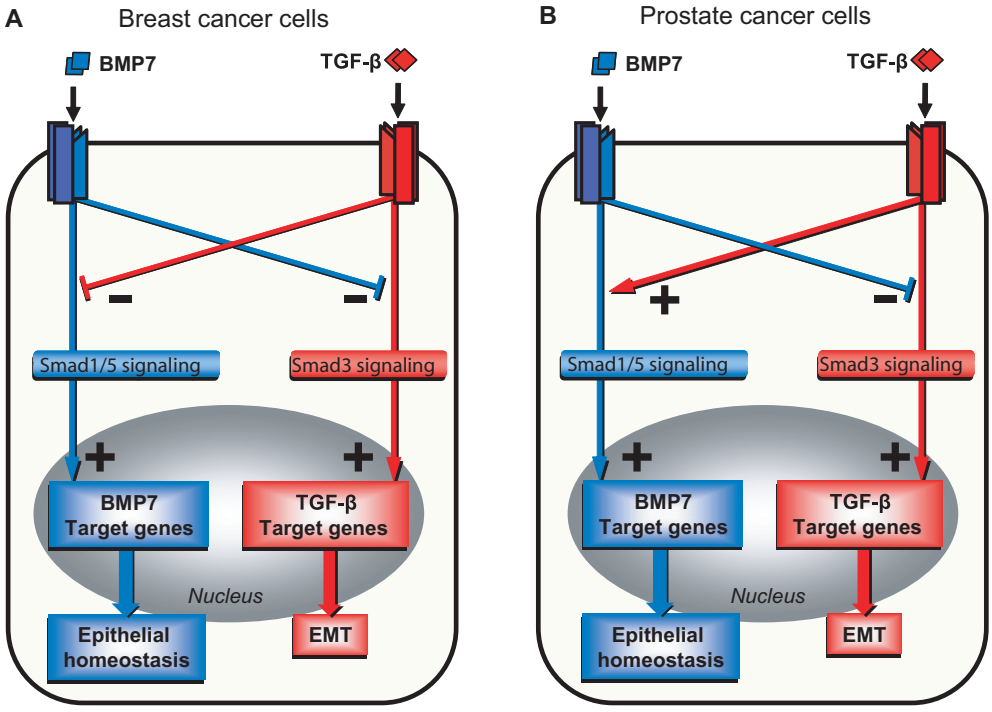

Figure 3 **Interactions between TGF-ß and BMP7 signaling.** The biological distinct effects of TGF-ß and BMP7 can be explained at the level of intracellular signaling. *A,* in breast cancer cells, BMP7 can inhibit Smad-dependent TGF-ß-signaling, and vice versa, TGF-ß can inhibit Smad-dependent BMP7-signaling. *B.* In prostate cancer cells, TGF-ß has an stimulatory rather than an inhibitory effect on BMP7-signaling. Consequently, BMP7 alone or in combination with TGF-ß, results in epithelial maintenance. However, when BMP7 expression is lost, TGF-ß may still trigger the TGF-ß-induced EMT and acquisition of a metastatic phenotype. So, whereas in breast cancer prevailed TGF-ß-signaling might already result in induction of an EMT, in prostate cancer, loss of BMP7 is a prerequisite for EMT to occur.

that endoglin inhibits TGF-ß1-induced ALK5–Smad3 signaling and promotes BMP7–Smad1/Smad5 signaling [105,106]. Therefore, we suggest that the inhibitory effects of BMP7 on prostate cancer cell migration and invasion are most likely mediated via its type I receptor ALK2 and is Smad-dependent.

Similarly, expression of BMP receptors was reduced, and BMP signaling was diminished in colorectal cancer, indicating that loss of BMP signaling also correlates tightly with progression of adenomas to colorectal cancer occuring relatively early during cancer progression [107,108].

Compared to prostate cancer, even less is known about the BMP effects in breast cancer cells. A dominant negative truncated BMPRII inhibited proliferation of T47D breast cancer cells suggesting a stimulatory role for BMPs [109]. In contrast, a dominant negative mutated

BMPRII — inhibiting BMP–Smad signaling, but not $p38^{MAPK}$ signaling — stimulated proliferation of NMuMG breast cancer cells suggesting a stimulatory role for BMPs via $p38^{MAPK}$ [110]. In breast cancer, BMP7 has not yet been studied in many functional studies. BMP2, however, is one the the most investigated BMPs in breast cancer. BMP2 can inhibit proliferation [111,112], inhibit hypoxia-induced apoptosis [75], stimulate migration of cancer cells, and induce tumor formation *in vivo* after subcutaneous implantation in nude mice [113]. In **chapter 6**, we describe that BMP7 does not affect proliferation, induces MET, and inhibits TGF-ß induced EMT in MDA-231 breast cancer cells. In line with its inhibitory role in cancer progression, we show that stable overexpression of BMP7 in MDA-231 breast cancer cells inhibits *de novo* formation and progression of osteolytic bone metastases.

In mammary (and other) epithelial cells, members of TGF-ß superfamily strongly regulate the expression of Inhibitor of DNA binding (Id) proteins in normal and cancerous cells in a Smad-dependent manner. Id proteins antagonize basic helix-loop-helix transcription factors by inhibiting them from DNA binding and transactivation of their target genes, thereby playing critical roles in animal development and cancer [114]. Kowanetz and co-workers have shown that Id2 and Id3 showed long-term repression by TGF-ß and sustained induction by BMP7 in NMe mammary, lens and other epithelial cells (Fig. 2*B*) [115,116]. Moreover, overexpression of Id2, and to a lesser extent Id3, blocked TGF-ß-induced EMT in these cells. Furthermore, BMP7 could counteract TGF-ß-induced EMT by overriding the downregulation of Id2 and Id3 by TGF-ß in lens epithelial cells. Surprisingly, Id2 knockdown in these cells not only enhanced TGF-ß-induced EMT, but also permitted EMT by BMP7. Thus, during tumor progression, misregulation of epithelial Id2 and Id3 expression could possibly allow even BMP pathways to cause EMT and enhance tumor invasiveness. Accordingly, Id2 was found to play an important role in the preservation and maintenance of the differentiated and non-invasive phenotype of breast cancer cells [117]. However, the role of Id proteins in our models has not yet been addressed. If regulation of Id proteins is also critically involved in biological responses in other carcinomas, such as prostate, the absence or very low basal level of Id2 and Id3 proteins in the PC-3 cells used by Yang might explain that BMP7 was capable to induce EMT [97].

Recently, it was demonstrated that BMP7 is a novel target of the p53 family in breast cancer [116]. In fact, Id2 is also regulated by p53, and whereas a functional BMP7 or an active p53 pathway was sufficient to maintain basal levels of Id2, loss of both pathways abrogated Id2 expression. Subsequently, loss of Id2 resulted in inhibition of cell proliferation [116]. Interestingly, p53 is the most frequently mutated gene found in human cancers, including breast cancer. For this reason, it is tempting to speculate that loss of both p53 and BMP7, which is the case for MDA-231 cells, may be a prerequisite for EMT in cancer cells that have already escaped from the anti-proliferative effects exerted by restrained Id2 signaling.

Although much remains to be understood about the complexity of signaling from BMPs in cancer, there is emerging evidence from a variety of tumor systems that the observed

Jeroen_Buijs_18.indd 210 26-11-2008 10:19:05

effects are cell specific and could be either pro- or anti-tumorigenic. Consequently, results derived from the study of one cell system frequently could not be applied to other systems of the same cancer type. While the BMPs themselves may hold some of the answers, BMP receptors are probably also determining factors in distinguishing between the pro- or anti-tumorigenic effects seen in cancer cells. There is a good possibility that further understanding of the expression pattern of the type I and type II receptors and their relationship to the development and progression of cancer may provide much more information on this phenomenon. In addition, the physiological response of many different types of cancer cells might also very well be explained by the basal level and regulation of sensitive gene targets, such as *Id2* and *Id3*.

It is important to note that analogous to its protective role in breast and prostate cancer progression (**chapter 6** + **7**), we have recently demonstrated that decreased BMP7 expression also contributes to progression of uveal melanoma [118].

BMP7 Treatment in Experimental Models

It has never been specifically addressed whether systemic treatment with (any) BMP might influence the progression of (breast and prostate) cancer. In line with our earlier observations that BMP7 inhibits tumorigenicity in breast cancer, we describe in **chapter 6** that daily intra venous administration of BMP7 (100 µg/kg/d) significantly inhibited orthotopic and intra-bone growth of MDA-231-B/Luc+cells in nude mice. In addition, we describe in **chapter 7** that BMP7 treatment also inhibits PC-3M-Pro4/Luc+ prostate cancer bone metastatic growth. However, prostate cancer growth was not inhibited after orthotopic implantation. Clearly, the tumor microenvironment is an important determinant of the therapeutic response to BMP7 in prostate cancer. In fact, it cannot be excluded that the successful treatment may also be explained by direct effects of BMP7 on tumor stroma. This question may, for example, be adequately addressed in an experiment in which cancer cells are transfected with a constitutively active form of ALK2, excluding the direct BMP7 effects on the stroma.

Interestingly, the effects of BMP7 can be further potentiated in prostate cancer cells by an environment rich in TGF-ß, such as in bone, because the combination of BMP7 and TGF-ß increased E-cadherin and decreased vimentin expression to greater extent than BMP7 alone (Fig. 1-3). In prostate cancer, these synergistic actions of BMP7 and TGF-ß may explain the successful experimental treatment of skeletal metastases and intra-bone growth, but not of orthotopic growth. For the full beneficial effects of BMP7 in prostate (cancer) cells, paradoxically, the presence TGF-ß may be needed for BMP7 to fully function as a growth factor that maintains the epithelial homeostasis. Taken together, the tumor microenvironment is an important determinant of the therapeutic response to BMP7 in prostate cancer.

In the bone matrix, TGF-ß is highly concentrated in an inactive form that can be released and activated by osteoclastic resorption [119]. Upon activation, TGF-ß may act as a paracrine

growth factor for neighboring cancer cells that may have colonized the BM [120]. In this context, our observation that BMP7 could counteract TGF-ß signaling in both breast and prostate cancer cells (Fig. 1-3), may be very important in explaining the successful treatment of osteolytic bone metastases from breast and prostate cancer (Fig. 4). The important role of TGF-ß in the progression of bone metastasis was established in experiments that showed that interference with TGF-ß signaling by either small-molecule inhibitors of ALK5 (TßRI) kinase [121,122], overexpression of the inhibitory Smad7 [123], or introduction of a dominant negative TßRII [58] could reduce osteolytic tumor burden. Nevertheless, we did not provide direct evidence that BMP7 inhibits TGF-ß signaling *in vivo* as it does *in vitro*. We are in the process

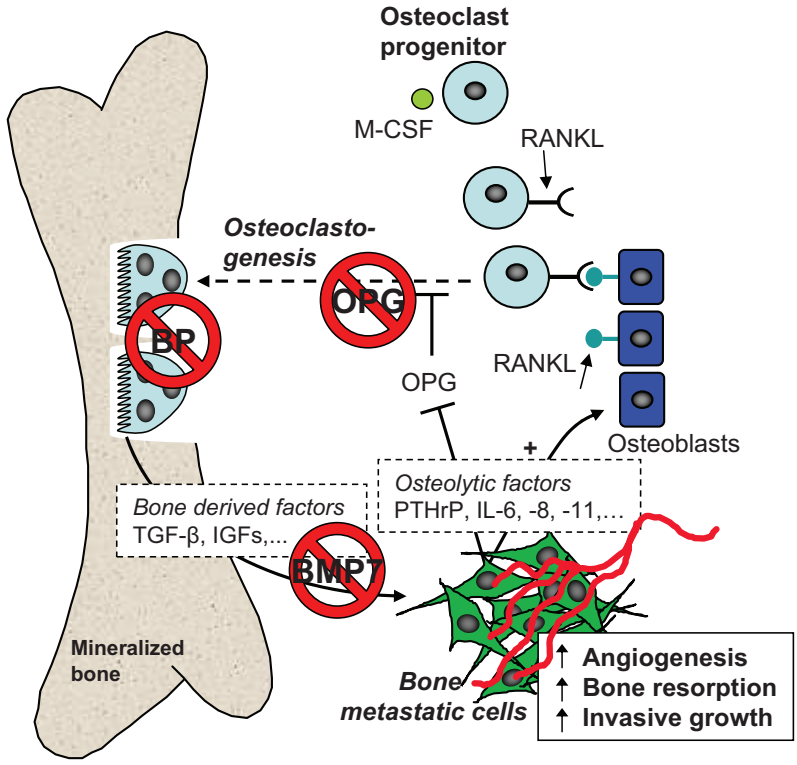

Figure 4 **Potential mechanisms to inhibit bone metastatic growth**. Osteoclastic bone resorption results in release of growth factors, such as TGF-ß, from the bone matrix that may stimulate (cancer) cell growth. Therefore, inhibition of bone resorption provide a potential mechanism for treatment and prevention of bone metastasis. Either treatment with OPG, inhibiting the formation of osteoclasts, or treatment with a bisphosphonate (BP), reducing the number of active osteoclasts, may not only inhibit osteolysis but also the development and growth of bone metastases. It is important to note that in both blastic and lytic lesions the osteoclastic bone resorption is increased and plays an important role in the pathophysiology of the bone metastasis. BMP7, either endogenously expressed or given as a therapeutic agent, can inhibit TGF-ß signaling in cancer cells. Therefore, BMP7 may also represent a novel therapeutic molecule that may also halt or slow down the progression and development of bone metastases.

Jeroen_Buijs_18.indd 212 26-11-2008 10:19:05

of addressing this using an *in vivo* model in which cancer cell line lines stably expressing the TGF-ß-specific reporter construct CAGA-luciferase are monitored (manuscript in preparation). Using this enhancement of our *in vivo* models, the effects of various compounds, such as BMP7, on TGF-ß signaling in cancer cells will be elegantly monitored.

In conclusion, we provide a role for BMP7 expression in the maintenance of epithelial cell behavior in the breast and prostate. We propose a model wherein BMP7 can induce the expression of E-cadherin, repress vimentin synthesis, and prevent EMT in normal epithelial cells. In later stages of tumorigenesis, cancer cells lose BMP7 expression or become resistant to the BMP7 secreted by surrounding normal epithelial cells. Consequently, malignant cells may lose their expression of E-cadherin under the influence of TGF-ß, resulting in EMT and subsequent metastatic spread. In prostate cancer, TGF-ß may even contribute to the epithelial homeostasis as long as BMP7 remains present as well. This model re-emphasizes the double-edged-sword properties and the complexity of members of the TGF-ß superfamily in cancer biology. It also provides a rationale for further investigation of BMP7 in the prevention of osteolytic bone metastases from breast and prostate cancer. Overall, we provide novel and possibly clinically relevant perspectives for the therapeutic use of BMP7, but also raise numerous questions regarding the molecular mechanisms involved, and its role at different stages of cancer that exemplify the promises but also the versatility of the members of the TGF-ß superfamily.

BMP7, Future Perspectives

Since we position BMP7 as a promising novel therapeutic molecule for repression of systemic breast and prostate cancer progression, it is of utmost interest to unravel the molecular and biological roles of BMP7 in cancer progression and bone metastasis formation that have not yet been addressed. Given the correlation between BMP7 and androgens — BMP7 expression is associated with androgen receptor status, and stimulated by androgens — it is of great interest to study the effects of BMP7 treatment on androgen-positive cell lines in experimental models as well. In addition, the effect of BMP7 on the initial phases of metastasis and on osteosclerotic lesions also remains to be investigated.

In our animal models, orthotopic breast and prostate cancer growth does not lead to distant metastases. Hence, studying the role of BMP7 in inhibiting EMT in the process of metastasis requires investigation in animal models in which tumor cells metastasize from the primary site to distant sites, such as bone. For this, very few models are available that recapitulate the events of the entire metastatic cascade attributable to prostate or breast cancer. A relevant model that fulfills this requirement, and shows enhanced metastasis with increased TGF-ß signaling uses a genetically engineered expression of the proto-oncogene Her2/Neu (erBB2), a receptor tyrosine kinase under the control of the mouse mammary tumor virus in mouse mammary gland [124]. In this system, mammary tumors spontaneously

developed and metastasized to lung. Overexpression of either active TGF-ß [125] or a constitutively active form of ALK5 [126] increased metastasis formation, whereas impairment of the TGF-ß pathway in mammary cells with a dominant negative form of the TßRII [126], or administering a soluble form of TßRII [125], decreased the frequency of metastasis to the lungs. Analysis of endogenous expression of BMP7 and EMT markers, as well as testing the effects of a BMP7 treatment could answer questions about BMP7 antagonism of TGF-ß-induced EMT and the early steps of metastasis. However, bone metastases do not develop in this model.

Particularly, transgenic mice that spontaneously develop primary breast or prostate tumors may very well be used to further elucidate the role of BMP7 in development and progression of these carcinomas [128]. For example, in these transgenic mice the BMP7 gene could be knocked-out using the Cre/loxP system in a prostate or breast specific manner.

In another model, inoculation of the 4T1 murine breast cancer cells into the mammary gland results in formation of a primary tumor that disseminates to lung, adrenal glands, and bone. Using this model, Muraoka and co-workers showed that inhibition of TGF-ß signaling with a soluble type II receptor significantly reduced metastases [127]. Unfortunately, EMT or bone metastases have not been studied in this model.

Most patients with prostate cancer metastases manifest with radiologically osteoblastic lesions. However, enhanced osteoclastic bone resorption is also clearly evident and contributes to the pathophysiology of bone metastasis in this setting. In fact, the bone resorption marker N-telopeptide is increased in prostate cancer patients with bone metastases and is a stronger predictor of death than prostate specific antigen [46]. Furthermore, BPs also improve skeletal morbidity in patients with osteoblastic disease [129]. Although our animal model lacks a strong osteoblastic component that is often evident in humans with prostate cancer bone metastases, important information can be gleaned regarding the role of BMP7 in osteolytic prostate (and breast) cancer bone metastases. Nonetheless, the effect of BMP7 on bone metastases with a sclerotic phenotype has not yet been established, and should, therefore, also be evaluated in osteoblastic models such as those induced by the breast cancer cell line ZR-75-1 [130], and prostate cancer cell lines LuCap 23.1 [131] or C4-2B [132].

Cancer Stem Cells and the Bone Metastatic Process

It is becoming increasingly clear that tumor cell populations arising in breast and prostate are organized much like normal tissues, in which self-renewing stem cell populations are responsible for spawning the bulk of the cells [133]. The bulk populations (>>95%) of tumor cells behave much like the transit-amplifying cells found in a normal tissue [134,135]. While the cancer stem cells are tumorigenic, in that they can seed a new tumor mass when implanted into the host, the non-stem cells (i.e., the transit-amplifying cells) in the tumor mass are unable to do so, because they are endowed with only a limited replicative potential. Strikingly, TGF-ß and BMPs affect stem cell renewal and induction of differentiation into spe-

Jeroen_Buijs_18.indd 214 26-11-2008 10:19:05

cialized-epithelial structures (reviewed in [136-139]). These observations may have important implications for the process of metastasis. If the non-stem cells in a primary tumor mass are truly non-tumorigenic, then these cells may well succeed in leaving the primary tumor and lodging in distant sites, but they will be unable to colonize these sites because of their limited proliferative potential. Accordingly, the ability to create macroscopic metastases may be limited to the relatively small number of tumor stem cells that escape from the primary tumor. These MICs may possess the ability to replicate to an unlimited extent and are therefore ideally suited to found new metastatic colonies that eventually expand to a life-threatening size. Such dynamics may well contribute to metastatic inefficiency — the failure of the vast majority of DTCs to colonize the tissue sites in which they have landed [140-143].

In addition to the TGF-ß and BMP pathways, the Notch, hedgehog and Wnt pathway are critically involved in normal and cancer stem cell proliferation (reviewed in [134]). Interestingly, multiple interactions between these pathways and different BMPs have been established. BMP7 could inhibit Notch signaling in normal prostate gland development [144], and BMP signaling can inhibit intestinal stem cell-renewal through suppression of Wnt/ß-catenin signaling [145]. For instance, we have found that BMP7 is able to inhibit Wnt signaling in PC-3M-Pro4 prostate cancer cells (unpublished data). Furthermore, recent data suggest that BMP(4)-induced Smad-signaling can inhibit the tumorigenic potential of human brain-tumor initiating cells, mediated via a significant reduction in the stem-like, tumor-initiating precursors [146]. Accumulating evidence suggests that cancer stem cells with tumor-initiating potential exist in human breast [147] and prostate cancer [141]. Although speculative at present, some of the observed effects of BMP7 described in this thesis may be mediated, at least in part, by osteotropic cancer cells with tumor-initiating (and metastatic) potential.

Further research is certainly warranted to address the role of BMP7 and other members of the TGF-ß superfamily in these pathways that are crucially important in developmental processes as well as in cancer progression. Furthermore, identification and characterization of MICs may provide new strategies for the treatment of patients with (as yet) incurable metastatic bone disease.

Summary and Conclusion

In this thesis, several processes have been unraveled that are critically important in the formation of metastases, particularly to bone. The presence of PAS+ networks in lymph node metastases from breast cancer is a prognostic factor for the formation of distant metastases. In addition, low BMP7 mRNA expression levels in primary breast cancer may be used as a prognostic indicator for the formation of bone metastases. After validation, these markers may be used to predict which patients are at high risk for distant metastases and become the rationale to offer patients a more adequate treatment, e.g., prophylactic BP treatment for patients that have low BMP7 levels.

Furthermore, we propose a model in which DTCs from osteotropic cancers are spread throughout the body, but with a modestly higher propensity for bone. Only DTCs with stem-cell like characteristics, i.e., MICs, which end up in a suitable environment can ultimately develop into a metastasis. In the bone environment, MICs can stay dormant for many years until a BMU comes into close proximity. When this happens the BMU may induce high local concentrations of growth factors such as TGF-ß, which can stimulate the outgrowth of a micrometastatic deposit to an overt bone metastasis. So, only MICs that are in the close proximity of a BMU may be activated to form a bone metastasis. Also, therapies that may reduce the actual number of BMUs, like OPG and BP, may inhibit the formation of bone metastases (Fig. 4). This may also be true for treatments that antagonize the pro-tumorigenic effects of TGF-ß. In addition, BMP7 may not only inhibit TGF-ß-induced EMT, but also induce epithelial homeostasis in normal breast and prostate epithelium, representing a putative novel therapeutic molecule for breast and prostate cancer.

References

1. Coleman RE. Metastatic bone disease: clinical features, pathophysiology and treatment strategies. *Cancer Treat Rev* 2001; 27:165-76.
2. Galasko C Incidence and distribution of skeletal metastases. In: *Skeletal Metastasis*, pp. 14-21. London, Butterworths, 1986.
3. Paget S. The distribution of secondary growths in cancer of the breast. *Lancet* 1889; 1:571-3.
4. Rubens RD The nature of metastatic bone disease. In: RD Rubens and Fogelman I. (eds.), *Bone metastases – diagnosis and treatment*, pp. 1-10. London, Springer-Verlag, 1991.
5. Weigelt B, Peterse JL, 't Veer LJ. Breast cancer metastasis: markers and models. *Nat Rev Cancer* 2005; 5:591-602.
6. Foss AJ, Alexander RA, Hungerford JL, Harris AL, Cree IA, Lightman S. Reassessment of the PAS patterns in uveal melanoma. *Br J Ophthalmol* 1997; 81:240-6.
7. Ruoslahti E. Specialization of tumour vasculature. *Nature Cancer Reviews* 2002; 2:83-90.
8. Clarijs R, Otte-Holler I, Ruiter DJ, de Waal RM. Presence of a fluid-conducting meshwork in xenografted cutaneous and primary human uveal melanoma. *Invest Ophthalmol Vis Sci* 2002; 43:912-8.
9. Engels K, Fox SB, Harris AL. Angiogenesis as a biologic and prognostic indicator in human breast carcinoma. *EXS* 1997; 79:113-56.:113-56.
10. Folberg R, Pe'er J, Gruman LM, Woolson RF, Jeng G, Montague PR *et al*. The morphologic characteristics of tumor blood vessels as a marker of tumor progression in primary human uveal melanoma: a matched case-control study. *Hum Pathol* 1992; 23:1298-305.
11. Thies A, Mangold U, Moll I, Schumacher U. PAS-positive loops and networks as a prognostic indicator in cutaneous malignant melanoma. *J Pathol* 2001; 195:537-42.
12. Folberg R, Rummelt V, Parys-Van Ginderdeuren R, Hwang T, Woolson RF, Pe'er J *et al*. The prognostic value of tumor blood vessel morphology in primary uveal melanoma. *Ophthalmology* 1993; 100:1389-98.
13. Warso MA, Maniotis AJ, Chen X, Majumdar D, Patel MK, Shilkaitis A *et al*. Prognostic significance of periodic acid-Schiff-positive patterns in primary cutaneous melanoma. *Clin Cancer Res* 2001; 7:473-7.
14. Hendrix MJ, Seftor EA, Kirschmann DA, Seftor RE. Molecular biology of breast cancer metastasis. Molecular expression of vascular markers by aggressive breast cancer cells. *Breast Cancer Res* 2000; 2:417-22.
15. McDonald DM, Munn L, Jain RK. Vasculogenic mimicry: how convincing, how novel, and how significant? *Am J Pathol* 2000; 156:383-8.

Jeroen_Buijs_18.indd 216 26-11-2008 10:19:05

16. Folberg R, Hendrix MJ, Maniotis AJ. Vasculogenic mimicry and tumor angiogenesis. *Am J Pathol* 2000; 156:361-81.
17. Fausto N. Vasculogenic mimicry in tumors. Fact or artifact? *Am J Pathol* 2000; 156:359.
18. Maniotis AJ, Folberg R, Hess A, Seftor EA, Gardner LM, Pe'er J *et al*. Vascular channel formation by human melanoma cells in vivo and in vitro: vasculogenic mimicry. *Am J Pathol* 1999; 155:739-52.
19. Bissell MJ. Tumor plasticity allows vasculogenic mimicry, a novel form of angiogenic switch. A rose by any other name? *Am J Pathol* 1999; 155:675-9.
20. Sood AK, Seftor EA, Fletcher MS, Gardner LM, Heidger PM, Buller RE *et al*. Molecular determinants of ovarian cancer plasticity. *Am J Pathol* 2001; 158:1279-88.
21. Sharma N, Seftor RE, Seftor EA, Gruman LM, Heidger PM, Jr., Cohen MB *et al*. Prostatic tumor cell plasticity involves cooperative interactions of distinct phenotypic subpopulations: Role in vasculogenic mimicry. *Prostate* 2002; 50:189-201.
22. Shirakawa K, Wakasugi H, Heike Y, Watanabe I, Yamada S, Saito K *et al*. Vasculogenic mimicry and pseudo-comedo formation in breast cancer. *Int J Cancer* 2002; 99:821-8.
23. Hendrix MJ, Seftor EA, Meltzer PS, Gardner LM, Hess AR, Kirschmann DA *et al*. Expression and functional significance of VE-cadherin in aggressive human melanoma cells: role in vasculogenic mimicry. *Proc Natl Acad Sci U S A* 2001; 98:8018-23.
24. Arguello F, Baggs RB, Graves BT, Harwell SE, Cohen HJ, Frantz CN. Effect of IL-1 on experimental bone/bone-marrow metastases. *Int J Cancer* 1992; 52:802-7.
25. Sasaki A, Boyce BF, Story B, Wright KR, Chapman M, Boyce R *et al*. Bisphosphonate risedronate reduces metastatic human breast cancer burden in bone in nude mice. *Cancer Res* 1995; 55:3551-7.
26. Yoneda T, Williams PJ, Hiraga T, Niewolna M, Nishimura R. A bone-seeking clone exhibits different biological properties from the MDA-MB-231 parental human breast cancer cells and a brain-seeking clone in vivo and in vitro. *J Bone Miner Res* 2001; 16:1486-95.
27. Hanahan D, Folkman J. Patterns and emerging mechanisms of the angiogenic switch during tumorigenesis. *Cell* 1996; 86:353-64.
28. Liotta LA, Kohn EC. The microenvironment of the tumour-host interface. *Nature* 2001; 411:375-9.
29. Hill PA. Bone remodelling. *Br J Orthod* 1998; 25:101-7.
30. Kostenuik PJ, Singh G, Suyama KL, Orr FW. Stimulation of bone resorption results in a selective increase in the growth rate of spontaneously metastatic Walker 256 cancer cells in bone. *Clin Exp Metastasis* 1992; 10:411-8.
31. Schneider A, Kalikin LM, Mattos AC, Keller ET, Allen MJ, Pienta KJ *et al*. Bone turnover mediates preferential localization of prostate cancer in the skeleton. *Endocrinology* 2005; 146:1727-36.
32. Vaananen K. Mechanism of osteoclast mediated bone resorption--rationale for the design of new therapeutics. *Adv Drug Deliv Rev* 2005; 57:959-71.
33. Michaelson MD, Smith MR. Bisphosphonates for treatment and prevention of bone metastases. *J Clin Oncol* 2005; 23:8219-24.
34. Body JJ, Greipp P, Coleman RE, Facon T, Geurs F, Fermand JP *et al*. A phase I study of AMGN-0007, a recombinant osteoprotegerin construct, in patients with multiple myeloma or breast carcinoma related bone metastases. *Cancer* 2003; 97:887-92.
35. Coleman RE. Bisphosphonates in breast cancer. *Ann Oncol* 2005; 16:687-95.
36. Elte JW, Bijvoet OL, Cleton FJ, van Oosterom AT, Sleeboom HP. Osteolytic bone metastases in breast carcinoma pathogenesis, morbidity and bisphosphonate treatment. *Eur J Cancer Clin Oncol* 1986; 22:493-500.
37. Antic VN, Fleisch H, Muhlbauer RC. Effect of bisphosphonates on the increase in bone resorption induced by a low calcium diet. *Calcif Tissue Int* 1996; 58:443-8.
38. Dunford JE, Thompson K, Coxon FP, Luckman SP, Hahn FM, Poulter CD *et al*. Structure-activity relationships for inhibition of farnesyl diphosphate synthase in vitro and inhibition of bone resorption in vivo by nitrogen-containing bisphosphonates. *J Pharmacol Exp Ther* 2001; 296:235-42.
39. Rosen LS, Gordon DH, Dugan W, Jr., Major P, Eisenberg PD, Provencher L *et al*. Zoledronic acid is superior to pamidronate for the treatment of bone metastases in breast carcinoma patients with at least one osteolytic lesion. *Cancer* 2004; 100:36-43.

40. Hiraga T, Williams PJ, Mundy GR, Yoneda T. The bisphosphonate ibandronate promotes apoptosis in MDA-MB-231 human breast cancer cells in bone metastases. *Cancer Res* 2001; 61:4418-24.
41. Hall DG, Stoica G. Effect of the bisphosphonate risedronate on bone metastases in a rat mammary adenocarcinoma model system. *J Bone Miner Res* 1994; 9:221-30.
42. Krempien B, Wingen F, Eichmann T, Muller M, Schmahl D. Protective effects of a prophylactic treatment with the bisphosphonate 3-amino-1-hydroxypropane-1,1-bisphosphonic acid on the development of tumor osteopathies in the rat: experimental studies with the Walker carcinosarcoma 256. *Oncology* 1988; 45:41-6.
43. Kostenuik PJ, Orr FW, Suyama K, Singh G. Increased growth rate and tumor burden of spontaneously metastatic Walker 256 cancer cells in the skeleton of bisphosphonate-treated rats. *Cancer Res* 1993; 53:5452-7.
44. Brown JE, Thomson CS, Ellis SP, Gutcher SA, Purohit OP, Coleman RE. Bone resorption predicts for skeletal complications in metastatic bone disease. *Br J Cancer* 2003; 89:2031-7.
45. Brown JE, Cook RJ, Major P, Lipton A, Saad F, Smith M *et al*. Bone turnover markers as predictors of skeletal complications in prostate cancer, lung cancer, and other solid tumors. *J Natl Cancer Inst* 2005; 97:59-69.
46. Coleman RE, Major P, Lipton A, Brown JE, Lee KA, Smith M *et al*. Predictive value of bone resorption and formation markers in cancer patients with bone metastases receiving the bisphosphonate zoledronic acid. *J Clin Oncol* 2005; 23:4925-35.
47. Costa L, Demers LM, Gouveia-Oliveira A, Schaller J, Costa EB, de Moura MC *et al*. Prospective evaluation of the peptide-bound collagen type I cross-links N-telopeptide and C-telopeptide in predicting bone metastases status. *J Clin Oncol* 2002; 20:850-6.
48. Zheng Y, Zhou H, Modzelewski JR, Kalak R, Blair JM, Seibel MJ *et al*. Accelerated bone resorption, due to dietary calcium deficiency, promotes breast cancer tumor growth in bone. *Cancer Res* 2007; 67:9542-8.
49. Diel IJ, Solomayer EF, Costa SD, Gollan C, Goerner R, Wallwiener D *et al*. Reduction in new metastases in breast cancer with adjuvant clodronate treatment. *N Engl J Med* 1998; 339:357-63.
50. Kanis JA, Powles T, Paterson AH, McCloskey EV, Ashley S. Clodronate decreases the frequency of skeletal metastases in women with breast cancer. *Bone* 1996; 19:663-7.
51. Saarto T, Vehmanen L, Virkkunen P, Blomqvist C. Ten-year follow-up of a randomized controlled trial of adjuvant clodronate treatment in node-positive breast cancer patients. *Acta Oncol* 2004; 43:650-6.
52. van Holten-Verzantvoort AT, Hermans J, Beex LV, Blijham G, Cleton FJ, Eck-Smit BC *et al*. Does supportive pamidronate treatment prevent or delay the first manifestation of bone metastases in breast cancer patients? *Eur J Cancer* 1996; 32A:450-4.
53. Powles T, Paterson A, McCloskey E, Schein P, Scheffler B, Tidy A *et al*. Reduction in bone relapse and improved survival with oral clodronate for adjuvant treatment of operable breast cancer [ISRCTN83688026]. *Breast Cancer Res* 2006; 8:R13.
54. Kang Y, Siegel PM, Shu W, Drobnjak M, Kakonen SM, Cordon-Cardo C *et al*. A multigenic program mediating breast cancer metastasis to bone. *Cancer Cell* 2003; 3:537-49.
55. Woelfle U, Cloos J, Sauter G, Riethdorf L, Janicke F, van Diest P *et al*. Molecular signature associated with bone marrow micrometastasis in human breast cancer. *Cancer Res* 2003; 63:5679-84.
56. Smid M, Wang Y, Klijn JG, Sieuwerts AM, Zhang Y, Atkins D *et al*. Genes associated with breast cancer metastatic to bone. *J Clin Oncol* 2006; 24:2261-7.
57. Bendre MS, Gaddy-Kurten D, Mon-Foote T, Akel NS, Skinner RA, Nicholas RW *et al*. Expression of interleukin 8 and not parathyroid hormone-related protein by human breast cancer cells correlates with bone metastasis in vivo. *Cancer Res* 2002; 62:5571-9.
58. Yin JJ, Selander K, Chirgwin JM, Dallas M, Grubbs BG, Wieser R *et al*. TGF-beta signaling blockade inhibits PTHrP secretion by breast cancer cells and bone metastases development. *J Clin Invest* 1999; 103:197-206.
59. Zhao Y, Bachelier R, Treilleux I, Pujuguet P, Peyruchaud O, Baron R *et al*. Tumor alphavbeta3 integrin is a therapeutic target for breast cancer bone metastases. *Cancer Res* 2007; 67:5821-30.

Jeroen_Buijs_18.indd 218 26-11-2008 10:19:05

60. 't Veer LJ, Dai H, van de Vijver MJ, He YD, Hart AA, Mao M *et al*. Gene expression profiling predicts clinical outcome of breast cancer. *Nature* 2002; 415:530-6.
61. Wang Y, Klijn JG, Zhang Y, Sieuwerts AM, Look MP, Yang F *et al*. Gene-expression profiles to predict distant metastasis of lymph-node-negative primary breast cancer. *Lancet* 2005; %19-25;365:671-9.
62. Braun S, Kentenich C, Janni W, Hepp F, de Waal J, Willgeroth F *et al*. Lack of effect of adjuvant chemotherapy on the elimination of single dormant tumor cells in bone marrow of high-risk breast cancer patients. *J Clin Oncol* 2000; 18:80-6.
63. Berg A, Berner A, Lilleby W, Bruland OS, Fossa SD, Nesland JM *et al*. Impact of disseminated tumor cells in bone marrow at diagnosis in patients with nonmetastatic prostate cancer treated by definitive radiotherapy. *Int J Cancer* 2007; 120:1603-9.
64. Thiery JP. Epithelial-mesenchymal transitions in development and pathologies. *Curr Opin Cell Biol* 2003; 15:740-6.
65. Dudley AT, Lyons KM, Robertson EJ. A requirement for bone morphogenetic protein-7 during development of the mammalian kidney and eye. *Genes Dev* 1995; 9:2795-807.
66. Luo G, Hofmann C, Bronckers AL, Sohocki M, Bradley A, Karsenty G. BMP-7 is an inducer of nephrogenesis, and is also required for eye development and skeletal patterning. *Genes Dev* 1995; 9:2808-20.
67. Vukicevic S, Kopp JB, Luyten FP, Sampath TK. Induction of nephrogenic mesenchyme by osteogenic protein 1 (bone morphogenetic protein 7). *Proc Natl Acad Sci U S A* 1996; 93:9021-6.
68. Barnes J, Anthony CT, Wall N, Steiner MS. Bone morphogenetic protein-6 expression in normal and malignant prostate. *World J Urol* 1995; 13:337-43.
69. Bentley H, Hamdy FC, Hart KA, Seid JM, Williams JL, Johnstone D *et al*. Expression of bone morphogenetic proteins in human prostatic adenocarcinoma and benign prostatic hyperplasia. *Br J Cancer* 1992; 66:1159-63.
70. Harris SE, Harris MA, Mahy P, Wozney J, Feng JQ, Mundy GR. Expression of bone morphogenetic protein messenger RNAs by normal rat and human prostate and prostate cancer cells. *Prostate* 1994; 24:204-11.
71. Ye L, Lewis-Russell JM, Kyanaston HG, Jiang WG. Bone morphogenetic proteins and their receptor signaling in prostate cancer. *Histol Histopathol* 2007; 22:1129-47.
72. Masuda H, Fukabori Y, Nakano K, Takezawa Y, CSuzuki T, Yamanaka H. Increased expression of bone morphogenetic protein-7 in bone metastatic prostate cancer. *Prostate* 2003; 54:268-74.
73. Thomas R, Anderson WA, Raman V, Reddi AH. Androgen-dependent gene expression of bone morphogenetic protein 7 in mouse prostate. *Prostate* 1998; 37:236-45.
74. Masuda H, Fukabori Y, Nakano K, Shimizu N, Yamanaka H. Expression of bone morphogenetic protein-7 (BMP-7) in human prostate. *Prostate* 2004; 59:101-6.
75. Raida M, Clement JH, Ameri K, Han C, Leek RD, Harris AL. Expression of bone morphogenetic protein 2 in breast cancer cells inhibits hypoxic cell death. *Int J Oncol* 2005; 26:1465-70.
76. Helms MW, Packeisen J, August C, Schittek B, Boecker W, Brandt BH *et al*. First evidence supporting a potential role for the BMP/SMAD pathway in the progression of oestrogen receptor-positive breast cancer. *J Pathol* 2005; 206:366-76.
77. Alarmo EL, Rauta J, Kauraniemi P, Karhu R, Kuukasjarvi T, Kallioniemi A. Bone morphogenetic protein 7 is widely overexpressed in primary breast cancer. *Genes Chromosomes Cancer* 2006; 45:411-9.
78. Wang N, Lin KK, Lu Z, Lam KS, Newton R, Xu X *et al*. The LIM-only factor LMO4 regulates expression of the BMP7 gene through an HDAC2-dependent mechanism, and controls cell proliferation and apoptosis of mammary epithelial cells. *Oncogene* 2007; 26:6431-41.
79. Guhaniyogi J, Brewer G. Regulation of mRNA stability in mammalian cells. *Gene* 2001; 265:11-23.
80. Zhang W, Dahlberg JE, Tam W. MicroRNAs in tumorigenesis: a primer. *Am J Pathol* 2007; 171:728-38.
81. Constam DB, Robertson EJ. Regulation of bone morphogenetic protein activity by pro domains and proprotein convertases. *J Cell Biol* 1999; 144:139-49.
82. Alarmo EL, Korhonen T, Kuukasjarvi T, Huhtala H, Holli K, Kallioniemi A. Bone morphogenetic protein 7 expression associates with bone metastasis in breast carcinomas. *Ann Oncol* 2007.
83. Rothhammer T, Wild PJ, Meyer S, Bataille F, Pauer A, Klinkhammer-Schalke M *et al*. Bone morphogenetic protein 7 (BMP7) expression is a potential novel prognostic marker for recurrence in patients with primary melanoma. *Cancer Biomark* 2007; 3:111-7.

84. Kwak C, Park YH, Kim IY, Moon KC, Ku JH. Expression of bone morphogenetic proteins, the subfamily of the transforming growth factor-beta superfamily, in renal cell carcinoma. *J Urol* 2007; 178:1062-7.
85. Korchynskyi O, van Bezooijen RL, Löwik CWGM, and Ten Dijke P Bone morphogenetic protein receptors and nuclear effectors in bone formation. In: S Vukicevic and KT Sampath (eds.), *Bone Morphogenetic Proteins: Regeneration of Bone and Beyond*, pp. 9-44. Basel, Birkhäuser, 2004.
86. Ten Dijke P, Korchynskyi O, Valdimarsdottir G, Goumans MJ. Controlling cell fate by bone morphogenetic protein receptors. *Mol Cell Endocrinol* 2003; 211:105-13.
87. Dai J, Kitagawa Y, Zhang J, Yao Z, Mizokami A, Cheng S *et al*. Vascular endothelial growth factor contributes to the prostate cancer-induced osteoblast differentiation mediated by bone morphogenetic protein. *Cancer Res* 2004; 64:994-9.
88. Groppe J, Greenwald J, Wiater E, Rodriguez-Leon J, Economides AN, Kwiatkowski W *et al*. Structural basis of BMP signalling inhibition by the cystine knot protein Noggin. *Nature* 2002; 420:636-42.
89. Feeley BT, Gamradt SC, Hsu WK, Liu N, Krenek L, Robbins P *et al*. Influence of BMPs on the formation of osteoblastic lesions in metastatic prostate cancer. *J Bone Miner Res* 2005; 20:2189-99.
90. Schwaninger R, Rentsch CA, Wetterwald A, van der HG, van Bezooijen RL, van der PG *et al*. Lack of noggin expression by cancer cells is a determinant of the osteoblast response in bone metastases. *Am J Pathol* 2007; 170:160-75.
91. Feeley BT, Krenek L, Liu N, Hsu WK, Gamradt SC, Schwarz EM *et al*. Overexpression of noggin inhibits BMP-mediated growth of osteolytic prostate cancer lesions. *Bone* 2006; 38:154-66.
92. Dai J, Keller J, Zhang J, Lu Y, Yao Z, Keller ET. Bone morphogenetic protein-6 promotes osteoblastic prostate cancer bone metastases through a dual mechanism. *Cancer Res* 2005; 65:8274-85.
93. Ao M, Franco OE, Park D, Raman D, Williams K, Hayward SW. Cross-talk between paracrine-acting cytokine and chemokine pathways promotes malignancy in benign human prostatic epithelium. *Cancer Res* 2007; 67:4244-53.
94. Miyazaki H, Watabe T, Kitamura T, Miyazono K. BMP signals inhibit proliferation and in vivo tumor growth of androgen-insensitive prostate carcinoma cells. *Oncogene* 2004; 23:9326-35.
95. Qiu T, Grizzle WE, Oelschlager DK, Shen X, Cao X. Control of prostate cell growth: BMP antagonizes androgen mitogenic activity with incorporation of MAPK signals in Smad1. *EMBO J* 2007; 26:346-57.
96. Yang S, Lim M, Pham LK, Kendall SE, Reddi AH, Altieri DC *et al*. Bone morphogenetic protein 7 protects prostate cancer cells from stress-induced apoptosis via both Smad and c-Jun NH2-terminal kinase pathways. *Cancer Res* 2006; 66:4285-90.
97. Yang S, Zhong C, Frenkel B, Reddi AH, Roy-Burman P. Diverse biological effect and Smad signaling of bone morphogenetic protein 7 in prostate tumor cells. *Cancer Res* 2005; 65:5769-77.
98. Brubaker KD, Corey E, Brown LG, Vessella RL. Bone morphogenetic protein signaling in prostate cancer cell lines. *J Cell Biochem* 2004; 91:151-60.
99. Kim IY, Lee DH, Lee DK, Ahn HJ, Kim MM, Kim SJ *et al*. Loss of expression of bone morphogenetic protein receptor type II in human prostate cancer cells. *Oncogene* 2004; 23:7651-9.
100. Zeisberg M, Hanai J, Sugimoto H, Mammoto T, Charytan D, Strutz F *et al*. BMP-7 counteracts TGF-beta1-induced epithelial-to-mesenchymal transition and reverses chronic renal injury. *Nat Med* 2003; 9:964-8.
101. Zeisberg M, Shah AA, Kalluri R. Bone morphogenic protein-7 induces mesenchymal to epithelial transition in adult renal fibroblasts and facilitates regeneration of injured kidney. *J Biol Chem* 2005; 280:8094-100.
102. Ye L, Lewis-Russell JM, Kynaston H, Jiang WG. Endogenous Bone Morphogenetic Protein-7 Controls the Motility of Prostate Cancer Cells Through Regulation of Bone Morphogenetic Protein Antagonists. *J Urol* 2007;..
103. Kim IY, Lee DH, Ahn HJ, Tokunaga H, Song W, Devereaux LM *et al*. Expression of bone morphogenetic protein receptors type-IA, -IB and -II correlates with tumor grade in human prostate cancer tissues. *Cancer Res* 2000; 60:2840-4.

Jeroen_Buijs_18.indd 220 26-11-2008 10:19:05

104. Craft CS, Romero D, Vary CP, Bergan RC. Endoglin inhibits prostate cancer motility via activation of the ALK2-Smad1 pathway. *Oncogene* 2007; 26:7240-50.
105. Letamendia A, Lastres P, Botella LM, Raab U, Langa C, Velasco B *et al*. Role of endoglin in cellular responses to transforming growth factor-beta. A comparative study with betaglycan. *J Biol Chem* 1998; 273:33011-9.
106. Scherner O, Meurer SK, Tihaa L, Gressner AM, Weiskirchen R. Endoglin differentially modulates antagonistic transforming growth factor-beta1 and BMP-7 signaling. *J Biol Chem* 2007; 282:13934-43.
107. Kodach LL, Bleuming SA, Musler AR, Peppelenbosch MP, Hommes DW, van den Brink GR *et al*. The bone morphogenetic protein pathway is active in human colon adenomas and inactivated in colorectal cancer. *Cancer* 2008; 112:300-6.
108. Bleuming SA, He XC, Kodach LL, Hardwick JC, Koopman FA, Ten Kate FJ *et al*. Bone morphogenetic protein signaling suppresses tumorigenesis at gastric epithelial transition zones in mice. *Cancer Res* 2007; 67:8149-55.
109. Pouliot F, Blais A, Labrie C. Overexpression of a dominant negative type II bone morphogenetic protein receptor inhibits the growth of human breast cancer cells. *Cancer Res* 2003; 63:277-81.
110. Rudarakanchana N, Flanagan JA, Chen H, Upton PD, Machado R, Patel D *et al*. Functional analysis of bone morphogenetic protein type II receptor mutations underlying primary pulmonary hypertension. *Hum Mol Genet* 2002; 11:1517-25.
111. Arnold SF, Tims E, Mcgrath BE. Identification of bone morphogenetic proteins and their receptors in human breast cancer cell lines: importance of BMP2. *Cytokine* 1999; 11:1031-7.
112. Ghosh-Choudhury N, Woodruff K, Qi W, Celeste A, Abboud SL, Ghosh CG. Bone morphogenetic protein-2 blocks MDA MB 231 human breast cancer cell proliferation by inhibiting cyclin-dependent kinase-mediated retinoblastoma protein phosphorylation. *Biochem Biophys Res Commun* 2000; 272:705-11.
113. Clement JH, Raida M, Sanger J, Bicknell R, Liu J, Naumann A *et al*. Bone morphogenetic protein 2 (BMP-2) induces in vitro invasion and in vivo hormone independent growth of breast carcinoma cells. *Int J Oncol* 2005; 27:401-7.
114. Perk J, Iavarone A, Benezra R. Id family of helix-loop-helix proteins in cancer. *Nat Rev Cancer* 2005; 5:603-14.
115. Kowanetz M, Valcourt U, Bergstrom R, Heldin CH, Moustakas A. Id2 and Id3 define the potency of cell proliferation and differentiation responses to transforming growth factor beta and bone morphogenetic protein. *Mol Cell Biol* 2004; 24:4241-54.
116. Yan W, Chen X. Targeted repression of bone morphogenetic protein 7, a novel target of the p53 family, triggers proliferative defect in p53-deficient breast cancer cells. *Cancer Res* 2007; 67:9117-24.
117. Itahana Y, Singh J, Sumida T, Coppe JP, Parrinello S, Bennington JL *et al*. Role of Id-2 in the maintenance of a differentiated and noninvasive phenotype in breast cancer cells. *Cancer Res* 2003; 63:7098-105.
118. Notting I, Buijs J, Mintardjo R, van der Horst G, Vukicevic S, Lowik C *et al*. Bone morphogenetic protein 7 inhibits tumor growth of human uveal melanoma in vivo. *Invest Ophthalmol Vis Sci* 2007; 48:4882-9.
119. Pfeilschifter J, Mundy GR. Modulation of type beta transforming growth factor activity in bone cultures by osteotropic hormones. *Proc Natl Acad Sci U S A* 1987; 84:2024-8.
120. Kang Y, He W, Tulley S, Gupta GP, Serganova I, Chen CR *et al*. Breast cancer bone metastasis mediated by the Smad tumor suppressor pathway. *Proc Natl Acad Sci U S A* 2005; 102:13909-14.
121. Bandyopadhyay A, Agyin JK, Wang L, Tang Y, Lei X, Story BM *et al*. Inhibition of pulmonary and skeletal metastasis by a transforming growth factor-beta type I receptor kinase inhibitor. *Cancer Res* 2006; 66:6714-21.
122. Ehata S, Hanyu A, Fujime M, Katsuno Y, Fukunaga E, Goto K *et al*. Ki26894, a novel transforming growth factor-beta type I receptor kinase inhibitor, inhibits in vitro invasion and in vivo bone metastasis of a human breast cancer cell line. *Cancer Sci* 2007; 98:127-33.

123. Javelaud D, Mohammad KS, McKenna CR, Fournier P, Luciani F, Niewolna M *et al*. Stable overexpression of Smad7 in human melanoma cells impairs bone metastasis. *Cancer Res* 2007; 67:2317-24.
124. Guy CT, Webster MA, Schaller M, Parsons TJ, Cardiff RD, Muller WJ. Expression of the neu protooncogene in the mammary epithelium of transgenic mice induces metastatic disease. *Proc Natl Acad Sci U S A* 1992; 89:10578-82.
125. Muraoka RS, Koh Y, Roebuck LR, Sanders ME, Brantley-Sieders D, Gorska AE *et al*. Increased malignancy of Neu-induced mammary tumors overexpressing active transforming growth factor beta1. *Mol Cell Biol* 2003; 23:8691-703.
126. Siegel PM, Shu W, Cardiff RD, Muller WJ, Massague J. Transforming growth factor beta signaling impairs Neu-induced mammary tumorigenesis while promoting pulmonary metastasis. *Proc Natl Acad Sci U S A* 2003; 100:8430-5.
127. Muraoka RS, Dumont N, Ritter CA, Dugger TC, Brantley DM, Chen J *et al*. Blockade of TGF-beta inhibits mammary tumor cell viability, migration, and metastases. *J Clin Invest* 2002; 109:1551-9.
128. Derksen PW, Liu X, Saridin F, van der GH, Zevenhoven J, Evers B *et al*. Somatic inactivation of E-cadherin and p53 in mice leads to metastatic lobular mammary carcinoma through induction of anoikis resistance and angiogenesis. *Cancer Cell* 2006; 10:437-49.
129. Saad F, Gleason DM, Murray R, Tchekmedyian S, Venner P, Lacombe L *et al*. A randomized, placebo-controlled trial of zoledronic acid in patients with hormone-refractory metastatic prostate carcinoma. *J Natl Cancer Inst* 2002; 94:1458-68.
130. Yin JJ, Mohammad KS, Kakonen SM, Harris S, Wu-Wong JR, Wessale JL *et al*. A causal role for endothelin-1 in the pathogenesis of osteoblastic bone metastases. *Proc Natl Acad Sci U S A* 2003; 100:10954-9.
131. Corey E, Quinn JE, Bladou F, Brown LG, Roudier MP, Brown JM *et al*. Establishment and characterization of osseous prostate cancer models: intra-tibial injection of human prostate cancer cells. *Prostate* 2002; 52:20-33.
132. Thalmann GN, Anezinis PE, Chang SM, Zhau HE, Kim EE, Hopwood VL *et al*. Androgen-independent cancer progression and bone metastasis in the LNCaP model of human prostate cancer. *Cancer Res* 1994; 54:2577-81.
133. Wicha MS, Liu S, Dontu G. Cancer stem cells: an old idea--a paradigm shift. *Cancer Res* 2006; 66:1883-90.
134. Reya T, Morrison SJ, Clarke MF, Weissman IL. Stem cells, cancer, and cancer stem cells. *Nature* 2001; 414:105-11.
135. Tang DG, Patrawala L, Calhoun T, Bhatia B, Choy G, Schneider-Broussard R *et al*. Prostate cancer stem/progenitor cells: identification, characterization, and implications. *Mol Carcinog* 2007; 46:1-14.
136. Zhang J, Li L. BMP signaling and stem cell regulation. *Dev Biol* 2005; 284:1-11.
137. Mishra L, Shetty K, Tang Y, Stuart A, Byers SW. The role of TGF-beta and Wnt signaling in gastrointestinal stem cells and cancer. *Oncogene* 2005; 24:5775-89.
138. Mishra L, Derynck R, Mishra B. Transforming growth factor-beta signaling in stem cells and cancer. *Science* 2005; 310:68-71.
139. Varga AC, Wrana JL. The disparate role of BMP in stem cell biology. *Oncogene* 2005; 24:5713-21.
140. Arguello F, Baggs RB, Frantz CN. A murine model of experimental metastasis to bone and bone marrow. *Cancer Res* 1988; 48:6876-81.
141. Collins AT, Berry PA, Hyde C, Stower MJ, Maitland NJ. Prospective identification of tumorigenic prostate cancer stem cells. *Cancer Res* 2005; 65:10946-51.
142. Langley RR, Fidler IJ. Tumor cell-organ microenvironment interactions in the pathogenesis of cancer metastasis. *Endocr Rev* 2007; 28:297-321.
143. Wetterwald A, van der Pluijm G, Que I, Sijmons B, Buijs J, Karperien M *et al*. Optical imaging of cancer metastasis to bone marrow: a mouse model of minimal residual disease. *Am J Pathol* 2002; 160:1143-53.
144. Grishina IB, Kim SY, Ferrara C, Makarenkova HP, Walden PD. BMP7 inhibits branching morphogenesis in the prostate gland and interferes with Notch signaling. *Dev Biol* 2005; 288:334-47.

Jeroen_Buijs_18.indd 222 26-11-2008 10:19:06

145. He XC, Zhang J, Tong WG, Tawfik O, Ross J, Scoville DH *et al*. BMP signaling inhibits intestinal stem cell self-renewal through suppression of Wnt-beta-catenin signaling. *Nat Genet* 2004; 36:1117-21.
146. Piccirillo SG, Reynolds BA, Zanetti N, Lamorte G, Binda E, Broggi G *et al*. Bone morphogenetic proteins inhibit the tumorigenic potential of human brain tumour-initiating cells. *Nature* 2006; 444:761-5.
147. Al Hajj M, Wicha MS, Benito-Hernandez A, Morrison SJ, Clarke MF. Prospective identification of tumorigenic breast cancer cells. *Proc Natl Acad Sci U S A* 2003; 100:3983-8.

Jeroen_Buijs_18.indd 224 26-11-2008 10:19:06

Chapter 9

Summary
Samenvatting
List of Abbreviations
List of Publications
Curriculum Vitae

Jeroen_Buijs_18.indd 226 26-11-2008 10:19:06

Summary

The skeleton is one of the most common organs to be affected by metastatic disease. However, only a restricted number of solid cancers, especially those of the breast and prostate, are responsible for the majority of the bone metastases. Bone metastases are a major cause of morbidity, characterized by severe pain and high incidence of fractures, spinal cord compression and bone marrow aplasia requiring hospitalization. Despite the high frequency of skeletal metastases, the molecular mechanisms underlying the predisposition for tumors to colonize bone are poorly understood and treatment options are often unsatisfactory. The focus of this thesis was to better understand the processes that contribute to the formation of distant metastasis (**chapter 2**), particularly to bone (**chapter 4–7**), as well as to explore new treatment strategies with conventional (**chapter 4** and **5**) and novel therapeutic molecules (**chapter 6** and **7**) using optical imaging to sensitively monitor growth, dissemination and metastasis in mouse models (**chapter 3–7**).

Although current clinicopathologic parameters are widely used to predict clinical outcome, the clinical behavior of prostate and breast cancer can still be quite different. In order to improve breast and prostate cancer management, better and reliable markers are needed to distinguish patients with good and poor prognosis.

In **chapter 2** we demonstrated that, in addition to the tumor blood vessels, thin periodic acid-Schiff-positive (PAS+) patterns may exist in invasive ductal carcinoma (IDC) of the breast and their lymph node metastases. More importantly, the complexity of the PAS+ patterns in lymph node metastases was related to poor prognosis. Moreover, we found that the presence of the most complex thin PAS+ pattern — the PAS+ network — in lymph node metastases and stage classification of the tumor were the only two independent risk factors associated with the occurrence of a distant metastasis. Additionally, the presence of a PAS+ network in a positive lymph node is the factor most strongly associated with poor prognosis. Therefore, by examining IDC patients for the presence of PAS+ networks in their lymph node metastases, the clinical behavior of this heterogeneous group of breast cancer patients can be better predicted. This may ultimately lead to improved management of the disease.

Animal models have become important tools to study the molecular mechanisms that are involved in the formation of bone metastases and have adequately served as pre-clinical models to test new drug compounds and strategies. The formation of bone metastases after injection of MDA-MB-231 breast cancer cells into the left cardiac ventricle of immunodeficient (*nu/nu*) mice has been one of the most widely used bone metastasis models. The subsequent formation of cancer-induced osteolysis can be monitored by

radiographic detection. However, radiographic detection is an indirect and insensitive method to analyze bone metastases. Therefore, we described in **chapter 3** a technique that is able to directly monitor and quantify the distribution and growth of luciferase-transfected (luc+) cancer cells in intact animals using whole-body bioluminescent reporter imaging (BLI). In comparison with indirect detection using radiography, the BLI method yields higher sensitivity, reliability, and statistical power. The remarkable sensitivity of the optical imaging in detecting microscopic bone marrow metastases allowed us to detect bone micrometastatic deposits of 0.5 mm^3 volume, preceding the appearance of radiological evident osteolysis by 2 weeks. At present, the use of new CCD cameras and better luciferase expression have yielded even higher sensitivity. In the subsequent chapters **(4–7)**, BLI was used to study the molecular mechanisms in bone metastasis, as well as to develop new treatment strategies with novel and conventional compounds.

Interference with the microenvironmental growth support has been proposed as an attractive strategy for decreasing metastatic tumor growth. Agents that specifically decrease bone resorption and remodeling, such as bisphosphonates, are available and are used clinically for the protection of bone destruction by metastases from different primary tumors. In **chapter 4**, we have shown that clinically relevant doses of bisphosphonates, administered before the establishment of micrometastases (preventive protocol), reduced the number of developing bone metastases by 70%. Bisphosphonate treatment also inhibited the early progression of tumor growth in the small number of still developing metastases. However, when bisphosphonates were given to animals with established bone metastases (curative protocol) they did not inhibit the growth of breast cancer cells in the bone microenvironment, despite a substantial anti-osteolytic effect.

The lack of tumor growth response may be due to the magnitude of suppression of bone resorption and hence the potency or dose of bisphosphonates given, or due to the mechanism of bone resorption inhibition by bisphosphonates. In **chapter 5** we investigated these mechanisms in more detail in an experimental model of intra-tibial injection of human breast cancer cells. We assessed the effects of very high doses of the most potent bisphosphonate currently available, zoledronic acid, and we compared these to the effects of osteoprotegerin, which inhibits bone resorption by a different mechanism of action. As expected, both zoledronic acid and osteoprotegerin treatment markedly suppressed bone resorption, protected the integrity of bone trabeculae and prevented the development of osteolytic lesions. At the end of the experiment intraosseous tumor burden was reduced, but extramedullary growth was not affected. Although total (intra-bone and extramedullary) tumor burden in treated groups appeared less compared to controls, this difference was not significant. Taken together, using BLI for monitoring and quantifying tumor burden, our data favor the hypothesis that metastatic cancer cells in

Jeroen_Buijs_18.indd 228 26-11-2008 10:19:06

bone, after an initial growth phase that depends on their interaction with the BM stroma and extracellular bone matrix, become increasingly independent of microenvironmental growth factor support and are self-maintained by autocrine mechanisms.

In order to become invasive, cancer cells have to lose epithelial characteristics, such as expression of E-cadherin. The acquisition of an invasive phenotype is reminiscent of the epithelial-to-mesenchymal transition (EMT) that occurs during embryonic development. It has long been recognized that transforming growth factor-ß (TGF-ß), by signaling via the Smad pathway, can induce EMT in many different cell types in different settings, including embryogenesis, wound healing, and carcinogenesis. In contrast, bone morphogenetic protein 7 (BMP7) was shown to counteract TGF-ß–induced EMT and induce the opposite process, a mesenchymal-to-epithelial transition (MET), in renal epithelial cells.
In **chapter 6 and 7**, we described that BMP7 expression in breast and prostate cancer cell lines *in vitro* correlated with E-cadherin expression, and inversely correlated with aggressiveness and expression of the mesenchymal marker vimentin. Furthermore, we demonstrated that BMP7 induced MET and inhibited TGF-ß–induced EMT in breast and prostate cancer cells. In clinical samples, decreased BMP7 expression was observed in prostate cancer cells when compared to normal epithelial prostatic cells. In addition, decreased BMP7 mRNA expression levels in primary tumor were correlated with formation of bone metastases in breast cancer patients. In line with its inhibitory role in cancer progression, we show that stable overexpression of BMP7 in MDA-MB-231-BO2/luc+ breast cancer cells inhibited *de novo* formation and progression of osteolytic bone metastases. In **Chapter 6**, we examined the effects of daily intra-venous administration of BMP7 (100 µg/kg/d) and observed significant inhibition of orthotopic and intra-bone growth of luciferase transfected MDA-MB-231-B/luc+ cells in nude mice. BMP7 treatment also inhibited PC-3M-Pro4/Luc+ prostate cancer bone metastatic growth, but not orthotopic growth. Clearly, the tumor microenvironment is an important determinant of the therapeutic response to BMP7 in prostate cancer.

To summarize our data described in **chapter 6 and 7**, we propose a role for BMP7 expression in the maintenance of epithelial cell behavior in the breast and prostate. In normal epithelial cells BMP7 can induce the E-cadherin expression, repress vimentin synthesis, and prevent EMT. In later stages of tumorigenesis, because of loss of BMP7 expression by cancer cells and/or resistance of these cells to the BMP7 secreted by surrounding normal epithelial cells, malignant cells may lose their expression of E-cadherin under the influence of TGF-ß leading to EMT and subsequent metastatic spread. In prostate cancer, TGF-ß may even contribute to the epithelial homeostasis as long as BMP7 remains present as well.

In this thesis, several processes have been unraveled that are critically important in the formation of metastases, particularly to bone. The presence of PAS+ networks in lymph node metastases from breast cancer is a prognostic factor for the formation of distant metastases. In addition, low BMP7 mRNA expression levels in primary breast cancer may be used as a prognostic indicator for the formation of bone metastases. Both these markers may be used to predict which patients are at high risk for distant metastases and become the rationale to offer patients a more adequate treatment, e.g., prophylactic bisphosphonate treatment for patients that have low BMP7 levels.

Altogether, we propose a model in which disseminating tumor cells (DTCs) from osteotropic cancers are spread throughout the body with a modest higher propensity for bone. Only DTCs with stem-cell like characteristics such as an indefinite capacity of self-renewal, which end up in a suitable environment, can ultimately develop into a metastasis. In the bone environment cancer cells can stay dormant for many years until a bone remodeling unit (or basic multicellular unit, BMU) comes into close proximity. Osteoclastic bone resorption within the BMU induces high local concentrations of growth factors such as TGF-ß, which may stimulate the outgrowth of a micrometastatic deposit into an overt bone metastasis. Also, therapies that can reduce the actual number of BMUs, like treatment with osteoprotegerin and bisphosphonates, may inhibit the formation of bone metastases. This may also be true for compounds that antagonize the pro-tumorigenic effects of TGF-ß, such as BMP7. In addition, BMP7 may not only inhibit TGF-ß–induced EMT, but also be involved in the homeostasis of normal breast and prostate epithelium, representing thus a putative novel therapeutic molecule for breast and prostate cancer.

Jeroen_Buijs_18.indd 230 26-11-2008 10:19:06

Samenvatting

Van een tumor kunnen cellen losraken, die via het bloed en de lymfe op andere plekken in het lichaam terechtkomen en daar ook een tumor kunnen vormen. Dit proces heet uitzaaien. Al sinds de 19e eeuw is bekend dat bepaalde type tumoren, zoals borst- en prostaatkanker, vaker naar bot uitzaaien ('metastaseren') dan andere tumoren. In de Westerse wereld komen borst- en prostaatkanker bovendien het vaakst, bij respectievelijk vrouwen en mannen, voor. Uitzaaiingen in het bot veroorzaken grote morbiditeit, gekenmerkt door botpijnen, botbreuken en verzakkingen van de wervelkolom. Volgens welke exacte moleculaire mechanismen bepaalde tumoren naar bot uitzaaien is echter nog niet bekend. Daarnaast is er nog geen genezende behandeling voor handen.

Het onderzoek dat beschreven is in dit proefschrift was erop gericht om de processen die betrokken zijn bij (bot)metastasering te ontrafelen (**hoofdstuk 2, 4–7**), en tevens nieuwe behandelstrategieën te ontwikkelen met conventionele (**hoofdstuk 4 en 5**) én nieuwe (**hoofdstuk 6 en 7**) potentiële medicijnen, gebruikmakend van een techniek waarmee je tumorgroei direct en gevoelig kunt meten (**hoofdstuk 3–7**).

Ondanks dat in de kliniek verscheidene prognostische factoren worden gebruikt om het verloop van borst- en prostaatkanker te voorspellen, is het ziekteverloop nog heel divers. Betere prognostische factoren zijn dan ook hard nodig om een beter passende behandeling te kunnen aanbieden aan deze patiënten.

In **hoofdstuk 2** werd beschreven dat met een histologische "periodic acid-Schiff" (PAS)-kleuring in borstkanker naast aankleuring van de basaalmembraan van tumorbloedvaten ook andere structuren worden aangekleurd. De complexiteit van deze dunne PAS-positieve (PAS+) structuren bleek geassocieerd met een slechte prognose voor de patiënt. Bovendien waren de aanwezigheid van de meest complexe structuur, een PAS+ netwerk, in lymfekliermetastasen en de classificatie van het stadium van de kwaadaardige tumor ('stagering') de enige twee onafhankelijke risicofactoren voor de vorming van een metastase op afstand. De aanwezigheid van een PAS+ netwerk in een lymfekliermetastase bleek zelfs de sterkste indicatie voor een slechte prognose. De waarneming van een PAS+ netwerk in een lymfekliermetastase zou in de kliniek dus kunnen worden gebruikt om het ziekteverloop van een heterogene groep borstkankerpatiënten beter te kunnen voorspellen, zodat de behandeling daarop aangepast kan worden.

Diermodellen zijn van essentieel belang bij zowel het ontrafelen van moleculaire mechanismen betrokken bij botmetastasering als bij het preklinisch testen van nieuwe behandelingen gericht tegen de vorming en verdere groei van botmetastasen. Het meest bekende model dat gebruik wordt voor botmetastasering is de injectie van MDA-MB-231 borstkankercellen

Jeroen_Buijs_18.indd 231 26-11-2008 10:19:06

in het linker hartventrikel van naakte imuundeficiënte muizen. Deze tumorcellen metastaseren via de bloedbaan naar bot, waar ze botafbrekende cellen ('osteoclasten') stimuleren tot botafbraak ('osteolyse'). De tumor-geïnduceerde osteolytische plekken zijn dan na drie á vier weken te meten met behulp van röntgenapparatuur. Deze vorm van detectie is echter een indirecte en relatief onnauwkeurig methode om botmetastasen te meten. Een nieuwe techniek, bioluminescentie, werd beschreven in **hoofdstuk 3**. Deze techniek maakt gebruik van het *luciferase*-gen, dat wanneer het in de tumorcellen is gezet het enzym luciferase maakt. Na toediening van het substraat luciferine oxideert dit enzym de luciferine, waarbij er licht vrijkomt in de tumorcellen. Vervolgens kunnen deze lichtgevende tumorcellen in een diermodel met een lichtgevoelige CCD camera worden gevolgd en gemeten. In vergelijking met detectie met behulp van röntgenapparatuur kan met bioluminescentie botmetastasen in een eerder stadium gedetecteerd worden, vaak al na 2 weken. In de volgende hoofdstukken **(4–7)** werd bioluminescentie gebruikt als techniek om tumorgroei nauwkeuriger te meten.

Bisfosfonaten zijn botresorptieremmers die in de kliniek worden gegeven als behandeling tegen tumor-geïnduceerde botafbraak. Tijdens botafbraak komen veel groeifactoren zoals transforming growth factor-ß (TGF-ß) vrij, die mogelijk kunnen bijdrage aan tumorgroei. In **hoofdstuk 4 en 5** werd onderzocht of botresorptieremming naast remming van tumor-geïnduceerde botafbraak ook de groei en ontwikkeling van borstkanker in het bot kon remmen. In **hoofdstuk 4** werd beschreven dat een preventieve behandeling met klinisch relevante doseringen van bisfosfonaten de vorming van botmetastasen remde. Ondanks een grote remming van tumor-geïnduceerde botafbraak, kon een behandeling met bisfosfonaten nadat botmetastasen al ontwikkeld waren de tumorgroei niet meer remmen (curatieve behandeling).
Het is echter niet uit te sluiten dat een potenter of hogere dosering van een bisfosfonaat, of een botresorptieremmer met een ander werkingsmechanisme verdere groei van borstkanker in de bot wel zou kunnen remmen. Daarom hebben we in een model van borstkankergroei in de tibia (scheenbeen) in **hoofdstuk 5** zowel de effecten bestudeerd van een hoge dosering zoledronine zuur (Zometa®), het nu meest krachtige bisfosfonaat beschikbaar, als het effect van osteoprotegerine, dat botresorptie via een ander mechanisme remt. Zoals verwacht remden behandeling met zoledronine zuur of osteoprotegerine de vorming van tumor-geïnduceerde osteolytische plekken en voorkwamen ze de afbraak van bottrabekels, die in het bot onder andere voor extra stevigheid zorgen. De hoeveelheid tumor binnen-bot was na behandeling met zoledronine zuur of osteoprotegerine minder groot, echter een gedeelte van de tumor groeide buiten-bot en deze hoeveelheid tumor was even groot in vergelijking met de controlebehandeling. De totale tumor grootte (binnen-bot + buiten-bot) leek bij de behandelde groepen iets minder groot, maar gaf geen significant verschil in vergelijking met de controlebehandeling. De data beschreven in dit proefschrift wijzen er op dat de initiële tumorgroei in

Jeroen_Buijs_18.indd 232 26-11-2008 10:19:06

het bot afhankelijk is van de interacties met het botmilieu, maar dat tijdens verdere progressie de tumorgroei steeds onafhankelijker wordt van het botmilieu.

Zoals de meeste kankers ontstaan borst- en prostaatkanker uit epitheelcellen: cellen met een duidelijke onder- en bovenkant, die de eigenschap hebben dat ze aan elkaar vastzitten en die het oppervlak bekleden van onder andere huid, slijmvliezen, luchtwegen, maag-darmkanaal, en borst- en prostaatklieren. De ondergrond van een laag epitheel bestaat uit bindweefsel, ook wel mesenchym genoemd. Echter, tijdens het ontstaan en de groei van kanker ('carcinogenese') kunnen tumorcellen bepaalde epitheliale eigenschappen verliezen. Kwaadaardige tumorcellen aan de rand van de primaire tumor kunnen doordat ze niet meer goed aan elkaar hechten, losraken van de primaire tumor, binnendringen in het omliggende gezonde (bind)weefsel en uiteindelijk uitzaaien naar andere organen. De kanker is dan invasief geworden. Het verkrijgen van een invasief fenotype lijkt veel op een epitheliale-mesenchymale transitie (EMT), een proces dat van essentieel belang is tijdens de embryonale ontwikkeling van verscheidene organen zoals de nier. TGF-ß (transformerende groeifactor-beta) is een van de belangrijkste factoren die via intracellulaire Smad eiwitten EMT kan stimuleren in verschillende processen zoals bij wondgenezing, embryogenese en carcinogenese. BMP7 (bot morfogenese proteïne-7) kan daarentegen EMT remmen en het tegenovergestelde proces, een mesenchymale-epitheliale transitie (MET), induceren in nierepitheelcellen.

In **Hoofdstuk 6 en 7** werd de hypothese getest of BMP7 ook MET kon induceren in borst- en prostaatkanker. De hoeveelheid BMP7-eiwit ('de expressie') in borst- en prostaatkankercellijnen was gecorreleerd met de expressie van de epitheliale factor E-cadherine, en omgekeerd evenredig gecorreleerd met de mesenchymale marker vimentine, en de mate van kwaadaardigheid. BMP7 remde TGF-ß geïnduceerde EMT en stimuleerde MET in borst- en prostaatkankercellijnen. In klinische monsters van prostaatkankerpatiënten was BMP7 expressie verlaagd in tumorcellen ten opzichte van gezonde prostaatcellen. Bij borstkankerpatiënten was verlaagde BMP7 mRNA expressie in de primaire tumor bovendien gecorreleerd met de vorming van nieuwe botmetastasen. Wanneer BMP7 tot overexpessie werd gebracht in een borstkankercellijn, waardoor er meer BMP7 eiwit werd aangemaakt, remde dit het ontstaan van het aantal tumor-geïnduceerde osteolytische plekken. Groei van borstkanker in de borst en in het bot werd bovendien geremd door dagelijkse behandeling met BMP7. Behandeling met BMP7 bleek tevens de groei van prostaatkanker in het bot, maar niet in de prostaat te remmen. De omgeving van de tumor bepaalt dus mede de therapeutische respons van BMP7 op prostaatkanker.

De data beschreven in **hoofdstuk 6 en 7** suggereren dat er een belangrijke rol voor BMP7 is weggelegd in het behoud van epitheliale homeostase in de gezonde borst en prostaat. Hier stimuleert BMP7 de expressie van epitheliale eiwitten zoals E-cadherine, remt het

de synthese van het mesenchymale eiwit vimentine, en voorkomt het EMT. Tijdens tumorprogressie kan verlies van BMP7 expressie mogelijk leiden tot verlies van E-cadherine en leiden tot EMT en metastasering. In de prostaat zou in aanwezigheid van BMP7, TGF-ß zelfs kunnen bijdrage aan de epitheliale homeostase.

In dit proefschrift zijn verschillende processen beschreven die betrokken zijn bij metastasering, in het bijzonder botmetastasering. De aanwezigheid van PAS+ netwerken in lymfekliermetastasen van borstkanker is een prognostische factor voor de ontwikkeling van metastasen op afstand, en lage BMP7 mRNA expressie in primair borstkanker is een goede indicator voor de ontwikkeling van botmetastasen. Deze factoren kunnen worden gebruikt om te bepalen welke patiënten een verhoogd risico hebben op metastasering, zodat sneller en adequater met bv. een bisfosfonaatbehandeling gestart kan worden.

Op basis van de bevindingen beschreven in dit proefschrift en in de literatuur stellen wij een model voor waarbij tumorcellen van borst- en prostaatkanker via de bloedbaan door heel het lichaam verspreid worden met een voorkeur om naar bepaalde organen, zoals bot, uit te zaaien. Van de uitgezaaide tumorcellen kunnen alleen die cellen met bepaalde stamceleigenschappen, zoals de mogelijkheid tot oneindig delen, in staat zijn uiteindelijk uit te groeien tot een macrometastase. Tumorcellen kunnen in het bot jarenlang in ruste zijn en pas bij een locale hoge concentratie van groeifactoren van bv. TGF-ß en IGF, veroorzaakt door een normale botresorptie unit ('basic multicellular unit', BMU), worden gestimuleerd tot groei en vorming van een macrometastase. Behandelstrategiën die erop gericht zijn het aantal botresorptie units te verminderen, zoals bisfosfonaten en osteoprotegerine, zouden dus de vorming van nieuwe botmetastasen kunnen remmen. Dit geldt ook voor behandelingen die de pro-tumorigene effecten van TGF-ß kunnen remmen, zoals BMP7. BMP7 zou bovendien kunnen zorgen voor epitheliale homeostase in de borst en prostaat, waardoor dit een goede nieuwe behandeling kan worden in strijd tegen borst- en prostaatkanker.

Jeroen_Buijs_18.indd 234 26-11-2008 10:19:06

List of Abbreviatons

ActRII	activin type II receptor
ActRIIB	activin type IIB receptor
ALK	activin receptor-like kinase
AMHRII	Anti-Müllerian hormone type II receptor
bFGF	basic fibroblast growth factor
BLI	bioluminescent imaging
BMP	bone morphogenetic protein
BMPRI	BMP type I receptor
BMPRII	BMP type II receptor
BM	bone marrow
BMU	basic multicellular unit
BP	bisphosphonate
BRE	BMP-responsive element
BSP	bone sialoprotein
CDKI	cyclin-dependent kinase inhibitor (CDKI)
CMV	cytomegalovirus
CSC	cancer stem cell
CT	connective tissue
DFS	disease free survival
DKK-1	dickkopf
DTC	disseminating tumor cell
ECM	extracellular matrix
EGF	epidermal growth factor
EMT	epithelial-to-mesenchymal transition
ER	estrogen receptor
ERK	extracellular signal-related kinase
ET-1	endothelin-1
FCS	fetal calf serum
FGF	fibroblast growth factor
GFP	green fluorescent protein
GM-CSF	granulocyte-macrophage colony stimulating factor (alias CSF2)
HGF	hepatocyte growth factor (alias scatter factor)
Hh	hedgehog
HRPC	hormone refractory prostate cancer
HSC	hematopoietic stem cell
i.c.	intracardiac
i.m.	intramuscle
i.o.	intraosseous
i.v.	intravenous
IBC	inflammatory breast cancer
Id	Inhibitor of DNA binding
IDC	invasive ductal carcinoma
IGF	insulin growth factor
IGFBP	insulin-like growth factor binding protein
IHC	immunohistochemistry
IL	interleukin
ILC	invasive lobular carcinoma
JNK	JunN-terminal kinase
LAP	latency-associated peptide
LCM	laser capture microdissection
LLC	large latent complex
LSD	least significant difference
LTBP	large latent TGF-ß-binding protein
Luc	luciferase

M-CSF	macrophage colony stimulating factor (alias CSF1)
MAPK	mitogen-activated protein kinase
MET	mesenchymal-to-epithelial transition
MIC	metastasis-initiating cell
MRD	minimal residual disease
MSC (cell)	migrating cancer stem (cell)
n.s.	not significant
NF-κB	nuclear factor κB
OPG	osteoprotegerin
OPN	osteopontin
PAS	periodic acid-Schiff
PCR	polymerase chain reaction
PDGF	platelet-derived growth factor
PR	progesteron receptor
PSA	prostate-specific antigen
PTH	parathyroid hormone
PTHrP	parathyroid hormone-related protein
qPCR	quantitative real-time reverse transcription PCR
R-Smads	receptor-regulated Smads
RANK	receptor activator of nuclear factor κB
RANKL	receptor activator of nuclear factor κB ligand
RLU	relative light unit
Runx2	runt-related transcription factor 2 (alias core-binding factor α1)
s.c.	subcutaneous
s.e.m.	standard error of the mean SBE smad-binding element
SCID	severely compromised immunodeficient
SCS (cell)	stationary cancer stem (cell)
SDF-1	stromal derived growth factor-1
SLC	small latent complex
SMA	smooth muscle actin
Smad	Sma-Mad related proteins
Smurf	Smad ubiquitin regulatory factor
SNO (cells)	spindle-shaped N-cadherin+ CD45- osteoblastic (cells)
SRE	skeletal-related events
sALP	serum alkaline phosphatase
TßRII	transforming growth factor-ß type II receptor
TBV	trabecular bone volume
TGF-ß	transforming growth factor-ß
TGIF	TGF-ß-induced factor
TMA	tissue microarray
TNF	tumor necrosis factor
Tob	transducer of ErbB-2
TRAcP	tartrate-resistant acid phosphatase
uPA	urokinase-type plasminogen activator
VCAM	vascular cell adhesion molecule
VEGF	vascular endothelial growth factor
VEGFR	vascular endothelial growth factor receptor
VM	vasculogenic mimicry
vWF	von Willebrandt Factor
Wnt	wingless int
ZO	zona occludens
ZOL	zoledronic acid

Jeroen_Buijs_18.indd 236 26-11-2008 10:19:06

List of publications

1. **Buijs JT**, van der Pluijm G. Osteotropic cancers: From primary tumor to bone. Review. *Cancer Letters* 2008. *in press*.
2. **Buijs JT**, Que I, Löwik CWGM, Papapoulos SE, van der Pluijm G. Inhibition of bone resorption and growth of breast cancer in the bone microenvironment. *Bone,* 2008, *in press.*
3. Kaijzel EL, Snoeks TJ, **Buijs JT,** van der Pluijm G, Löwik CWGM. Multimodal imaging and treatment of bone metastasis. *Clin Exp Metastasis* 2008, *in press*.
4. Notting IC, **Buijs JT,** Speetjens FM, Mintardjo RE, Henriquez NV, Schalij-Delfos NE, Keunen JEE, van der Pluijm G. Expression of tumor-suppressor gene DAN in uveal melanoma: a new prognostic marker? *submitted for publication*.
5. **Buijs JT**, Henriquez NV, van Overveld PG, van der Horst G, Ten Dijke P, van der Pluijm G. TGF-ß and BMP7 interactions in tumour progression and bone metastasis. *Clin Exp Metastasis* 2007; 24:609-17.
6. **Buijs JT**, Henriquez NV, van Overveld PG, van der Horst G, Que I, Schwaninger R, Rentsch C, Ten Dijke P, Cleton-Jansen AM, Driouch K, Lidereau R, Bachelier R, Vukicevic S, Clézardin P, Papapoulos SE, Cecchini MG, Löwik CW, van der Pluijm G. Bone Morphogenetic Protein 7 in the Development and Treatment of Bone Metastases from Breast Cancer. *Cancer Res* 2007; 67:8742-51.
7. **Buijs JT**, Rentsch CA, van der Horst G, van Overveld PG, Wetterwald A, Schwaninger R, Henriquez NV, Ten Dijke P, Borovecki F, Markwalder R, Thalmann GN, Papapoulos SE, Pelger RC, Vukicevic S, Cecchini MG, Löwik CWGM, van der Pluijm G. BMP7, a Putative Regulator of Epithelial Homeostasis in the Human Prostate, is a Potent Inhibitor of Prostate Cancer Bone Metastasis In Vivo. *Am J Pathol* 2007; 171:1047-57.
8. Henriquez NV, van Overveld PG, Que I, **Buijs JT**, van der Horst G, Bachelier R, Kaijzel EL, Löwik CWGM, Clezardin P, van der Pluijm G. Advances in optical imaging and novel model systems for cancer metastasis research *Clin Exp Metastasis* 2007; 24:699-705.
9. Notting IC, **Buijs JT**, Mintardjo R, van der Horst G, Vukicevic S, Löwik CWGM, Schalij-Delfos N, Keunen J, van der Pluijm G. Bone Morphogenetic Protein 7 inhibits tumor growth of uveal melanoma *Invest Ophthalmol Vis Sci* 2007 48:4882-9.
10. Deckers M, van Dinther M, **Buijs JT**, Que I, Löwik CWGM, van der Pluijm G, ten Dijke P. The tumor suppressor Smad4 is required for transforming growth factor beta-induced epithelial to mesenchymal transition and bone metastasis of breast cancer cells. *Cancer Res* 2006; 66:2202-9.
11. Notting IC, **Buijs JT**, Que I, Mintardjo RE, van der Horst G, Karperien M, Missotten GS, Jager MJ, Schalij-Delfos NE, Keunen JE, van der Pluijm G. Whole-body bioluminescent imaging of human uveal melanoma in a new mouse model of local tumor growth and metastasis. *Invest Ophthalmol Vis Sci*. 2005; 46:1581-7.
12. van der Pluijm G, **Buijs JT**. Angiogenesis and lymphangiogenesis in metastatic bone disease: a matter of networking. *In:* Singh G, Orr W (eds.) *Bone Metastasis and Molecular Pathophysiology* volume 6:139-62. Kluwer Academic Publishers 2004.
13. **Buijs JT**, Cleton A-M, Smit VTHBM, Löwik CWGM, Papapoulos SE, van der Pluijm G. Prognostic significance of periodic acid-Schiff-positive patterns in primary breast cancer and its lymph node metastases. *Breast Cancer Res Treat*. 2004; 84:117-30.
14. Wetterwald A, van der Pluijm G, Que I, Sijmons B, **Buijs JT**, Karperien M, Lowik CWGM, Gautschi E, Thalmann GN, Cecchini MG. Optical imaging of cancer metastasis to bone marrow: a mouse model of minimal residual disease. *Am J Pathol* 2002; 160:1143-53.
15. Van Duijn MM, **Buijs JT**, Van der Zee J, Van den Broek PJA. The ascorbate: ascorbate free radical oxidoreductase from the erythrocyte membrane is not cytochrome b561. *Protoplasma* 2001; 217:94-100.

Jeroen_Buijs_18.indd 238 26-11-2008 10:19:06

Curriculum Vitae

Jeroen Theodorus Buijs werd geboren op 27 januari 1979 in Amsterdam. Na het behalen van zijn VWO diploma in juni 1997 aan het Thorbecke Lyceum in Rotterdam, begon hij aan de studie Biomedische Wetenschappen aan de Universiteit Leiden. Tijdens deze studie werden stages gelopen bij de afdeling Moleculaire Celbiologie in het Sylviuslaboratorium onder leiding van Dr. M.M. van Duijn en Dr. P.J.A. van den Broek, bij de afdeling Endocrinologie en Stofwisselingsziekten van het Leids Universitair Medisch Centrum (LUMC), onder leiding van Dr. G. van der Pluijm en Prof. Dr. C.W.G.M. Löwik, en bij de afdeling Pathologie van het LUMC, onder leiding van Dr. A.M. Cleton-Jansen. Nog tijdens de studie werd in nauwe samenwerking met de afdeling Endocrinologie en Stofwisselingsziekten een werkbezoek van drie maanden afgelegd bij de afdeling 'Gene Therapy' van het 'Inselspital' in Bern (Zwitserland) onder leiding van Dr. M.G. Cecchini. Na zijn afstuderen in September 2001, was hij werkzaam als promovendus bij de afdeling Endocrinologie en Stofwisselingsziekten van het LUMC, onder leiding van Dr. G. van der Pluijm en Prof. Dr. S.E. Papapoulos. Het hier uitgevoerde onderzoek staat beschreven in dit proefschrift, en is gehonoreerd met een prijs voor beste researchposter op het '*Vth International Conference on Cancer-Induced Bone Disease*' in Davos (Zwitserland) in 2005 en geselecteerd voor een mondelinge presentatie op de '*17th Scientific Meeting of the International Bone & Mineral Society (IBMS)*' in Montréal (Canada) in 2007. Sinds april 2006 zet hij zijn onderzoek naar processen die betrokken zijn bij metastasering naar bot voort als postdoc bij de afdeling Urologie van het LUMC op het door EU gefinancierde zesde kader programma PRIMA (FP-504587)

Jeroen Theodorus Buijs was born on 27th of January 1979 in Amsterdam. After graduation from high school in 1997 at the 'Thorbecke Lyceum' in Rotterdam, he started to study Biomedical Science at the University of Leiden. During his study he performed internships at the department of 'Molecular Cell Biology' at the Sylvius under supervision of Dr. M.M. van Duijn and Dr. P.J.A. van den Broek, at the department of 'Endocrinology and Metabolic Diseases' at the Leiden University Medical Center (LUMC) under supervision of Dr. G. van der Pluijm and Prof. Dr. C.W.G.M. Löwik, and at the department of Pathology at the LUMC under supervision of Dr. A.M. Cleton-Jansen. At the end of his study, he worked, in close collaboration with the department of 'Endocrinology and Metabolic Diseases', at the department of Gene Therapy at the 'Inselspital' in Berne (Switzerland) under supervision of Dr. M.G. Cecchini. After graduation in September 2001, he started his PhD research at the department of 'Endocrinology and Metabolic Diseases' under supervision Dr. G. van der Pluijm and Prof. Dr. S.E. Papapoulos. The work from this period is described in this thesis, and was awarded with the prize for best research poster at the *Vth International Conference on Cancer-Induced Bone Disease* in Davos (Switzerland) in 2005, and selected for oral presentation at the '*17th Scientific Meeting of the International Bone & Mineral Society (IBMS)*' in Montréal (Canada) in

2007. Since April 2006 he works as a postdoctoral researcher at the department of Urology at het LUMC on an EU-financed sixth framework program PRIMA (FP-504587), studying the pathogenesis and treatment of bone metastasis.

Jeroen_Buijs_18.indd 240 26-11-2008 10:19:06